THE DEVELOPMENT AND ASSESSMENT OF SUSTAINED RELEASE NEVIRAPINE TABLETS

A Thesis Submitted to Rhodes University in

Fulfilment of the Requirements for the Degree of

MASTER OF SCIENCE (PHARMACY)

By

Chiluba Mwila

FEBRUARY 2013

Faculty of Pharmacy

Rhodes University

Grahamstown

South Africa

ABSTRACT

The use of antiretroviral (ARV) agents in the management of HIV/AIDS has significantly improved the lifestyle and wellbeing of patients. Despite the success that has been achieved with the use of ARV therapy, the occurrence of adverse effects and unpredictable bioavailability associated with most of these drugs remains a major concern. Nevirapine (NVP) is a non-nucleoside reverse transcriptase inhibitor (NNRTI) that is used in combination with other ARV compounds for the treatment of HIV-1 infections. It is also used for the prevention of mother to child transmission of the HIV-1 virus. NVP is a Biopharmaceutics Classification System (BCS) Class II compound.

Although NVP exhibits good oral absorption, it induces self-metabolism leading to low and sometimes unpredictable bioavailability. NVP is commercially available as an immediate release and extended release dosage form, *viz.,* Viramune® XR. Formulation of a generic sustained release (SR) dosage form for once daily dosing would result in delivery of constant amount of the drug to the circulation, reduce dose related adverse effects, improve patient compliance to medication and reduce the costs of therapy.

A simple RP-HPLC method was developed and optimised using a central composite design approach. The method was validated using ICH guidelines and was found to be linear, precise, specific and accurate for the analysis of NVP both in bulk and dosage forms.

Direct compression was used as the method of tablet manufacture. Different polymers were assessed for suitability as rate retarding polymers and included Methocel® K4M, Carbopol® 71G NF and Eudragit® RSPO. Powder blends were assessed for flow properties using the angle of repose, bulk and tapped density, Carr's Compressibility index and Hausner's ratio. The traditional approach of changing the amount of polymers and diluents systematically to achieve a desired NVP release profile was used for the development of a preliminary formulation. Response surface methodology was used for the optimisation of the formulation using a Box-Behnken quadratic design.

Physical characteristics of the tablets such as thickness, weight, hardness, tensile strength and friability were assessed and the tablets passed Pharmacopoeial testing. NVP assay and content uniformity were assessed using a validated RP-HPLC method.

Initially, USP Apparatus 2 was used to study NVP release over a 24 hour period and subsequently dissolution studies were performed using USP Apparatus 3 as it can be used to simulate GIT conditions. The dissolution profiles generated were used to determine the agitation rate for USP Apparatus 3 that would be equivalent to an agitation rate of 50 rpm when using USP Apparatus 2. The effect of the mesh screen pore size, buffer molarity strength and concentration of surfactant on NVP release were also investigated in order to select discriminatory dissolution test conditions for the test formulation.

Dissolution profiles were compared to those of the commercially available Viramune® XR using the FDA recommended difference (f_1) and similarity (f_2) factors. The calculated values for f_1 and f_2 revealed that the dissolution profile for the optimised formulation that was identified was statistically similar to Viramune® XR.

In vitro release data were fitted to different kinetic models to study the release kinetics of NVP. The overall mechanism of NVP release was best described using the Korsmeyer-Peppas diffusion exponent value, *n*. NVP release was found to be anomalous, implying that the release was influenced by a combination of diffusion, swelling and polymer chain relaxation. The Hixson-Crowell model revealed that there was constant change in surface area of the dosage form suggesting that erosion and swelling were significant factors affecting NVP release from the hydrophilic matrix technology. The release kinetics data were also used to design the optimised formulation.

Tablets manufactured using the optimised formulation were subjected to water uptake and erosion studies and the results revealed that swelling and erosion occur simultaneously. The effects of pH and molarity on the swelling and erosion of the tablets were also investigated. The data suggest that increase in pH resulted in a slight increase in swelling while an increase in molarity did not have a significant effect on swelling. The change in pH did not have a significant effect on erosion while an increase in molarity strength resulted in a decrease in matrix erosion.

The effect of HPMC grade on swelling, erosion and NVP release revealed that the grade of HPMC used had a significant effect on NVP release, with the release rate decreasing, swelling increasing and erosion decreasing as the viscosity of the HPMC grade increased. The effect of the particle size of MCC on NVP release was also studied by manufacturing tablets containing different grades of MCC and these studies revealed that particle size did

not appear to have a significant effect on NVP release. Similarly the use of different types of lactose did not appear to have a significant impact on NVP release.

In conclusion a sustained release NVP tablet formulation that has the potential for further development and optimisation has been developed, assessed and manufactured successfully and has been shown to exhibit similar dissolution behaviour to Viramune® XR, a commercially available NVP extended release product.

ACKNOWLEDGEMENTS

I would like to express my sincere gratitude to the following people:

My supervisor and Dean of the Faculty of Pharmacy: Professor Roderick B. Walker, for the opportunity to be part of his research group. Thank you very much for your support, guidance, assistance, understanding and patience throughout the course of my studies. Thank you for providing me with the materials and laboratory facilities.

The Beit Trust for funding and giving me the opportunity to be part of the elite group of Beit Scholars, I will forever be grateful.

Aspen® Pharmacare (South Africa): for the generous donation of anhydrous nevirapine.

Dr. S. M. M. Khamanga: for the tremendous assistance and guidance during my studies.

Dr. K. Wa Kasongo: for the ever timely advice, guidance, support and shared wisdom.

Mr. T. Samkange and Mr. L. Purdon: for the technical assistance throughout my studies.

Ms. Ayeshah B. F. Fauzee: for the support and advice.

Tendai Maynard Chiwakata: from the Pharmaceutical Chemistry Laboratory for all the help.

My lovely fiancée Elizabeth Mutale: for the support and patience. I know things were very hard but you remained strong and supportive through difficult times.

My parents mum Rosemary T. Mwila and dad Edward Mwila: for the support and encouragement. My brothers and sisters: Gilgrest, Chisanga, Mulinda, Chewe, Mwelwa, Mulenga and Chinyimba for the support and understanding during the period of my studies.

My colleagues in the Biopharmaceutics Research Laboratory: Farai J. Mhaka, Tawanda G. Dube, Chiedza C. Zindove, Tendai J. Chanakira, Pedzisai Makoni, Samantha Y. Mukozhiwa, Henusha Jhundoo, Laura Magnus, Bianca Dagnolo and Ashmita Ramanah. Thank you very much for the great support and friendship.

I would like to give thanks to the almighty God for everything he has done in my life and making the seemingly impossible things possible.

STUDY OBJECTIVES

HIV/AIDS is a well-known health challenge globally, with more than 34 million people living with HIV/AIDS worldwide [1]. Sub-Saharan Africa has the highest prevalence of HIV infection and death accounting for 67 percent of the death toll and with approximately 60 percent of new infections occurring in 2010 [2]. The use of HAART has helped save many lives in low and middle income settings, and approximately 1.8 million deaths have been prevented in Sub-Saharan Africa [3]. However, many challenges still exist with current regimens as most ARV agents have short half-lives and require frequent administration, or present with undesirable adverse effects and unpredictable bioavailability. These factors result in poor adherence to medication and ultimately, treatment failure [4].

The use of novel drug delivery systems in the management of HIV/AIDS has received attention as there is the potential to overcome many of the challenges faced with the use of currently available ARV dosage forms. NVP has exhibited dose dependent side effects in addition to unpredictable bioavailability and was selected as a model ARV candidate for formulation into a SR dosage form.

The objectives of this study were:

1. To develop and validate a reversed-phase high performance liquid chromatographic (RP-HPLC) method for the quantitation of NVP as bulk API and in dosage forms.
2. To develop and validate a dissolution method for *in vitro* testing of NVP release from SR tablets.
3. To assess the suitability of powder blends for direct compression and investigate the potential for drug-excipient interactions using differential scanning calorimetry (DSC) and infrared spectroscopy (FT-IR).
4. To investigate the possibility of using HPMC alone or in combination with other polymers such as carbomers and methacrylates for the development of directly compressible SR tablets.
5. To use response surface methodology (RSM) to optimise the NVP formulation.
6. To evaluate NVP release from the tablets produced and compare the dissolution profiles to Viramune® XR, using statistical methods.
7. To study and use the release kinetics of NVP in the optimisation process.
8. To investigate factors that affect NVP release from tablets and to identify key aspects of the formulation that require further study.

TABLE OF CONTENTS

LIST OF TABLES

LIST OF FIGURES

CHAPTER ONE

ANHYDROUS NEVIRAPINE (NVP)

1.1 INTRODUCTION

It is estimated that more than 34 million people worldwide are living with acquired immunodeficiency syndrome (AIDS) caused by human immunodeficiency virus (HIV) [1]. Sub-Saharan Africa is the region with the highest prevalence and accounted for approximately 1.9 million, slightly over 60 % of the 2.7 million newly reported infections with the virus in 2010 [2]. The region also accounts for about 91 % of the children living with HIV in the world. Approximately 1.2 million adults and children died of AIDS and HIV-related causes in 2010 accounting for 67 % of the total deaths in the world that year [1, 2].

New infections and deaths from HIV/AIDS have been decreasing steadily. The decline varies from region to region, with some regions have showing a slight increase in the incidence of new infections and deaths. In Sub-Saharan Africa, a decline of approximately 16 % in new infections was recorded in 2010, representing a significant decline compared to the infection rates that were reported in 2001. There were also 20 % fewer deaths of children aged < 15 years in 2010 compared to the deaths reported in 2005 [2].

With the advent of highly active antiretroviral therapy (HAART) in 1995, approximately 2.5 million deaths have been avoided in low and middle income countries, with approximately 1.8 million deaths prevented in Sub-Saharan Africa [2].

Although HAART usually results in an improved lifestyle and wellbeing of patients, the occurrence of adverse effects leads to patient inconvenience and reduced adherence to medication regimens [3-5]. Extensive hepatic first pass metabolism and intestinal degradation of many drugs has led to reduced and difficult to predict bioavailability of anti-retroviral (ARV) agents [3]. The short half-life of most ARV agents requires frequent administration of doses to maintain adequate levels of antiviral activity. This may result in reduced adherence to treatment which may ultimately result in treatment failure [4]. Sustained drug delivery from technologies that are designed to produce predictable and reproducible drug level profiles and kinetics over an extended period of time can help minimise most of the problems associated with ARV drug therapy [3-5].

NVP is a non-nucleoside reverse transcriptase inhibitor (NNRTI) used in combination with other ARV in the treatment of HIV-1 infections and for the prevention of mother-to-child transmission of the HIV-1 virus [6-8]. NVP exhibits good oral absorption properties, however it induces its own metabolism leading to reduced and sometimes unpredictable bioavailability [8]. NVP has also been found to show solubility limited absorption [9, 10]. Formulation of a sustained release dosage form for once daily dosing may result in the delivery of constant amount of the drug to the systemic circulation, reduce dose related adverse effects, improve patient adherence to medication and reduce the cost of therapy.

1.2 PHYSICO-CHEMICAL PROPERTIES

1.2.1 Description

Anhydrous NVP occurs as a white to off-white odourless crystalline powder [7, 11]. Structurally NVP belongs to the dipyridodiazepinone class of compounds [8]. The chemical name for NVP is 11-cyclopropyl-5, 11-dihydro-4-methyl-6H-dipyrido (3, 2-b: 2', 3'-e) (1, 4) diazepin-6-one [8, 12, 13]. NVP has a molecular weight of 266.30 g/mol, a molecular formula of $C_{15}H_{14}N_4O$ and the structural formula is depicted in Figure 1.1 [8].

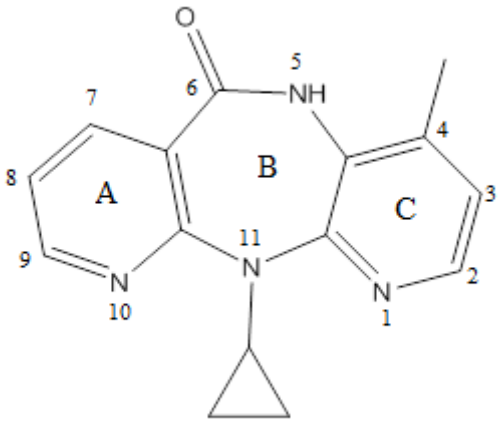

Figure 1.1. Chemical structure of NVP.

1.2.2 Solubility

NVP exhibits a very low intrinsic aqueous solubility of approximately 0.06 mg/mL [10, 14]. It is freely soluble in acetone and chloroform, sparingly soluble in methylene chloride, alcohol and methanol [9, 15]. The solubility of NVP has been shown to be pH dependent,

exhibiting high aqueous solubility in buffers of pH values less than the pKa of the compound. The solubility of NVP decreases as the pH of solution increases. For example at pH 1.5 the solubility of NVP is 1.9 mg/mL whereas at pH 4.0 the solubility is 0.1 mg/mL. The solubility remains fairly constant at higher pH values, for example the solubility is 0.1 mg/mL at pH 8.0 [16].

1.2.3 Biopharmaceutics Classification System (BCS)

NVP has low solubility and high intestinal permeability and is thus classified as a BCS class II compound [17].

1.2.4 pKa and Partition Coefficient

NVP is a weakly basic drug with a pKa of 2.8. It is lipophilic in nature and has a log octanol-water partition coefficient (Log P) of 2.5. It is unionised at physiological pH [10, 11, 17].

1.2.5 Ultraviolet (UV) Absorption Spectrum

NVP has been reported to show maximum UV (λ_{max}) absorption at 280 nm [18, 19]. Other reported λ_{max} values occur at 282 nm [20, 21] and 283 nm [22]. The λ_{max} of NVP in a mixture of methanol and water was found to be 283.4 nm. The UV absorption spectrum of NVP in methanol showing a λ_{max} of 284 nm is depicted in Figure 1.2.

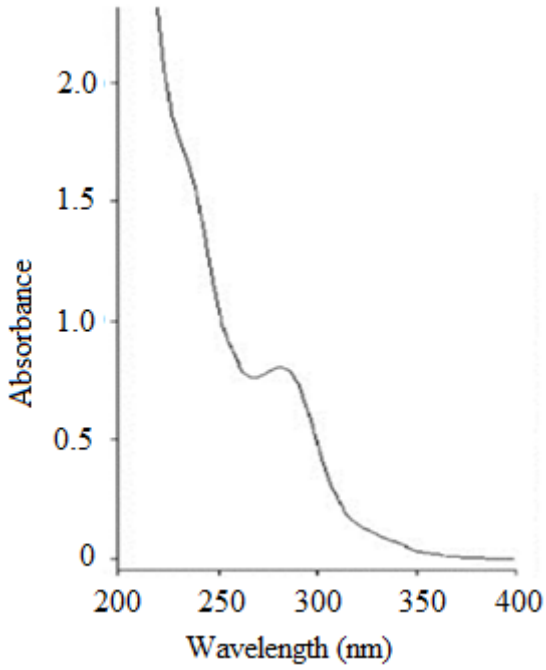

Figure 1.2. UV absorption spectrum of NVP in methanol [23].

1.2.6 Melting Range

The melting range of nevirapine is 244-250 °C [10, 11, 13].

1.2.7 Hygroscopicity

On exposure to 75% relative humidity at 30 °C, NVP did not adsorb moisture and is therefore considered non-hygroscopic [24].

1.2.8 Stability

The degradation of NVP in 1 M NaOH, 1 M HCl and in 10 % v/v H_2O_2 at 80 °C after 2 hours with the presence of unknown degradation products was reported by Filho *et al*, however NVP remained stable after neutral hydrolysis in water at 80 °C for 2 hours [25]. In another study NVP was found to be relatively stable in 1 M HCl, 1 M NaOH and 10 % v/v H_2O_2 when stored at room temperature for 24 hours [26]. Solutions of NVP have been shown to be stable for at least two days when stored at ambient temperature [27]. The stability of NVP in 0.1M HCl, 0.1M NaOH, 30 % v/v H_2O_2, refluxed at 90 °C for 8 hours and sunlight was assessed in these studies. NVP was found to degrade in HCl, NaOH and H_2O_2 with the degradation more prominent under oxidative conditions. NVP was found to be stable after refluxing in water at 90 °C and exposure to sunlight for 8 hours.

1.2.9 Stereospecificity and Polymorphism

NVP does not show isomerism but does exhibit polymorphism. NVP is known to occur as a pseudopolymorph, in the anhydrous form, hemihydrate and hemiethyl acetate forms. The hemiethyl acetate form is unstable and is converted to the hemihydrate form [28]. The anhydrous form of NVP is formulated in tablets whereas the hemihydrate form is used to manufacture suspensions [24].

1.2.10 Particle Shape

The hemihydrate form is reported to exist as prismatic crystals while the anhydrous form is found in fine grained opaque aggregates when viewed using a polarised light microscope [11].

1.3 SYNTHETIC PATHWAY

The synthetic procedure of NVP is summarised in Figure 1.3. The first step of the synthetic process involves the reaction of 2-halo-3-pyridinecarbonitrile (I) with cyclopropylamine (II) in an inert, organic solvent, at temperatures between 77 – 100 °C to yield 2-(cyclopropylamino)-3-pyridinecarbonitrile (III). The preferred organic solvents are C_1 to C_6 straight or branched chain alcohols, tetrahydrofuran, dimethylformamide, diglyme or toluene. The solvents of choice are ethanol and 1-propanol. A strong acidic or basic solution, preferably a mixture of 1-propanol and potassium hydroxide is then used to hydrolyse the 2-(cyclopropylamino)-3-pyridinecarbonitrile to produce 2-(cyclopropylamino)-3 pyridine carboxylic acid (IV). The product is then chlorinated to yield 2-(cyclopropylamino)-3-pyridinecarbonyl chloride (V). Chlorinating agents that are used include thionyl chloride, phosphorous oxychloride, phosphorous trichloride, phosphorous pentachloride, phosgene or oxalyl chloride. The 2-(cyclopropylamino)-3-pyridinecarbonyl chloride is then reacted with 2-halo-4-methyl-3-pyridinamine (VI) to form N-(2-halo-4-methyl-3-pyridinyl)-2-(cyclopropylamino)-3-pyridinecarboxamide (VII) which is cyclised by reacting with a strong base such as sodium hydride (NaH) in an inert anhydrous organic solvent at temperatures ranging between -30 °C to 130 °C to produce NVP [29].

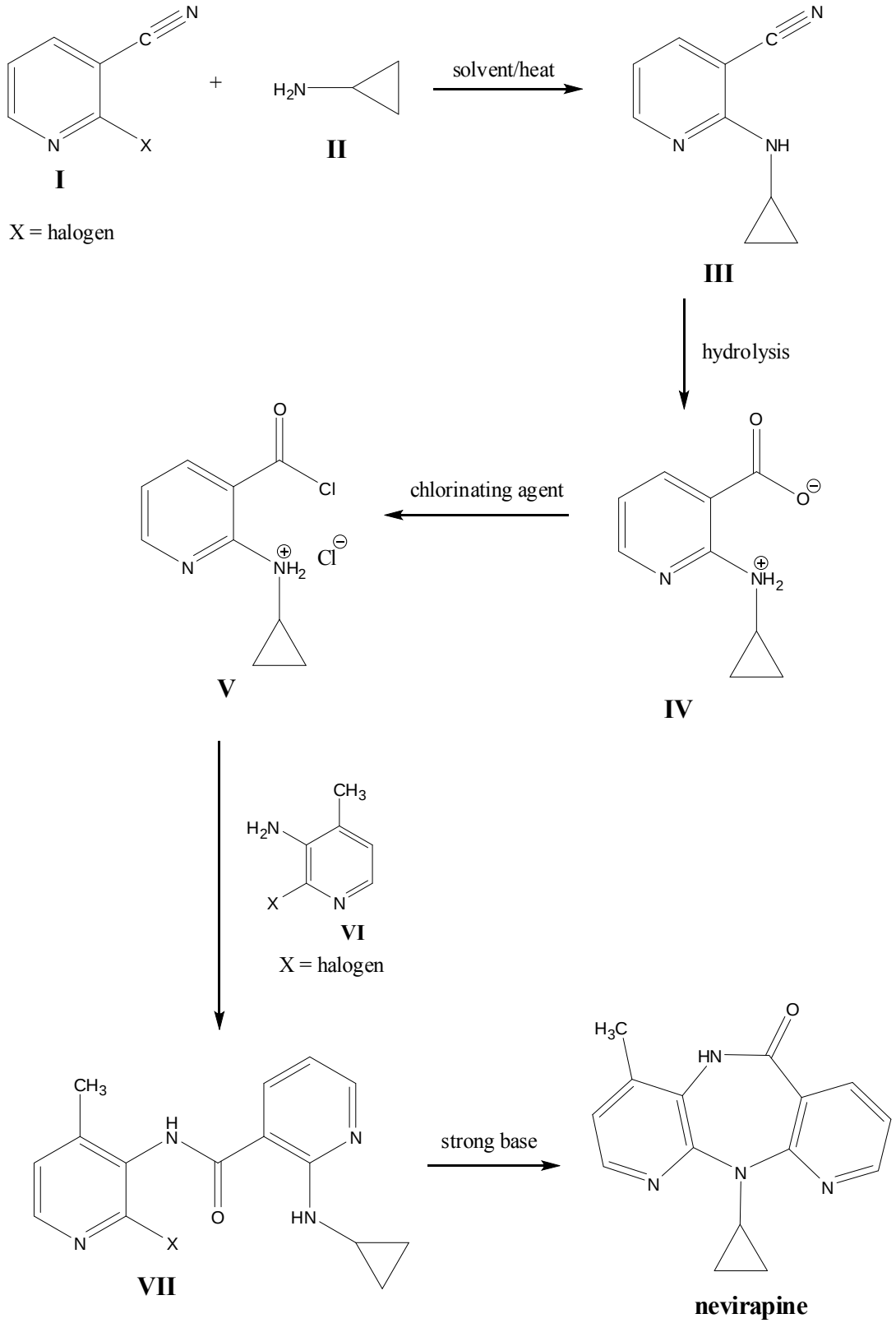

Figure 1.3. Synthesis reaction scheme for the production of NVP

1.4 STRUCTURE ACTIVITY RELATIONSHIP (SAR)

The preparation and evaluation of four series of dibenzo-, pyridobenzo- and dipyridodiazepinone analogs that included molecules that belong to classes of compounds such as pyrido (2,3-b)(1,5) benzodiazepinones, dipyrido (3,2-b:3',4'-e)(1,4) diazepinones in addition to pyrido (2,3-b)(1,4) benzodiazepinones and dibenzo (b,e)(1,4) diazepinones for treatment of HIV-1 infections and inhibition revealed a number of general SAR characteristics.

1.4.1 Dipyridodiazepinone Analogs

The dipyrido (3,2-b:3',4'-e)(1,4) diazepinones showed the same or slightly improved potency compared to the corresponding pyrido (2,3-b)(1,5) benzodiazepinones and pyrido (2,3-b((1,4) benzodiazepinones. Nevertheless, the dibenzo (b, e)(1, 4) diazepinones seemed to have lower activity compared to the corresponding mono- or dipyrido- analogs. It was observed that the presence of a pyrimidine ring was essential for adequate HIV-1 inhibitory activity to be present and consistent [30].

1.4.2 Pyridobenzodiazepinone Analogs

All pyrido (2,3-b)(1,5) benzodiazepinones compounds with a hydrogen or methyl group located at the lactam nitrogen, the presence of an ethyl group at position N-11 and methyl group or chloro atom on the A-ring, exhibited the highest degree of potency with IC_{50} values in the 36-62 nM range. The addition of either electronegative groups such as nitro, methoxy-, carbonyl, carboxy, aminocarbonyl and (N,N-diethylamino) carbonyl functional groups or electron donating groups such as methoxy, hydroxy, hydroxymethyl and aminomethyl on the 8-position of the A-ring produced analogs that exhibited lower potency than unsubstituted compounds. Substitution with electronegative groups such as trifluoromethyl, azido and chloro functionalities at the 9-position of the A-ring resulted in increased activity, however the use of electron donating groups such as amino and acetamido functionalities decreased the activity of the compounds. In order to produce a compound with improved activity in the pyrido (2,3-b)(1,5) benzodiazepinones class, it requires appropriate substitution on the A-ring. This was evident from the fact that introduction of a chlorine atom on the 8 and 9-position of the A-ring resulted in compounds with greater potency than those which had a chlorine atom located at the 3-position of the C-ring [30].

1.4.3 Dibenzodiazepinone Analogs

Compounds in the dipyrido (3,2-b:3',4'-e)(1,4) diazepinone class that were not substituted at the nitrogen of the lactam ring, the ethyl or cyclopropyl functional group at position N-11 and the methyl or chlorine at position 4 on ring A exhibited IC_{50} values in the 35-95 nM range, indicating a high degree of potency. Substitution at position 2 did not have an impact on potency and these compounds showed similar activity to the corresponding material that was not substituted at position 2. Substitution of the same functional groups at position 3 had a negative effect on potency when compared to molecules that did not have substitution at position 2. The introduction of methyl, chloro or ethyl functionalities at position 4 in combination with unsubstituted lactam nitrogen was vital for the production of compounds with improved HIV-1 inhibitory activity. However, substituting the lactam nitrogen with any functional group resulted in a sharp decrease in potency. Functional groups such as methyl, hydroxy and chlorine located at positions 7, 8 or 9-position also reduced the potency of the molecule. The location of short chain alkyl groups such as ethyl and cyclopropyl functionalities at position N-11 gave preferable potency compared to substitution with larger molecular weight groups [30].

1.5 CLINICAL PHARMACOLOGY

1.5.1 Mechanism of Action

NVP is a HIV-1 inhibitor that acts as a non-nucleoside reverse transcriptase inhibitor. NVP exerts activity by binding directly to the reverse transcriptase enzyme and prevents RNA- and DNA-dependent polymerase activities by disruption of the catalytic site of the enzyme [31]. NVP attaches to the hydrophobic pocket of the p66 subunit of the HIV-1 reverse transcriptase enzyme to produce a conformational change in the three-dimensional structure of the enzyme, that significantly decreases activity and also behaves as a non-competitive inhibitor of the virus [8]. NNRTI have a binding site which is virus strain specific and therefore acts only against the HIV-1 virus strain and not HIV-2 or other retrovirus strains [8, 32].

1.5.2 Clinical Indications

NVP is used in combination with other ARV compounds for the treatment of HIV-1 infection [6, 8]. A single dose of NVP administered at the onset of labour to a pregnant mother and to the neonatal infant following delivery is used to prevent mother to child transmission of HIV. Current thinking at the World Health Organization (WHO) suggests that a single dose of NVP is no longer effective in preventing vertical transmission of the virus and has now recommended that this practice be discontinued. Some studies also suggest such an indication has contributed to the emergence of NVP resistant strains of HIV [33, 34].

1.5.3 Contraindications

NVP should not be used in patients with clinically significant hypersensitivity to any of the components contained in the tablets or oral suspension of the product [6, 8]. NVP should not be used in patients with moderate to severe hepatic impairment [35]. Current guidelines recommend avoiding NVP in women with CD4 counts > 250 cells/mm^3 and in men with CD4 counts > 400 cells/mm^3 [36].

1.5.4 Precautions

1.5.4.1 Geriatric Patients

Elderly patients frequently suffer from decreased hepatic, renal and cardiac function. They also present with concomitant disease states and may be on therapy for other conditions. All these factors should be considered when selecting an appropriate dose of NVP for such patients [37].

1.5.4.2 Paediatric Patients

The adverse effects of NVP in children are similar to those that occur in adults (§1.5.6), with the exception that granulocytopenia is more prevalent in children. Therefore full blood count (FBC) should be performed regularly in paediatric patients who are on NVP regimen [38].

1.5.4.3 Breastfeeding Mothers

Lactating mothers should be advised that breastfeeding be stopped when being treated with NVP as there is a risk of transmission of the HIV virus and the potential occurrence of serious adverse effects of NVP in breastfeeding infants [6, 8].

1.5.4.4 Pregnancy

There have been reports of severe hepatic events with fatality in pregnant women on NVP therapy when administered as part of HAART. As a consequence NVP should only be used in pregnant individuals when the potential benefits of use, outweigh the associated risks to both the mother and the foetus [39].

1.5.4.5 Renal Impairment

Metabolites of NVP may accumulate in patients who are on dialysis but the clinical significance of such accumulation is not known. When a patient presents with a creatinine clearance (CrCL) of ≥ 20 mL/min an adjustment in the dose of NVP is not required but lower CrCL may necessitate dose adjustment [40, 41].

1.5.4.6 Hepatic Impairment

Clinical and laboratory monitoring of liver function should be performed regularly in patients treated with NVP as approximately 1% of patients treated with NVP present with clinical hepatitis, while approximately 14% of patients show elevated transaminase levels [35]. Severe and fatal hepatitis has been reported in women with CD4 counts > 250 cells/mm^3 [42]. Administration of NVP to patients with severe hepatic impairment should be avoided and liver function tests must be performed in patients who present with signs and symptoms of hepatitis or hypersensitivity reactions [43]. If a patient develops a rash during the first 18 weeks of treatment, liver function tests should be performed immediately and treatment changed if the results show any signs of liver damage [44-46].

1.5.5 Drug Interactions

The enzymes responsible for the metabolism of NVP in the liver are cytochrome P450 iso-enzymes 3A4 and B26 [47]. NVP induces CYP3A4 and CYPB26 enzyme systems and consequently lowers plasma concentrations of drugs that are also metabolised by these enzymes. Concurrent administration of such drugs with NVP may require dose adjustment [8, 48].

The plasma concentrations of ethinyl estradiol and norethindrone are lowered significantly when these molecules are administered at the same time as NVP. Consequently additional

contraceptive methods should be used when NVP is prescribed and used in women of child bearing age [49].

The concomitant administration of fluconazole with NVP should be undertaken with caution as plasma concentration levels of NVP tend to be increased in these patients. The increase in plasma levels of NVP must be monitored to avoid occurrence of adverse events [50].

The efficacy of ketoconazole is reduced when administered concurrently with NVP as plasma levels of ketoconazole are decreased. Therefore ketoconazole and NVP should not be prescribed and used concomitantly [50].

The plasma concentrations of methadone are reduced by NVP and therefore an upward adjustment of methadone dose may be necessary to avoid the occurrence of opiate withdrawal symptoms. Patients that have been maintained on methadone and are due to commence NVP therapy should be monitored for signs of withdrawal and dosages may need to be adjusted, accordingly [51].

The blood levels of NVP decrease when rifampicin, an inducer of liver metabolism, is used in the same patient. This may lead to a reduction in the efficacy of NVP and the emergence of HIV-1 resistant strains. Patients co-infected with HIV-1 and tuberculosis that require NVP should be treated with rifabutin rather than rifampicin. However the plasma concentrations of rifabutin increase with concomitant NVP therapy and therefore patient monitoring is necessary [52, 53].

The metabolism of protease inhibitors (PI) such as saquinavir, lopinavir/ritonavir, nelfinavir and indinavir is increased by NVP. There is reduction in the plasma concentration of NVP and the PI, consequently increased doses of NVP and the PI of choice may be necessary [48, 54, 55].

Anti-arrhythmics, anti-convulsants, anti-fungals, calcium channel blockers, ergot alkaloids, immunosuppressants, motility agents and opiate agonists are additional examples of drugs for which the plasma concentrations may be reduced by NVP, when used concomitantly [48]. The use of anti-thrombotics such as warfarin requires monitoring of anticoagulant levels as plasma concentrations are decreased when co-administered with NVP, an inducer of warfarin metabolism [48].

St. John's Wort (*Hypericum perforatum*) or products that contain St. John's Wort should be used with caution in HIV positive patients as the plasma concentrations of NVP are significantly reduced by this complementary medicine. The sub-therapeutic levels of NVP that result, may lead to failure to reduce the viral load and induce possible resistance to NVP and/or other NNRTI compounds [48, 56].

1.5.6 Adverse Effects

1.5.6.1 Hepatic

Patients have been reported to experience fatal hepatotoxicity including fulminant and cholestatic hepatitis, hepatic necrosis and hepatic failure [43]. Non-specific signs of illness such as fatigue, malaise, anorexia, nausea, jaundice, liver tenderness or hepatomegaly with or without abnormal transaminase levels initially, may be experienced by some patients treated with NVP [57]. Approximately 50% of patients that present with hepatic events also present with a rash and frequent monitoring may be necessary in the early stages of NVP treatment [58]. Hepatic failure coupled with elevated transaminase levels with or without hyperbilirubinemia, hepatic encephalopathy, prolonged partial thromboplastin time or eosinophilia may also occur when patients are treated with NVP. Consequently hepatic function monitoring in patients is critical and NVP therapy should be stopped in those who exhibit signs and symptoms of hepatitis [8, 46, 59].

1.5.6.2 Dermatological

Life threatening and fatal skin reactions such as Stevens-Johnson syndrome and toxic epidermal necrolysis are common in patients that are on NVP therapy [58]. Severe hypersensitivity reactions such as fever, general malaise, fatigue, muscle or joint aches, blisters, oral lesions, conjunctivitis and facial oedema, may occur and permanent discontinuation of NVP should be considered in these cases [60]. Patient should not be re-challenged with NVP following the occurrence of severe hypersensitivity reactions and withdrawal of NVP therapy [61, 62].

1.5.6.3 Metabolic

Patients that are treated with NNRTI compounds have been observed to present with redistribution and accumulation of body fat. Trunk obesity, accumulation of fat in the dorsocervical region that is commonly known as "buffalo hump", thinning of peripheral parts

of the body, loss of fat on the face, gynecomastia and a Cushing syndrome appearance have been observed in patients on chronic NVP treatment [63, 64].

1.5.6.4 Gastrointestinal

Patients that are prescribed NVP often experience gastrointestinal disturbance such as nausea, vomiting, diarrhoea and abdominal pain [65].

1.5.6.5 Haematological

The use of NVP has been associated with anaemia, eosinophilia and neutropenia, therefore FBC should be undertaken periodically when patients are prescribed and treated with NVP over a prolonged period [66, 67].

1.5.6.6 Musculoskeletal and Neurological

Patients that have used NVP have reported arthralgia and paraesthesia events [68, 69].

1.5.7 Resistance

The use of NVP as monotherapy or as an additional single agent to a failing regimen for the treatment of HIV-1 infections results in rapid development of resistance to the drug [8]. Resistance develops as a consequence of a single mutation at either codon 103 or 181 of the reverse transcriptase enzyme and leads to a decrease in the susceptibility of the virus by more than two orders of magnitude [8]. Resistance to NVP has also been associated with mutations at codons 100, 106, 108, 188, and 190 [70]. However, mutation at either the K103N or Y181C sites is sufficient to result in the development of high level resistance and failure of therapy [71]. Resistance to NVP may result in resistance to efavirenz and delavirdine and the use of these compounds should be avoided in patients that have developed resistance to NVP [72].

1.6 CLINICAL PHARMACOKINETICS

1.6.1 Dosage and Administration

1.6.1.1 Adult Patients

NVP therapy is initiated with a 200 mg per day dose for the first two weeks to minimise the occurrence of hypersensitivity skin reactions. Patients are then maintained on a 400 mg per day dose administered as either a 200 mg twice daily or a single 400 mg extended release (XR) tablet daily, usually in combination with other ARV agents [6, 73].

1.6.1.2 Paediatric Patients

Paediatric patients between 2 months and 8 years of age are usually administered 4 mg/kg daily doses following initiation of therapy for up to 14 days after which the dose is increased to 7 mg/kg twice daily, as maintenance therapy. A recommended dose of 4 mg/kg administered once daily during the first two weeks of therapy and a maintenance dose of 4 mg/kg twice daily is used for patients of 8 years and older. The maximum total daily dose for any paediatric patient is 400 mg [6, 74, 75].

The administration of NVP suspension requires the product to be thoroughly shaken, prior to administration and it has been recommended that a dosing syringe or cup is used for administration of the doses that are < 5 mL. Thorough rinsing of the dosing cup with water and administration of the rinse solution is advised to ensure that the entire, measured dose is delivered [6].

1.6.1.3 Patient Monitoring

Liver function and other relevant laboratory tests in addition to clinical monitoring should be included in patient management strategies and should be mandatory for the lead-in and the first 18 weeks of NVP therapy. The recommended frequency of monitoring has not yet been established but it is suggested that once a month monitoring may be appropriate [59, 68].

1.6.1.4 Dosage Adjustment

Treatment should be discontinued in patients who develop a severe rash. The occurrence of a rash and test results such as abnormal liver function also necessitate the termination of treatment. Dose increases should not be effected if patients experience a rash during the first

14 days of therapy and should only be undertaken after complete clinical resolution of the rash has been achieved [68, 69].

The occurrence of clinically significant hepatic events requires that NVP treatment cease immediately and that no further exposure to NVP be attempted after recovery [59, 62].

When a patient does not adhere to the dosing requirements for longer than a week, treatment should be started *ab initio* using the recommended treatment and dosing guidelines [70].

Patients that require dialysis should receive an additional 200 mg dose of NVP in order to ensure that the NVP that is eliminated during dialysis is replaced. The additional NVP that is administered may result in the accumulation of NVP metabolites and it has not yet been established whether this accumulation is clinically significant [76, 77].

1.6.1.5 Overdosage

Overdosing with NVP may occur when patients receive NVP doses in the range 800 mg to 1800 mg per day, for approximately 15 days [6]. Such patients may suffer from adverse effects such as oedema, erythema nodusum, fatigue, fever, headache, insomnia, nausea, vomiting, rash, vertigo, weight loss and pulmonary infiltration [6, 78]. Other reported adverse effects of NVP overdose include psychiatric symptoms [79]. There is no known antidote for NVP overdosage and therefore NVP must be withdrawn from the treatment regimen for the adverse events to be resolved [6].

1.6.2 Absorption and Bioavailability

The absorption of NVP following oral administration is relatively good and the bioavailability of NVP is > 90% [80]. The absorption of NVP from the GIT exhibits the highest extent from the jejunum and the lowest from the descending colon [81]. The absorption of NVP when administered at doses of > 50 mg shows characteristics of solubility rate limited absorption which includes delayed time to peak, multiple peak concentrations and a slight decrease in bioavailability [80, 82].

Peak plasma concentrations of approximately 2.0 ± 0.4 μg/mL are reached within 4 hours of administration of a single 200 mg dose and peak concentrations appear to increase in direct proportion to the administered dose for the dose range 200 mg – 400 mg/day on multiple dose

administration. A median steady state trough NVP concentration of 4.50 ± 1.90 µg/mL was achieved following dosing of 400 mg/day to steady state [80, 82].

The bioavailability of NVP tablets and suspension has been shown to be comparable and as a result these products can theoretically be interchanged when doses of up to 200 mg per day are required [74].

The effect of food on the extent of absorption of NVP following administration of 200 mg NVP to 24 adults (12 male, 12 female) was studied and revealed that the extent of NVP absorption (Area Under the Curve, AUC) was comparable to that observed when administered under fasting conditions. Therefore NVP absorption does not appear to be affected by food [80, 83].

1.6.3 Distribution

NVP is a lipophilic compound that remains unionised at physiological pH. The apparent volume of distribution at steady state (Vd_{ss}) of NVP following intravenous administration to healthy adults was found to be 1.21 ± 0.09 L/kg, implying that NVP is widely distributed in the human body [80, 82].

NVP is approximately 60% bound to plasma proteins in the plasma concentration range 1–10 µg/mL. NVP also crosses the blood brain barrier and in one study concentrations in cerebrospinal fluid were approximately 45 ± 5% of those observed in plasma, which is approximately equivalent to the concentration of NVP that is unbound in plasma [80, 82].

1.6.4 Metabolism

Biotransformation of NVP takes place in the liver via the cytochrome P450 enzyme system. NVP undergoes oxidative metabolism to form several hydroxylated metabolites. Oxidative metabolism occurs primarily by cytochrome P450 isoenzymes from the CYP3A4 and CYP2B6 families although other isoenzymes may play a secondary role [84].

NVP is known to induce the hepatic cytochrome 3A4 and 2B6 enzymes by a magnitude of approximately 20 – 25 %. Induction of CYP3A4 and CYP2B6 mediated metabolism results in an approximately two-fold increase in the elimination of NVP as treatment is scaled from a single dose to 200 – 400 mg/day between two and four weeks. Enzyme induction also leads

to a decrease in the half-life of NVP in plasma, from approximately 45 hours (single dose) to approximately 25 – 30 hours following multiple dosing with 200 – 400 mg/day [84].

1.6.5 Elimination

Cytochrome P450 enzyme systems primarily metabolise NVP through glucuronide conjugation. The glucuronidated metabolites are then excreted *via* the renal system in the urine. Several metabolites have been identified in urine and include 2-hydroxynevirapine glucuronide (18.6 %), 3-hydroxynevirapine glucuronide (25.7%), 12-hydroxynevirapine glucuronide (23.7%), 8-hydroxynevirapine glucuronide (1.3%), 3-hydroxynevirapine (1.2%), 12-hydroxynevirapine (0.6%), and 4-carboxynevirapine (2.4%). No more than 3 % of parent drug is excreted unchanged in the urine. The steady state elimination half-life of NVP can be as long as 25 – 30 hours but the half-life shows individual variability and patients of african descent tend to exhibit much longer elimination half-lives [47].

1.6.6 Pharmacokinetics in Special Populations

1.6.6.1 Renal Patients

The pharmacokinetics of NVP in patients with mild, moderate and severe renal impairment are similar to that observed in patients that exhibit normal renal function. Nevertheless, subjects requiring dialysis showed a 44% decrease in the AUC of NVP following exposure for one week, with additional evidence of the accumulation of hydroxy-metabolites of NVP in the plasma [76, 77].

1.6.6.2 Hepatic Impairment

A study undertaken in subjects with mild to moderate liver impairment did not show significant variability in the pharmacokinetic parameters for NVP. However, a patient with child-Pugh class B ascites exhibited an increased AUC which implies that patients with severe hepatic failure and ascites may accumulate NVP [85].

1.6.6.3 Gender

The apparent volume of distribution adjusted for weight was found to be slightly higher in females (1.54 L/kg) than males (1.38 L/kg). The shorter terminal half-life of NVP observed in females ensures that the difference in the clearance of NVP observed between males (19 ± 3.9 mL/kg/hr.) and females (24.6 ± 7.7 mL/kg/hr.) following administration of a single oral

dose, is not significant. The plasma concentrations observed following either single or multiple dose administration are almost similar in males and females [80, 86, 87].

1.6.6.4 Race

No significant difference in the pharmacokinetics of NVP was observed following administration to subjects of different races. Patients (27 Black, 24 Hispanic, and 189 Caucasian) did not exhibit significant differences in NVP steady state concentration ($Cmin_{ss}$ = 4.7 µg/mL (black), 3.8 µg/mL (hispanic) and 4.3 µg/mL (caucasian) following treatment with 400 mg NVP daily. However, it is important to note that the pharmacokinetics of NVP have not yet been specifically studied or analysed for ethnicity effects [80, 86, 87].

1.6.6.5 Geriatric Patients

The pharmacokinetics of NVP in patients over the age of 55 years has not been widely studied but do not appear to change with age over the range of 18 to 68 years [37].

1.6.6.6 Paediatric Patients

The apparent total body clearance of NVP in children < 8 years of age is higher than in adults. The clearance reaches the maximum at the age of 1 to 2 years and then starts to decrease with increasing age after the age of 8 [75, 88].

1.7 CONCLUSIONS

NVP is a BCS class II compound with HIV-1 antiviral activity. NVP is a NNRTI and is used in combination with other ARV compounds for the management of HIV/AIDS. NVP has also been used as single dose therapy for the prevention of mother to child transmission of HIV-1, however questions relating to the efficacy of this regimen have led to the WHO recommendation that this practice be stopped.

NVP has a melting point range of 244 - 250 °C and has been shown to exist as polymorphs, *viz*., the hemihydrate, hemiethyl acetate or anhydrous form. The hemihydrate is used in the formulation of suspensions whereas the anhydrous form is used to produce solid oral dosage forms, such as tablets.

NVP is practically insoluble in water and is sparingly soluble in methylene chloride, ethanol and methanol. NVP is freely soluble in acetone and chloroform and exhibits pH dependent solubility with the highest solubility at pH values below the pKa and lower solubility at higher pH values. NVP has a λ_{max} of between 280 – 284 nm.

NVP solutions are stable at room temperature (22 °C) for approximately two days. NVP degrades on exposure to 0.1M HCl, 0.1 NaOH and 30 % v/v H_2O_2 after refluxing for > 8 hours at 90 °C but is stable under hydrolytic conditions at a temperature of 90 °C following refluxing for 8 hours.

NVP is well absorbed from the GIT and has a bioavailability of > 90%, however the rate of absorption decreases following multiple administration revealing characteristics of solubility limited absorption. The biological half-life of NVP is approximately 45 hours and NVP induces its own metabolism following multiple dosing resulting in a significant reduction in the half-life to between 25 and 30 hours.

The most common adverse effects associated with NVP administration are skin reactions. Other side effects include hepatic events, renal failure, metabolic and GIT associated disturbances.

Resistance to NVP is common and as a result it should not be used as monotherapy for the treatment of HIV/AIDS. Resistance to NVP may also result in resistance to other non-nucleoside reverse transcriptase inhibitors.

Patient adherence to medication is essential for the successful treatment of HIV/AIDS. Most ARV treatment regimens require multiple administrations per day in order to maintain antiviral activity, often resulting in patient inconvenience. The adverse effects associated with ARV are also a challenge for patients and in many cases result in treatment failure due to non-adherence.

Novel methods of drug delivery are capable of reducing patient inconvenience and other challenges that are associated with the use of currently available technologies and may improve patient adherence to medication regimens. One example of such delivery systems are sustained release dosage forms.

NVP was selected as a model drug for inclusion in a sustained release dosage form. NVP is a weakly basic drug with a pKa of 2.8, implying that its unionised form exists at all pH values

and hence shows pH independent absorption. The lipophilic nature of NVP also means its absorption in the GIT would not be a problem. These characteristics of NVP make it a good candidate for inclusion into sustained release dosage form as bioavailability can be significantly influenced by modifying the characteristics of the dosage form. Furthermore, the costs of ARV therapy in the developing world may be reduced by use of multisource products. Consequently the development of a sustained release NVP multisource product was attempted in these studies.

CHAPTER TWO

HPLC ANALYSIS OF NEVIRAPINE

2.1 INTRODUCTION

Chromatography exists in many forms and is used as a separation technique in the pharmaceutical and chemical industry [89]. Liquid chromatographic methods are commonly used in almost every stage of pharmaceutical development from initial synthesis and isolation of an API, pharmacological testing, product development and quality control of the marketed product [90]. Typically chromatography includes gas and liquid separation techniques including paper, thin-layer, ion–exchange and size-exclusion chromatography [89].

High performance liquid chromatography (HPLC) is also known as high speed liquid chromatography (HSLC), high efficiency liquid chromatography (HELC) and high pressure liquid chromatography [89]. Ultra performance liquid chromatography (UPLC), a more recent variant of HPLC uses smaller particle size column packing and hence exhibits faster separations with enhanced peak capacity [91].

The principles and theories of HPLC are derived from gas chromatography. However, HPLC exhibits advantages over gas chromatography in terms of column efficiency and speed of analysis [89, 92, 93].

Chromatographic separations can also be broadly classified as normal-phase chromatography (NPC) and reversed-phase chromatography (RPC). In RPC the stationary phase is less polar than the mobile phase whereas the converse is true for NPC [94].

RPC is usually selected for the separation of most pharmaceutical samples as it is more convenient and reliable than other forms of liquid chromatography since the columns are efficient, stable and behave in a reproducible manner [95]. The typical solvents used for RPC separations also facilitate detection using Ultraviolet (UV) detectors [96]. The limited aqueous solubility of most organic compounds is not a practical limitation for RPC separations as only small volumes of the sample of interest are usually injected onto the HPLC system [97].

2.2 PRINCIPLES OF RP-HPLC

A separation using reversed-phase high performance liquid chromatography (RP-HPLC) is achieved using a silica-based support chemically bonded with different organic chains of compounds. The organic chains of compounds impart the necessary hydrophobicity to the bonded stationary phase [98]. To achieve a separation, the compound to be analysed must partition into an organic modifier component of the mobile phase [96, 97]. Non-polar compounds are preferentially attracted to the hydrophobic stationary phase which typically consists of carbon chains of lengths C_3, C_4, C_8 or C_{18} bonded to the silica backbone or support [97]. The mobile phase is more polar than the stationary phase and the analytes of interest partition between the polar mobile phase and non-polar stationary phase. The more hydrophobic the compound is the more likely it will be retained on the stationary phase [96, 97, 99].

In RPC, the retention time of a specific compound depends on the polarity, mobile phase composition, stationary phase, column and temperature used in a separation [96, 97]. The more polar a compound of interest the shorter the retention time of that compound for a set of separation conditions. The retention of a compound varies with the nature of the bonded phase and usually increases with an increase in chain length or hydrophobicity of the material [97]. Sample retention is also influenced by temperature and an increase in temperature of 1 °C will usually decrease retention times by 1 to 2 % for non-ionic compounds [92, 97].

2.2.1 Column Selection

The column forms a critical component of a RP-HPLC analytical separation. It is important to ensure that a stable high-performance column is available if an efficient, rugged and reproducible method is to be developed [100]. When selecting an HPLC column, consideration must be given to understanding column-to-column reproducibility which is guaranteed by several manufacturers on the basis of specific column performance criteria. Factors such as column plate number (N), selectivity for certain analytes and conditions, backpressure and retention (k) values for specified test solutions are often used for this purpose [97].

Most HPLC columns are packed with silica particles as the backbone or support, however some columns based on a porous-polymer support are also commercially available [98]. Silica based packing materials are the most commonly used HPLC stationary phases as they

exhibit favourable physical characteristics such as mechanical strength and form efficient packed beds that are stable under high operating pressures over a long period of time. Silica based columns exhibit the highest column efficiencies. The rigid high-strength particles produce columns that operate with low backpressures, and have longer column life times [97, 101].

The silica support is a chemically bonded material with an organic surface layer of different functionalities such as C_3, C_8 or C_{18} carbon chains. Silica based phases are compatible with water and organic solvents exhibiting no swelling of the silica backbone with changes in mobile phase composition and/or solvents [97, 102].

A variety of particle types can be packed into an HPLC column, however totally porous microspheres are the most commonly used materials. This is due to their desirable properties such as separation efficiency, sample loading capacity, durability, convenience and availability. The particles are available with different diameters, pore size and surface areas facilitating the development of a variety of separations by HPLC with these materials. Spherically shaped particles have an advantage over irregularly shaped particles as they are more easily and reproducibly packed so as to produce efficient columns [97, 103].

Due to the presence of fine materials that may form following fracture of random-shaped particles, columns with irregular particles often develop high operating backpressures on prolonged use [97, 104, 105].

A disadvantage of using a silica-based stationary phase is that the material is soluble in solutions of high pH. An increase in the life span of some silica based columns can be achieved by avoiding the use of mobile phases of pH > 8 in which the silica support is rapidly dissolved. The dissolving of the silica support results in subsequent collapsing of the packed bed with a corresponding decrease in column efficiency and an increase in peak asymmetry [97, 106, 107].

A further disadvantage of some silica-based stationary phases is that surface acidity may pose a challenge when separating basic compounds. However, newer supports constructed with highly purified silica minimise the problems usually associated with the analysis of basic solutes [103, 105, 108, 109].

Silica materials for HPLC analysis are fully hydroxylated in order to achieve a homogeneous silica surface [103]. Hydrated silica columns have a surface layer of –SiOH functional groups

with a maximum surface silanol concentration of 8 μmol/m^2, and free and bound silanol groups can exist on the hydrated silica surface. Free silanol groups tend to occur in low concentration and affect the binding of basic analytes that exhibit broad tailing peaks in a separation. Chromatographic analysis of basic analytes is best achieved using fully hydroxylated, silica-based packings with a high concentration of geminal and associated silanol functional groups [103]. Geminal silanol functional groups tend to be less acidic than isolated groups and are preferred for the separation of basic compounds [110]. Associated hydrogen bonded silanol functional groups in high concentration are suitable for the separation of basic compounds and are available in fully hydroxylated HPLC silica-based columns [104, 110].

The surface area of bonded phase supports influences the retention of a solute on stationary phases, with a large surface area exhibiting longer retention times [96]. Provided that organic ligands are completely accessible to a solute, the retention times tend to increase with an increase in the carbon content, where the separation is only dependent on hydrophobic interactions [89, 97]. In cases where a separation involves a mixed mechanism of retention that includes hydrophobic interactions with an organic stationary phase and normal phase interactions with exposed silanol functional groups on the silica support, the percent carbon is not a significant indicator of the retention characteristics of that column. The retention time(s) of solutes are normally longer for bonded phase columns of greater length *viz.,* $C_{18} > C_8 > C_3 > C_1$ [111, 112].

2.2.2 Methods of Detection

In most cases, HPLC method development is performed using UV detection with a variable wavelength spectrophotometric or diode-array detector (DAD) [97, 112]. Factors to consider when selecting a method of detection include the physicochemical properties and concentration of the analyte of interest and the sensitivity of the analytical system. UV detection may produce a linear response in the range 0.0001 to 2.0 absorbance units when analyte concentrations are low so as not to deviate from Beer-Lambert Law [97, 112, 113]. High sensitivity for analytes of interest, predictable specificity, non-destructive and insensitivity to temperature effects and mobile phase flow velocity changes are other characteristics to be considered when selecting a method of detection. Furthermore detectors should be reliable and convenient to use [89].

2.2.3 Mobile Phase Selection

The composition of the mobile phase may affect the selectivity and separation of analytes when using HPLC [97]. Organic solvents such as methanol, acetonitrile, ethanol and tetrahydrofuran can be used to produce mobile phase for RP-HPLC [97, 100] that usually consist of water or buffer and an organic modifier or solvent.

In RP-HPLC, the retention times of an analyte can be modified by adjusting the composition of the mobile phase and/or the solvent strength of the organic modifier used in the mobile phase [92]. Since organic solvents affect the polarity and selectivity of a mobile phase, initial consideration of use of a specific solvent should involve an understanding of the physicochemical properties of the solvent to be used in the mobile phase [90, 92, 95].

Solvents are attracted to analyte molecules in the mobile phase by a combination of dipole and hydrogen-bonding interactions [90, 95]. Therefore, solvent selectivity is, in part, dependent on the dipole moment, acidity and basicity of the solvent molecule. It is vital that the organic solvent to be used does not absorb UV radiation at the same wavelength as that of the λ_{max} of the analyte of interest as this will compromise the efficiency of the analytical method [89, 97].

Organic solvents for use in HPLC method development should possess certain physical properties such as have a low viscosity, vapour pressure, a boiling point > 40 °C, good transmittance of low-wavelength UV light and minimal toxicity. Other factors to consider when selecting an organic solvent include the need for pure, low cost materials and the effect of the organic solvent on the retention time(s) of the analytes of interest and band spacing [89, 97].

2.3 RESPONSE SURFACE METHODOLOGY (RSM)

2.3.1 Overview

The traditional and widely used approach of changing one experimental variable at a time sequentially involves performing a large number of experiments to achieve a specific end-point and does not permit an evaluation of multiple parameters, simultaneously [114]. Experimental design methodology has the advantage of enabling the simultaneous screening

of multiple factors that may affect a response in addition to establishing the magnitude of the effect and also permits identification of a possible interaction between factors [114-116].

RSM refers to a group of statistical and mathematical techniques used in the development of an adequate functional relationship between a response of interest, say Y and a number of associated control or input variables denoted X_1, X_2,….X_k. Such a relationship is generally unknown but can be approximated by use of a low-degree polynomial model as depicted by Equation 2.1.

$$Y = f'(X)\,\beta + \in \qquad \textbf{Equation 2.1}$$

where,

$X = X_1, X_2, \ldots X_k$,
f' (X) = a vector function of elements that consists of powers and cross-products of powers of $X_1, X_2, \ldots X_k$ up to a certain degree denoted by $d \geq 1$,
β = a vector of unknown constant coefficients referred to as parameters, and
$\in$ = random experimental error assumed to have a zero mean.

This approach is conditioned on the belief that the relationship depicted in Equation 2.1 provides an adequate representation of the response being monitored. The parameter f' (X) β represents the mean response, which is the expected value of Y [117].

Two important models are commonly used in RSM [117] and these are special cases of models represented by Equation 2.2 as a first degree model (d = 1),

$$Y = \beta_0 + \sum_{i=1}^{k} \beta i\, Xi + \in \qquad \textbf{Equation 2.2}$$

where,

Y = expected response,
β_i and β_0 = constant coefficients,
X_i = coded independent factor, and
$\in$ = random experimental error assumed to have zero mean.

and Equation 2.3 as a second-degree model (d =2),

$$Y = \beta_0 + \sum_{i=1}^{k} \beta i\, Xi + \sum_{i<j} \sum \beta ij\, XiXj \; + \sum_{i=1}^{k} \beta ii\, Xi^2 + \in \qquad \textbf{Equation 2.3}$$

where,

β_0, β_i, β_{ii} and β_{ij} = constant coefficients,
X_i and X_j = coded independent factors, and

$\in$ = random experimental error assumed to have zero mean.

There are three purposes for considering the model represented by Equation 2.2 and these include the establishment of an approximate relationship between Y and X_1, X_2, ..., X_k that can be used to predict response values for specific settings of the control variables under investigation, in order to determine through hypothesis testing the significance of factors for which the levels are represented by X_1, X_2, …, X_k. Furthermore, the optimum settings for X_1, X_2… X_k that result in a maximum or minimum response over a certain range of interest can also be established. In order to achieve these objectives a series of n experiments should be performed initially in which the response, Y, is measured for a range of specific settings of the control variables to be considered. The totality of these settings constitutes the response surface design [117, 118].

The appropriate selection of a design is critical for any response surface model since the quality of prediction, measured by the size of the prediction variance, is dependent on the design matrix. Furthermore, the determination of the optimum response amounts to finding an optimal value within the design matrix [118].

The first- and second-degree models are the most frequently used approximating polynomial models in classical RSM experiments. The most commonly used first order designs are 2^k factorial designs where k represents the number of control variables, the Plackett-Burman and Simplex designs. For the 2^k factorial, each control variable is measured at two levels which can be coded as +1 and -1, corresponding to the high and low levels to be used for each control variable under investigation. For the factorial design the number of experimental runs, n, is equal to 2^k provided that no design point is replicated [118, 119].

The Plackett-Burman design allows for two levels of each of the control variables (k) to be evaluated, just as for the 2^k factorial design and requires fewer experimental runs, especially if k is large, and is therefore an economical approach to consider. This design is available only when n is a multiple of 4 and can therefore be used when the number of control variables, k, is 3, 7, 11, 15, etc. [118, 119].

The Simplex design is a less frequently used approach as the actual setting for the design are, in general, difficult to achieve exactly in a real experimental situation [118, 119].

The most commonly used second-degree order designs are the 3^k factorial, Central Composite (CCD) and the Box-Behnken (BBD) designs**.** The 3^k factorial design consists of all combinations of levels of the control variables (k) which are tested at three levels each. For equally spaced levels, codes are used and correspond to -1, 0, and 1. The number of experimental runs for this design is 3^k which can be very large when a large number of input factors are to be evaluated [117-119].

The CCD approach is the most popular of all second-order designs and consists of three sections *viz*., a complete or fraction of a 2^k factorial design with factor levels coded as -1 and 1 and is termed the factorial portion, an axial portion consisting of 2k points for which two points are selected on the axis of each control variable at a distance of α from the design centre that is also selected as the point at the origin of coordinates, and n_0 centre points [117, 118].

The CCD approach is obtained by augmenting a first-order model (2^k factorial) with additional experimental runs *viz.,* 2k axial points and n_0 centre point replications. The CCD is developed in a manner that is consistent with the sequential nature of a response surface investigation. This starts with a first-order design, to fit a first-degree model, followed by the addition of design points to fit a larger second-order model [117].

The first-order design serves in a preliminary phase to obtain initial information about the response system and to assess the importance of the factors selected for a specific experiment. The additional experimental runs are used to generate information that can lead to the establishment of optimum operating conditions for the control variables using a second-degree model [117, 118].

The BBD provides for evaluation of three levels of each factor and consists of a particular subset of the factorial combinations from a 3^k factorial design. The BBD is popular in industrial research settings as it is economical and requires the use of only three levels *viz.,* -1, 0 and +1 for each factor under investigation [117-119].

RSM has been successfully used to develop and optimise several HPLC methods [114, 116, 120-125]. RSM generally involve performing experiments in the region of the best known solution, fitting the experimental data to a response model and then optimising the estimated response model to produce the best possible conditions for the responses that are to be evaluated [116, 123, 126].

2.4 ANALYSIS OF NEVIRAPINE

A number of analytical methods have been developed for the quantitation of NVP in different matrices and the conditions for these separations are summarised in Table 2.1. The methods include isocratic RP-HPLC [18-20, 127-130], gradient elution HPLC [131], ion-pair RP-HPLC [21], liquid chromatography-mass spectrophotometry (LC-MS) [12], gas chromatography-mass spectrophotometry (GC-MS) [132] and gas chromatography (GC) [133]. The majority of the methods involve the determination and quantitation of NVP in human plasma [18-20, 127, 133, 134], as bulk drug [20, 128, 130, 135] and in dosage forms [20, 130, 135-137]. Most of the methods are tedious as they involve long analysis times and may therefore not be suitable for routine laboratory use were a large number of samples need to be analysed within a short period of time. Therefore the objective of this study was to develop and optimise a simple, rapid, selective, precise and accurate RP-HPLC method for the analysis of NVP, using RSM.

Table 2.1. Analytical methods for the analysis of NVP

Sample	Technique	Mobile Phase	Column	Internal standard	Wavelength nm	Flow rate mL/min	Ref
Tablets	HPLC	Phosphate buffer (pH3.5): acetonitrile 85:15% v/v	C_8 Intersil® 250x 4.6 mm, 10 µm	-	266	1.0	[136]
Human plasma	HPLC	Ammonium acetate buffer (pH 4.0 ± 0.05): acetonitrile 85 : 15% v/v	Hypersil® BDS C_{18} 150 x 4.6 mm, 5 µm	oxcarbazepine	254	1.2	[127]
Tablets	HPLC	Acetonitrile: phosphate buffer (pH 3.0) 65:35 % v/v	XTerra® symmetry C_{18} 150 x 4.6 mm, 5 µm	-	283	0.8	[137]
Tablets/bulk drug	HPLC	Methanol: acetate buffer (pH = 3.0)	ODS C_{18} 250 x 4.6 mm, 5 µm	-	280	1.0	[135]
Human plasma	HPLC	25mM potassium phosphate buffer (pH 6.0): methanol: acetonitrile, 63:21.5:15.5% v/v/v	Supelcosil® LC-8 150 x 4.6 mm, 5 µm	-	280	1.0	[134]
Human plasma	HPLC	25mM triethylamine in water: acetonitrile 65:35% v/v	Zorbax® Extend 150 x 2.1 mm, 5 µm	carbamazepine	275	0.2	[20]
Human plasma	HPLC	15mM phosphate buffer: acetonitrile 65:35% v/v	Waters® RP- C_{18} 250 x 4.6 mm, 10 µm	carbamazepine	283	1.0	[129]
Human plasma	HPLC	Solvent A: Acetonitrile and 0.025M tetramethylammonium perchlorate in 0.2 % v/v trifluoroacetic acid 55:45 % v/v. Solvent B: methanol in place of acetonitrile in solvent A, same ratio	Waters® Symmetry C_{18} 250 x 4.6 mm, 5 µm	-	320	0.9	[131]
Human plasma	Ion-pair RP-HPLC	25mM phosphate buffer (pH 5.5): methanol: acetonitrile 7:2:1 v/v/v containing 25 mM hexane-1-sulfuric acid	C_8 150 x 4.6 mm, 5 µm	-	282	-	[21]
Human plasma	HPLC/MS/MS	Acetonitrile: water 70:30% v/v containing 10 mM of formic acid	Genesis® C_{18} 150 x 4.6 mm, 4 µm	dibenzepine	_	0.7	[138]

2.5 EXPERIMENTAL

2.5.1 HPLC Apparatus

The modular HPLC system consisted of a SpectraSERIES® P100 pump (Thermo Separation Products, San Jose, USA), a Model AS100 fixed loop autosampler (Thermal Separation Products, San Jose, USA) and a Spectra® 100 variable wavelength detector (Spectraphysics®, San Jose, USA) set at 284 nm. Chromatograms were recorded on a Model SP4290 Integrator (Spectraphysics®, San Jose, USA) and the stationary phase was a Phenomenex® C_{18} (2), 5µm, 250 x 4.6mm i.d. column.

2.5.2 Chemicals and Reagents

All chemicals used in these studies were at least of analytical reagent grade. Bulk NVP was donated by Aspen Pharmacare® (Aspen Pharmacare®, Port Elizabeth, South Africa). Acetonitrile 200 far UV Romil-SpS™ Super Purity Solvent and methanol UV cut-off of 215nm (Romil® Ltd, Waterbeach, UK) were used to prepare the mobile phase and samples of NVP and internal standard, respectively. Carbamazepine (CBZ) was used as the internal standard and was purchased from Sigma Aldrich® (Sigma Aldrich®, St Louis, USA). HPLC grade water was prepared using a Milli-Q Academic A10 water purification system (Millipore®, Bedford, USA) that consisted of an Ionex®Ion-Exchange cartridge and a quantum EX-ultrapore organex cartridge, which was fitted with a 0.22 µm Millipak® 40 sterile filters (Millipore®, Bedford, USA). NaOH (0.1M) was prepared by dissolving 0.4 g of sodium hydroxide pellets (Rochelle Ltd, Johannesburg, South Africa) in 100 mL of HPLC grade water. HCl (0.1 M) was prepared by accurately pipetting 3.14 mL of 32 % v/v HCl (Merck chemical Ltd, Wadeville, South Africa) and adding to 1 L of HPLC grade water.

2.5.3 Preparation of Stock Solutions

Standard stock solutions of NVP (1 mg/mL) were prepared by accurately weighing approximately 20 mg of NVP using a Mettler® Model AE163 top-loading analytical balance (Mettler®, Zurich, Switzerland) and quantitatively transferring into a 20 mL A-grade volumetric flask. Approximately 10 mL of methanol was added and the solution was sonicated for 10 minutes using a Branson® B12 sonicator (Branson®, Shelton, USA). The solution was then made up to volume using mobile phase. Analytical standards were prepared

by serial dilution with mobile phase to produce solutions of NVP of 1, 10, 20, 40, 120, 240 µg/mL NVP.

2.5.4 Preparation of Internal Standard

Approximately 20 mg of CBZ was accurately weighed using a Mettler® Model AE163top-loading analytical balance (Mettler®, Zurich, Switzerland) and quantitatively transferred into a 20 mL A-grade volumetric flask. Approximately 10 mL of methanol was added and the solution was sonicated for 10 minutes using a Branson® B12 sonicator (Branson®, Shelton, USA) and then was made up to volume using mobile phase to make a solution of 1 mg/mL. The solution was diluted with mobile phase to a concentration of 100 µg/mL before adding to the standard solutions of NVP. Approximately 1.0 mL of 100 µg/mL CBZ was added to 0.5 mL of NVP solution and mixed in vial prior to analysis.

2.5.5 Preparation of Mobile Phase

The mobile phase, comprised of acetonitrile and water, was prepared by accurately measuring appropriate volumes of each component using an A-grade measuring cylinder, adding to a 1000 mL beaker and mixing. The mobile phase was filtered through a 0.45 µm HVLP Millipore® membrane filter (Millipore®, Bedford, USA) and degassed under vacuum using an Eyela® Aspirator A-2S vacuum pump (Rikakikai® Co. Ltd, Tokyo, Japan). The mobile phase was prepared on a daily basis, transferred to a 1000 mL Scott® Duran bottle (Scott® Duran GmbH, Wertheim, Germany) and was not recycled during analysis.

2.5.6 Selection of Internal Standard

An internal standard is used during quantitative analysis to minimise system and procedural variability that can arise during sample preparation, as a consequence of analytical technique or due to equipment variability [95, 139, 140]. The use of an internal standard compensates for variable injection volumes and day to day instrumental changes and therefore can improve the accuracy of an analytical method [139, 140]. The internal standard selected for use should have similar characteristics as the analyte of interest so as to achieve a similar response for a specific analytical procedure [141-143]. The internal standard should be compatible with the analyte and must not be present in the original samples that are to be analysed [95].

Perusal of the literature reveals that dipenzepine [137], CBZ [129, 136] and oxcarbazepine [11] have been used as internal standards for HPLC methods that have been developed for the analysis of NVP. Diazepam, chlordiazepoxide, nitrazepam, imipramine and CBZ were considered as possible choices for use as an internal standard as they exhibit structural similarities to NVP. The response produced for CBZ revealed a relatively good peak shape and a peak that was well resolved from NVP with a retention time of 9.25 min before optimisation. Therefore CBZ was selected as the internal standard for use in these studies.

2.5.7 System Suitability Testing

2.5.7.1 Theoretical Number of Plates (N)

The column number of theoretical plates is a characteristic that provides an indication of the suitability of a column to produce sharp, narrow peaks with adequate resolution between the peaks with an associated low selectivity value [97]. The theoretical number of plates of the analytical column can be calculated using Equation 2.4 [144].

$$N = 16 \left(\frac{RT}{W}\right)^{1/2} \qquad \textbf{Equation 2.4}$$

where,

N = number of theoretical plates,
RT = retention time of the test peak, and
W = peak width at the baseline.

2.5.7.2 Peak Asymmetry Factor (Peak Tailing Factor)

The peak shape was determined by calculating the peak asymmetry factor, A_s, using Equation 2.5.

$$A_s = \frac{B}{A} \qquad \textbf{Equation 2.5}$$

where,

B = width of the peak to the tailing edge at 10% of the peak height, and
A = width of the peak to the leading edge of the peak at 10% of the peak height.

Poor peak asymmetry can result in the determination of an inaccurate plate number, resolution measurement, imprecise quantitation, poor resolution, undetected minor bands in the peak tail and/or poor retention time reproducibility. As a result peak shape is an important consideration during HPLC method development. Peak asymmetry factor values of between 0.95 and 1.1 are associated with good column performance and column manufacturers specify A_s values of between 0.95 to 1.3, for new columns. However, values < 1.5 for analytes of interest are generally considered acceptable. Exactly symmetrical peaks have an A_s value of 1.0.

The peak tailing factor (PTF) is another parameter that can be used to determine the shape of a peak and can be calculated using Equation 2.6 [97, 144].

$$PTF = \frac{A+B}{2A} \qquad \textbf{Equation 2.6}$$

where,

A = width of the peak to the leading edge of the peak at 10% of the peak height, and
B = width of the peak to the tailing edge at 10% of the peak height.

2.5.7.3 Resolution Factor

The resolution factor (R_s) indicates the extent and quality of a separation between the peaks of interest in a sample. The resolution can be a function of the column and operating conditions, instrumental effects or variable separation conditions. It is desirable that R_s values be > 2.0 which indicate that an adequate separation has been achieved and values < 1.5 are indicative of a poor separation [97]. The R_s can be calculated using Equation 2.7.

$$Rs = \frac{RT2 - RT1}{0.5(TW1 - TW2)} \qquad \textbf{Equation 2.7}$$

where,

RT_1 = retention time for the first peak,
RT_2 = retention time of the second peak,
T_{W1} = width of the first peak at the baseline, and
T_{W2} = is width of the second peak at the baseline.

2.5.7.4 Capacity Factor

The capacity factor (*K'*) is an indicator of the length of time that a compound is retained on a column relative to the peaks observed for the void volume. The *K'* provides an indication of the rate at which an analyte migrates through a column [97]. Factors that may influence *K'* include the mobile phase composition, age of the column and temperature of the operating system [97, 112]. The *K'* can be calculated using Equation 2.8.

$$K' = \frac{V1 - V0}{V0} \qquad \textbf{Equation 2.8}$$

where,

V_0 = Void volume of the column, and
V_1 = Retention volume of the analyte (retention time x flow rate).

The void volume is calculated using the retention time of a molecule, such as uracil, that is not retained on a column and a capacity factor ≥ 2.0 is desirable and chromatographic conditions resulting in *K'* values < 2.0 are considered unacceptable to produce an effective separation [97, 112].

2.5.8 Experimental Design

A CCD approach was selected for the optimisation of process variables of the method that was developed for the purposes of analysing NVP. Based on preliminary studies, three independent factors that were considered as important were the organic solvent composition of the mobile phase, flow rate and column temperature. The retention times of NVP, CBZ and the resolution factor were the responses or dependent variables that were monitored. The levels of each factor, both coded and actual that were used in the CCD are listed in Table 2.2. The constraints were selected based on preliminary experiments and desire to achieve best possible chromatographic conditions to yield well separated peaks within 10 minutes. The experiments that were performed are listed in Table 2.3. The experiments were performed in a randomised manner and in replicates (n=3) to minimise any potential bias.

Table 2.2. Experimental factors and levels used in CCD

Factor	**Level**				
Independent/Input Factor	[-1.68]	[-1]	[0]	[+1]	[+1.68]
Organic solvent (%) = X_1	33.2	40	50	60	66.8
Column temperature (°C) = X_2	21.6	25	30	35	38.4
Flow rate (mL/min) = X_3	0.5	0.7	1.0	1.3	1.5
Dependent/Output Factor	**Constraints**				
NVP retention time (min) = Y_1	$Y_1 = 4.0$				
CBZ retention time (min) = Y_2	$Y_2 = 7.0$				
Resolution factor = Y_3	$Y_3 = 4.0$				

Table 2.3. CCD Experiments performed, coded and actual factors

			Coded values			Actual values		
Experimental run	**Standard run number**	**Type**	**Organic solvent %**	**Column temperature °C**	**Flow rate mL/min**	**Organic solvent %**	**Column temperature °C**	**Flow rate mL/min**
1	0	Center	0.00	0.00	0.00	50	30	1.0
2	4	Fact	1.00	1.00	-1.00	60	35	0.7
3	5	Fact	-1.00	-1.00	1.00	40	25	1.3
4	0	Center	0.00	0.00	0.00	50	30	1.0
5	1	Fact	-1.00	-1.00	-1.00	40	25	0.7
6	11	Axial	0.00	-1.68	0.00	50	21.6	1.0
7	13	Axial	0.00	0.00	-1.68	50	30	0.5
8	2	Fact	1.00	-1.00	-1.00	60	25	0.7
9	0	Center	0.00	0.00	0.00	50	30	1.0
10	10	Axial	1.68	0.00	0.00	66.8	30	1.0
11	12	Axial	0.00	1.68	0.00	50	38.4	1.0
12	6	Fact	1.00	-1.00	1.00	60	25	1.3
13	0	Center	0.00	0.00	0.00	50	30	1.0
14	9	Axial	-1.68	0.00	0.00	33.2	30	1.0
15	7	Fact	-1.00	1.00	1.00	40	35	1.3
16	8	Fact	1.00	1.00	1.00	60	35	1.3
17	0	Center	0.00	0.00	0.00	50	30	1.0
18	3	Fact	-1.00	1.00	-1.00	40	35	0.7
19	0	Center	0.00	0.00	0.00	50	30	1.0
20	14	Axial	0.00	0.00	1.68	50	30	1.5

Design Expert® Version 7.0.1 (Stat-Ease Inc., Minneapolis, USA) statistical software was used to analyse the data and to predict values of input variables that would produce responses that were desired and produce a usable separation. Fisher's statistical test for Analysis of Variance (ANOVA) for the response surface quadratic model was used to determine the significance of each factor. The effectiveness of the model was evaluated by computing the F-ratio, Coefficient of Variation (C.V), adequate precision, adjusted R^2, predicted R^2 and the predicted residual error sum of squares (PRESS).

2.5.9 RP-HPLC Method Validation

2.5.9.1 Introduction

Analytical method validation can be defined as the process by which, through laboratory studies, the performance characteristics of a method are verified and meet the requirements for the intended analytical application of that method [97, 145]. Validation is an essential procedure as the acceptability of a method, using prescribed conditions, is tested. Validation is also used to determine the limits of allowed variability for the conditions needed to perform and use an analytical method [97, 146]. A well-conceived validation plan for testing a method and the associated acceptance criteria should be in place prior to commencing the validation process. A number of guidelines and standard procedures for method validation have been published by the International Conference on Harmonization (ICH) [147] and the United States Food and Drug Administration (FDA) [148].

A new or amended analytical method must undergo a validation process to ensure that it will produce reliable and reproducible results when used by different operators using the same equipment in the same or different laboratory [149]. Validation is also an important component of the quality control system in the pharmaceutical industry and forms an integral part of the assurance of product quality [150-152].

The parameters assessed during method validation include linearity, range, accuracy, precision, selectivity, reproducibility and the limits of quantitation (LOQ) and detection (LOD). These parameters are usually prioritised after which stability and ruggedness studies are undertaken at a later stage [146, 150-152].

2.5.9.2 Linearity and Range

The linearity of an analytical method is defined as the ability of a method to generate results that are, directly or after mathematical transformation, proportional to the concentrations of sample that are tested within a specified range. The range is the interval between the upper and lower concentration levels of the analyte that have been determined with acceptable precision, accuracy and linearity [97, 150, 152].

Linearity was determined using least squares linear regression analysis and establishing the equation for the line. The R^2 value is a measure of linearity and the closer the value is to unity, the more linear the line and therefore the response of the analytical method [97, 148, 150].

2.5.9.3 Precision

The precision of an analytical method is a measure of the degree of agreement among individual test results when the method is used to analyse multiple units of a homogeneous sample [97, 150]. The precision of a method is a measure of the reproducibility of analytical method and associated processes including sampling, sample preparation and analysis under normal operating circumstances [153].

The ICH guidelines recommend that precision studies should be performed in three different ways *viz*., repeatability (intra-assay precision), intermediate precision (inter-day precision) and reproducibility (different laboratories or analyst) [147].

FDA recommends that precision at selected concentration levels should not exceed a % relative standard deviation (RSD) of 15% for analysis of biological matrices [148]. However, the acceptance limit for % RSD in these studies was set at ≤ 5% at all concentration levels as dosage form analysis is not usually associated with the variability that is usually observed when analysing samples from biological matrices.

2.5.9.3.1 Repeatability

Repeatability of a method is an indication of the performance of an analytical method when used in analysis of samples within a laboratory over a short period of time by a single analyst using the same equipment [97, 146, 148].

Repeatability was evaluated by determining the % RSD of the peak height ratios of the standard solutions used to construct the calibration curve (n = 5) on a single day.

2.5.9.3.2 Intermediate Precision

Intermediate precision refers to the precision of a method when used to analyse samples within a laboratory on different days by different analysts and/or equipment [97, 146, 148].

The intermediate precision of this method was established by determining the % RSD of the peak height ratios of standard solutions (n = 5) used to construct a calibration curve, on three consecutive days.

2.5.9.3.3 Reproducibility

Reproducibility is the precision of the analytical method when it is used to analyse samples in different laboratories or with different equipment and is an essential part of inter-laboratory crossover studies [149, 153]. If intermediate precision is evaluated, the reproducibility of a method is normally not required [149]. Therefore, reproducibility studies where not performed for this method as intermediate precision was determined and the analytical method was to be used by a single analyst in the same laboratory, using the same equipment for the duration of these studies.

2.5.9.4 Accuracy

The accuracy of a method is a measure of the closeness of the test results generated using a method, to the accepted true value for a sample and indicates the deviation between the mean value obtained and the true value [97, 146]. Accuracy is determined by analysing samples to which a known amount of analyte has been added. Accuracy is used in combination with precision to determine the magnitude of error associated with an analytical procedure and is a vital and important part of analytical method validation [146, 148].

The ICH guidelines recommend that a minimum of nine determinations should be performed at a minimum of three concentrations covering a specific range of the analytical procedure to establish the accuracy of a method [146, 147]. Three samples representing low (5 µg/mL), medium (100 µg/mL) and high (200 µg/mL) concentrations of the calibration range were prepared as previously described and analysed in replicates of five (n = 5).

The results for accuracy were reported as % recovery, % RSD and % Bias. Bias is the difference between the calculated mean value and the true value for a sample and is used to assess the influence of an analyst on the performance of an analytical method. Bias is designed to measure the effectiveness of the sample preparation procedure undertaken prior to analysis [154]. The % recovery and % bias were calculated using equations 2.9 and 2.10 respectively.

$$\%\ Recovery = \frac{actual\ concentration}{theoretical\ concentration}\ X\ 100 \qquad \textbf{Equation 2.9}$$

$$\%\ Bias = \frac{True\ value - measured\ value}{True\ value}\ X\ 100 \qquad \textbf{Equation 2.10}$$

2.5.9.5 Limits of Quantitation (LOQ) and Detection (LOD)

The LOQ or the Lower Limit of Quantitation (LLOQ) is the lowest concentration of an analyte that can be accurately quantified with the necessary precision and accuracy [154]. The LOQ can also be defined as the level at which precision of the method is higher than a specified value e.g., RSD < 3% [97].

The LOD is the lowest level of an analyte that produces a measurable response but that cannot be quantified as an exact value with the necessary precision [154, 155].

Four techniques may be used to determine the LOQ and LOD of an analytical method [155], and include the lowest concentration at which the % RSD ≤ 5% or other specified value, plotting the standard deviation versus concentration for a sample of a specific concentration, establishing a confidence interval for the best-fit line or by use of signal to noise ratio methods.

The LOQ and LOD values established during method validation are affected by separation conditions such as the column, reagents and instrumentation. Changes in an instrument, particularly the solvent delivery module, detectors or the use of contaminated reagents may result in large changes in the signal to noise ratio [97].

The LOQ and LOD for this method were determined by using a precision of ≤ 5% and by convention, the LOD value was then taken as 30% of the LOQ value [155]. Five potential concentration values were selected and tested for consideration as the LOQ.

2.5.9.6 Specificity

The specificity of a method is described as the ability of the analytical method to produce a response to only the analyte of interest and no other compounds that may be present in the sample matrix [156, 157].

The specificity of the method was established by comparing chromatograms of standard solutions containing the analyte only, with chromatograms generated from samples following preparation of commercially available Aspen® NVP tablets for analysis.

2.5.9.7 Assay

The applicability of the method for the analysis of NVP in dosage forms was established by testing commercially available Aspen® nevirapine 200 mg and Viramune® XR 100 mg tablets using the method that was developed. Twenty tablets were weighed and ground and an amount equivalent to 100 mg NVP was transferred into a 100 mL A-grade volumetric flask. Approximately 40 mL methanol was added and the mixture was sonicated for 10 minutes before making up to volume with mobile phase. The solution was then filtered with 0.45 µm HVLP Millipore® filter membrane and diluted with mobile phase to 100 µg/mL prior to analysis.

2.5.10 Stability Studies

2.5.10.1 Introduction

The ICH guidelines require analytical methods to be stability indicating and that the method must allow discrimination between the analyte of interest and any degradation products that may be produced during forced degradation studies [158].

Forced degradation studies are performed in light, acidic, basic, oxidative and elevated temperature conditions [158, 159]. There is also a requirement for degradation products to be analysed qualitatively and quantitatively, however only qualitative analyses were performed in these studies.

2.5.10.2 Oxidative, Acidic and Alkali Degradation Studies

Samples of NVP, weighing approximately 100 mg each, were transferred into three 100 mL A-grade volumetric flasks. Methanol (40 mL) was added to each flask and the solutions were sonicated for 10 minutes. The resultant solutions were made up to volume with 30% v/v H_2O_2 (Allied Drug Company Ltd, Durban, KwaZulu-Natal, South Africa), 0.1 M HCl and 0.1 M NaOH for the oxidative, acidic and alkali degradation studies, respectively. The samples were refluxed for 8 hours at 90 °C. Sample aliquots of 1.2 mL were collected at 2, 4, 6 and 8 hours and diluted to a theoretical concentration of 60 µg/mL with mobile phase in 20 mL A-grade volumetric flasks. Sample aliquots of 0.5 mL were then collected and 1 mL of internal standard solution was added and the solutions were vortexed prior to analysis by HPLC.

2.5.10.3 Photo Degradation Studies

Approximately 100 mg NVP was accurately weighed and transferred into a 100 mL A-grade volumetric flask. Methanol (40 mL) was added and the solution was sonicated for 10 minutes and then made up to volume with mobile phase. The sample was exposed to light of 500 w/m^2 at a temperature of 27 °C using a model CPS+ SUNTEST® Weathering unit (ATLAS Material Testing Technology B.V, Linsengericht, Germany) for 8 hours. Sample aliquots of 1.2 mL were collected at 2, 4, 6 and 8 hours and diluted to a concentration of 60 µg/mL with mobile phase in a 20 mL volumetric flask. Sample aliquots of 0.5 mL were then collected and 1 mL of internal standard solution added and the solutions vortexed prior to analysis by HPLC.

2.5.10.4 Neutral Hydrolytic Studies

Approximately 100 mg NVP was accurately weighed and transferred into a 100 mL A-grade volumetric flask. Methanol (40 mL) was added and the solution sonicated for 10 minutes and then made up to volume with water. The sample was then refluxed at 90 °C after which sample aliquots of 1.2 mL were collected at 2, 4, 6 and 8 hours and diluted to a concentration of 60 µg/mL with mobile phase in a 20 mL volumetric flask. Sample aliquots of 0.5 mL were then collected and 1 mL of internal standard solution added and the solutions vortexed prior to analysis by HPLC.

2.6 RESULTS AND DISCUSSION

2.6.1 Chromatographic System Suitability Tests

A summary of results of chromatographic system suitability tests are listed in Table 2.4. The results indicate that the results of all tests were within the limits that had been set and the analytical system and method were declared suitable for the analysis of NVP.

Table 2.4. System suitability results (n = 3)

Factor	Value	%RSD
Number of plates (N)	19 328	0.76439
Resolution factor (R_s)	3.82	0.88231
Asymmetry factor (A_s)	N/A (no tailing evident)	-
Capacity factor (K')	4.20	0.92175

2.6.2 Central Composite Design

Twenty experiments were performed using a CCD and a summary of experiments and respective responses are summarised in Table 2.5. All experiments were performed in a randomised fashion resulting in simplified data sets being generated in order to minimise the effects of uncontrolled factors that may introduce bias to the observed responses.

Table 2.5. CCD experiments and measured responses

Std. Exp. ID	Run	Organic solvent	Column temp.	Flow rate	RT NVP	RT CBZ	R_s
		%	°C	mL/min	Min	Min	
0	1	50	30	1.0	3.49	4.93	3.60
4	2	60	35	0.7	4.43	5.54	1.85
5	3	40	25	1.3	3.30	5.86	5.11
0	4	50	30	1.0	3.49	4.93	3.60
1	5	40	25	0.7	5.99	10.61	4.62
11	6	50	21.6	1.0	3.48	4.88	2.79
13	7	50	30	0.5	6.78	9.57	2.78
2	8	60	25	0.7	4.41	5.46	1.75
0	9	50	30	1.0	3.49	4.93	3.60
10	10	66.8	30	1.0	2.99	3.49	1.26
12	11	50	38.4	1.0	3.49	4.92	2.39
6	12	60	25	1.3	2.42	3.02	1.49
0	13	50	30	1.0	3.49	4.93	3.60
9	14	33.2	30	1.0	5.44	12.37	6.93
7	15	40	35	1.3	3.19	5.45	4.50
8	16	60	35	1.3	2.44	3.02	1.46
0	17	50	30	1.0	3.49	4.93	3.60
3	18	40	35	0.7	5.74	9.76	4.02
0	19	50	30	1.0	3.49	4.93	3.60
14	20	50	30	1.5	2.39	3.34	2.43

The responses listed in Table 2.5 were evaluated using Design Expert® software and the data were fitted to a number of quadratic models. The adequacy of each quadratic model in describing the relationship between the independent variables and responses were determined and ANOVA used to identify the significant parameters. The evaluation of model adequacy and ANOVA for the retention time of NVP and resolution factor will be discussed in detail. ANOVA for the retention time of CBZ is not discussed as CBZ was only used as an internal standard in this method. The relationships that had been established were then used to derive and predict a set of independent variables that would yield the desired responses for this analytical system.

2.6.1.1 Evaluation of Model Adequacy for Retention Time of NVP

The values of the factors that were assessed to determine the adequacy of the model are summarised in Table 2.6. The most important parameters in the evaluation of model adequacy are the model F-value, coefficient of variation, adequate precision, PRESS and R^2 values. The importance of these parameters in Table 2.6 and their respective values are discussed in detail.

Table 2.6. Summary of model adequacy parameters and associated values

Parameter	Value	Parameter	Value
Std. Deviation	0.15	R-Squared	0.9917
Mean	3.87	Adjusted R-Squared	0.9842
% Coefficient of variation	3.99	Predicted R-Squared	0.9369
PRESS	1.81	Adequate precision	38.864
F-Value	132.67		

2.6.1.1.1 Model F-Value

The model F-value is used to ascertain the utility of a model that the data has been fitted to and to determine whether a model best fits the data set. The F-value produces a ratio of explained and unexplained variability and the larger the value for F, the more useful the model [117, 160]. A model F-value of 132.67 was obtained and represents a 0.01% chance that a model F-value this large could occur due to noise. This implies that the model would be able to describe the fitted data set accurately and there is only 0.01% chance of the model being inaccurate.

2.6.1.1.2 Coefficient of Variation

The coefficient of variation is the ratio of the standard deviation and mean and is indicative of the normalised measure of dispersion of a probability distribution [161, 162]. The % C.V is a measure of the reproducibility of a model and a value of < 10% is desirable [163]. The value of 3.99 was within this limit and implies that the model would be able to produce reproducible results over time, which is important in any laboratory analytical procedure.

2.6.1.1.3 Adequate Precision

Adequate precision compares the range of predicted values at the design points of the CCD to the average prediction error and a ratio of > 4 indicates that there is adequate model discrimination [119, 160]. The value of 38.864 was well above the limit implying that the model can be used to predict possible experimental outcomes with acceptable accuracy.

2.6.1.1.4 R^2, Predicted R^2 and Adjusted R^2 Values

It is important to determine whether a model is able to describe the experimental data under consideration adequately [119, 160]. The process of evaluation includes the determination of different coefficients of correlation. The R^2 coefficients have values between 0 and 1 and the closer the value to 1, the more reliable the model. All values that were obtained were > 0.9 signifying that the model is reliable and when used to predict experimental outcomes, the actual values will be reasonably close to the predicted values.

2.6.1.1.5 Residual Analysis

The adequacy of a model is also investigated by examination of residuals. Residuals are the difference between the respective observed and predicted responses [119]. Residuals are examined using normal probability plots of residuals and the plot of residuals versus predicted responses. If a model is adequate, the points of the normal probability plot of residuals should fall on a straight line. On the other hand, the location of points on the plots of residuals versus the predicted responses should be structureless, i.e. should not be seen to follow a specific pattern [117, 119, 160]. The data depicted in Figures 2.1 and 2.2 clearly indicate that these criteria have been met and the model was therefore deemed adequate.

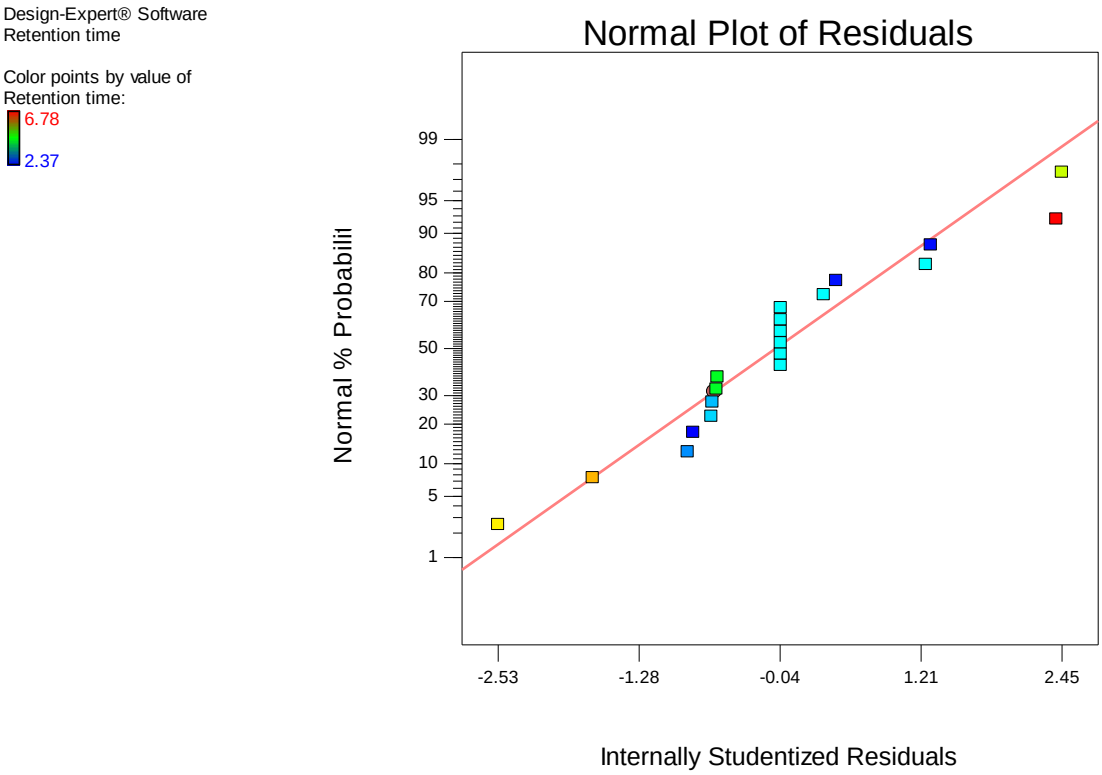

Figure 2.1. Normal probability plots of residuals for the retention time of NVP.

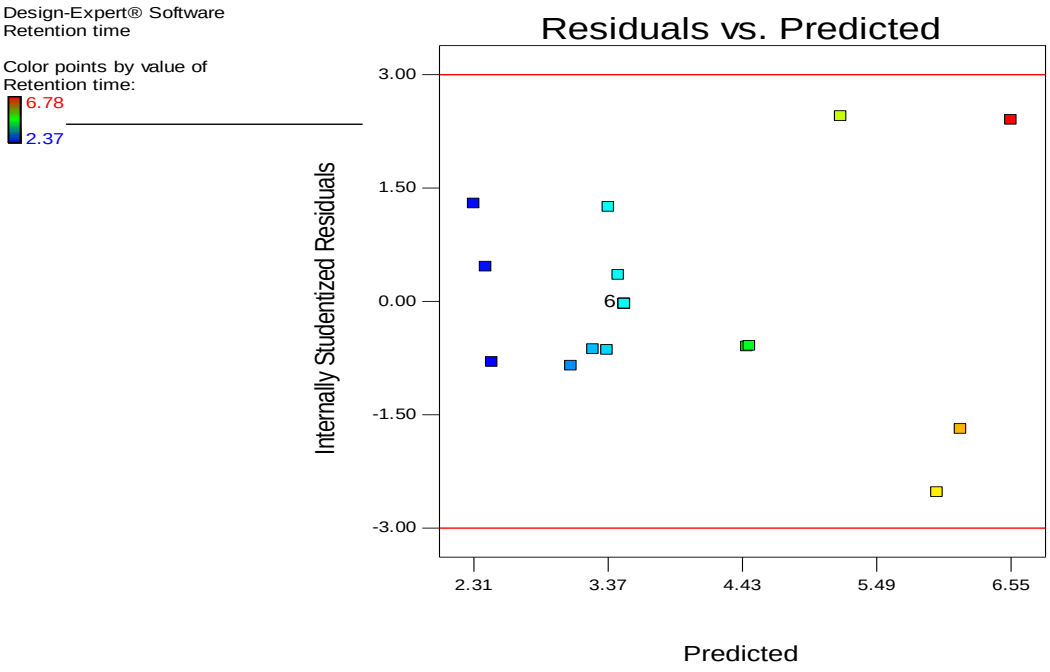

Figure 2.2. Plot of residuals versus predicted responses for the retention time of NVP.

2.6.1.1.6 PRESS

The PRESS value is the sum of squares of residuals and is a measure of the discrepancy between experimental data and those estimated by the model. A small PRESS value indicates a good fit of the data under investigation to the model selected [160]. The value of 1.81 suggests that the data was well fitted to the model, indicating that the model selected was accurate and can be used to describe the data set adequately.

2.6.1.1.7 Box-Cox Plot for Power Transformations

Most statistical tests and intervals are based on the assumption of normality of distribution of data as this leads to tests that are simple, mathematically tractable and powerful compared to tests that do not make any assumption of normality [117, 160]. However, many data sets are neither in fact, nor approximately normal and transformation of results may be necessary to yield data that follow a normal distribution, albeit approximately in some cases. Box-Cox plots of normality are used when transformation is required to increase the applicability and usefulness of an applied statistical test [164]. In this case, inspection of the Box-Cox plot suggests that transformation of the power $\lambda = -1.76$ should be made to the data set and this is depicted in Figure 2.3.

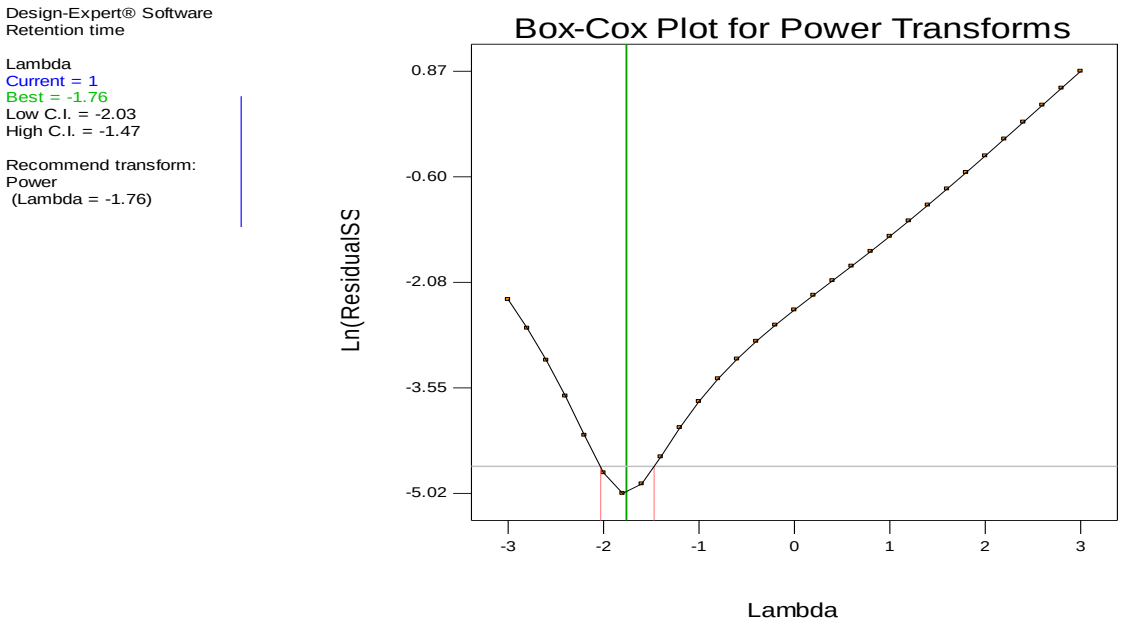

Figure 2.3. Box-Cox plot for power transformation of retention time data for NVP.

The resultant response range was between 2.39 and 6.78 and the ratio of maximum to minimum response was 2.8368. A ratio > 10 indicates that transformation is required. However ratios of < 3 indicate power transformations have little effect on the experimental responses, therefore transformation was not performed for these data.

2.6.1.2 ANOVA: Retention Time of NVP

2.6.1.2.1 Significant Factors Affecting the Retention Time of NVP

The results of ANOVA following CCD and the significant factors affecting the retention time of NVP are summarised in Table 2.7. Values of "P > F" that are < 0.0500 indicate that the model terms investigated are significant.

Table 2.7. ANOVA for response surface quadratic model analysis of variance table [partial sum of squares-type III] for the retention time of NVP

Source	Sum of squares	Df	Mean square	F-value	P-value Prob > F
Model	28.46	9	3.16	132.67	< 0.0001
X_1	5.48	1	5.48	229.91	< 0.0001
X_2	0.007.182	1	0.007.182	0.30	0.5951
X_3	20.29	1	20.29	851.42	< 0.0001
X_1X_2	0.021	1	0.021	0.88	0.3699
X_1X_3	0.20	1	0.20	8.46	0.0156
X_2X_3	0.002.813	1	0.002813	0.12	0.7383
X_1^2	0.75	1	0.75	31.28	0.0002
X_2^2	0.014	1	0.014	0.57	0.4683
X_3^2	1.81	1	1.81	76.08	< 0.0001
Residuals	0.24	10	0.024		
Lack of fit	0.24	5	0.048		
Pure error	0.000	5	0.000		
Cor total	28.69	19			

Dark red = significant model terms.

The relationship between independent variables and the retention time of NVP as a function of interaction amongst the parameters are described by Equation 2.11.

$$Y_1 = 3.49 - 0.63X_1 - 0.23X_2 - 1.22X_3 + 0.051X_1X_2 - 0.16X_1X_3 + 0.019X_2X_3 - 0.23X_1^2 - 0.031X_2^2 - 0.35X_3^2 \quad \textbf{Equation 2.11}$$

The data generated reveal that linear contributions of X_1, X_3 and X_1X_3, as well as quadratic interactions of X_1^2 and X_3^2 model terms had a significant and antagonistic effect on the retention time of NVP, as indicated by the negative sign of the model terms in the equation.

The amount of organic solvent, X_1, and flow rate, X_3, have a significant effect on the retention time of NVP. Increasing the amount of organic solvent resulted in a decrease in the retention time of NVP which can be attributed to a decrease in hydrophobic interactions between NVP and the stationary phase of the column [97, 165]. Increasing the flow rate also reduced the retention time and can be attributed to faster elution of NVP from the column at the higher mobile phase flow rate.

The effect of column temperature on the retention time of NVP was not significant but the negative sign associated with this parameter *viz.,* $-0.23X_2$ as shown in Equation 2.11 indicates that an increase in temperature results in a decrease in the retention time that may be attributed to a decrease in the viscosity of the mobile phase [97, 166].

2.6.1.2.2 Response Surface Model Plots for Retention Time

The relationship between the significant factors and the retention time of NVP can be visualised using contour plots as depicted in Figures 2.4 - 2.6. An increase in concentration of organic solvent, whilst keeping the column temperature constant, resulted in a significant decrease in retention time as shown in Figure 2.4. The retention time of NVP decreased almost linearly with an increase in the concentration of the organic solvent when the column temperature was kept constant. The insignificance of the effect of column temperature on the retention time of NVP when keeping the concentration of the organic solvent constant was typified by almost straight lines on the contour plots as shown in Figure 2.4. Increasing both the concentration of the organic solvent and the column temperature resulted in a decrease in the retention time.

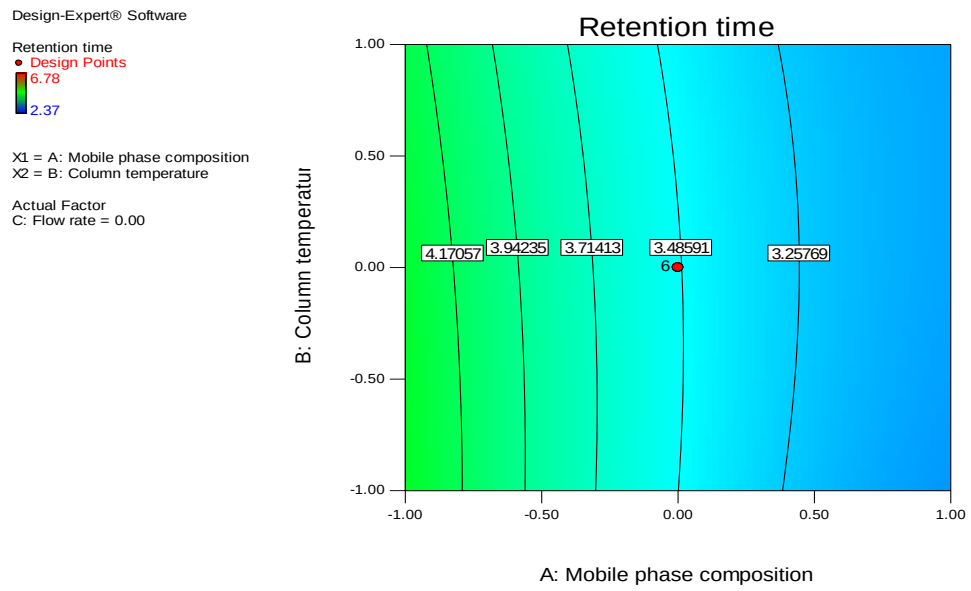

Figure 2.4. Contour plot showing the effect of changes in column temperature and organic solvent concentration on the retention time of NVP.

Organic solvent concentration and flow rate have an inverse relationship with retention time as depicted in Figure 2.5, as increasing the organic solvent concentration while keeping the flow rate constant resulted in a decrease in the retention time and increasing the flow rate while keeping the organic solvent concentration constant also resulted in a decrease in the retention time. Increasing both the concentration of the organic solvent and the column temperature resulted in a decrease in the retention time of NVP.

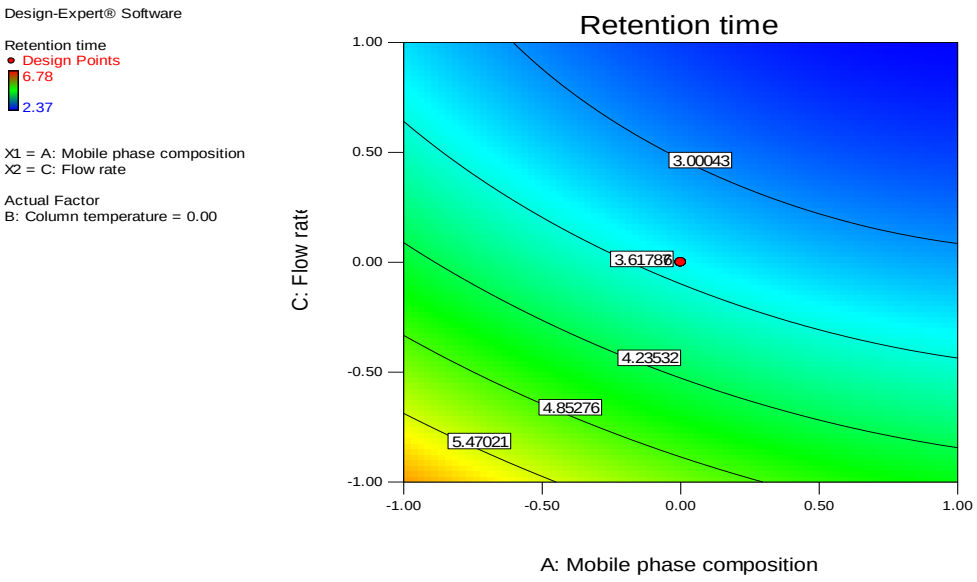

Figure 2.5. Contour plot showing the effect of changes in flow rate and organic solvent concentration on the retention time of NVP.

A study of the effect of column temperature and flow rate on the retention time of NVP showed that increasing the flow rate while keeping the temperature constant resulted in a significant decrease in the retention time, whereas increasing the temperature of the column did not have a significant effect on the retention time of NVP, signified by the straight lines on the contour plots as shown in Figure 2.6. Increasing both the column temperature and the flow rate resulted in a decrease in the retention time.

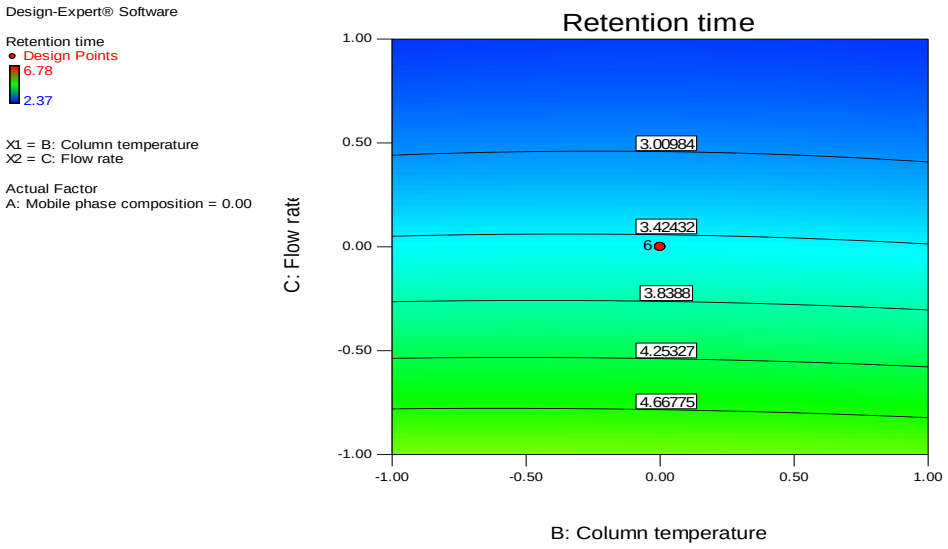

Figure 2.6. Contour plot showing the effect of changes in flow rate and column temperature on the retention time of NVP.

2.6.1.3 Evaluation of Model Adequacy for Resolution Factor

The results of these determinations are summarised in Table 2.8. All parameters that were considered for determining the adequacy of the model revealed that the quadratic model that was selected was appropriate to navigate the design space for this separation.

Table 2.8. Summary of model parameters and values used to evaluate adequacy of the model for resolution factor

Parameter	Value	Parameter	Value
Std. Deviation	0.15	R-Squared	0.9937
Mean	3.25	Adjusted R-Squared	0.9880
C.V %	4.75	Predicted R-Squared	0.9521
PRESS	1.81	Adequate precision	49.471
F-Value	175.14		

2.6.1.4. ANOVA: Resolution Factor

2.6.1.4.1 Significant Factors Affecting Resolution Factor

ANOVA results for CCD of the factors that significantly affect the resolution between NVP and CBZ are listed in Table 2.9. Model terms with p-value < 0.05 were considered significant. As can be seen from the table, the resolution factor for NVP and CBZ peaks was found to be significantly affected by the model terms X_1, X_2, X_1X_2, X_1X_3, X_1^2, X_2^2 and X_3^2. The column temperature and the amount of organic solvent had a significant effect on the resolution for this separation, implying that the viscosity of the mobile phase at a particular time, in addition to hydrophobic interactions between the compounds and the stationary phase affected resolution factor. The mobile phase flow rate did not have a significant effect on peak resolution. However, the linear interactions between flow rate and organic solvent composition were significant.

Table 2.9. ANOVA for response surface quadratic model analysis of variance table (partial sum of squares-type III) for the resolution factor

Source	Sum of squares	Df	Mean square	F-value	P-value Prob > F
Model	37.56	9	4.17	175.14	< 0.0001
X_1	32.80	1	32.80	1376.45	< 0.0001
X_2	0.24	1	0.24	10.25	0.0095
X_3	0.005.834	1	0.005.834	0.24	0.6314
X_1X_2	0.20	1	0.20	8.33	0.0162
X_1X_3	0.34	1	0.34	14.11	0.0037
X_2X_3	0.003.200	1	0.003.200	0.13	0.7217
X_1^2	0.45	1	0.45	18.88	0.0015
X_2^2	1.77	1	1.77	74.12	< 0.0001
X_3^2	1.68	1	1.68	70.43	< 0.0001
Residual	0.24	10	0.024		
Lack of fit	0.24	5	0.048		
Pure error	0.000	5	0.000		
Cor total	37.80	19			

Dark red = significant model terms.

The relationship between the resolution factor and interacting parameters is described by Equation 2.12.

$$Y_3 = 3.60X_1 - 1.55X_2 - 0.13X_2 - 0.021X_3 - 0.16X_1X_2 - 0.20X_1X_3 - 0.020X_2X_3 - 0.18X_1^2 - 0.35X_2^2 - 0.34X_3^2$$ **Equation 2.12**

The equation shows that the resolution factor was significantly affected by the antagonistic linear contributions of the model terms X_1, X_2, X_1X_2, X_1X_3 and antagonistic quadratic interaction effects of X_1^2, X_2^2 and X_3^2. These relationships implied that increasing the concentration of the organic solvent, column temperature and mobile phase flow rate resulted in a decrease in the resolution factor.

2.6.1.4.2 Response Surface Model Plots for Resolution Factor

The relationship between the independent variables and the resolution factor was visualised using 3-dimentional Response Surface Plots (RSP). Increasing both the column temperature and the amount of organic solvent resulted in a slight decrease in the resolution factor as depicted in Figure 2.7. An increase in the concentration of the organic solvent while keeping the column temperature constant resulted in a decreased resolution. An increase in the column temperature while keeping the concentration of the organic solvent constant resulted in an increase in the resolution factor. The figure also shows that the highest values of resolution were achieved with high temperatures and low concentrations of the organic solvent compared to low temperatures and high concentrations of organic solvent.

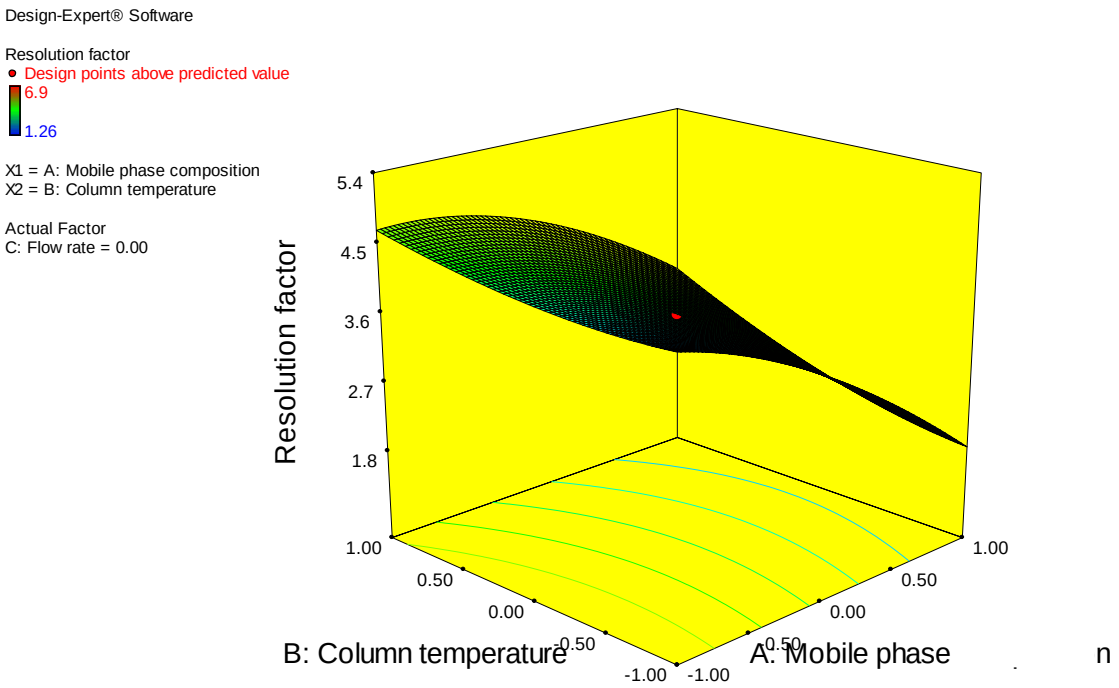

Figure 2.7. RSM plot showing the effect of column temperature and amount of organic solvent on the resolution factor.

Increasing both the amount of the organic solvent in the mobile phase and flow rate significantly decreased the resolution factor, while an increase in the flow rate with constant organic solvent also resulted in a slightly decreased resolution factor as shown in Figure 2.8. The figure also shows that increasing the concentration of the organic solvent while keeping the flow rate constant resulted in a decrease in the resolution factor and that highest values of resolution factor was achieved when low flow rates and high concentrations of organic solvent concentration in the mobile phase were used as compared to high flow rates and low organic solvent concentration.

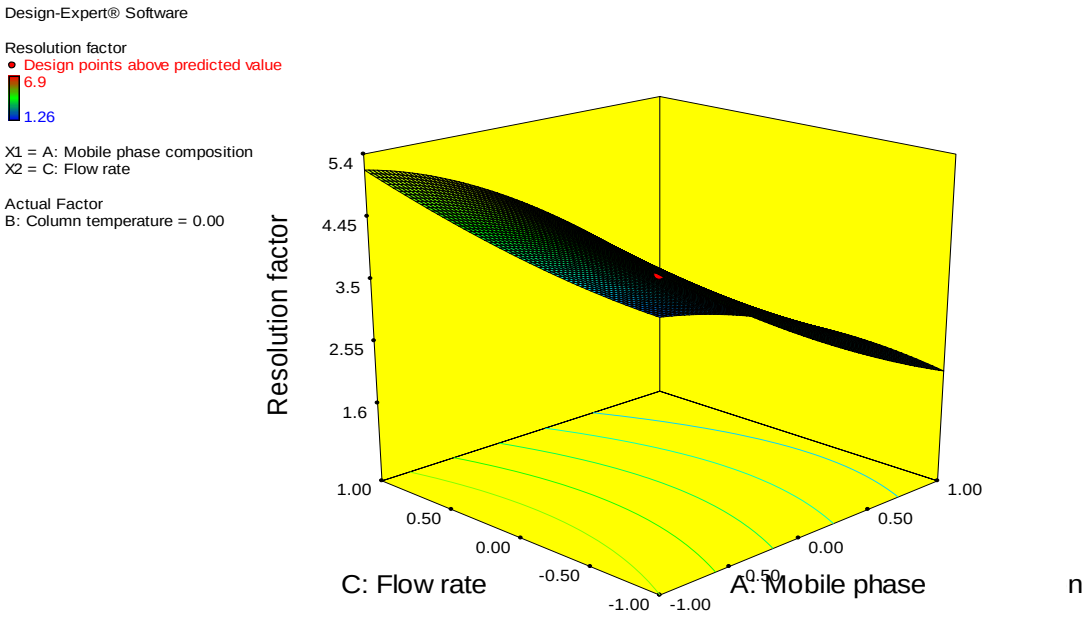

Figure 2.8. RSM plot showing the effect of changes in mobile phase composition and flow rate on the resolution factor.

An increase in both temperature and flow rate resulted in a slight decrease in the resolution factor. An increase in flow rate did not have a significant effect on the resolution factor as shown in Figure 2.9. The figure also shows that increasing the column temperature up to approximately 30 °C while keeping the flow rate constant resulted in an increase in the resolution factor, thereafter an increase in the column temperature resulted in a decrease in the resolution factor. An increase in flow rate of mobile phase with constant column temperature did not have a significant effect on the resolution factor. The resolution factors for conditions of low temperatures and high flow rates were similar to those of conditions of low temperature and low flow rates. Furthermore, high temperatures and low flow rates

resulted in resolution factors that were similar to those from high temperatures and high flow rates. These effects resulted in the formation of a 'molehill' shaped response surface plot shown in Figure 2.9. The figure also shows that highest values of resolution factor were achieved when medium low flow rates (approximately 1 mL/min) and medium temperatures (approximately 30 °C) were used.

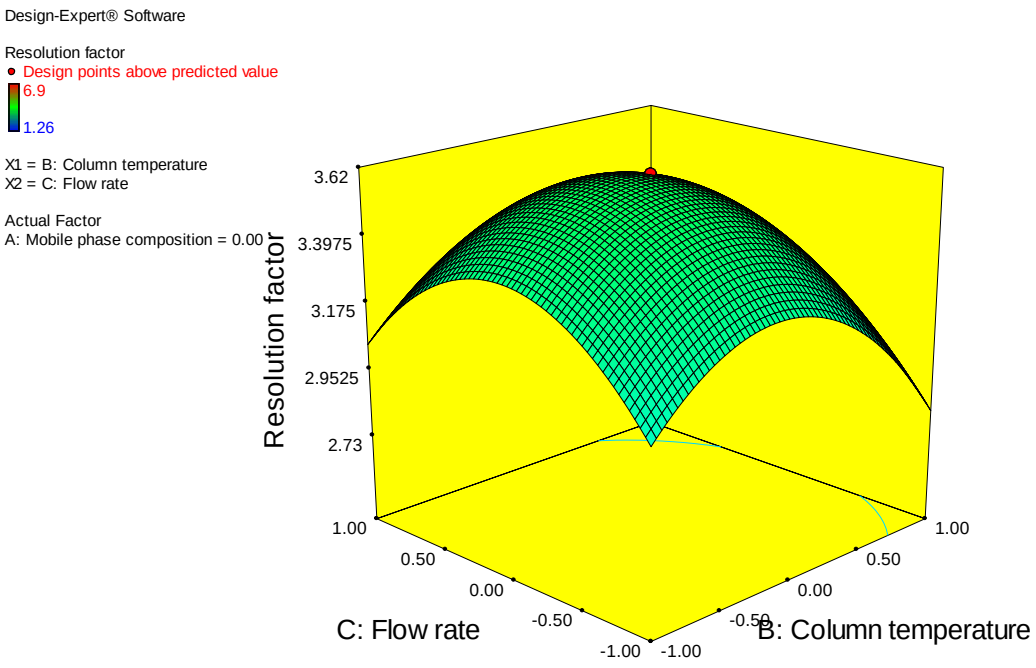

Figure 2.9. RSM plot of the effect of flow rate and column temperature on the resolution factor.

2.6.1.5 Validation of Experimental Design

The optimised chromatographic conditions selected for the quantitation of NVP are summarised in Table 2.10.

Table 2.10. Summary of chromatographic conditions

Parameter	Setting
Integrator: Speed	0.25 cm/min
Input voltage	10 mV full scale
Attenuation (AT)	128
Offset (OF)	5
Peak height (PH)	1
Peak threshold (PT)	250
Minimum area (MA)	2500
Peak width (PW)	6
Sensitivity	0.1 AUFS
Flow rate	1.0 mL/min
Injection volume	20 µL
Wavelength	284 nm
Temperature	30 °C
Mobile phase composition	44:56 % v/v acetonitrile: water

The optimised chromatographic conditions resulted in a separation for which the retention time of NVP and CBZ were 4.30 ± 0.014 min and 7.60 ± 0.014 min, respectively with a resolution factor of 3.82 ± 0.012 (n =5). A typical chromatogram of the separation of a standard solution of NVP and CBZ is depicted in Figure 2.10.

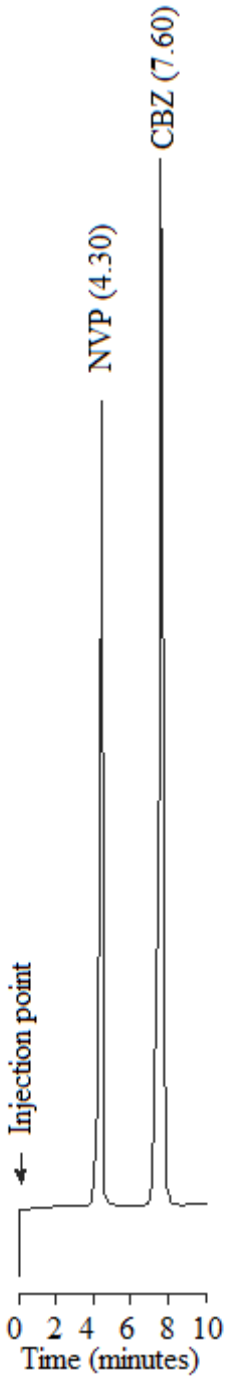

Figure 2.10. Typical chromatogram of the separation of NVP (60 µg/mL) and CBZ (100 µg/mL).

The experimental design model was validated by comparing the predicted values and the actual experimental values obtained using calculated residual and percentage errors. The predicted retention times of NVP and CBZ, and the resolution factor in addition to the calculated residual and percent prediction errors (% P.E) are summarised in Table 2.11.

Table 2.11. Validation of experimental model: comparison of predicted and actual responses

Response	Predicted	Actual	Residuals	% Prediction error
RT NVP	4.00	4.30	0.30	6.98
RT CBZ	7.00	7.60	0.60	7.89
R_S	4.00	3.82	0.12	3.00

The percent error between the predicted and actual retention times were 6.98 and 7.89 for NVP and CBZ, respectively while the percentage error for the resolution factor was 3%. It can be concluded that the empirical models that were developed were reasonably accurate, particularly for resolution that had a percentage error < 5%. Slightly lower prediction errors could have been obtained if transformation of the data was performed, however, the responses observed were within the set limits and the separation was rapid and produced reliable analyses.

The preliminary chromatographic conditions achieved using the traditional method of sequentially changing one variable at a time produced a mobile phase that was comprised of 40% acetonitrile and 60% water, and yielded retention times of 5.23 minutes and 9.25 minutes for NVP and CBZ, respectively whereas the RSM optimised mobile phase was comprised of 44% acetonitrile and 56% water with retetions times of 4.30 minutes and 7.6 minutes for NVP and CBZ, respectively. The use of RSM enabled achievement of conditions that resulted in much shorter retention times and adequate resolution between the peaks of interest.

2.6.2 HPLC Method Validation

2.6.2.1 Linearity and Range

A plot of peak height ratio of NVP/CBZ versus the concentration of NVP yielded a calibration curve with a slope of 0.0064, a y-intercept of – 0.0016 and a correlation coefficient of 0.9996 and is depicted in Figure 2.11. These results indicate that the method was linear over the concentration range studied.

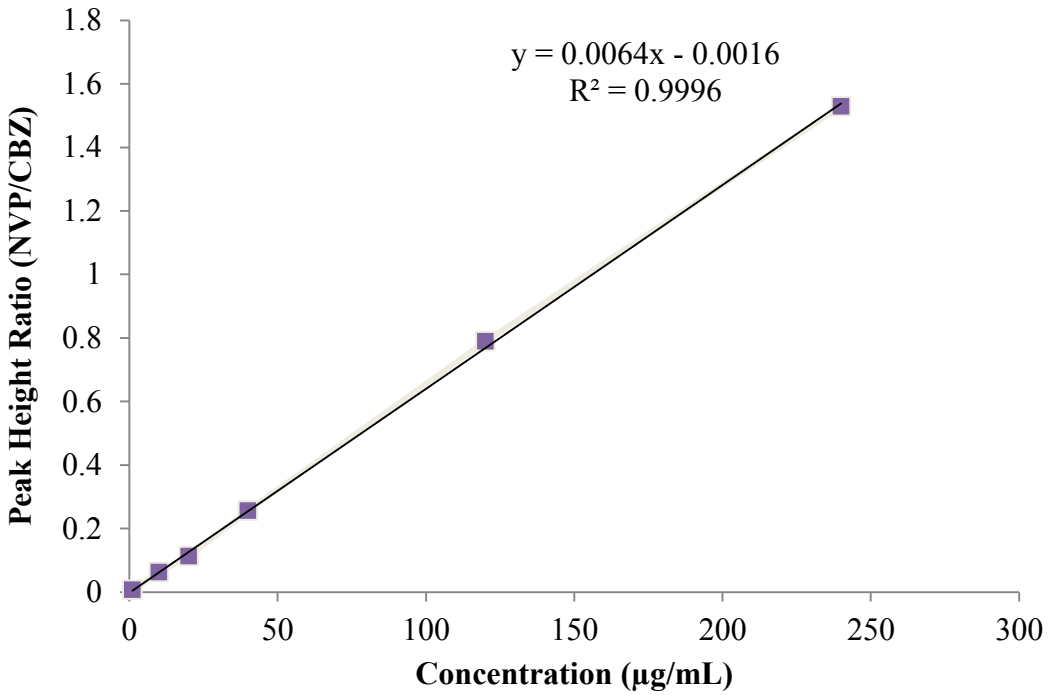

Figure 2.11. Calibration curve for NVP over the concentration range 1 - 240 µg/mL (n = 5).

2.6.2.2 Precision

2.6.2.2.1 Repeatability

The results of repeatability studies are summarised in Table 2.12 and indicate that the method was repeatable and the % RSD values for samples of all concentration levels were < 5%.

Table 2.12. Summary of results of repeatability studies

Concentration µg/mL	Average Peak Height Ratio (n = 5)	Standard Deviation (SD)	%RSD
1	0.0042	0.00018	4.282
10	0.0416	0.00028	0.6713
20	0.0771	0.00032	0.4097
40	0.1702	0.00021	0.1254
120	0.5285	0.00083	0.1577
240	0.9962	0.00096	0.0964

2.6.2.2.2 Intermediate Precision

A summary of the results of intermediate precision studies are listed in Table 2.13. All % RSD values were within the acceptance criterion of ≤ 5% indicating that the method is precise for the analysis of NVP when conducted on different days.

Table 2.13. Results of intermediate precision studies

Day	Concentration µg/mL	Average peak height ratio n =5	SD	%RSD
1	**1**	0.0085	0.0000462	0.54499
	10	0.0621	0.0001709	0.27522
	20	0.1272	0.0004357	0.34266
	40	0.2639	0.0002695	0.10212
	120	0.8145	0.0006800	0.08348
	240	1.5980	0.0015676	0.09822
2	**1**	0.0201	0.0000865	0.42981
	10	0.0671	0.0017270	2.57331
	20	0.1282	0.0027920	2.17819
	40	0.2753	0.0018870	0.68547
	120	0.8432	0.0005270	0.06250
	240	1.5890	0.0018770	0.11813
3	**1**	0.0200	0.0001080	0.54126
	10	0.0673	0.0000825	0.12268
	20	0.1289	0.0003640	0.28224
	40	0.2722	0.0004250	0.15631
	120	0.8308	0.0020070	0.24154
	240	1.5776	0.0015850	0.10048

2.6.2.3 Accuracy

A summary of results of accuracy studies is listed in Table 2.14 and indicates the method is accurate, with all % RSD and % Bias values < 5%.

Table 2.14. Summary of results of accuracy studies (n = 5)

Theoretical concentration µg/mL	Actual Concentration µg/mL	SD	%RSD	% Recovery	%Bias
5	5.0283	0.00035	0.80079	100.566	-0.5660
100	100.209	0.00059	0.08798	100.209	-0.2090
200	198.544	0.00145	0.11213	99.272	0.7280

2.6.2.4 LOQ and LOD

The LOQ was found to be 1.0 µg/mL with a % RSD of 1.50 while the LOD was set at 0.3 µg/mL. The results for the determination of LOQ are summarised in Table 2.15.

Table 2.15. Results for LOQ determination for HPLC analysis of NVP (n = 5)

Concentration µg/mL	NVP/CBZ HT ratio	SD	% RSD
0.5	0.003342	0.0002455	7.3467
1	0.006760	0.0001000	1.4947
1.5	0.009820	0.0000263	0.2679
2	0.011820	0.0000190	0.1635
2.5	0.015160	0.0003235	0.2134

2.6.2.5 Specificity

The results of specificity studies reveal that there was no interference with the NVP peak from excipients used in commercially available Aspen® nevirapine tablets as shown in Figure 2.12 and the method was therefore deemed specific for the analysis of NVP in pharmaceutical dosage forms.

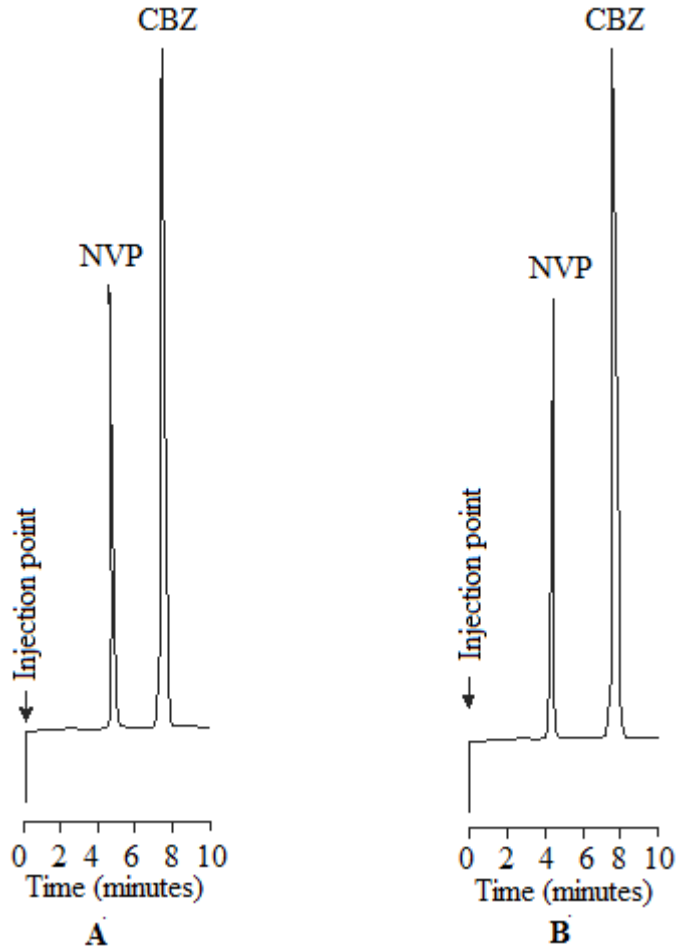

Figure 2.12. Comparison of chromatograms of a standard solution of NVP (A) and NVP solution from commercially available tablets (B) at a concentration of 60 µg/mL.

2.6.2.6 Assay

The average NVP content was found to be between 97.35 and 99.79% of the label claim for the two products tested. The results are summarised in Table 2.16 and the % recovery and corresponding %RSD values were all < 5% showing that the method was accurate.

Table 2.16. Assay results for commercially available products

Product	NVP added mg	NVP found mg ± SD	Recovery %	% RSD
Aspen® Nevirapine 200 mg	100	97.35 ± 0.652	97.35	0.6697
Viramune® XR 100 mg	100	98.45 ± 0.884	98.45	0.8977

2.6.3 Stability Indicating Studies

2.6.3.1 Oxidative Degradation Studies

NVP was found to degrade by 11.72 ± 1.12% in 30 % v/v H_2O_2 after refluxing for 8 hours. However chromatograms reveal that no degradation peaks were present for the duration of the study. Typical chromatograms of NVP following exposure to oxidative conditions at 2, 4, 6 and 8 hours are shown in Figure 2.13. These results are in agreement with previously reported results [167].

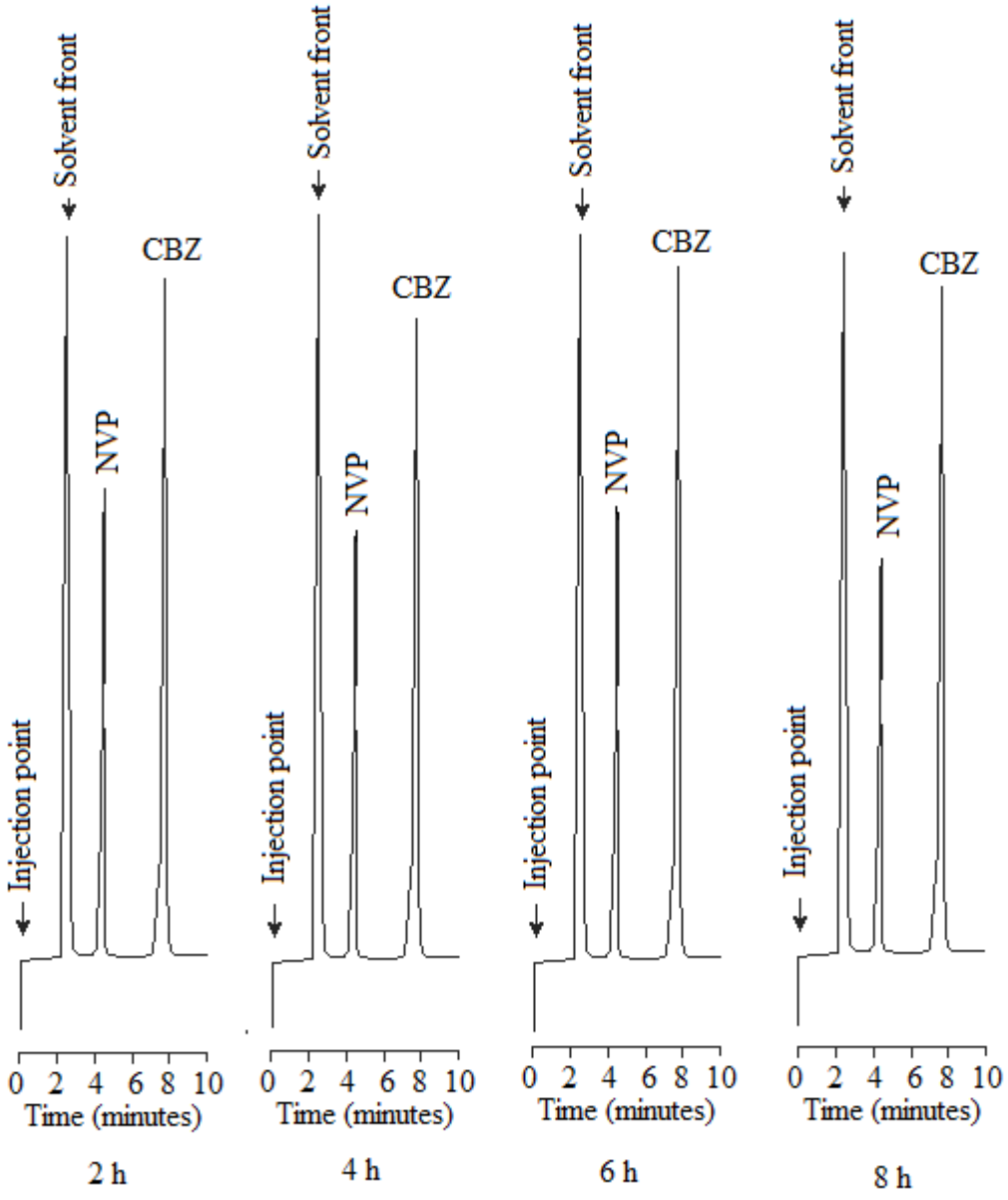

Figure 2.13. Typical chromatograms of NVP (60 µg/mL) following exposure to 30% v/v H_2O_2 at 2, 4, 6 and 8 hour time points.

2.6.3.2 Acidic Degradation Studies

NVP was found to degrade by 7.11 ± 0.87% in 0.1 M HCl after refluxing at 90 °C for 8 hours. There were no degradation peaks observed for the duration of the studies and the chromatograms of NVP exposure to acidic conditions at 2, 4, 6 and 8 hours are shown in Figure 2.14.

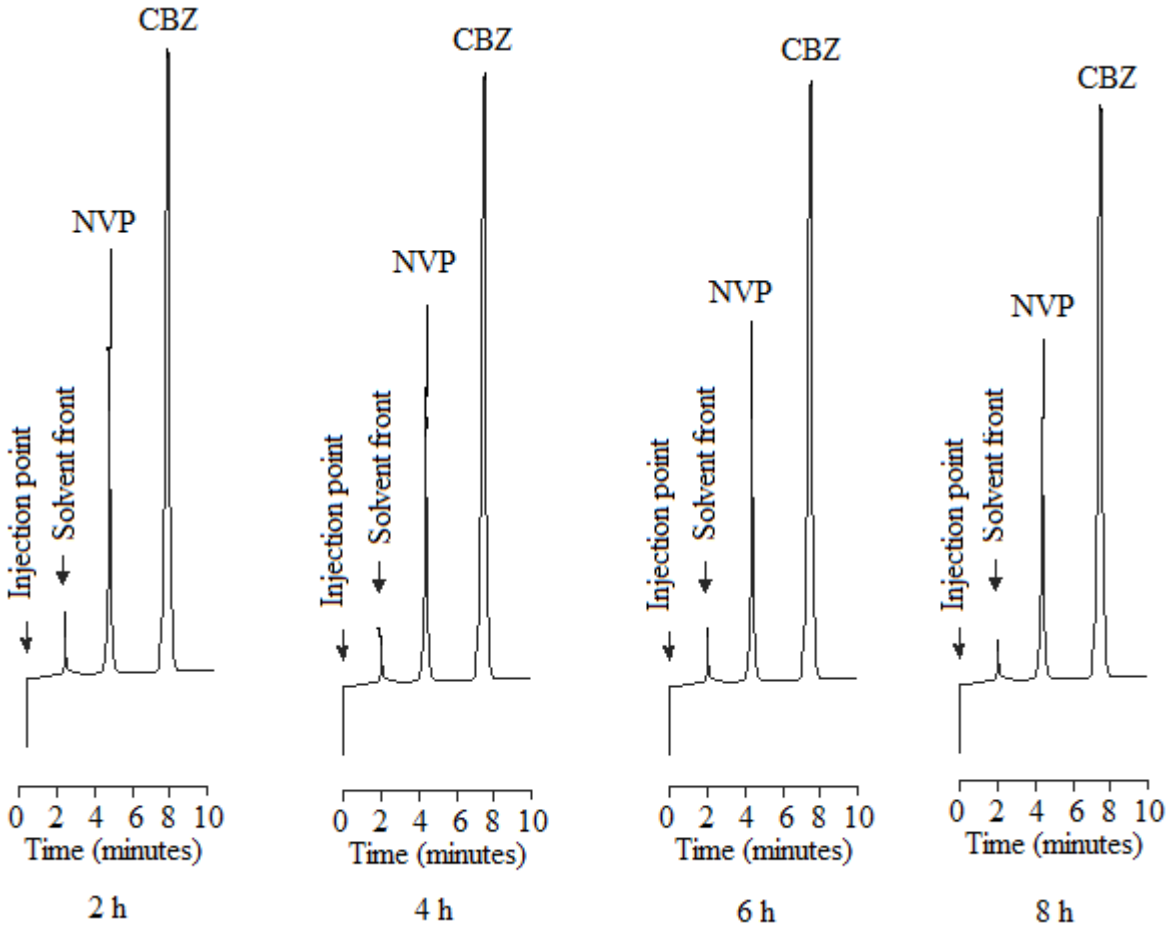

Figure 2.14. Typical chromatograms of NVP (60 µg/mL) following exposure to 0.1 M HCl at 2, 4, 6 and 8 hour time points.

2.6.3.3 Alkali Degradation Studies

NVP degraded by approximately 4.83 ± 1.07% after exposure to 0.1 M NaOH and refluxing at 90°C for 8 hours. No degradation peaks were present for the duration of the study as can be seen in the chromatograms of NVP at 2, 4, 6 and 8 hours in alkali as shown in Figure 2.15.

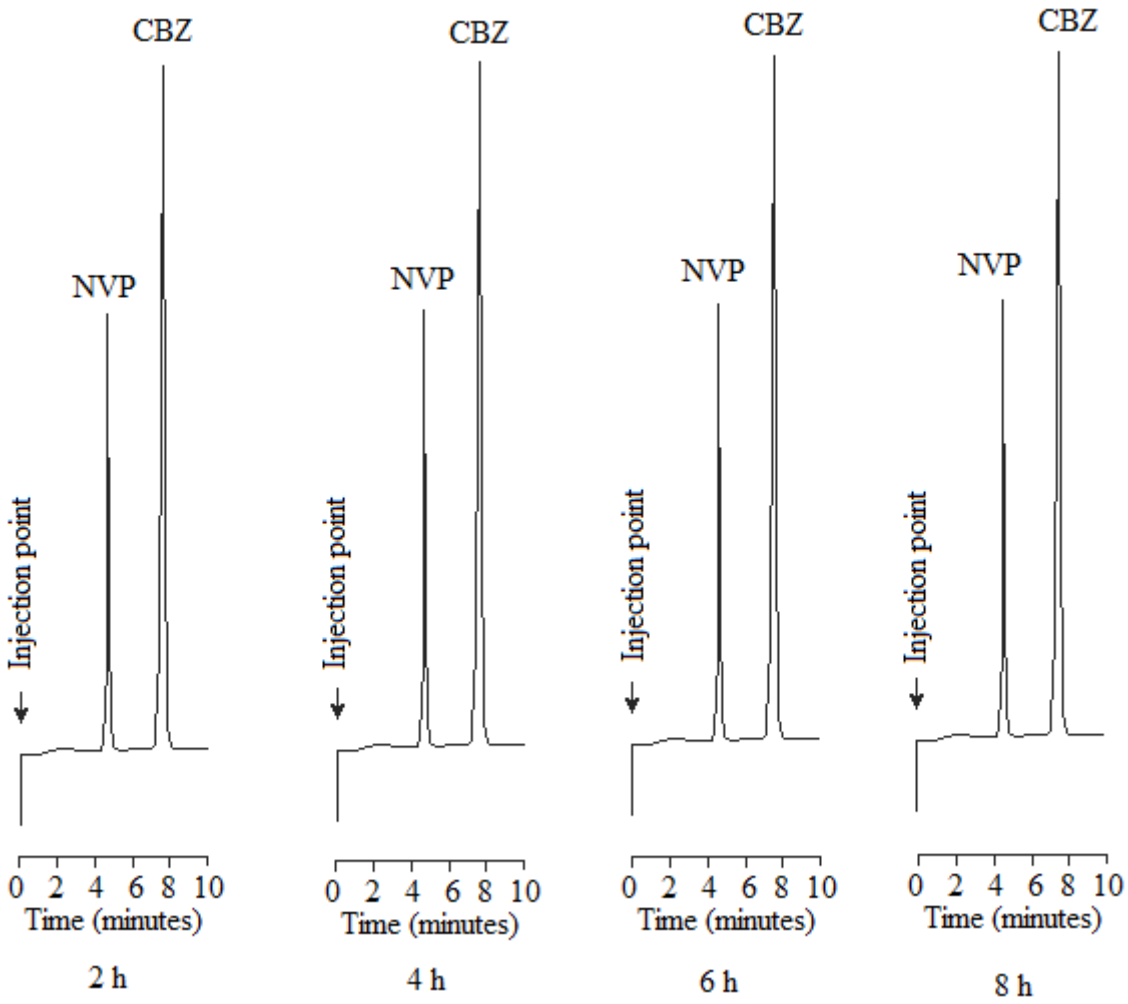

Figure 2.15. Typical chromatograms of NVP (60 µg/mL) following exposure to 0.1 M NaOH at 2, 4, 6 and 8 hours.

2.6.3.4 Neutral Hydrolytic Studies

NVP was found to be stable at an elevated temperature of 90 °C and refluxing for 8 hours in a neutral medium. Typical chromatograms at 2, 4, 6 and 8 hours are shown in Figure 2.16.

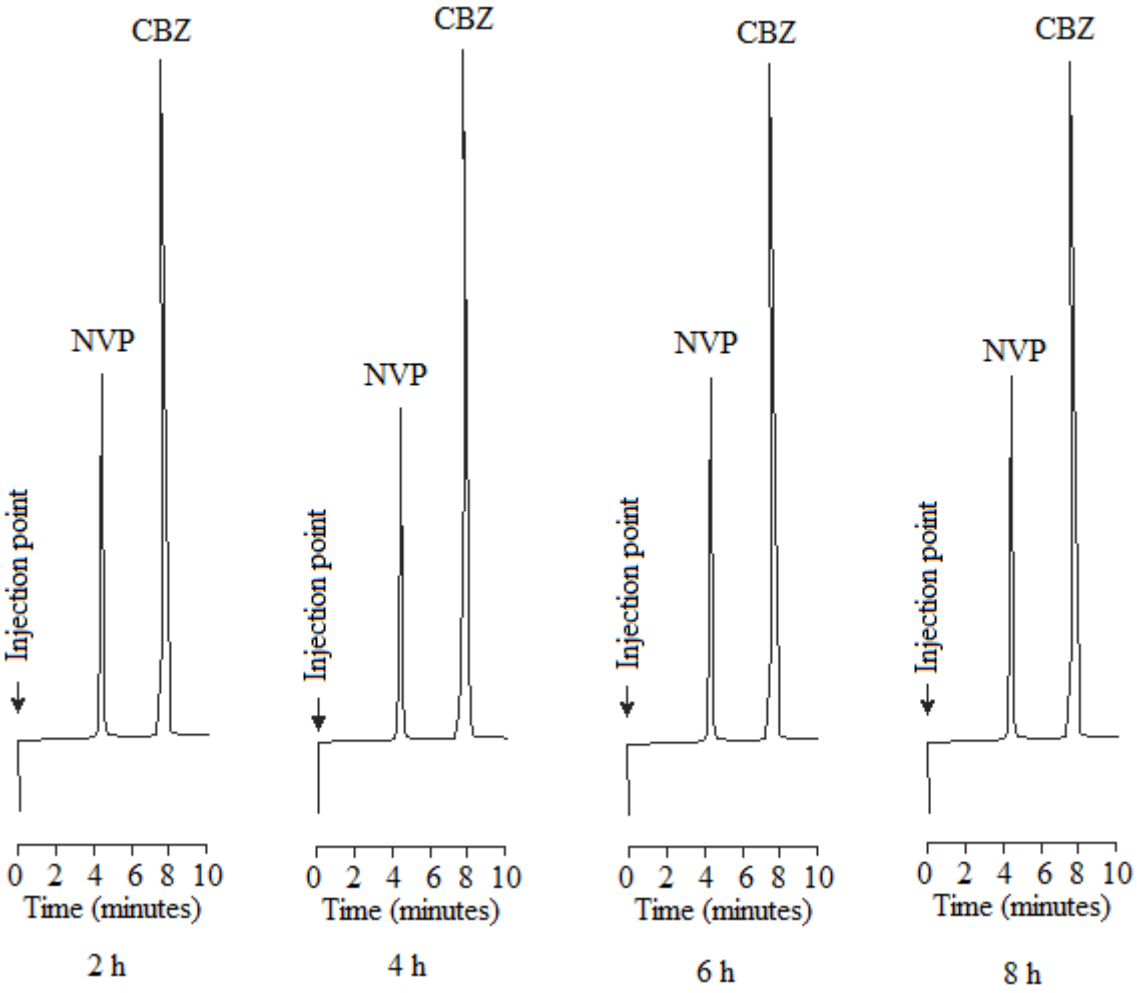

Figure 2.16. Typical chromatograms of NVP (60 µg/mL) following exposure to neutral hydrolysis at 2, 4, 6 and 8 hours.

2.6.3.5 Photo Degradation Studies

NVP was also found to be stable following exposure to light conditions of 500 w/m^2 at 27 °C following exposure for 8 hours and chromatograms at 2, 4, 6 and 8 hours are depicted in Figure 2.17.

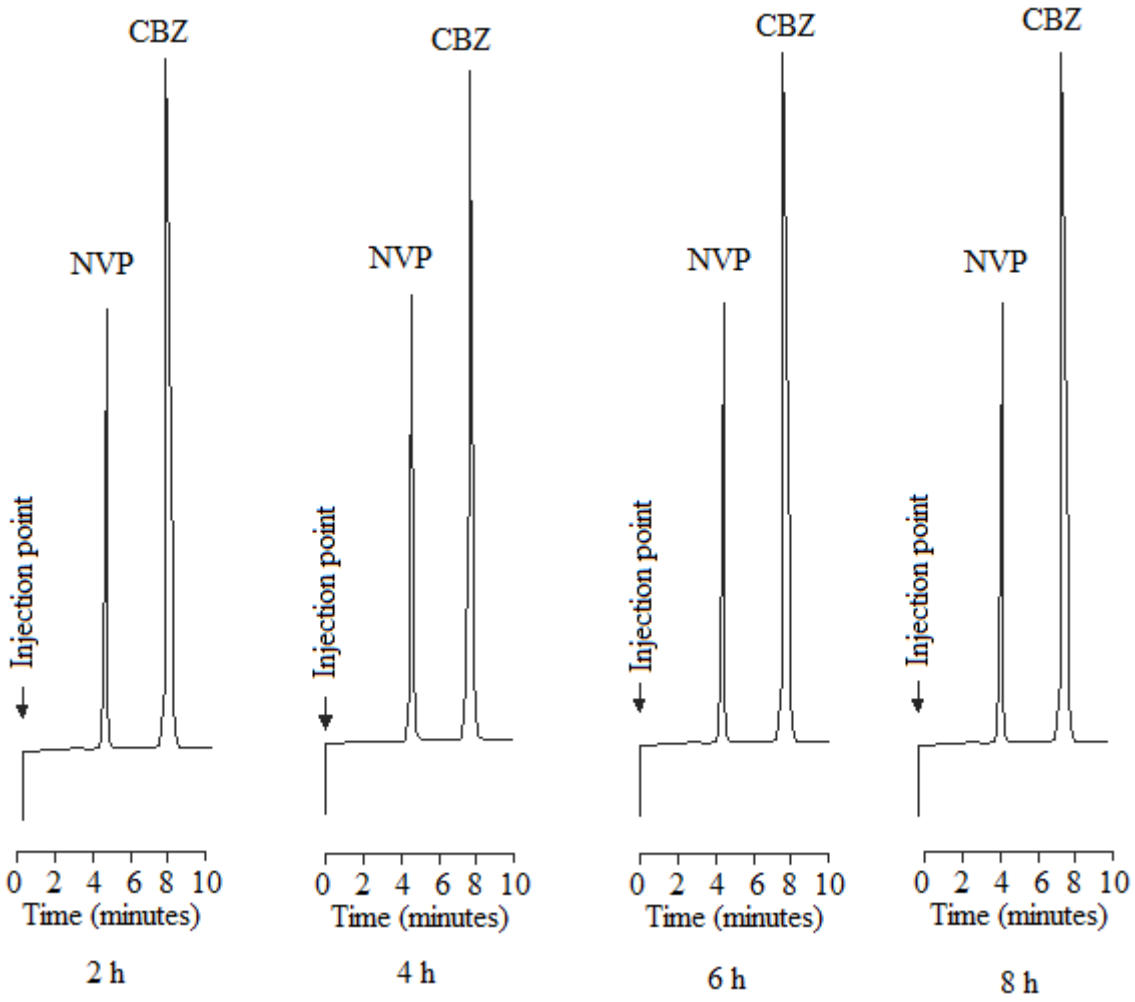

Figure 2.17. Typical chromatograms of NVP (60 µg/mL) following exposure to 500 w/m^2, at 27 °C at 2, 4, 6 and 8 hours.

The results of stability studies in terms of % recovery under different stress conditions at different time points are summarised Table 2.17. The results show a decrease in % recovery of NVP after exposure to 30% v/v H_2O_2, 0.1 M HCl and 0.1 M NaOH and refluxing at 90 °C for 8 hours, indicating degradation. The % recovery of NVP remained relatively unchanged after exposure to neutral hydrolytic conditions at 90 °C and 500 w/m^2 at 27 °C for 8 hours showing that NVP was stable under these conditions.

Table 2.17. Summary of stability data of NVP in different stress conditions

Time h	% Recovery				
	Stress condition				
	30% v/v H_2O_2	0.1 M HCl	0.1 M NaOH	Neutral, 90 °C	500 w/m^2 at 27 °C
0	99.3 ± 0.118	99.2 ± 0.455	99.5 ± 0.662	98.9 ± 0.244	99.4 ± 0.743
2	96.2 ± 0.255	97.5 ± 0.336	97.7 ± 0.559	98.8 ± 0.331	99.2 ± 0.447
4	92.7 ± 0.677	94.8 ± 0.128	95.8 ± 0.578	99.0 ± 0.566	98.8 ± 0.512
6	89.6 ± 0.558	92.1 ± 0.556	94.6 ± 0.442	98.6 ± 0.864	99.0 ± 0.211
8	86.5 ± 1.121	91.3 ± 0.870	93.6 ± 1.072	98.4 ± 0.773	98.9 ± 0.323

2.7 CONCLUSIONS

A simple, precise, accurate, selective and rapid RP-HPLC method for the quantitation of NVP has been successfully developed, optimised and validated. RSM was used for method optimisation to establish the optimum chromatographic conditions for the separation of NVP and the internal standard, CBZ. The amount of acetonitrile and flow rate affect the retention times of NVP and CBZ significantly, whereas column temperature and the amount of acetonitrile had a significant effect on the resolution of NVP and CBZ.

The separation using the optimised conditions produced sharp and well resolved symmetrical peaks with retention times of approximately 4.30 and 7.60 minutes for NVP and CBZ, respectively. The residuals and percent errors for the predicted responses and actual responses showed that the experimental model used was reasonably accurate and could therefore be applied to generate the optimum chromatographic conditions for the separation.

The method is simple, precise and accurate and can be used for the analysis of NVP in bulk and pharmaceutical dosage forms. The method is an improvement on most of the methods reported in the literature as it is isocratic whereas most methods have used gradient elution that may result in longer analysis times. The use of a simple mobile phase with no buffers also makes this method a better and cheaper alternative to previously reported methods.

NVP was found to be more stable in 0.1 NaOH than in 0.1 M HCl and 30% v/v H_2O_2 following exposure to these media, for up to 8 hours. NVP was also stable under neutral

hydrolytic conditions at an elevated temperature of 90 °C and was also stable following exposure to light at 500 w/m^2 at 27 °C for 8 hours. The forced degradation studies did not yield any degradation products during the 8 hour period of study.

The method that was developed is specific for NVP analysis in pharmaceutical dosage forms as no interfering peaks were observed during the analysis of commercially available Aspen® NVP tablets. The method is therefore suitable for use in formulation development studies of a NVP sustained release multisource product.

CHAPTER THREE

DISSOLUTION TESTING OF NEVIRAPINE SUSTAINED RELEASE TABLETS

3.1 INTRODUCTION

Dissolution is defined as the process by which solid particles are solubilised in a solvent and it can be considered a type of heterogeneous reaction in which mass transfer is a result of the net effect between escape and deposition of solute molecules at a solid interface [168, 169]. The dissolution rate of an API is defined as the amount of that substance that is transferred into solution per unit time under standard conditions of the solid/liquid interface, temperature and solvent composition [169]. Dissolution has also been described as a process by which solid particles of acceptable solubility characteristics only, will enter into solution [170].

During the process of dissolution, solid particles located at the solid-liquid interface are initially transferred into solution resulting in the formation of a stagnant film of defined thickness, *h*, around the particle. The solute particles that are dissolved migrate across the film to the bulk dissolution medium and this represents the initial rate limiting step in the process of dissolution of an API in a solvent [171].

The earliest reference to dissolution was described by Noyes and Whitney who reported the process of dissolution of solid particles based on a diffusion layer model, in which the rate of drug diffusion was a function of a thin layer of saturated solution surrounding the solid particle. The relationship between dissolution rate and diffusion parameters are described by what is known as the Noyes-Whitney Equation (Equation 3.1) [171].

$$\frac{dc}{dt} = k\frac{DS}{vh}(C_s - C_t) \qquad \textbf{Equation 3.1}$$

where,

$\frac{dc}{dt}$ = the dissolution rate,
k = the intrinsic dissolution rate constant of an API,
D = the diffusion coefficient of the API,
S = the surface area of API particles,
v = the volume of dissolution medium,
h = the thickness of the stagnant diffusion layer,
C_s = the saturation concentration of API in the dissolution medium, and
C_t = the concentration of API in solution at time *t*.

In vitro dissolution testing has been widely used as a quality control tool for testing the performance of solid oral dosage forms. A meaningful dissolution test should, as far as possible, be representative of the *in vivo* release characteristics of a dosage form in order for it to be adequately correlated with *in vivo* performance and bioavailability. *In vitro* dissolution testing is the single most important tool for the provision of process control and quality assurance of a dosage form. It confirms constant and reproducible characteristics of an API and product performance and is used to fulfil regulatory requirements when formulation changes are made post registration [172].

Dissolution testing of modified release dosage forms also provides an indication of how a formulation may perform *in vivo*. Therefore a major objective is to develop and evaluate, where possible an *in vitro in vivo* correlation (IVIVC) to establish whether dissolution testing can be used as a surrogate approach to establishing bioequivalence, that may then reduce the number of bioequivalence studies needed during the initial approval process in addition to permitting approval for scale-up and post approval changes [172].

Several dissolution Apparatus are available for use and have been described in the literature [173, 174]. The instruments for dissolution testing listed in the United States Pharmacopoeia (USP) are summarised in Table 3.1 and are considered official Apparatus [172, 175].

Table 3.1. Official USP dissolution Apparatus

Apparatus	USP Designation	Agitation Speed	Dosage Form
Basket	1	50 - 120 rpm	IR, DR, ER
Paddle	2	25- 75 rpm	IR, DR, ER
Reciprocating Cylinder	3	6 – 35 dpm	IR, ER
Flow-Through Cell	4	N/A	ER, PS API
Adaptations for transdermal patches, T = 32 °C:			
Disk assembly method	5	25- 50 rpm	Transdermal
Rotating cylinder method	6	N/A	Transdermal
Reciprocating Disk (transdermal)	7	30 rpm	ER

rpm = rotations per minute, dpm = dips per minute, IR = immediate release, DR = delayed release, ER = extended release, PS API = poorly soluble active pharmaceutical ingredient.

USP Apparatus 1 and 2 are the most commonly used apparatus for dissolution testing of solid oral dosage forms and have also been used for sustained release dosage form testing [176-

180]. The use of USP Apparatus 1 and 2 is easy as the equipment is readily automated, which is important for routine analysis.

Despite the fact that these apparatus are often used, USP Apparatus 1 and 2 exhibit certain disadvantages when applied to the assessment of dissolution rates of an API from modified release systems. For example, if a dissolution test method requires the pH of the test medium to be changed over time, the medium must be discharged manually during testing, resulting in a laborious and time-consuming experiment that may generate less accurate and precise data. These systems also exhibit complex hydrodynamics that are affected by the location of a dosage form in the test vessel and may impact the dissolution rate of an API, significantly [172]. USP Apparatus 1 and 2 are also not suitable for testing dosage forms containing drugs of low aqueous solubility as the design of the equipment makes it difficult to maintain sink conditions for testing that API [172, 174].

In order to overcome the challenges of testing low solubility compounds USP Apparatus 3 may be used. This apparatus consists of a set of cylindrical, flat-bottomed glass vessels and a set of glass cylinders fitted to a reciprocating rod in addition to stainless steel fittings and screens that are made of a suitable, non-adsorbing non-reactive material that fit into the top and bottom of each reciprocating cylinder. The cylinders are driven by a motor and drive assembly that reciprocates the chambers in a vertical manner inside the outer vessels that contain the test media. The vessels are partially immersed in a suitable water bath to maintain the dissolution media at a set temperature, during testing. The dosage form is placed in the reciprocating cylinder and the cylinder is allowed to move in an up- and downward direction at a predefined constant speed, permitting release of the drug into the dissolution fluid within the outer cylinder.

USP Apparatus 3 is purported to exhibit superior hydrodynamics when compared to USP Apparatus 1 and 2 and is particularly useful for the analysis of poorly water soluble drug containing products, modified release technologies and API that exhibit pH dependent dissolution characteristics [173].

The most useful advantage of USP Apparatus 3 over Apparatus 1 and 2 is that the reciprocating cylinders can be transferred to different dissolution media at specified times. The inner dissolution tubes move between successive rows of vessels, allowing dosage units to be exposed to media of different pH, such as for example simulated gastric fluid, simulated

intestinal fluid and simulated colonic fluid for a specified time and in a sequential manner [173].

USP Apparatus 4 or the flow-through cell dissolution system has a reservoir and pump to facilitate dissolution medium transport through the flow-through cell in which the dosage form is located. A dispersed flow pattern is produced due to the use of a porous glass plate or bed of beads and either laminar or turbulent fluid flow can be achieved. Although some studies have shown that USP Apparatus 4 is not as robust as other USP Apparatus it has been reported to be superior to the paddle or basket, for dissolution rate testing of modified release dosage forms [172, 181].

Due to the advantages that USP Apparatus 3 exhibits over USP Apparatus 1 and 2 in respect of media change and as NVP is a sparingly soluble API, a dissolution test method using USP Apparatus 3 was developed and validated for use in *in vitro* dissolution testing of NVP SR tablets.

Dissolution testing, as with any other analytical tool, should be reliable and yield valid, precise, accurate and repeatable data if the results of *in vitro* release testing are to be meaningful [182].

Dissolution testing has been reported to be a highly variable technique and in many cases the impact of formulation or manufacturing changes on API release properties, may not be observed but differences that are evident may rather be a consequence of the variability of the test method [183].

Therefore control of all experimental conditions is necessary to reduce test-to-test variability and to improve the reproducibility and reliability of a method [184]. The development and validation of a precise, accurate and reliable dissolution method for assessing NVP release from an oral sustained release dosage form was necessary to support product development studies and for quality control testing of manufactured dosage forms.

3.2 EXPERIMENTAL

3.2.1 Apparatus and Reagents

A Vankel® Bio-Dis dissolution test Apparatus (Vankel® Industries, New Jersey, USA) was used for dissolution testing of all batches of NVP tablets that were manufactured. A model VK 750 digitally controlled water circulation heater (Vankel® Industries, New Jersey, USA) was used to maintain the temperature of the dissolution media at 37 ± 0.5 °C.

Samples were analysed using the RP-HPLC method that was developed and validated and is reported in Chapter 2 of this dissertation. A Model GLP 21 Crison pH-meter (Crison Instruments, Johannesburg, South Africa) was used to measure the pH and 0.45 µm HVLP Millipore® nylon membrane filters were used to filter the samples prior to analysis. All chemicals that were used were at least of analytical reagent grade. Viramune® XR, a commercially available NVP extended release product was used for the development and validation of the dissolution method and was kindly donated by Boehringer Ingelheim Pharmaceuticals Ltd (Boehringer Ingelheim Ltd, Ridgefield, USA). The product was also used as the reference product for formulation development studies.

3.2.2 Preparation of Dissolution Media

The basis of the dissolution media used was phosphate buffer. The buffer strength of different media were 25, 50 and 75 mM and these were prepared by accurately pipetting 1.7 mL, 3.4 mL and 5.1 mL of 85% v/v ortho-phosphoric acid into a 1 L volumetric flask, respectively and making up to the volume with HPLC grade water. The pH of the buffer was then adjusted using a 0.1 M NaOH solution to a pH of 1.2, 1.6, 3.4, 4.7, 6.8 and 7.2. The pH was measured using a Model GLP 21 Crison pH meter (Crison Instruments, Johannesburg, South Africa) and 250 mL of each solution was transferred into the relevant outer dissolution vessels for each dissolution test (n=6).

3.3 METHOD DEVELOPMENT

3.3.1 Overview

Several authors have developed and validated dissolution test methods for different pharmaceutical products [185-190]. However, only one dissolution method specifically for the assessment of NVP release from SR dosage forms had been reported at the time of this

study [191]. The method that has been described involved the use of USP Apparatus 1 or 2 with 900 mL of a 50 mM phosphate buffer (pH 6.8) and 6% w/v sodium lauryl sulphate (SLS) maintained at 37.0 ± 0.5 °C and agitated at 50 rpm. This method was used during the initial stages of dissolution method development to characterise NVP release from Viramune® XR tablets in these studies. Subsequently the dissolution profiles were then compared to those generated using USP Apparatus 3.

3.3.2 Design of Experiments and Selection of Dissolution Test Conditions

The factors likely to have an impact on NVP release were evaluated individually, the effects on NVP release established and the level to be used determined to for use as dissolution test conditions. The dissolution method was validated using ICH guidelines [147].

3.3.2.1 Dissolution Medium

Phosphate buffer (50 mM) was used as the dissolution medium and was maintained at a temperature of 37.0 ± 0.5 °C. API liberation from modified release dosage forms should be monitored in dissolution media that cover the physiological pH of the gastro-intestinal tract *viz.,* pH 1 – 7.8 in an effort to simulate *in vivo* GIT pH. The NVP formulations were therefore tested in dissolution media of different pH as indicated in Table 3.2.

Table 3.2. Dissolution medium pH and duration of testing for formulation development studies and optimised product characterisation

Medium pH	Duration (hours)
Formulation development	
1.2	2
7.2	22
Optimised formulation	
1.6	2
3.4	2
4.7	4
6.8	6
7.2	10

3.3.2.2 Surfactant Use

The addition of a surfactant to a dissolution medium in a low concentration has been shown to improve the dissolution rate of poorly water soluble drugs [29, 172, 174]. Since NVP is poorly water soluble, a 50 mM phosphate buffer dissolution test medium of pH 6.8 with no

SLS and one with SLS at concentrations of 0.25% w/v, 0.5% w/v, 1.0% w/v and 2.0% w/v were used to establish the effect of surfactant concentration on the dissolution rate of NVP. The dissolution media for tests conducted using USP Apparatus 1 and 2 contained 6% w/v SLS [191].

3.3.2.3 Agitation Rate or Dip Speed

The agitation rate used during dissolution testing has been shown to have an impact on the dissolution rate of an API from dosage forms and studies have been undertaken to establish an equivalent dip speed for USP Apparatus 3 to basket and paddle rotational speeds for USP Apparatus 1 and 2 [192, 193]. It has been reported that a dip speed as high as 15 dpm for USP Apparatus 3 are equivalent to paddle rotation speeds of 50 rpm [192, 194]. Other studies have indicated that the extremely low end of available reciprocation rates for USP Apparatus 3 offer hydrodynamic conditions that are equivalent to 50 rpm and 100 rpm for USP Apparatus 1 and 2 [195]. In order to determine the dip speed to be used in these studies, dissolution testing was initially performed using USP Apparatus 2 with 50 mM phosphate buffer of pH 6.8 containing 6% SLS, 50 rpm at a temperature of 37 ± 0.5 °C [191]. Dissolution was also undertaken using USP Apparatus 3 with a 50 mM phosphate buffer of pH 6.8 containing 2% SLS, a temperature of 37 ± 0.5 °C at different reciprocation rates of 5, 10 and 15 dpm. The resultant dissolution profiles were compared using the difference (f_1) and similarity (f_2) factors [196] to select a dip rate that closely resembled the profile generated using USP Apparatus 2, at an agitation rate of 50 rpm.

3.3.2.4 Mesh Size

Different mesh sizes are available for use with USP Apparatus 3 and these are summarised in Table 3.3.

Table 3.3. Mesh sizes for use in USP Apparatus 3

Mesh Size	Pore Size µm
20	840
40	405
78	177
160	74

A study to investigate the effect of mesh size on API release showed that the top mesh screen size had an effect on release whereas the bottom did not [197]. Another study reported an insignificant effect of mesh size on API release [192]. Incomplete drainage of dissolution medium was observed when a mesh size of 74 μm was used by Khamanga and Walker [198]. In order to determine a suitable mesh size for these studies, the effect of mesh size on NVP release was investigated. The sizes of the bottom mesh screen that were tested included 20, 40 and 78 and the resultant dissolution profiles were compared using the f_1 and f_2 factors. An appropriate mesh size was selected based on visual inspection of the dissolution process and the amount of NVP released during dissolution testing.

3.3.2.5 Buffer Molarity

The effect of buffer molarity on NVP release was investigated in order to select a buffer of suitable strength. Phosphate buffers of molarities of 25 mM, 50 mM and 75mM were used to prepare dissolution media of pH 6.8 and were used to generate NVP release profiles that were compared using f_1 and f_2 factors to determine most appropriate molarity to use for dissolution studies.

3.4 VALIDATION OF DISSOLUTION METHOD

3.4.1 Specificity

The specificity of the method was established by exposing commercially available NVP SR tablets to 50 mM phosphate buffer of pH 6.8 for 2 h. An amount of NVP equivalent to the strength of a single tablet, *viz.,* 100 mg was transferred into the outer cylinders containing 250 mL of dissolution medium maintained at 37.0 ± 0.5 °C (n = 3) and stirred with a glass rod for 10 minutes and then left to stand for 2 h. The solutions were stirred for a further 5 minutes and then filtered using a 0.45 μm HVLP Millipore® nylon filter membrane prior to analysis by RP-HPLC (§2.6.1.5). The chromatograms from solutions of NVP prepared from the powdered tablets were compared to the chromatogram of a standard solution of NVP.

3.4.2 Linearity of Dissolution Method

A stock solution of pure NVP of approximately 1 mg/mL was prepared as described in §2.5.3. Aliquots of the stock solution were transferred into 20 mL A-grade volumetric flasks and diluted with 50 mM phosphate buffer of pH 6.8 to produce solutions with final concentrations of 1, 10, 20, 40, 120, and 220 μg/mL. The samples were mixed with an aliquot

of internal standard solution prior to RP-HPLC analysis (n = 3). Linearity was established using least squares linear regression analysis of the observed responses.

3.4.3 Precision

The precision of the method was evaluated by analysing the same samples used to establish the linearity of the method. The samples were analysed for repeatability and intermediate precision and the results were reported as %RSD with an acceptance limit set at ≤ 5%.

3.4.4 Accuracy

The accuracy of the method was established by spiking a known amount of NVP into each of the dissolution vessels with a final volume of 250 mL of 50 mM phosphate buffer medium of pH 6.8 to produce solutions corresponding to concentrations of 80, 100 and 120% of the nominal assay concentration. The solutions were then sampled and analysed in triplicate and the % recovery recorded.

3.4.5 Stability of Sample Solutions in Dissolution Medium

The stability of NVP in 50 mM phosphate buffer of all pH that were used in these studies was assessed by exposing a known quantity of pure NVP to dissolution test conditions and storing at 37.0 ± 0.5 °C, room temperature *viz*., 22.0 °C, and in a refrigerator between 2 – 8 °C for 48 hours. The samples were then analysed and the % recovery determined at 0 h, 24 h and 48 h following storage. ANOVA was used to analyse the stability of NVP samples in a 50 mM phosphate buffer of pH 1.6, 4.7 and 7.4 (representing low, medium and high pH range used for dissolution studies) stored at 37 ± 0.5 °C, 22.0 °C and 2 – 8 °C to determine how long NVP samples could be stored prior to analysis.

3.4.6 Comparison of Dissolution Profiles

A model independent method recommended for use by FDA [196] was used to compare the dissolution profiles that were generated. This method requires the calculation of an f_1 and f_2 factor for the two curves being compared and was first described by Moore and Flanner [199]. The f_1 factor measures the percent error between two curves over all time points and should result in a value between 0 and 15 for the two profiles to be considered statistically similar. The f_2 factor is a logarithmic transformation of the sum-squared error of the differences between a test and reference product over all time points under investigation and

will have a value between 50 and 100 for any two profiles to be considered similar [200]. The FDA only recommends the use of the f_2 factor as it has been shown to be more sensitive in describing differences between two profiles [201]. However, for the purposes of these studies both the f_1 and f_2 values were used to make decisions. The two factors, f_1 and f_2, can be calculated using Equations 3.2 and 3.3, respectively.

$$f_1 = \{[\sum_{t=1} n \, |R_t - T_t|]/ [\sum_{t=1} n \, R_t]\}*100 \qquad \textbf{Equation 3.2}$$

$$f_2 = 50*\log \{[1 + (1/n)\sum_{t=1} n \, (R_t-T_t)^2]^{-0.5} *100\} \qquad \textbf{Equation 3.3}$$

where,

R_t = the cumulative percentage API dissolved for reference product,
Tt = cumulative percentage API dissolved for test product, and
n = the number of time points.

The value of f_2 is sensitive to the number of dissolution time points that are used and only one time point should be used after 85% of the API in a dosage form has been released from a product [202].

3.5 RESULTS AND DISCUSSION

3.5.1 Effect of SLS on Dissolution Rate of NVP

The selection of an appropriate dissolution medium for assessing the dissolution rate of a sparingly soluble API is challenging, as it is often difficult to achieve sink conditions. Sink condition is defined as the volume of medium that is at least three times greater than that required to dissolve the total dose of an API in the product under investigation, for example this would be at least three times the volume required to dissolve 100 mg of NVP [173, 195, 203]. The addition of a small amount of surfactant to a dissolution test medium for testing poorly water soluble compounds has been suggested as an appropriate way to better simulate the GIT environment and to achieve sink conditions [195, 204]. However, the lowest possible concentration of surfactant to achieve 75-80% API release within a reasonable test time must be used [205].

The dissolution profiles depicting drug release in 50 mM phosphate buffer of pH 6.8 using different concentrations of SLS are depicted in Figure 3.1.

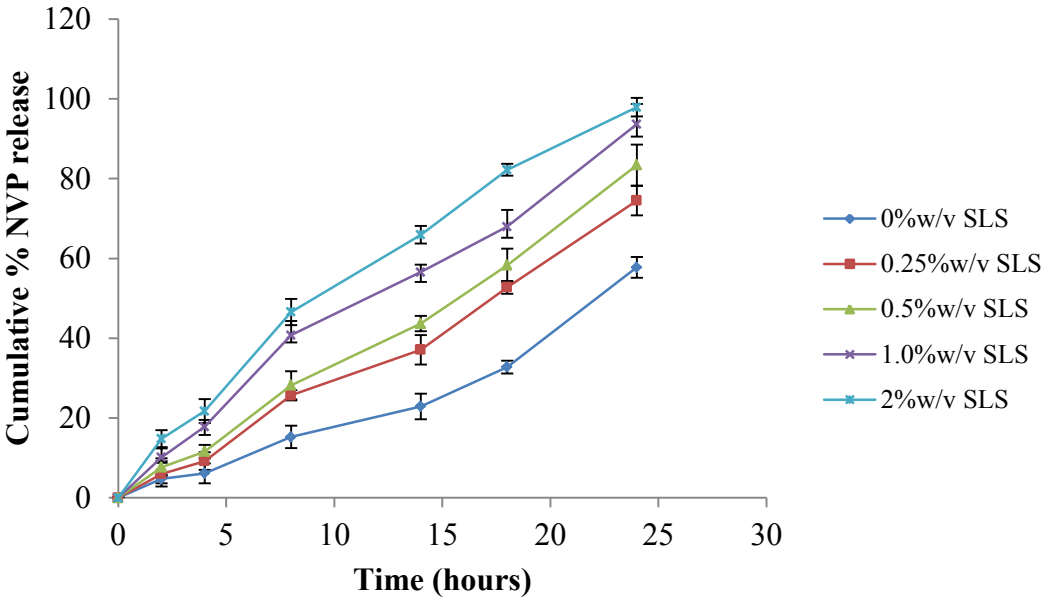

Figure 3.1. NVP dissolution profiles in 50 mM phosphate buffer with different amounts of SLS (n= 6, dip rate = 8 dpm, pH = 6.8).

Increasing the amount of SLS in the dissolution medium resulted in an increased rate and extent of dissolution of NVP which has also been reported for other compounds [195, 203, 205]. The increase in the extent of drug release can be attributed to the increased solubilisation of NVP due to improved wetting of the dosage form and NVP particles.

Comparison of the f_1 and f_2 factors in Table 3.4 revealed that dissolution profiles from media with different concentrations of SLS were different except for those with 1 and 2 % SLS, although inspection of the two profiles showed that the rate of NVP release was higher in medium containing 2% SLS and the profiles were slightly different. Therefore 2.0% w/v was selected as it resulted in slightly higher rate of release and resulted in the requisite 80% release from NVP tablets.

Table 3.4. Comparison of dissolution profiles of NVP release in medium with different concentrations of SLS

Profiles compared	f_1	f_2
0 % vs. 0.25 %	47.1	44.4
0 % vs. 0.5 %	66.8	37.2
0 % vs. 1 %	105.6	28.2
0 % vs. 2 %	135.9	23.0
0.25 % vs. 0.5 %	13.4	63.5
0.25 % vs. 1 %	39.8	41.6
0.25 % vs. 2 %	60.4	32.8
0.5 % vs. 1 %	23.2	50.5
0.5 % vs. 1 %	41.4	38.2
1 % vs. 2%	14.7	54.8

Red = out of specifications

3.5.2 Effect of Agitation Rate on Dissolution Rate

The dissolution profiles generated using agitation rates of 5 dpm, 10 dpm, 15 dpm or 50 rpm are shown in Figure 3.2 and the f_1 and f_2 values calculated from the comparison of dissolution profiles using data from USP Apparatus 3 (Test) to that of USP Apparatus 2 (Reference) are listed in Table 3.5.

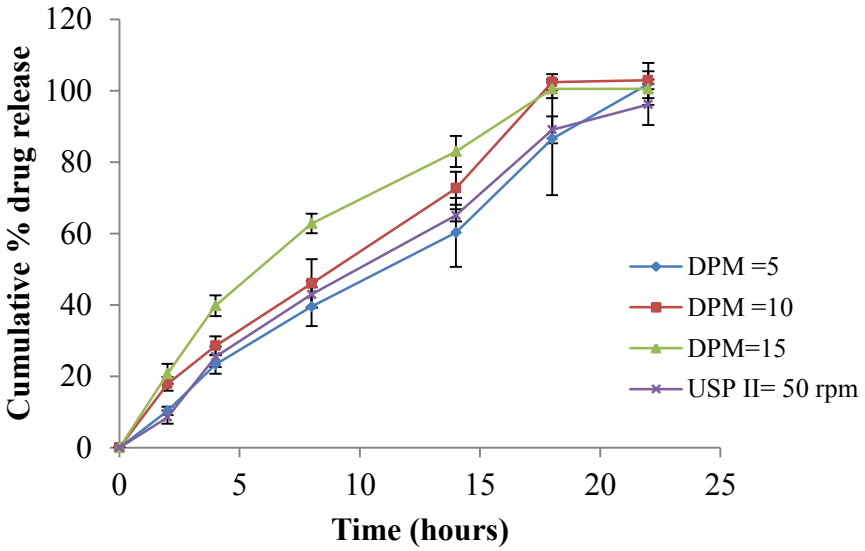

Figure 3.2. Dissolution profiles of NVP using different agitation rates in 50mM phosphate buffer, pH = 6.8.

Table 3.5. Comparison of dissolution profiles obtained from different dip speeds in USP Apparatus 3 to USP Apparatus 2 at 50 rpm

Reciprocation rate (dpm)	f_1	f_2
5	6.2	70.8
10	13.2	54.6
15	24.5	42.3

Red = out of specification.

These results indicate that the lower reciprocation rates of 5 and 10 dpm using USP Apparatus 3 produce dissolution profiles that are equivalent to a rotation speed of 50 rpm for USP Apparatus 2 and are in agreement with previously reported results [195]. Further inspection of the dissolution profiles generated using USP Apparatus 2 and 3 suggest that the f_2 factor may improve if dissolution testing were to be performed using dip rates of between 5 and 10 dpm. Consequently a dissolution test using USP Apparatus 3 was performed at a dip rate of 8 dpm and yielded f_1 and f_2 factors of 2.4 and 88.9, respectively. Therefore, a dip rate of 8 dpm was selected for use for all NVP dissolution studies. The results reveal that NVP release from tablets increases with an increase in agitation rate and are in agreement with previously reported data [170, 173, 192, 195]. Analysis of the f_1 and f_2 factors revealed statistical differences in the dissolution profiles as shown in Table 3.6, and showed that large differences in agitation rates yielded very different dissolution profiles.

Table 3.6. Comparison of NVP dissolution profiles at different agitation rates

Profiles compared	f_1	f_2
5 dpm vs. 10 dpm	15.7	50.5
5 dpm vs. 15 dpm	30.9	37.4
10 dpm vs. 15 dpm	13.1	50.8
8 dpm vs. 50 rpm	2.4	88.9

Red = out of specification

Most modified release dosage forms exhibit faster dissolution rates as agitation rates or speeds are increased. Mild agitation conditions are recommended for use during dissolution testing to permit use of the maximum discriminating power of a method in order to be able to detect products that may exhibit poor *in vivo* performance. Therefore, a desirable agitation rate or speed by rotation of the basket or paddle, dip rate of a reciprocating cylinder or flow rate for USP Apparatus 4 must be adjusted to yield a result for which 80% of the API is dissolved by the end of the specified test interval, as recommended in the FIP guidelines [206].

3.5.3 Effect of Mesh Size (MS) on the Rate and Extent of NVP Dissolution

Studies have been undertake to investigate the effect of mesh size on the rate and extent of drug release from dosage forms [192, 198]. In general the extent of API release increases with an increase in the mesh size used [197]. The impact of API release rates whilst, dependent on the size of the mesh of the top screen, release does not appear to be affected by that of the bottom mesh size as studies on the effect of the bottom mesh screen size did not reveal any differences in percent drug released [192]. However the lack of difference in the results observed were attributed to the use of a high agitation rate of 30 dpm which offsets the effect of mesh size within the first two hours of commencing dissolution testing.

The dissolution profiles of NVP from tablets using different sizes of mesh screens are shown in Figure 3.3.

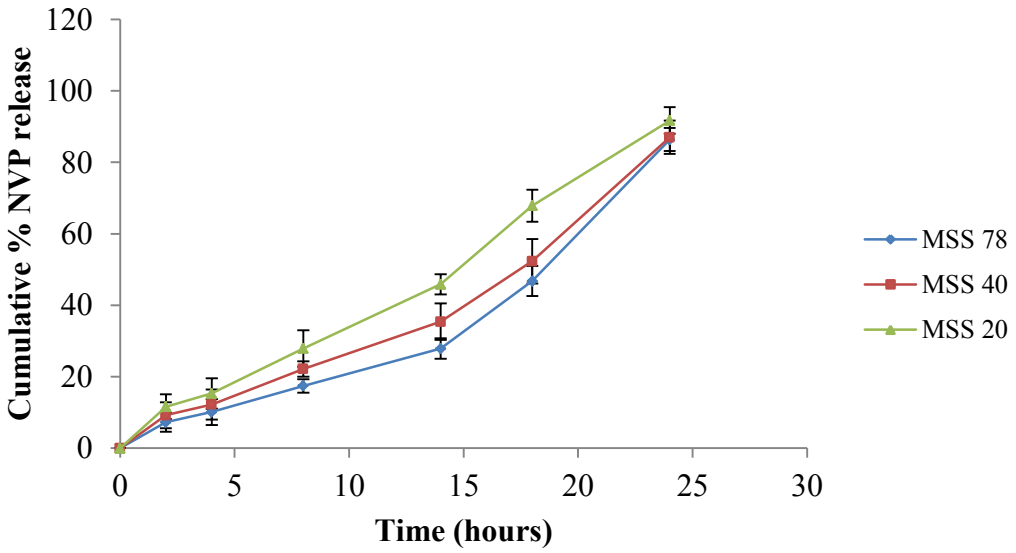

Figure 3.3. NVP dissolution profiles using mesh screens of different size in 50 mM phosphate buffer of pH 6.8 (n = 6, dip rate = 8 dpm).

The rate of NVP release increased with an increase in the mesh size, however the extent of API release from NVP tablets did not appear to be affected by the mesh size used. This may be attributed to the fact that complete drainage of the dissolution medium from the inner cylinders, regardless of the size of the mesh used occurred or may well be a consequence of hydrodynamic forces having a more pronounced effect on NVP release than the mesh size after a specific length of time during dissolution testing.

An analysis of the f_1 and f_2 factors revealed that the dissolution profiles generated with the use of MS 20 and 40 were similar whereas those from MS 20 and 78 were different as shown in Table 3.7.

Table 3.7. Comparison of dissolution profiles of NVP generated from using different mesh screen sizes

Profiles compared	f_1	f_2
20 vs. 40	11.5	67.1
20 vs. 78	32.9	44.9
40 vs. 78	19.2	53.7

Red = out of specification

A mesh of screen size 20 was selected for use as it appeared to produce better drainage which is an important aspect when using USP Apparatus 3.

3.5.4 Effect of Buffer Molarity on Dissolution Rate

The dissolution rate of NVP did not seem to be significantly affected by the molar strength of the buffer used, although a slight increase in the dissolution rate of NVP was observed with an increase in molarity up to 8 hours of dissolution testing as depicted in Figure 3.4. However, after 8 hours of dissolution testing the molarity did not appear to affect the rate of NVP release to any great extent.

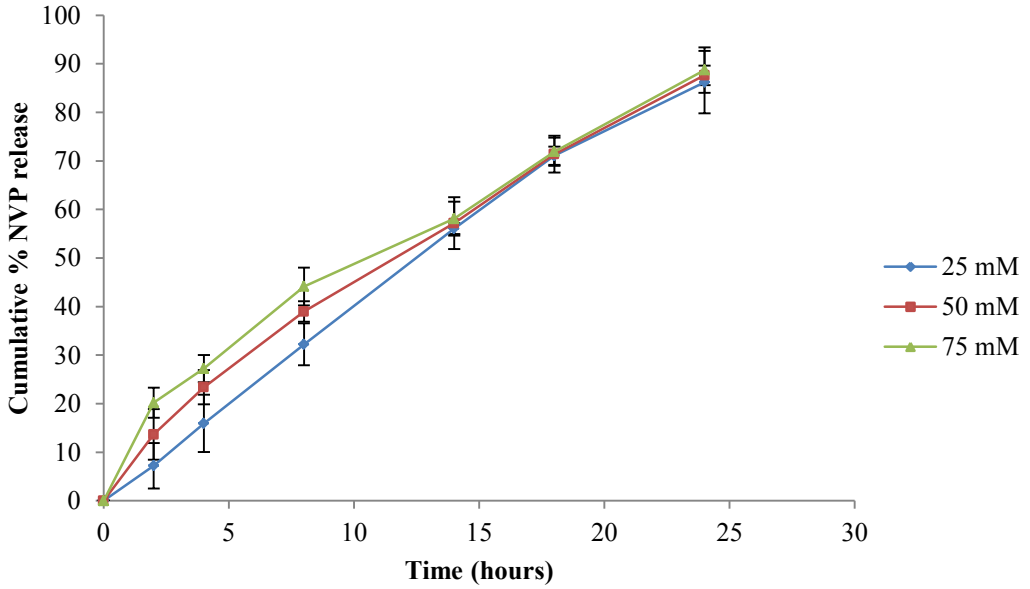

Figure 3.4. NVP dissolution profiles in media of different molarity (n = 6, dpm = 8, pH = 6.8).

Analysis of the f_1 and f_2 factors showed that dissolution profiles were similar but the f_2 factor decreased with an increase in the difference in molarity, for example a comparison of the profiles for NVP release in dissolution media of 25 mM and 50 mM revealed that they were more similar to each other compared to profiles for buffers of 25 mM and 75 mM. A summary of the f_1 and f_2 analysis is shown in Table 3.8.

Table 3.8. Comparison of dissolution profile of NVP generated from use of different molarity media. Red = out of specification

Profiles compared	f_1	f_2
25 mM vs. 50 mM	8.7	64.9
25 mM vs. 75 mM	15.5	53.0
50 mM vs. 75 mM	6.2	70.3

Red = out of specification

The studies revealed that any of the molarities studied could be used for dissolution testing and a 50 mM buffer was selected for all future experiments as it is the standard buffer used for dissolution studies in our laboratory.

Following evaluation of the dissolution parameters that may affect NVP release from tablets a specific set of dissolution conditions were selected for use and these are listed in Table 3.9.

Table 3.9. Summary of selected dissolution conditions

Parameter	**Settings**		
Medium	250 mL of 50 mM phosphate buffer containing 2.0% w/v SLS		
	Row	pH	Time in medium (h)
	Formulation development		
	1	1.2	2
	2	7.2	6
	3	7.2	6
	4	7.2	4
	5	7.2	4
	6	7.2	2
	Optimised formulation		
	1	1.6	2
	2	3.4	2
	3	4.7	4
	4	6.8	6
	5	7.2	4
	6	7.2	6
Agitation rate	8 dpm		
Mesh screen size	20 (840 µm) top and bottom		
Temperature	37 0.5 °C		

3.6. METHOD VALIDATION

3.6.1 Specificity

The chromatograms of NVP in 50 mM phosphate buffer of pH 6.8 containing 2% w/v SLS did not show any evidence of interference from tablet excipients as shown in Figure 3.5 and the method was therefore regarded as specific for NVP under these conditions.

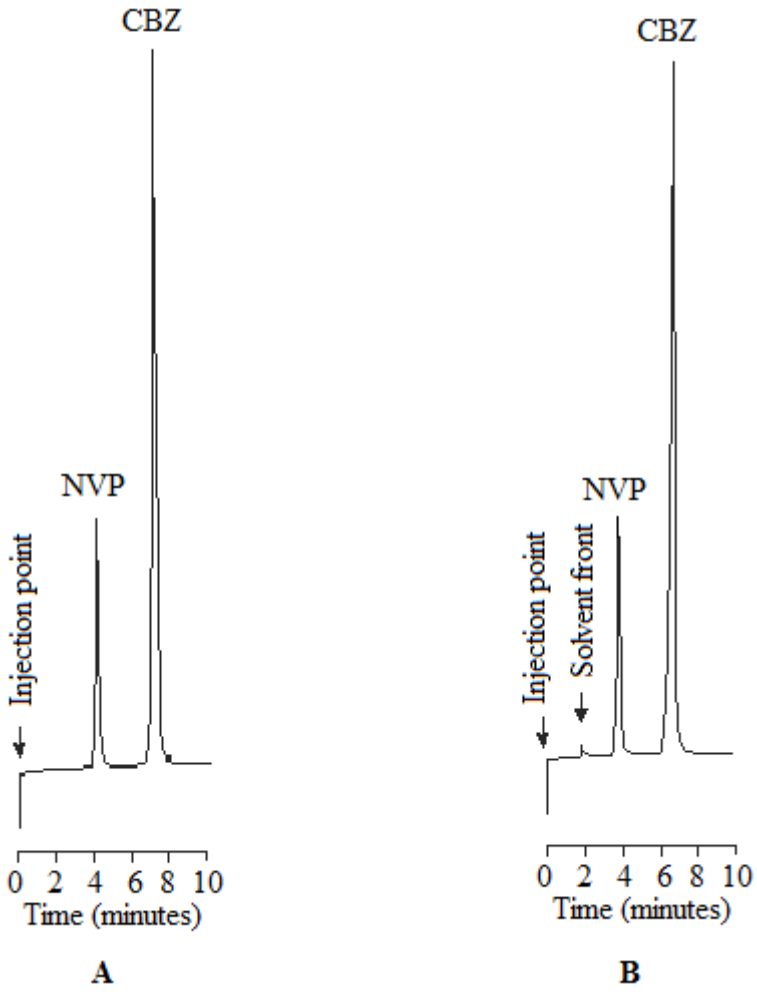

Figure 3.5. Comparison of chromatograms of a standard solution of NVP (A) and NVP from tablets in dissolution medium (B) (30 µg/mL).

3.6.2 Linearity and Range

The method was found to be linear over the concentration range 1 - 220 µg/mL with the calibration curve yielding a correlation coefficient value of 0.9997, a slope of 0.0047 and a y-intercept of - 0.006. The calibration curve for NVP in 50 mM phosphate buffer of pH 6.8 containing 2% w/v SLS is shown in Figure 3.6.

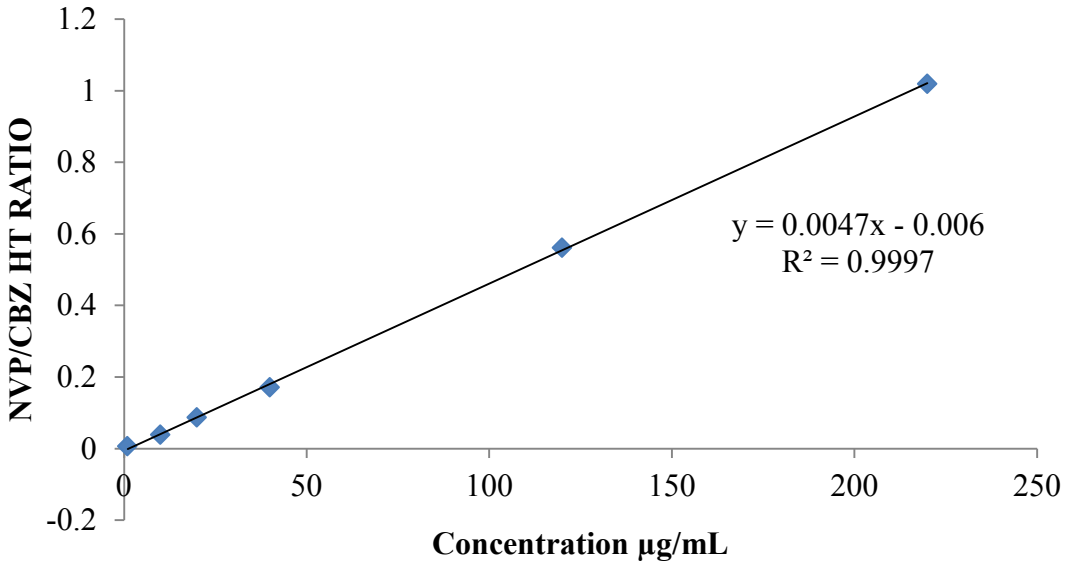

Figure 3.6. Calibration curve for NVP over the concentration range 1 – 220 µg/mL (n = 3).

3.6.3. Precision

The repeatability and the intermediate precision of the method were found to be acceptable with the acceptance criterion for % RSD ≤ 5% and these data are summarised in Tables 3.10 and 3.11.

Table 3.10. Results for repeatability studies

Concentration µg/mL	Average NVP/CBZ HT ratio n =3	SD	%RSD
1	0.0048	$4.3895E^{-05}$	0.9225
10	0.0394	$8.6958E^{-05}$	0.2208
20	0.0715	0.00051	0.7175
40	0.1591	0.00183	1.1475
120	0.4525	0.00269	0.5940
220	0.9339	0.00081	0.0873

Table 3.11. Results for intermediate or inter-day precision

Day	Concentration µg/mL	NVP/CBZ HT Ratio n = 3	SD	%RSD
1	**1**	0.0079	0.0001	1.3974
	10	0.0789	0.0003	0.3533
	20	0.1452	0.0009	0.5996
	40	0.3412	0.0015	0.4339
	120	1.0532	0.0024	0.2245
	220	2.0514	0.0032	0.1583
2	**1**	0.0053	0.0001	1.2775
	10	0.0907	0.0008	0.8927
	20	0.1845	0.0018	0.9810
	40	0.3167	0.0014	0.4414
	120	1.1142	0.0051	0.4584
	220	2.0304	0.0062	0.3046
3	**1**	0.0084	0.0003	3.1229
	10	0.0796	0.0008	1.0052
	20	0.1474	0.0008	0.5445
	40	0.3408	0.0004	0.1293
	120	1.0229	0.0009	0.0874
	220	1.8708	0.0246	1.3160

3.6.4 Accuracy

The percentage recoveries established through accuracy studies for the three concentrations under investigation are listed in Table 3.12.

Table 3.12. Results for accuracy studies

Theoretical concentration µg/mL	Average NVP/CBZ ratio (n=3)	Actual concentration µg/mL	% Recovery	SD	%RSD	%Bias
160	1.2832	157.54	98.46	0.03506	2.7321	1.5357
200	1.8935	198.22	99.11	0.02432	1.2844	0.8900
240	2.2733	236.49	98.54	0.0176	0.775	1.443

The % RSD and % Bias values were all within the acceptance criterion of ≤ 5% and therefore the method was considered accurate for *in vitro* analysis of NVP release from dosage forms.

3.6.5 Stability of NVP in Dissolution Medium

A summary of the % recoveries for the stability assessment of NVP in dissolution medium stored at different temperatures is listed in Table 3.13.

Table 3.13. Stability (%recovery) of NVP in dissolution media under different storage conditions

		%Recovery		
Condition	**pH**	**O h**	**24 h**	**48 h**
37.0 °C	1.6	98.67±0.0033	98.71 ±0.0094	98.52±0.026
	3.4	99.44±0.0012	98.95±0.0036	97.77±0.0012
	4.7	99.57±0.1120	99.48±0.0057	98.42±0.2087
	6.8	98.98±0.0052	98.80±0.0066	97.12±0.0076
	7.2	98.85±0.0252	99.04±0.0358	98.84±0.0271
22 °C	1.6	98.77±0.0093	98.78±0.0172	98.48±0.1727
	3.4	98.67±0.0092	97.99±0.0044	98.56±0.0042
	4.7	98.92±0.0137	98.66±0.0082	99.15±0.1276
	6.8	98.65±0.0079	98.93±0.0085	97.79±0.0084
	7.2	99.35±0.0014	98.68±0.0008	98.73±0.00123
2 – 8 °C	1.6	98.86±0.0025	98.89±0.0399	98.69±0.0100
	3.4	98.77±0.0037	98.49±0.0096	99.37±0.0069
	4.7	99.20±0.3804	99.12±0.0587	98.54±0.4297
	6.8	97.94±0.0039	98.36±0.0019	98.41±0.0045
	7.2	98.13±0.0004	97.92±0.0002	98.44±0.0020

Values reported as mean ± SD (n = 5)

NVP solutions (100 µg/mL) were found to be stable for 48 hours when stored at 37 °C in the dissolution medium that was selected for use. The NVP solution stored at 22 °C and 2-8 °C also remained stable for the entire storage period of analysis as all % recoveries remained unchanged.

ANOVA also confirmed that NVP was stable in 50 mM phosphate buffer of pH 1.6 stored at 37 °C, 22 °C and 2 – 8 °C for 48 hours. The results for ANOVA analysis for the stability of NVP in 50 mM phosphate buffer of pH 1.6 stored at these three temperatures are shown in Table 3.14.

Table 3.14. ANOVA single factor analysis for stability of NVP in 50 mM phosphate buffer of pH 1.6 stored at 37, 22 and 2-8 °C for 48 hours

Summary: 37 °C (n = 5)						
Time, h	**Count**	**sum**	**Average**	**Variance**		
0	5	494.67	98.6675	0.003292		
24	5	494.82	98.705	0.009367		
48	5	494.07	98.5175	0.026158		
ANOVA						
Source of variance	**SS**	**df**	**MS**	**F**	**p-value**	**F-critical**
Between Grps	0.07875	2	0.039375	3.043152	0.097829	4.25649
Within Grps	0.11645	12	0.012			
Total	0.1952	14				
Summary: 22 °C (n = 5)						
0	5	495.08	98.77	0.009333		
24	5	495.1	98.775	0.017233		
48	5	493.93	98.4825	0.172692		
ANOVA						
Between Grps	0.224317	2	0.112158	1.688637	0.238385	4.25649
Within Grps	0.597775	12	0.066419			
Total	0.822092	14				
Summary: 2 - 8 °C (n = 5)						
0	5	495.44	98.86	0.002467		
24	5	495.57	98.8925	0.039958		
48	5	494.77	98.6925	0.010025		
ANOVA						
Between Grps	0.09215	2	0.046075	2.635367	0.125627	4.25649
Within Grps	0.15735	12	0.017483			
Total	0.2495	14				

The null hypothesis was that NVP was stable in 50 mM phosphate buffer stored at 37 °C for 48 hours at 0.05 level of significance. The hypothesis was to be rejected if the value for the F-statistic was > F-critical value, or if the p-value was < 0.05. The F-value was 3.043152 which is smaller than the F-critical value of 4.25649 and the p-value was 0.09829 which is > 0.05 indicating that NVP was stable for 48 hour in 50 mM phosphate buffer of pH 1.6 stored at 37 °C.

Similarly, samples stored at 22 °C were stable with an F-value of 1.688637 which was < an F-critical value of 4.2549 and the p-value was 0.238385 as shown in Table 3.14. This indicated that NVP was stable in 50 mM phosphate buffer of pH 1.6 stored at 22 °C.

The ANOVA data for NVP concentrations following storage in a 50 mM phosphate buffer of pH 1.6 stored at 2 - 8 °C for 48 hours reveal that NVP was stable as the F-value of 2.635367 was smaller than the F-critical value of 4.25649 and the p-value was 0.125627 as listed in Table 3.14.

The ANOVA analysis for NVP stability in 50 mM phosphate buffer of pH 4.7 and 7.2 also revealed that samples stored at all temperatures investigated, *viz.,* 37°C, 22°C, and 2-8 °C, were stable having fulfilled the criteria of F-value < an F-critical value and p-value > 0.05 as shown in Tables 3.15 and 3.16.

Table 3.15. ANOVA single factor analysis for stability of NVP in 50 mM phosphate buffer of pH 4.7 stored at 37, 22 and 2-8 °C for 48 hours

Summary: 37 °C (n = 5)						
Time, h	**Count**	**sum**	**Average**	**Variance**		
0	5	497.83	99.566	0.11173		
24	5	497.41	99.482	0.00567		
48	5	490.73	98.416	0.20873		
ANOVA						
Source of variance	**SS**	**df**	**MS**	**F**	**p-value**	**F-critical**
Between Grps	0.07875	2	3.173627	2.919351	0.246	3.8852
Within Grps	0.11645	2	0.10871			
Total	0.1952	14				
Summary: 22 °C (n = 5)						
0	5	494.61	98.922	0.01367		
24	5	493.3	98.66	0.0082		
48	5	495.73	99.146	0.12763		
ANOVA						
Between Grps	1.184893	2	0.295847	3.885295	0.16129	5.9367
Within Grps	0.1208	12	0.049833			
Total	1.305693	14				
Summary: 2 - 8 °C (n = 5)						
0	5	495.98	99.196	0.38043		
24	5	495.96	99.12	0.05867		
48	5	492.68	98.536	0.42973		
ANOVA						
Between Grps	1.443253	2	0.721627	2.491719	0.124433	3.88529
Within Grps	3.47532	12	0.28961			
Total	4.918573	14				

Table 3.16. ANOVA single factor analysis for stability of NVP in 50 mM phosphate buffer of pH 7.2 stored at 37, 22 and 2-8 °C for 48 hours

Summary: 37 °C (n = 5)						
Time, h	**Count**	**Sum**	**Average**	**Variance**		
0	5	494.26	98.852	0.02522		
24	5	495.22	99.044	0.03578		
48	5	494.2	98.84	0.02705		
ANOVA						
Source of variance	**SS**	**Df**	**MS**	**F**	**p-value**	**F-critical**
Between Grps	0.13104	2	0.06552	2.232368	0.149885	3.88529
Within Grps	0.3522	2	0.02935			
Total	0.48324	14				
Summary: 22 °C (n = 5)						
0	5	496.74	99.348	0.00142		
24	5	493.42	98.684	0.00083		
48	5	493.63	98.726	0.00123		
ANOVA						
Between Grps	1.38257	2	0.691287	3.8852	0.0981	5.95937
Within Grps	0.01392	12	0.00116			
Total	1.396493	14				
Summary: 2 - 8 °C (n = 5)						
0	5	490.64	98.128	0.00037		
24	5	489.5	97.9	0.00025		
48	5	492.18	98.436	0.00203		
ANOVA						
Between Grps	0.723573	2	0.361787	3.885294	0.0906	4.09569
Within Grps	0.0106	12	0.000883			
Total	0.734173	14				

The stability of NVP in 50 mM phosphate buffer of pH 1.6, 4.7 and 7.2, which are representative of low, medium and high values of the pH range used in dissolution studies, as established by ANOVA and the % recovery gave an indication that NVP will be stable in 50 mM phosphate buffer media of various pH values used in these studies and that the samples could be stored for 48 hours prior to analysis.

3.7 CONCLUSIONS

Dissolution testing forms an integral part of the development and assessment of dosage forms and aids in the selection of initial formulation compositions. In addition dissolution testing facilitates the identification of suitable excipients to produce a desired release profile particularly for extended or sustained release formulations. The ultimate release profile that is selected may be critical for predicting the *in vivo* bioavailability of an API and the potential success of bioequivalence studies.

Dissolution testing is also a quality control tool that is used to assess the batch-to-batch performance of dosage forms and to provide continued assurance of product quality. The stability and shelf life of a product can also be assessed using *in vitro* dissolution data as any physicochemical changes associated with product aging may be revealed by altered dissolution characteristics of that dosage form over time. For example, a reduced dissolution rate may be associated with polymorphic transformations of an API to a more stable and less soluble crystalline form of that API that can be observed using a discriminatory dissolution test developed for that product.

Analytical methods for the assessment of pharmaceutical products need to be validated using regulatory guidelines, in order to produce meaningful, reliable and valid results. The rate at which drug particles are released into a dissolution medium are affected by a number of parameters including but not limited to the physicochemical properties of an API, formulation composition, manufacturing process variables, in addition to dissolution test apparatus type and method design.

Important factors to consider in respect to the test apparatus and effect on API release must be investigated and apparatus settings must be carefully selected in order to produce consistent and valid results. Such settings include for example, agitation rate, stirring element alignment, sample probe position, filter type, pore size and temperature of the dissolution medium. The effect of agitation rate on NVP release was investigated and different reciprocating rates for USP Apparatus 3 were tested to establish which rate would produce an equivalent response to that observed at 50 rpm when NVP tablets were tested using USP Apparatus 2. A low reciprocation rate of 5 – 10 dpm was found to produce dissolution profiles that were similar to the dissolution profiles generated using USP Apparatus 2 set at 50 rpm. Furthermore at these dip rates the dissolution method was able to permit discrimination of responses, which was not possible when a high agitation rate was used.

Close investigation of the dissolution profiles reveal that a reciprocation rate of 8 dpm produced a NVP dissolution profile that was closely related to the profile generated using USP Apparatus 2 and therefore, all dissolution studies were performed at a reciprocation rate of 8 dpm.

Parameters of the dissolution medium that should be considered when deciding on the parameters of a test method include buffer molarity, pH, presence of surfactants and volume. An increase in the molarity of the dissolution medium was found to increase the rate of NVP release slightly, however for each of the molarities tested the percent NVP released was above 85 % and 50 mM was selected for all future experiments. Increasing the concentration of SLS resulted in an increase in the dissolution rate of the NVP from the tablets and a 2% w/v SLS concentration was selected for all future experiments as the dissolution medium containing this concentration met the requisite of > 80% NVP release from the tablets.

The dissolution method passed the validation standards for stability of NVP in dissolution media, specificity, linearity and range, repeatability, intermediate precision and accuracy as defined by the ICH [147]. Therefore the dissolution method that was developed in these studies is regarded as an appropriate tool for use in the evaluation of NVP SR formulations and the impact of formulation composition and product quality attributes on drug release. Furthermore the method can be applied to quality control assessment of NVP dosage forms.

CHAPTER FOUR

PREFORMULATION AND ASSESSMENT OF POWDER BLENDS FOR NVP SUSTAINED RELEASE TABLETS

4.1 INTRODUCTION

Tablets are the most commonly used form of pharmaceutical solid oral dosage forms worldwide [207] and extensive data is required for the production of tablets of appropriate quality [208]. Preformulation approaches for the production of generic tablet products involve the study of the physicochemical properties of an API, excipients, API-excipient compatibility and stability [207]. Other preformulation procedures include defining the target product quality profile, designing and developing the product and manufacturing processes, identifying critical quality attributes, process parameters, sources of variability and controlling different manufacturing parameters to produce a product of consistent quality over time [208].

The challenges faced during dosage form development include excipient selection, poor powder flow, tableting process issues and the production of tablets of poor quality that lack tensile strength, exhibit high levels of friability, prolonged disintegration times and low dissolution rates amongst others. Most of these difficulties are a consequence of the mechanical properties of powders and include elasticity, brittleness, plasticity, compressibility and flow characteristics amongst others [207, 209].

4.2 SELECTION OF PHARMACEUTICAL EXCIPIENTS

The ICH guidelines [210] recommend that excipients should be selected with caution as the quality and sources of material vary by supplier and batch. The specifications for excipients should meet guidelines that have been put in place to aid the selection process and they should not be harmful, be physiologically inert, be non-toxic and must be listed as a GRAS (Generally Regarded As Safe) material [211]. The excipients should also exhibit stability with no evidence of drug-excipient incompatibility either as a physical or chemical interaction between the API and/or other excipients used in the formulation or with packaging materials [212, 213]. It is also important that excipients do not interfere with the validation process for manufacture and analytical testing [214]. The ease of accessibility, distribution, cost, satisfactory compliance with regulatory requirements, that may include

environmental issues in all countries where the product is marketed are other factors to be considered when selecting pharmaceutical excipients [207].

There are numerous other factors to be considered when selecting excipients for a formulation. For example, the type of excipient selected is highly dependent on the API to be delivered and the intended form and route of delivery. As a result appropriate formulation composition and parameters are critical and must be evaluated [215].

The formulation of sustained release tablets has been achieved using different polymers as release retarding agents that are often used in combination with other excipients that play different roles in the production of a successful dosage form.

4.2.1 Hydroxypropyl methylcellulose (HPMC)

HPMC is the most popular polymer used for matrix applications since it exhibits a number of key features and advantages, not the least of which is that it has been studied extensively, its use is well understood and HPMC has received global regulatory acceptance. HPMC exhibits excellent stability and the non-ionic nature of the polymer offers an advantage of producing formulations that exhibit pH independent performance. The different chemistry and viscosity grades of HPMC offer the formulation scientist versatility and ensure that a suitable grade is likely to be available for a variety of drug substances. HPMC can be used with ease when manufacture is to be achieved by direct compression or wet granulation and it is a readily available polymer [216].

Chemically, HPMC is a mixed alkyl-hydroxyalkyl cellulose ether that contains different numbers of methoxy and hydroxypropyl functional groups. The type and distribution of the functional group substitution and the average molecular weight of the polymer determine the physicochemical properties of that polymer and the grade designation. The grades of HPMC are distinguished by designation of a number that is indicative of the apparent viscosity of a 2% w/w aqueous solution of that polymer, measured at 20 °C [217].

HPMC has the ability to swell on contact with aqueous media, a property that has a considerable effect on the release kinetics of drugs dispersed in HPMC matrices. This characteristic is considered crucial to the successful use of the polymer in sustained drug delivery [218].

HPMC exhibits good compression characteristics and the swelling properties coupled with the ability to accommodate high levels of API make it an excellent candidate for it as a release rate retarding polymer [219]. The physicochemical properties of HPMC remain unaltered by shear forces that are applied to powder blends during aqueous granulation, during which water facilitates chain mobility and spreading and are thus able to produce dosage forms with consistent performance [220].

The solubility of the API is an important property to be considered when establishing the viscosity grade of polymer to be used to retard drug release [221-223]. NVP is a sparingly soluble compound in water and the use of high and low viscosity grades of HPMC were investigated for their suitability as matrices for the manufacture of SR NVP tablets. Methocel K4M, K15M and K100M were the grades of HPMC used in these studies.

4.2.2 Methacrylic Acid Copolymers

The most widely used methacrylic acid copolymers include Eudragit® RS and RL that are bio-compatible copolymers synthesised from acrylic and methacrylic acid esters. Eudragit® RS and RL differ in molecular structure due to different degrees of substitution of the quaternary ammonium functionality. Eudragit® RS exhibit a lower degree of substitution (5%) than Eudragit® RL (10%). The ammonium groups exist as salts that impart pH-independent permeability to the polymers [224].

Eudragit® RL is more hydrophilic than Eudragit® RS and thus allows water to permeate through films more readily and the polymers are useful for the formulation of extended release matrix tablets, for tablet coating and microencapsulation of particles [224].

Methacrylic acid copolymer is obtained following full polymerisation of methacrylic acid and an acrylic or methacrylic ester. Types A (Eudragit® L, Eudragit® RL), B (Eudragit® S, Eudragit® RS) and C (Eudragit® L 30 D-55) have been developed and vary in methacrylic acid ester content and viscosity of solution. These polymers have molecular weights in excess of 100 000 mass units and solid polymeric material is useful for use in direct compression tableting at concentrations of between 10 and 50% [225].

Eudragit® NE 30D is a neutral aqueous ester dispersion that consists of polymethacrylic acid esters with a milky-white appearance, has a low viscosity with an aromatic odour. It is

suitable for use in granulation processes for the manufacture of sustained release matrix tablets [226].

Eudragit® RL 30D and RS 30D are 30% w/v aqueous dispersion copolymers of acrylic and methacrylic acid esters with a low content of quaternary ammonium functional groups [226].

4.2.3 Carbomers

Carbomers are high molecular weight synthetic polymers of acrylic acid that are cross-linked with either allyl sucrose or allyl ethers of pentaerythritol and contain between 52% and 68% carboxylic acid (COOH) functional groups calculated on a dry basis [217, 227].

Carbomers are used in tablet formulations as controlled release agents or binders and unlike linear polymers, higher viscosity grades do not result in slower drug release as low cross-linked polymers are generally more efficient in controlling drug release than the highly cross-linked polymers [217].

Four carbomer polymers for use in oral dosage forms are available and include Carbopol® 934P NF, Carbopol® 974P NF, Carbopol® 971P NF and Carbopol® 71G NF [217]. Carbopol® 71G NF was selected for use in these studies.

Carbopol® 71G NF was designed for use in solid oral dosage applications and a unique feature of the polymer is its granular nature in contrast to other Carbopol® polymers that are supplied as powders [228, 229].

Carbopol® 71G NF is a free-flowing granular polymer for use in direct compression formulations that is manufactured by roller compaction and is chemically, the same product, with no additives as the powdered form of the polymer. The granules are free flowing, have increased bulk density and contain a minimal amount of small particles that cause dusting and/or static adherence that is usually observed with the powdered form of the polymer [228].

Typical levels of carbomer that are used to achieve extended release characteristics in tablets that are manufactured by direct compression are between 10 and 30 %w/w depending on the properties of the API and co-excipients used in the formulation [228, 230].

Carbopol® 71G NF can be combined with other extended release excipients to improve the flow properties of a formulation. Powdered or granular grades of Carbopol® polymers can be combined in a formulation to achieve a targeted release profile. The release rates can be

modulated by blending of powdered carbomer with granular carbomer in appropriate proportions [228, 230].

4.2.4 Dibasic Calcium Phosphate (DCP)

DCP occurs as a white, odourless, tasteless powder or as a monoclinic crystalline solid. Two particle size grades of DCP dihydrate are used in the pharmaceutical industry. Milled material is typically used in wet granulated, roller compacted or slugged formulations whereas the 'unmilled' or coarse grade material is typically used in direct compression formulations [231]. The coarse-grade DCP has good flow characteristics and is usually added to formulations to increase the general flow properties and compaction of a powder blend [232]. DCP is abrasive and the use of a lubricant such as magnesium stearate is essential to facilitate tablet production. The dehydrated form of DCP is non-hygroscopic and is stable at room temperature, however under certain conditions DCP can lose the water of crystallisation below 100 °C [231]. This phenomenon has implications for packaging and aqueous film coating processes, since the loss of water of crystallisation appears to be initiated by high humidity conditions. Therefore by implication, a high concentration of moisture vapour in the vicinity of DCP particles is expected [231, 232]. The surface of DCP dihydrate is alkaline and consequently it should not be used with drugs that are sensitive to alkaline pH [217]. The coarse grade of DCP dihydrate was selected for use in these studies.

4.2.5 Microcrystalline Cellulose (MCC)

MCC is purified, partially depolymerised cellulose that occurs as a white, odourless, tasteless, crystalline powder that is composed of porous particles. It exists in different particle size and moisture grades that have different properties and applications. Avicel® PH102 was used in these studies because of its good flow properties. Avicel® PH102 has a true density of 1.420-1.460 g/cm^3, a nominal mean particle size of 100 μm and specific surface area of 1.21-1.30 m^2/g with a moisture content ≤ 5.0%. MCC is a stable hygroscopic material and bulk material should be stored in a well closed container in a cool dry place [217].

4.2.6 Spray Dried Lactose (SDL)

Lactose exists as white to off-white crystalline particles or powder and is odourless with a slightly sweet taste [233]. Direct compression grades of SDL are generally composed of 80-90% specially prepared pure α-lactose monohydrate in addition to 10-20% amorphous lactose

[234, 235]. SDL is widely used as a binder, filler-binder and flow aid for direct compression tableting and SuperTab® 11SDL was used in this study due to its flow properties which would improve the flow characteristics of the powder blends to be manufactured in these studies [217].

4.2.7 Magnesium Stearate (Mg Stearate)

Mg stearate is comprised of magnesium and a mixture of solid organic acids that consists primarily of variable proportions of magnesium stearate and magnesium palmitate obtained from sources of vegetable or animal origin [236]. Mg stearate is a very fine, light white, precipitated or milled, impalpable powder of low bulk density that has a faint odour of stearic acid and a characteristic taste [236, 237].

Mg stearate is primarily used as a lubricant in capsule and tablet manufacture at concentrations between 0.25 and 5.0% w/w. The lowest possible amount of Mg stearate should be used as high levels may result in retardation of drug release from dosage forms due to the hydrophobic nature of the material [238, 239]. Mg stearate has a bulk and tapped density of 0.159 g/cm^3 and 0.286 g/cm^3, respectively, a true density of 1.092 g/cm^3 and melts between 117-150 °C [217].

4.2.8 Talc

Purified talc is hydrated magnesium silicate that may contain small and variable amounts of aluminium silicate and iron. Talc is a very fine, white to greyish-white, odourless, impalpable, unctuous crystalline powder that is used as a glidant and lubricant for tablet production at concentrations of between 1.0 and 10.0% w/w [240]. The particle size distribution of talc varies with the source and grade of the material and two typical grades exist *viz.,* a grade for which ≥ 99% of the particles pass through a 74 μm or #200 mesh or a grade for which ≥ 99% passes through a 44 μm or #325 mesh. Talc adsorbs an insignificant amount of water at 25 °C at a relative humidity of 90%. Talc has a specific gravity of 2.7-2.8 and a specific surface area of 2.41-2.42 m^2/g [217].

4.2.9 Colloidal Silicon Dioxide

Colloidal silicon dioxide is sub-microscopic fumed silica with a particle size of approximately 15 nm. It is a light, loose bluish-white coloured, odourless, tasteless and amorphous powder. Several grades of silicon dioxide are available for use and are produced

by modification of the manufacturing process. The small particle size and associated large specific surface area impart desirable flow characteristics that can be exploited to improve the flow properties of dry powders. Colloidal silicon dioxide is used as a glidant in tablet formulations at concentrations of 0.1-1.0% w/w [217].

A summary of the excipients that were investigated for use for the development of a NVP sustained release tablet with their respective sources and use is summarised in Table 4.1.

Table 4.1. Excipients used in NVP SR tablet formulation development

Excipient	Source	Use
Nevirapine	Boehringer Ingelheim, USA	API
HPMC (Methocel® K4M, K100M)	Colorcon® LTD, Dartford, Kent, UK	Release rate control polymer
Carbomer (Carbopol® 71G NF)	Noveon®, Inc., Brecksville, Cleveland, USA	Release rate control polymer
Ammonio methacrylate (Eudragit® RS PO)	Rohm Pharma Polymers, Darmstadt, Germany	Release rate control polymer
MCC (Avicel® PH102)	FMC® Biopolymer, USA	Filler
Spray-Dried Lactose (SuperTab®)	Lactose New Zealand	Diluent
Magnesium Stearate	Aspen® Pharmacare, SA	Lubricant
DCP (Emcompress®)	Penwest® Pharmaceutical Co., Mendel, UK	Flow-aid/filler
Talc	Aspen® Pharmacare, SA	Glidant
Colloidal Silicon Dioxide	Aspen® Pharmacare, SA	Glidant

4.3 PHYSICOCHEMICAL PROPERTIES

Prior to manufacturing solid dosage forms, it is necessary to understand and characterise the physical and chemical properties of the API, excipients and their powder mixtures, including crystal habit, particle size, shape, flow characteristics, density, hygroscopicity and compaction behaviour [241]. Successful tableting operations require the selection of excipients that balance desirable physical, flow and mechanical properties for tablet manufacturing [241, 242]. The bioavailability of an API can be affected by the physicochemical properties of excipients [243, 244], therefore the physical characteristics of API and excipients were examined and the characteristics investigated included particle size, shape, powder density and flow properties.

4.3.1 Particle Size and Shape

The measurement of particle size and distribution is an important parameter that must be evaluated during preformulation studies. The safety, stability and viability of an API and dosage form during and after manufacture can be significantly influenced by this parameter [207, 217].

Furthermore, the particle size of an API and excipients can affect uniform mixing, flow and, formulation characteristics, unit to unit content uniformity, dissolution rate and the bioavailability of an API [245].

Powder characteristics such as porosity and flowability are significantly affected by the particle size of excipients and API. Therefore detailed information of the particle size of an API, excipients and other materials or blends must be ascertained prior to tablet formulation development studies. During the tableting process the particle size of a material is important as it can have an impact on the homogeneity of a powder blend and of the final tablet. The ideal size range of particles for use in tableting is between 10 and150 μm and the particle size should be as consistent as possible throughout the production process [245].

Particle size is expressed in terms of the diameter and degree of asymmetry of particles and as asymmetry increases the difficulty of expressing size in terms of diameter is compounded [246]. A powder is regarded as monodisperse if all particles in a sample are of the same size and is polydisperse, if they are of different sizes. A monodisperse particle size distribution is more desirable than a polydisperse one [245].

Good powder flow properties are required for the successful manufacture of tablets as adequate fluidity of powders is necessary to facilitate the transport of material from a blender to the hopper and onto the die table of the tablet press. Elongated particle shape and small size may result in unacceptable blend uniformity, difficulty in filling die cavities and high variability of weight and strength of tablets [245-247].

The flow of powders into orifices is important when filling the die cavity of a tableting press and the flow into or through an orifice is dependent on the particle size of the material. Generally, as the particle size increases the powder flow rate increases up to a maximum and practically no flow occurs if the particle size of a powder is < 50 μm or > 1200 μm. Powders

with particles < 50 μm generally exhibit irregular or no flow due to particles agglomeration as a consequence of Van der Waal's forces [245].

The Hausner ratio (HR) and Carr compressibility index (CI) of powders provide an indication of powder flowability. The HR ranges from 1.2, for a free flowing powder, to 1.6 for a cohesive powder and the lower the CI of an excipient or powder blend the more acceptable the powder flow. The interpretation of the values of the HR and CI for powder flow is summarised in Table 4.2. The addition of a lubricant to a powder blend can significantly improve powder flow when the value of CI is above 20% [248].

Table 4.2. Interpretation of Hausner Ratio and Carr's Index

Hausner Ratio	**Flow**
< 1.25	Good
> 1.50	Poor
Carr Index %	
5-12	Excellent
12-16	Good
81-21	Fair
23-35	Poor
33-38	Very poor
> 40	Extremely poor

The angle of repose (AOR) is another common method that is used to measure powder flow when small sample quantities of material are available. The powder to be evaluated is poured from a funnel onto a horizontal surface so as to form a cone with only gravitational force, effecting the flow. The angle between the side of the cone and the horizontal is called the AOR and is a measure of the cohesiveness of a powder as it reflects the point at which inter-particulate attraction exceeds gravitational pull on the particles in that powder. A free flowing powder will form a cone with shallow sides and therefore a small AOR, whereas a cohesive powder will form a cone with steep sides. An AOR < 30° is indicative of good flow properties whereas powders with an AOR > 40° are likely to exhibit poor flow and the addition of a glidant may improve powder flow and the manufacturing process [245, 248]. The interpretation of the AOR is listed in Table 4.3.

Table 4.3. Interpretation of angle of repose

AOR	Flow
< 25	Excellent
25 – 30	Good
30 – 40	Fair (passable)
> 40	Very poor

4.3.2 Powder Density

The volume that a powder occupies when poured into a container is dependent on a number of factors including the particle size, shape and surface properties of the material. Subjecting a powder bed to vibration or pressure will result in the particles moving relative to one another in order to improve the packing arrangement in that container, by a process termed densification. Eventually a condition is reached where further densification of the powder is not possible without particle deformation. The density of the powder is therefore dependent on the conditions to which the material has been subjected to and several definitions can be used to describe the bulk powder or the individual particles of that power [245, 248].

4.3.2.1 Bulk Density

The bulk density of a powder refers to the volume of a specific mass of powder including the particulate and pore volume. The bulk density will vary depending on the packing arrangement of the powder. The minimum bulk density is achieved when the volume occupied by the powder is at a maximum, due to aeration that is present immediately prior to complete disruption of the bulk material [245, 248].

4.3.2.2 Tapped Density

The tapped density of a powder is the maximum bulk density that can be achieved without particle deformation [245]. It is established by tapping a fixed mass of material in the container in which the aerated sample is placed. If the structure of the powder is cohesive it will collapse significantly on tapping whereas a free flowing powder has little room for further consolidation [245-247].

The bulk and tapped densities were used to calculate CI, which was used in the assessment of powder flow characteristics of the materials used in these studies.

4.4 DRUG-EXCIPIENT COMPATIBILITY

Most of the approaches for the selection of an excipient for use in a formulation are often based on empirical approaches. Nevertheless excipients have the potential to precipitate chemical instability of an API and drug-excipient compatibility studies have been used as a basis for accepting or rejecting potential materials for inclusion in a formulation [245, 249-251].

Advanced analytical instrumentation is now available to facilitate the rapid identification of potential excipient induced instability and any material that exhibits an incompatibility with an API can be rejected early in development studies and removed from subsequent tablet formulation studies. The common approaches used for studying drug-excipient interactions include differential scanning calorimetry (DSC), thermogravimetric analysis (TGA), x-ray diffractiometry (XRD), Fourier transform infrared spectroscopy (FT-IR), Nuclear magnetic resonance spectroscopy (NMR) and scanning electron microscopy (SEM), amongst others. These methods and the utility of the information derived from these methods are summarised in Table 4.4.

Table 4.4. Techniques for testing drug-excipient compatibility and utility of data [207, 252]

Technique	Measurement	Utility of information
DSC	Energy is absorbed or released by a sample as it is heated, cooled or held at a constant temperature	Physicochemical compatibility of API and excipient, polymorph characterisation
TGA	Weight changes by a sample as it is heated, cooled or held at a constant temperature	Physicochemical compatibility of API and excipient, Stoichiometry of solvates and hydrates
Chromatographic Analysis	Chemical interactions of the sample with stationary and mobile phase	Excipient, API and drug product purity; excipient-API compatibility
Micro-calorimetry	Adsorption or release of API from a solution	Physicochemical compatibility of drug and excipients; solution application
X-ray Diffraction	Scattering of radiation by solid material	Polymorph characterisation
SEM	Magnified appearance of sample	Particle size and morphology
LC-MS/MS	Chromatographic separation and fragmentation of molecular species	Impurities, degradation product identification
FTIR	Absorption frequencies of functional groups	Characterisation and quantification of polymorphs, identification of interactions based on functional groups
NMR	Molecular arrangement	Studying molecular arrangement of polymorphs, hydrates and solvates
Hot-stage microscopy	Magnified appearance of sample	Studying solid state transition and desolvation events

DSC and TGA are techniques in which there is formation of a new peak as a result of an endothermic or exothermic reaction, and/or the disappearance of a peak. These two techniques have the advantage of being rapid analytical approaches [245]. TGA was used for thermal analysis of NVP while DSC and FT-IR where used to evaluate NVP-excipient compatibility in these studies. DSC and FT-IR were chosen as the equipment was readily available and were considered suitable to provide preliminary insight into NVP-excipient compatibility using thermal and non-thermal analytical techniques.

4.4.1 API-Excipient Interactions

Most excipients are pharmacologically inert, however chemical or physical interactions with API are often encountered and may affect the efficacy of a dosage form and/or API. The

multi-component nature of some excipients and formulations is usually the driving force of many of the interactions observed between an API and the components of a dosage form [253].

4.4.1.1 Mechanism of API-Excipient Interactions

4.4.1.1.1 Physical Interactions

A number of API excipient interactions do not involve any chemical changes in either of the compounds and whilst they are common, such interactions are difficult to detect. Physical interactions are frequently observed and/or used during the manufacturing process but are more often unintended and may cause manufacturing problems. Different physical interactions have been recognised and include the formation of solid dispersions, complexation and adsorption [254].

An example of a physical interaction that has been observed between primary amines and MCC results in the API binding to the MCC and is subsequently not released during dissolution testing and which is of particular importance for low dose drug products [253]. A further example of a physical interaction occurs during interactive mixing during which small particles interact with the surfaces of large carrier particles to ensure that a homogeneous powder blend is produced [253].

4.4.1.1.2 Chemical Interactions

Chemical interactions involve a reaction(s) between an API and an excipient and/or an API and impurities that may be present in the excipients. Chemical interactions are almost always detrimental to the stability and performance of a product as they generally result in the production of degradation products [253].

An example of a typical chemical interaction that often occurs is an interaction between the primary amine functional groups and the glycosidic hydroxyl group of the reducing sugars that precipitates a Maillard reaction to form imine that degrades further to form amidori type compounds and which has been observed with chlorpromazine and dextrose [255].

4.4.1.2 Beneficial API-Excipient Interactions

These interactions result in the formation of a dosage form with desirable characteristics and are usually physical in nature. An example is the simple manufacture of solid dosage forms in

the presence of Mg stearate which interacts with other excipients resulting in lubrication of powder blends. A further example includes cases where complexing agents such as cyclodextrins are reversibly bound to an API to form complexes that improve the bioavailability of poorly soluble drugs [256].

4.4.1.3 Detrimental API-Excipient Interactions

These interactions result in performance failure of dosage forms. For example, Mg stearate is known to cause reduced tablet strength and impact the dissolution rate of an API from tablets and capsules if it is used at high levels or if powders are subject to prolonged blending and this has been attributed to the hydrophobic nature of Mg stearate [257, 258].

The adsorption of API molecules onto the surface of an excipient(s) may result in an API being sequestered and not released during dissolution of a dosage form which may ultimately result in low bioavailability. An example of such an interaction includes the reduction of antibacterial activity of cetylpiridinium chloride when Mg stearate is used as a lubricant in a formulation. This is due to the adsorption of the cetylpiridinium cation by the stearate anion of the Mg stearate. [257-259].

Colloidal silica catalyses the degradation of nitrazepam in a solid dosage form, possibly due to adsorptive interactions altering the electron density of the labile azo functional group, thereby facilitating hydrolytic attack of the parent molecule [260]. Phenobarbital is known to form an insoluble complex with PEG-400 resulting in decreased dissolution and subsequently absorption of the API [261].

The release of diclofenac sodium from a matrix tablet was inhibited by the polymer chitosan at low pH, most likely due to the formation of an ionic complex between the diclofenac sodium and the ionised cationic chitosan polymer [262].

In a vitamin formulation it was reported that the decomposition of ascorbic acid was increased when silica gel was added to the formulation. This was possibly due to the presence of trace metals such as iron and/or copper that is known to catalyse the decomposition of ascorbic acid in solution [263].

4.5 EXPERIMENTAL

4.5.1 Particle Size and Shape

Particle size and shape were determined using a Vega® Scanning Electron Microscope (Tescan, Vega LMU, Czechoslovakia Republic). Approximately 0.5 mg of NVP and each of the excipients to be used during formulation development studies were separately dusted onto a graphite plate and then sputter coated with gold for 20 minutes under vacuum. The samples were then visualised using SEM at an accelerated voltage of 20 KV.

4.5.2 Angle of Repose

The AOR was determined by the height cone method. The end of a funnel was fixed at a height of 2 cm above a flat glass plate and powder blends to be tested allowed to flow under gravity onto the calibrated glass plate fixed on a horizontal surface and the AOR, θ, was calculated using Equation 4.1.

$$Tan\,\Theta = \frac{2h}{D} \qquad \textbf{Equation 4.1}$$

where,

h = height of the pile of powder,
D = diameter of the pile of powder, and
θ = angle of repose.

4.5.3 Powder Density

The tapped density of the powders was established using a Model SVM 203 Erweka® tapped density tester (Erweka, GmbH, Heuseastamm, Germany) at a rate of 220 taps per minute for 2 minutes. Approximately 20 g of the powder blends to be tested were filled into 100 mL graduated measuring cylinders. The bulk volume of the powder was recorded prior to tapping and the tapped volume at the end of tapping. All tests were conducted in triplicate for each powder blend under investigation and the bulk and tapped densities were calculated using Equation 4.2.

$$\rho = \frac{m}{v} \qquad \textbf{Equation 4.2}$$

where,

ρ = density,

m = mass of the powder, and
v = volume occupied by the powder.

The values of bulk and tapped densities were then used to calculate the CI and HR using Equations 4.3 and 4.4, respectively.

$$CI = \frac{Tapped\ density - bulk\ density}{Tapped\ density} \text{ x } 100 \qquad \textbf{Equation 4.3}$$

$$HR = \frac{Tapped\ density}{Bulk\ density} \qquad \textbf{Equation 4.4}$$

4.5.4 Thermogravimetric Analysis

TGA was performed using a Model TGA 7 Perkin Elmer Thermogravimetric Analyser (Perkin Elmer® Norwalk, Connecticut, USA) fitted with platinum sample holder. Approximately 2.5 mg of NVP was added to a platinum crucible and sealed and TGA was performed in a nitrogen atmosphere at a flow rate 20 mL/min over the temperature range 200 °C to 600 °C and heating at a rate of 20 °C/min. Data analysis was performed using Pyris™ Manager Software. TGA measurements were performed only once.

4.5.5 Differential Scanning Calorimetry

DSC thermograms were generated using a Model DSC 7 (Perkin Elmer®, Norwalk, USA) with a PC control unit TAC 7 (Perkin Elmer®, Norwalk, USA) at a heating rate of 10 °C/min and a nitrogen flow rate of 20 mL/min. Approximately 3.0 mg of individual samples to be tested and 1:1 binary mixtures of API and excipients were weighed directly into DSC aluminium pans, hermetically sealed prior to analysis and heated at a constant rate using an empty pan as the reference. The samples were placed directly onto a micro hot stage DSC and thermograms were generated at temperatures between 50 and 300 °C. The temperature of the DSC microscopy cell was monitored using a central processor and each spectrum generated during the heating process was performed using 10 scans with a resolution of 4 cm^{-1}. The DSC cell was calibrated for temperature and enthalpy with Indium (mp 156.6 °C; ΔH_{fus} = 28.4 j/g) and the resultant data were analysed using Pyris™ Manager Software.

4.5.6 FT-IR Spectroscopy

A Spectrum 100 FT-IR ATR Spectrophotometer (Perkin Elmer® Ltd Beaconsfield, England) was used to generate spectra of the potential components of the formulation individually and in 1:1 mixtures of API and excipients. The mixtures were prepared by physically mixing the components using a mortar and pestle. A small amount of each powder or blend was placed on a diamond crystal and a force of approximately 100 N applied before analysis over the wavelength number range 4000-650 cm^{-1} and resolution of 4 cm^{-1}.

4.6 RESULTS AND DISCUSSION

4.6.1 SEM

4.6.1.1 Particle Shape

The particle shapes of each of the excipients used in these studies are shown in Figure 4.1. SEM images reveal that Eudragit® RS PO particles (I) are sub-angular with low sphericity. SDL (II) exhibits rounded particles with high sphericity and images of Carbopol® 71G NF (III) show angular low sphericity particles. NVP particles (IV) are sub-rounded/irregularly shaped particles that occur in aggregates of medium sphericity as previously reported [11]. Avicel® PH102 (V) was shown to have angular particles of medium sphericity whereas Methocel® K4M (VI) occurs as angular flake like particles with low sphericity. Images of DCP (VII) reveal rounded particles of medium sphericity and Mg stearate (VIII) particles were sub-angular with low sphericity [264].

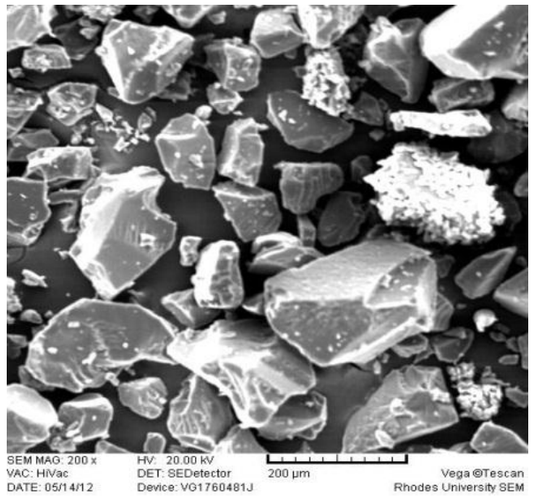

I (Eudragit® RS PO)

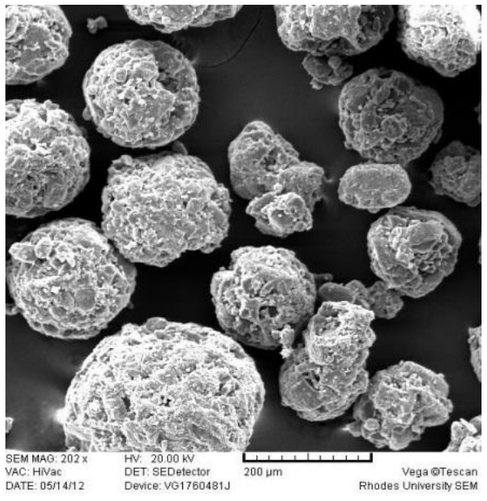

II (SDL)

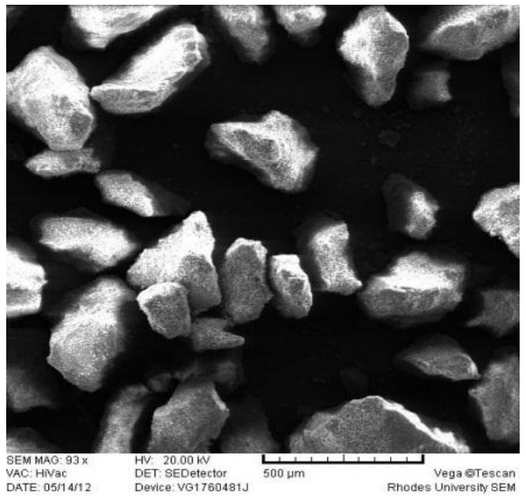

III (Carbopol® 71G NF)

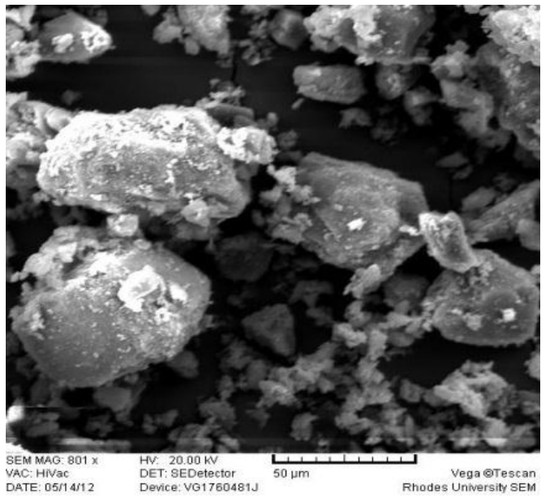

IV (NVP)

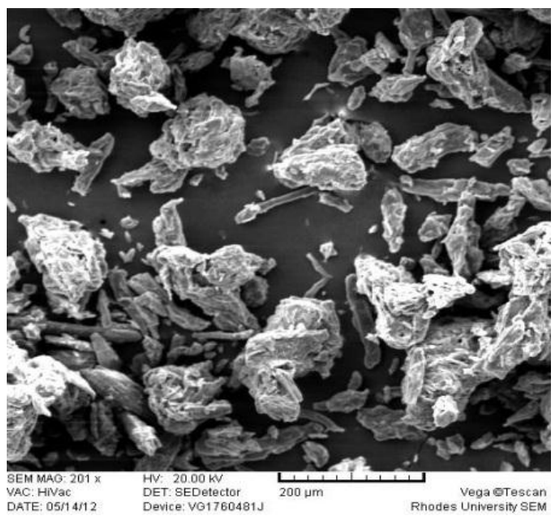

V (Avicel® PH102)

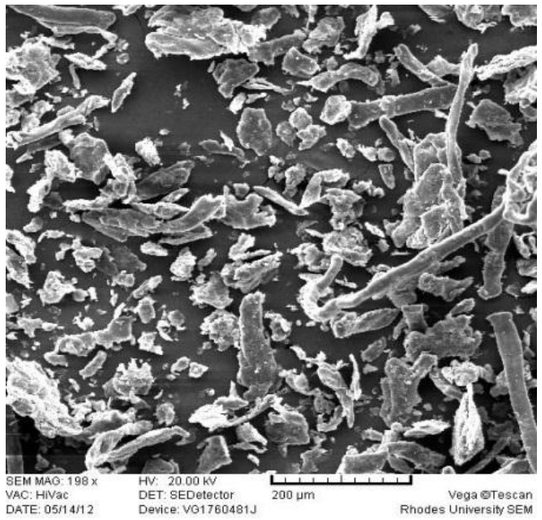

VI (Methocel® K4M)

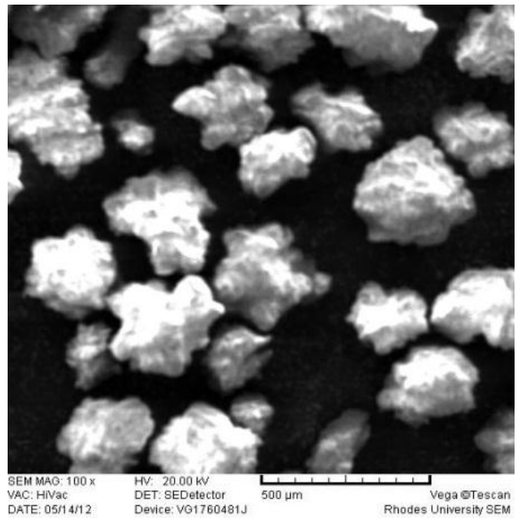

VII (DCP

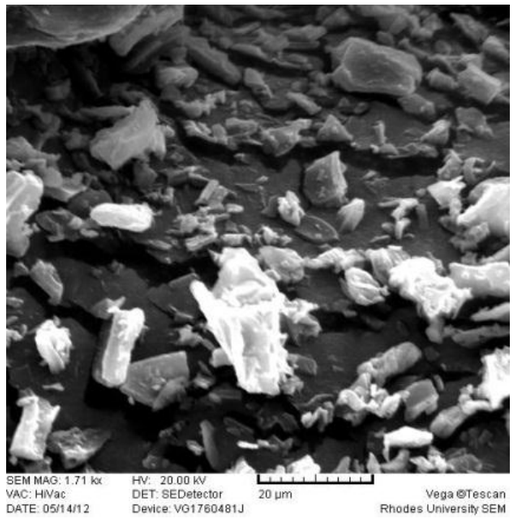

VIII (Mg stearate)

Figure 4.1. Particle shapes of excipients.

4.6.1.2 Particle Size Range

The SEM pictograms of particle size range of NVP and the excipients used in these studies are depicted in Figure 4.2 and Table 4.5 list a summary of the particle size distribution ranges for NVP and the excipients. The data showed that most excipients had particle size distribution which was suitable for tableting. However, wide variations in particle size of the excipients suggested potential for poor powder flow and thus sieving of the excipients and NVP to maintain a uniform particle size distribution and therefore powder flow was considered appropriate.

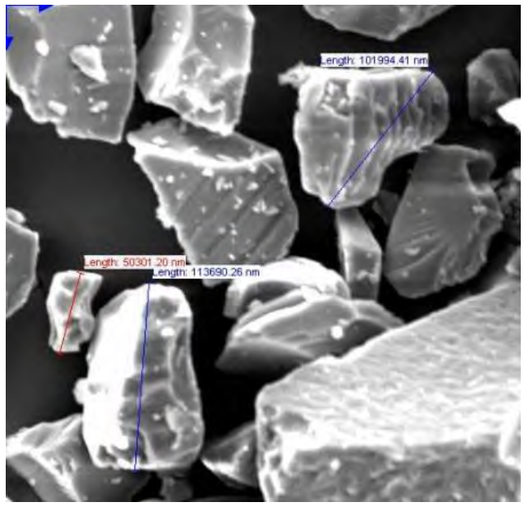

I

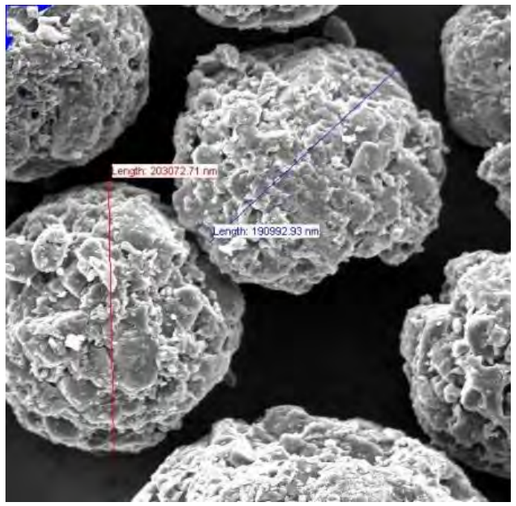

II

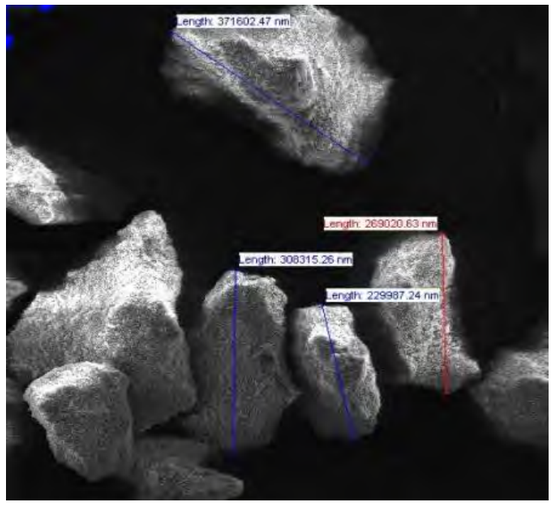

III

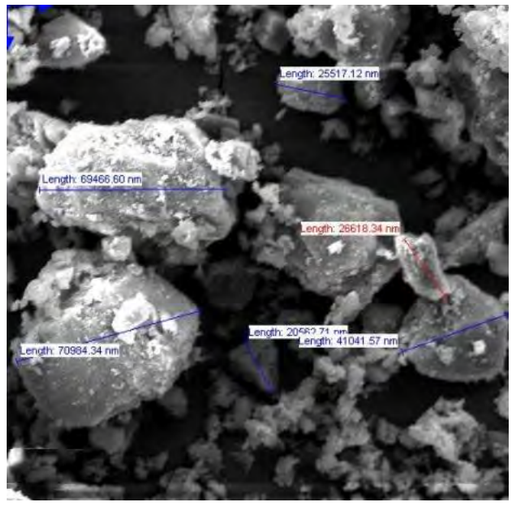

IV

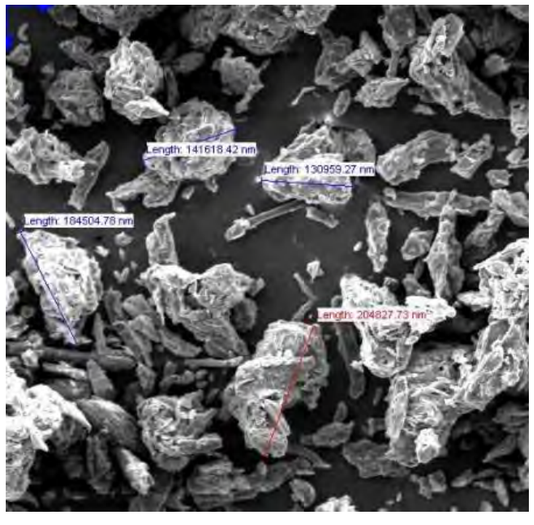

V

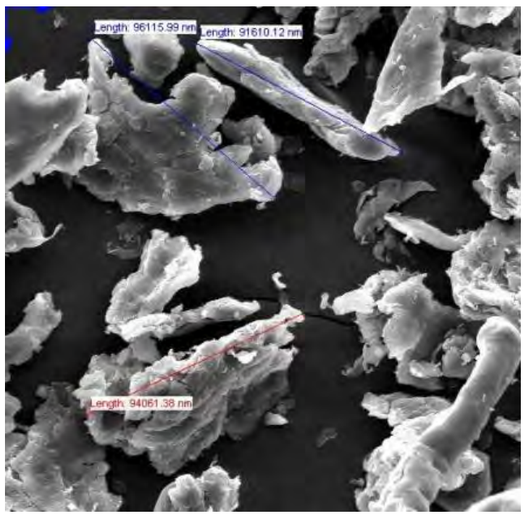

VI

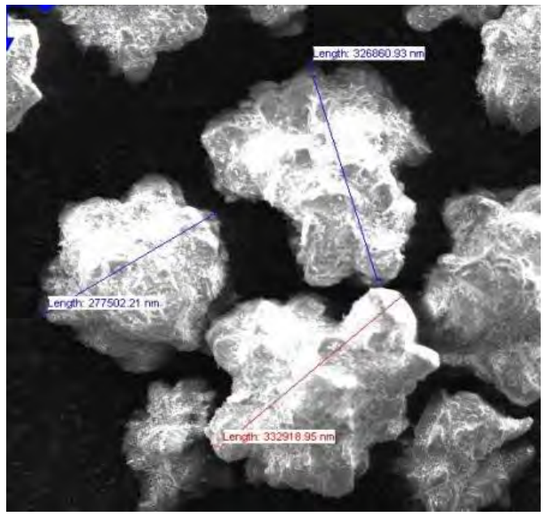

VII

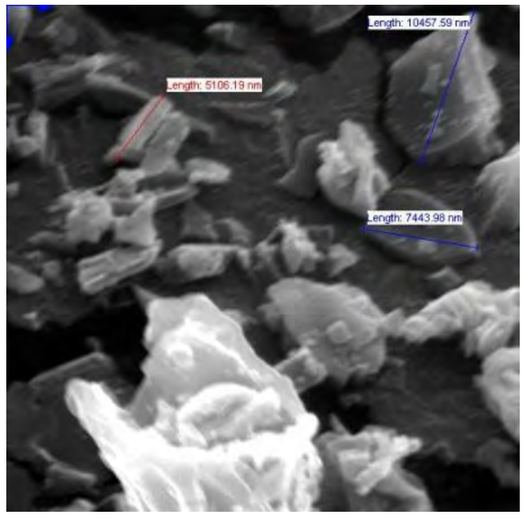

VIII

Figure 4.2. Particle size of excipients.

Table 4.5. Summary of particle size range of NVP and excipients

Excipient	Particle size range (μm)
NVP	20 – 70
Eudragit® RS PO	110 – 118
Carbopol® 71G NF	230 – 372
SuperTab® SDL	190 – 230
Avicel® PH102	130 – 204
Methocel® K4M	90 – 100
Mg. stearate	5 – 10

The particle size and shape of a material are known to affect the bulk properties of powders and have a significant effect on the ultimate compressibility of that powder. Any differences in the particle size distribution and shape can also significantly affect powder flow properties and subsequently the manufacturing process [265, 266].

Bulk powder behaviour is dependent on particle size, variation of particle size and the shape of particles. In general powders with large dry particles of > 250 μm in diameter are not cohesive, permeable and tend to flow adequately, however they exhibit low compressibility and shear strength and may thus not be suitable for direct compression. As the particle size of a powder decreases from 250 μm to 75 μm, the flowability decreases and flow becomes difficult when the particle size decreases < 75 μm in diameter. Fine powders with particles of < 10 μm diameter are cohesive, compressible, have high shear strength and exhibit poor flow properties which may result in tablets with poor quality attributes if directly compressed [266].

The particle shape tends to affect the flowability of powders and therefore the AOR. In general, spherical particles show good flowability and out of round particles with smooth edges also flow easily. Irregularly shaped particles such as flakes also flow with little difficulty whereas cubic and rectangular blocks with sharp edges do not flow readily. Irregularly shaped, interlocking and fibrous particles do not flow readily and usually result in powder flow stoppages by formation of semi-rigid structures in the powder bed [266, 267].

For powders with large particles, the mass of the individual particles is large and therefore flowability tends to be good. However, as the particle sizes of powders are reduced the mass of the particles reduces and with an increased surface area, surface forces are amplified and resistance to flow is observed. Small particles of < 75 μm diameter are difficult to blend due to a high surface area per unit volume ratio and may result in tablets with poor content

uniformity. The large surface area gives rise to strong electrostatic forces that occur during blending and inter-particulate friction between the smaller particles is also high resulting in low material movement compared to that observed with large particles. Powdered materials with particle sizes of 10 µm and smaller lead to the formation of weak polarising electrical or Van Der Waal's forces that may prevent the distribution of small particles throughout a blend due to fine particle agglomeration [245, 268, 269].

The size distribution and shape of a powder also affect the packing characteristics of the material and consequently have an impact on the bulk density of the material. Smaller powder particles occupy the interstitial spaces between large particles creating a densely packed powder with a high bulk density. The flowability of densely packed powder is lower than that of loosely packed powders and particle density affects the sedimentation or floating ability of the particles within a blender [266, 267].

It is ideal that the particle size distribution of a powder is within a narrow range to avoid poor flow and powder stratification and during tablet compression [245]. The excipients used in these studies were found to exhibit a wide range of particle sizes and shapes that are likely to impact negatively on the flowability of the powder blends. Furthermore the size distribution of NVP was also an indicator that powder flow would be poor. Consequently in order to improve manufacturability and in an attempt to create a uniform particle size distribution the excipients and NVP were passed through a sieve mesh size # 20 prior to blending for thirty minutes.

4.6.2 Angle of Repose

The values for the AOR for the powder blends used in formulation development studies are summarised in Table 4.6. The AOR ranged between 25.20° ± 2.44 to 36.89° ± 1.22 and the blends were considered suitable for use for direct compression manufacture of NVP SR tablets. The flowability of powder blends of the batches that have an AOR of > 30° was expected to improve following the addition of a lubricant and/or glidant to the powder blend.

Table 4.6. Flow characteristics of powder blends used in formulation development studies

Formulation	Angle of Repose °	Bulk Density g/cm^3	Tapped density g/cm^3	CI %	HR
NVP001	36.89 ± 1.22	0.385 ± 2.23	0.431 ± 2.54	10.59 ± 2.19	1.12 ± 1.12
NVP002	29.75 ± 1.31	0.393 ± 3.27	0.442 ± 3.13	11.02 ± 3.11	1.12 ± 2.21
NVP003	33.69 ± 1.42	0.379 ± 1.33	0.582 ± 3.22	34.89 ± 2.29	1.54 ± 2.11
NVP004	28.07 ± 2.11	0.469 ± 2.15	0.738 ± 1.83	36.54 ± 1.94	1.58 ± 3.08
NVP005	31.61 ± 3.04	0.473 ± 3.62	0.682 ± 1.26	30.65 ± 2.22	1.44 ± 2.07
NVP006	29.75 ± 2.28	0.432 ± 2.54	0.652 ± 2.33	33.82 ± 1.87	1.51 ± 1.10
NVP007	28.07 ± 1.78	0.489 ± 2.11	0.763 ± 1.75	35.93 ± 3.11	1.56 ± 2.04
NVP008	28.07 ± 2.35	0.456 ± 3.07	0.710 ± 3.72	35.82 ± 3.88	1.56 ± 2.06
NVP009	29.75 ± 1.97	0.427 ± 2.77	0.634 ± 1.44	32.76 ± 1.89	1.49 ± 2.01
NVP010	31.61 ± 3.61	0.446 ± 1.83	0.658 ± 2.01	32.20 ± 2.39	1.48 ± 2.02
NVP011	25.20 ± 2.44	0.485 ± 1.73	0.718 ± 2.29	32.44 ± 2.11	1.48 ± 3.11
NVP012	33.25 ± 3.18	0.462 ± 2.48	0.704 ± 1.72	34.49 ± 2.10	1.53 ± 2.04

Results shown as mean ± %RSD (n = 3)

4.6.3 Density

4.6.3.1 Bulk and Tapped Density

The bulk and tapped densities of the powder blends that were used to calculate the CI and HR are summarised in Table 4.6. These were used to assess the flowability and compressibility of the powder blends following calculation of HR and CI and ranged between 0.385 and 0.489 g/cm^3.

4.6.3.2 Carr's Index and Hausner Ratio

The CI values for the powder blends of all batches tested ranged between 10.59 ± 2.19 to 36.54 ± 1.94 and are shown in Table 4.6, indicating that the blends exhibited a high degree of variability in powder flow characteristics. Powders with CI values of between 30 and 40% are likely to exhibit improved flow properties following addition of a lubricant. Low CI values imply that there is a low level of cohesion between the particles in a blend thereby facilitating the tablet manufacturing process through improved powder flow.

The HR for the powder blends under investigation ranged between 1.12 ± 0.12 and 1.58 ± 3.08 as can be observed from the data summarised in Table 4.6 and are considered acceptable for tableting as the addition of a glidant or lubricant was expected to further improve powder flow properties.

4.6.4 Thermogravimetric Analysis

The TGA thermogram depicted in Figure 4.3 reveals that NVP is stable up to a temperature of approximately 244 °C after which almost complete decomposition of the compound (> 90%) occurs at 250 °C which is also the melting point of NVP. The results observed are in close agreement with previously reported values [11, 270] and suggest that it is unlikely that NVP would decompose under normal tableting conditions during which temperatures rarely exceed 100 °C.

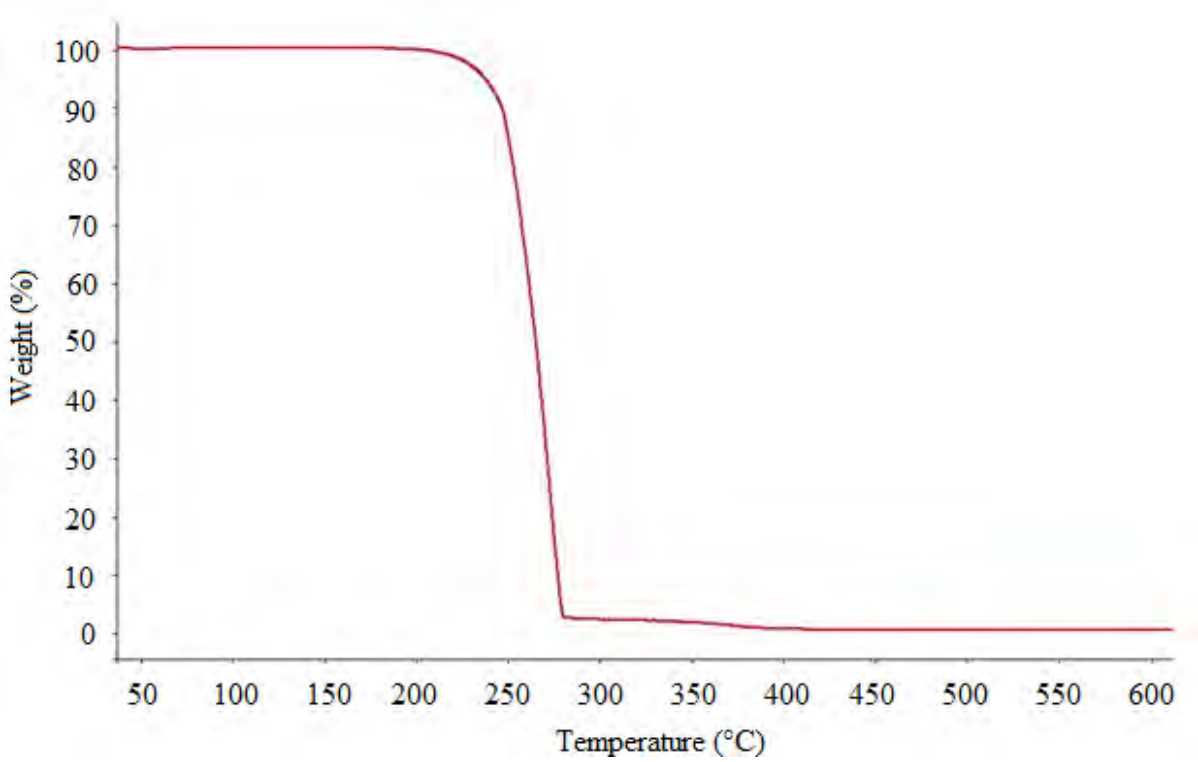

Figure 4.3. TGA thermogram of NVP generated at a heating rate of 10 °C/min.

4.6.5 Differential Scanning Calorimetry

DSC measures the change in energy that occurs as a sample is heated at a constant rate [271]. The principle involves heating two ovens to the same temperature at the same rate with one oven containing the sample to be tested in a sealed pan and the other containing an empty pan, serving as reference. Changes in the sample such as melting will result in consumption of energy and the process is classified as an endothermic event. Energy release will occur if a change such as crystallisation takes place and this process is called an exothermic event.

Since the reference pan remains constant, a thermogram displaying thermodynamic changes of a sample is produced indicating release or uptake of energy [271, 272].

The DSC thermogram of NVP revealed a single sharp symmetrical melting endotherm at 250 °C with a ΔH =504.5376 J/g and is depicted in Figure 4.4, indicating that NVP is not a hydrate or solvate. This value of the melting point was within the previously reported range of 244 - 250 °C [11, 270].

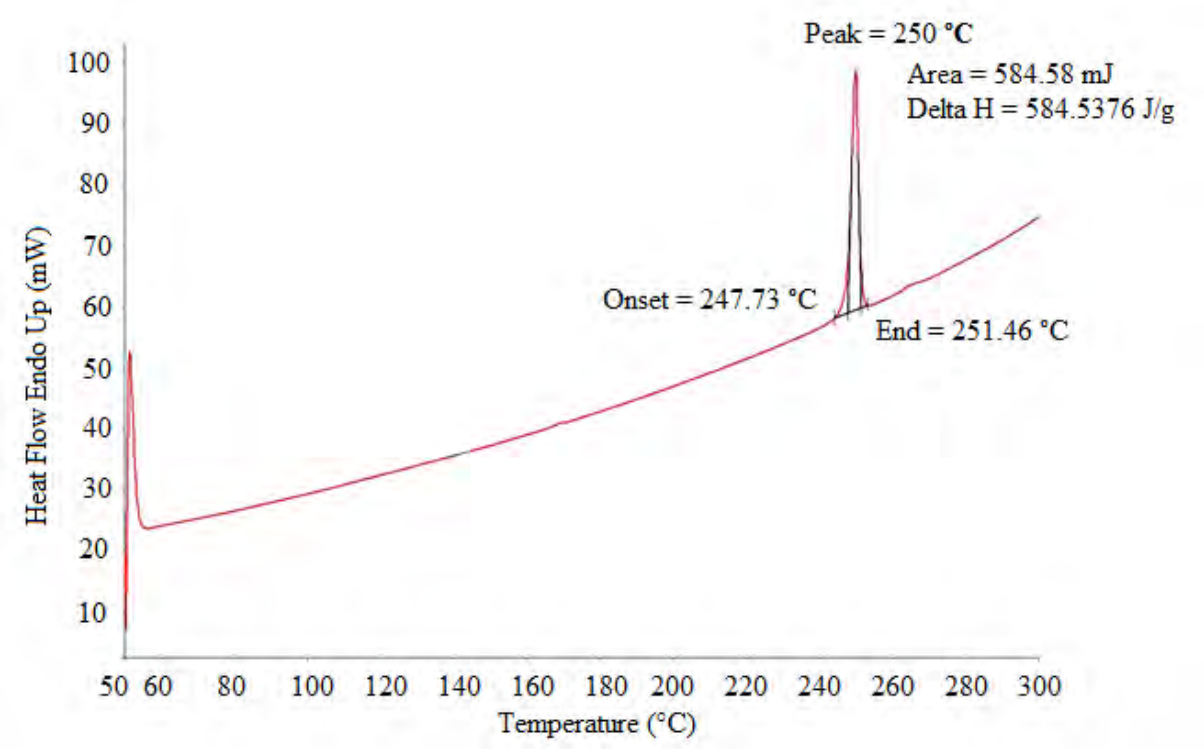

Figure 4.4. DSC thermogram of NVP generated at a heating rate of 10 °C/min.

The thermogram for DCP was broad and asymmetrical and revealed the presence of an endotherm at a temperature of 199.50 °C with a ΔH = 497.1446 and is shown in Figure 4.5. The endotherm may be attributed to the loss of a water of crystallisation [273].

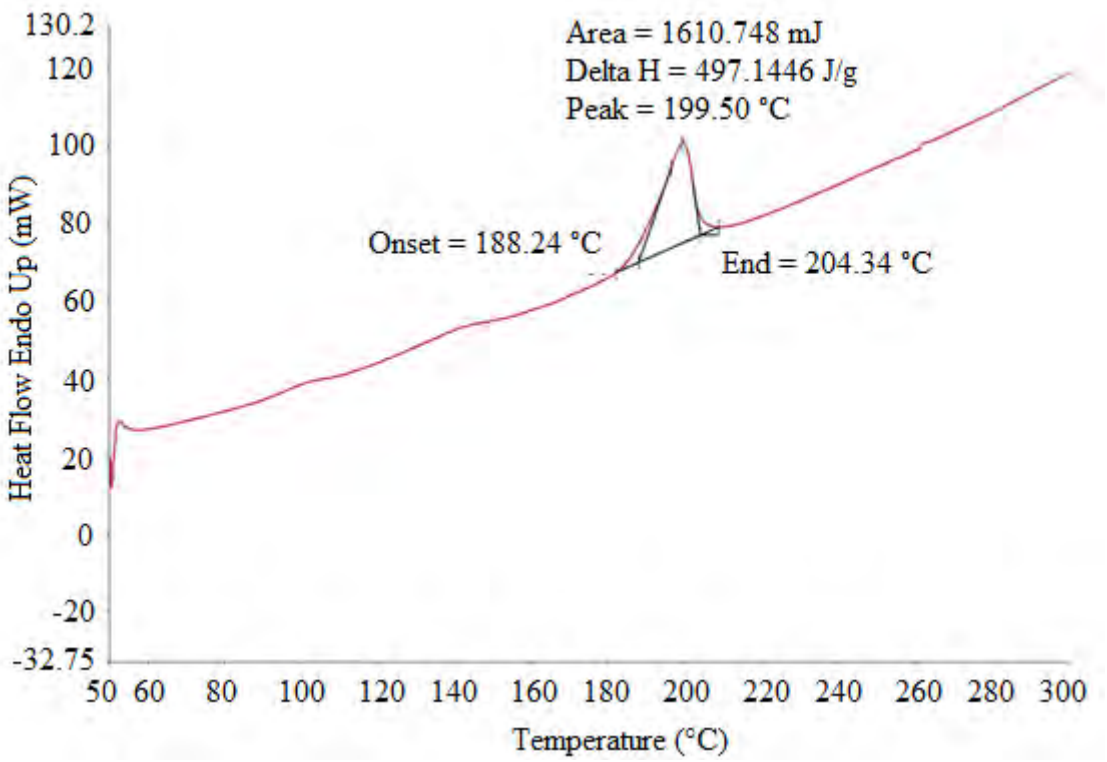

Figure 4.5. DSC thermogram of DCP generated at a heating rate of 10 °C/min.

The DSC thermogram of Mg stearate showed a broad and asymmetrical melting endotherm at 120.00 °C with a ΔH = 76.7026 J/g and is shown in Figure 4.6. The melting endotherm was in close agreement with the reported melting range of 110-120 °C and can be attributed to the fusion of Mg stearate [217, 274].

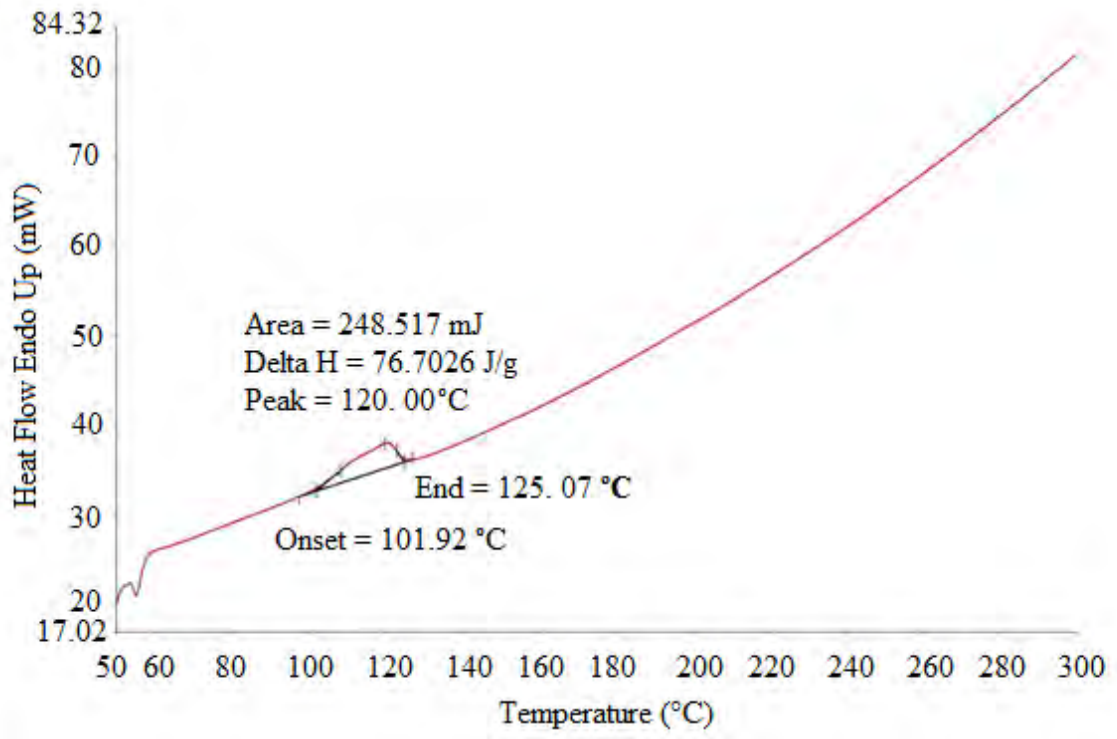

Figure 4.6. DSC thermogram of Mg stearate generated at a heating rate of 10 °C/min.

The DSC thermogram of SDL depicted in Figure 4.7 reveals the presence of a broad and symmetrical endothermic peak at 148.50 °C with a ΔH = 137.5859 J/g and can be attributed to dehydration of the lactose. The thermogram also revealed the presence of a broad asymmetrical endothermic peaks at 224.17 °C (ΔH = 129.1749 J/g) and at 234.17 °C (ΔH = 19.9389 J/g) which may be attributed to the heats of fusion of the α- and β forms of –lactose present in the SDL sample [275-277].

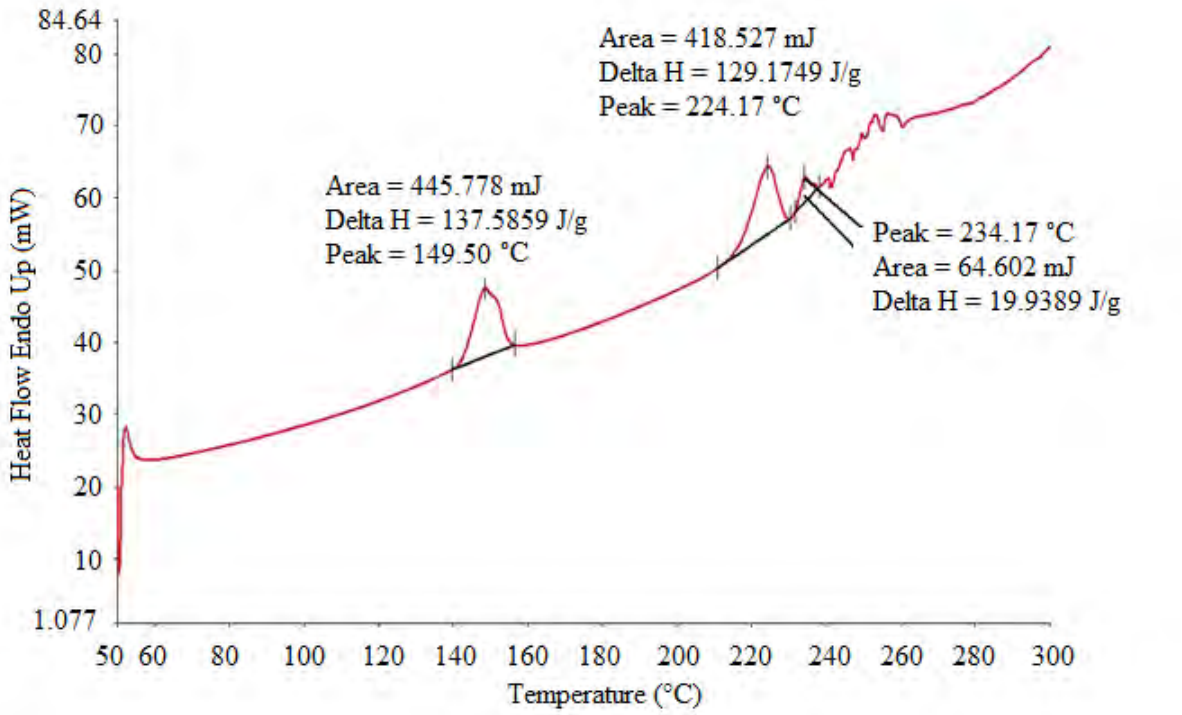

Figure 4.7. DSC thermogram of SuperTab® SDL generated at a heating rate of 10 °C/min.

The thermograms for colloidal silicon dioxide, talc, Eudragit® RS PO, Methocel® K4M, Avicel® PH102 and Carbopol® 71G NF did not show any significant enthalpy changes in the temperature ranges as can be observed in Figures 4.8a – 4.8f.

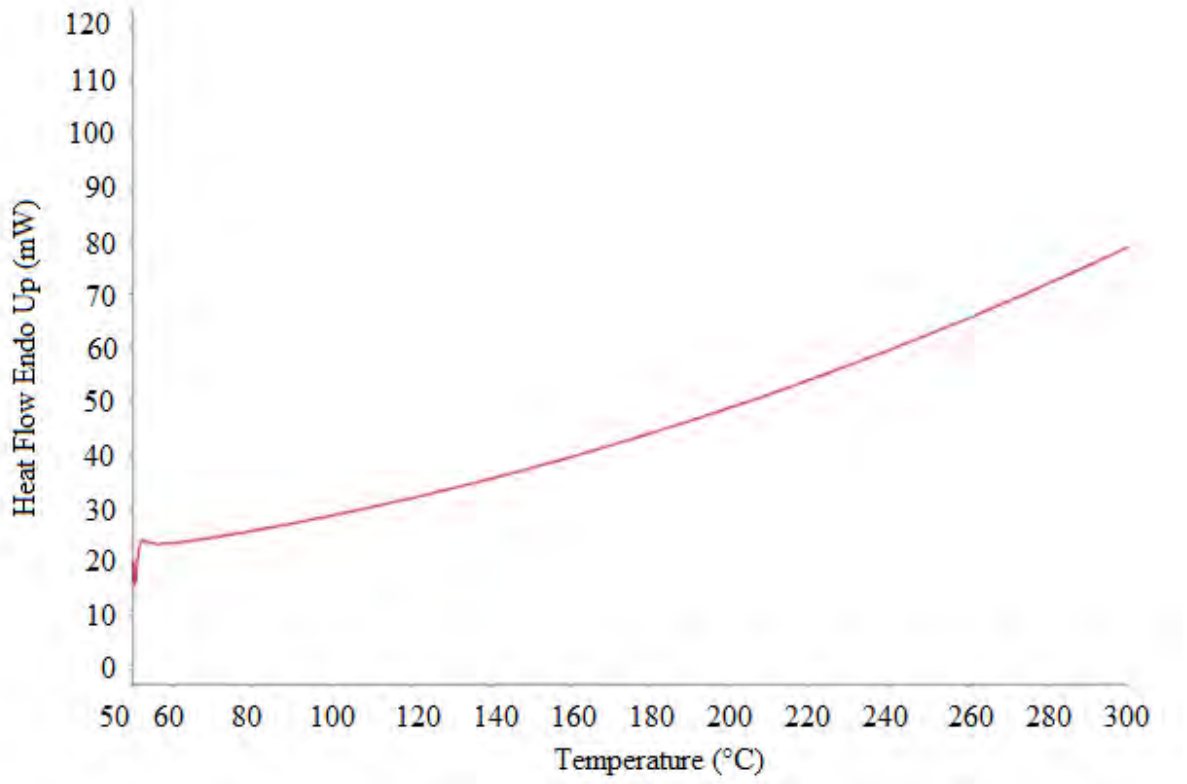

Figure 4.8a. DSC thermogram of colloidal silicon dioxide generated at a heating rate of 10°C/min.

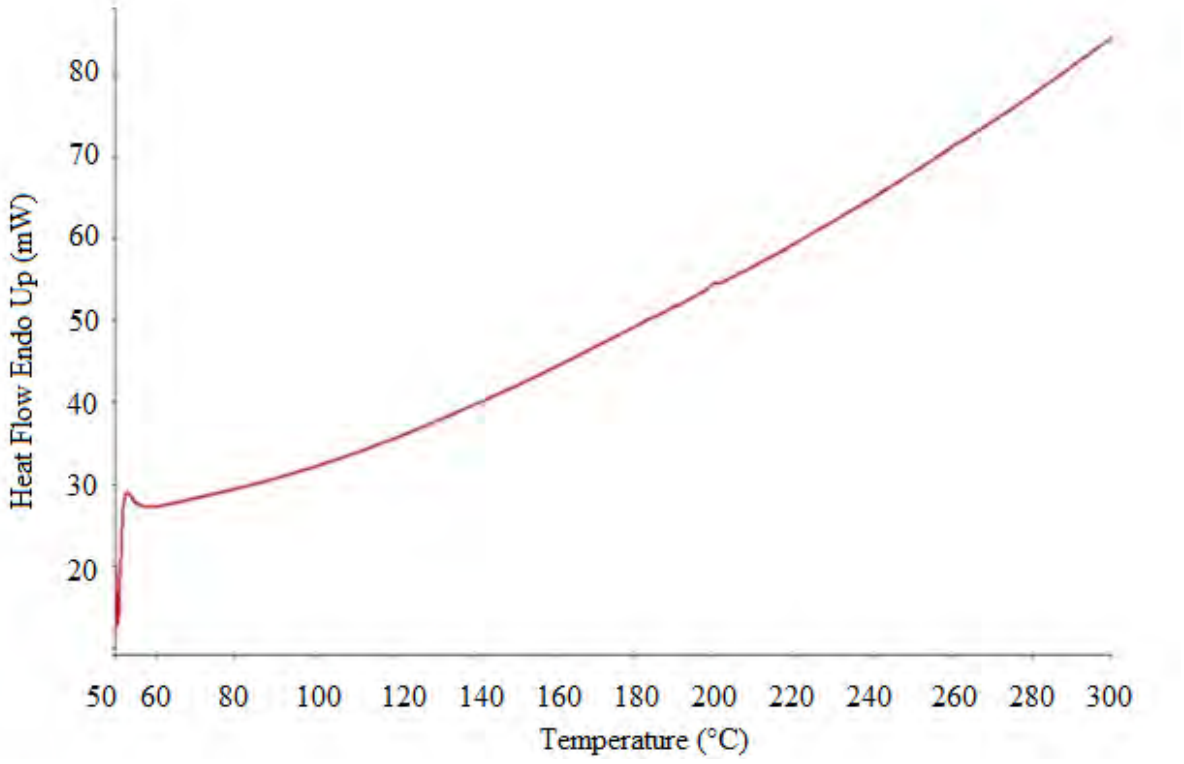

Figure 4.8b. DSC thermogram of Avicel® PH102 generated at a heating rate of 10 °C/min.

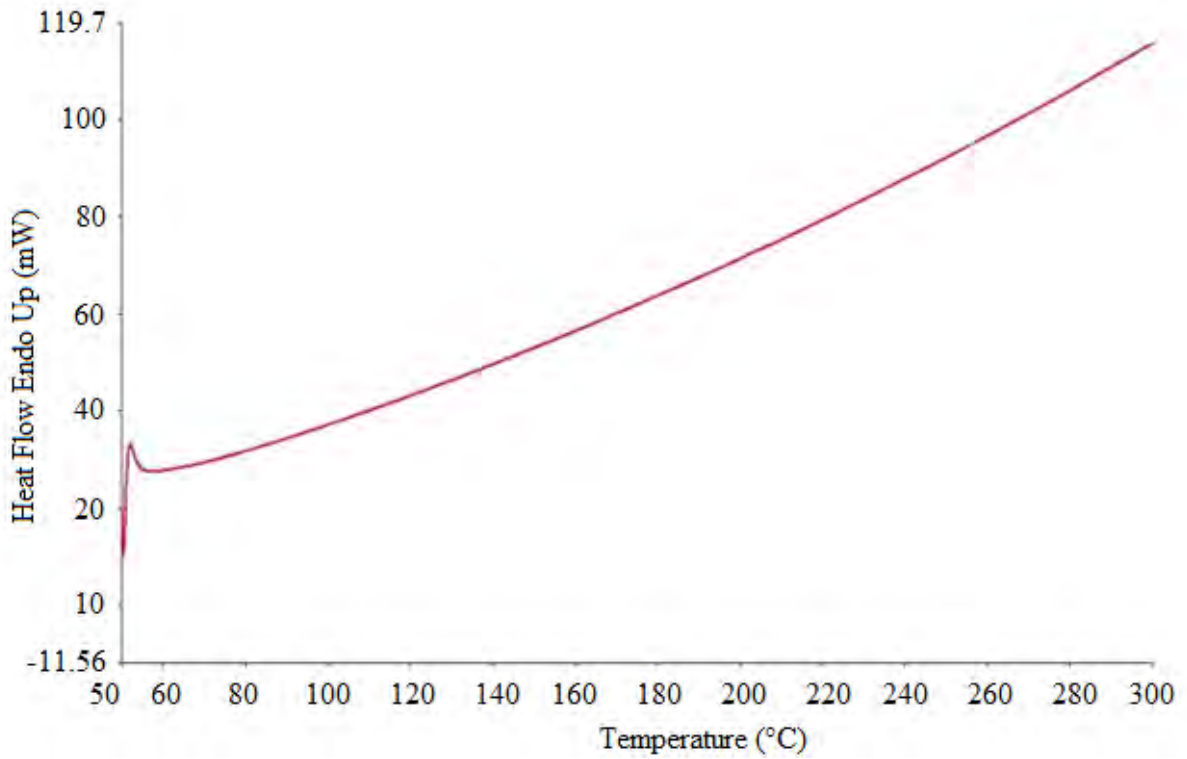

Figure 4.8c. DSC thermogram of Eudragit® RSPO generated at a heating rate of 10 °C/min.

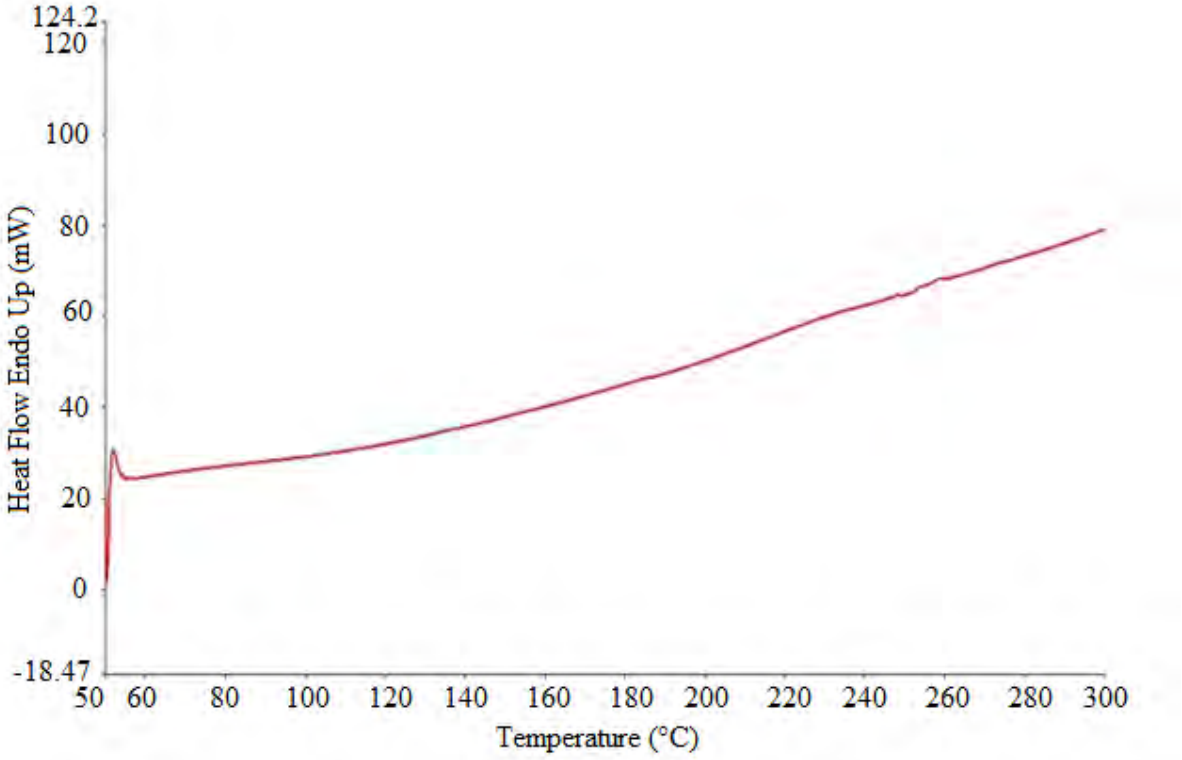

Figure 4.8d. DSC thermogram of Carbopol® 71G NF generated at a heating rate of 10 °C/min.

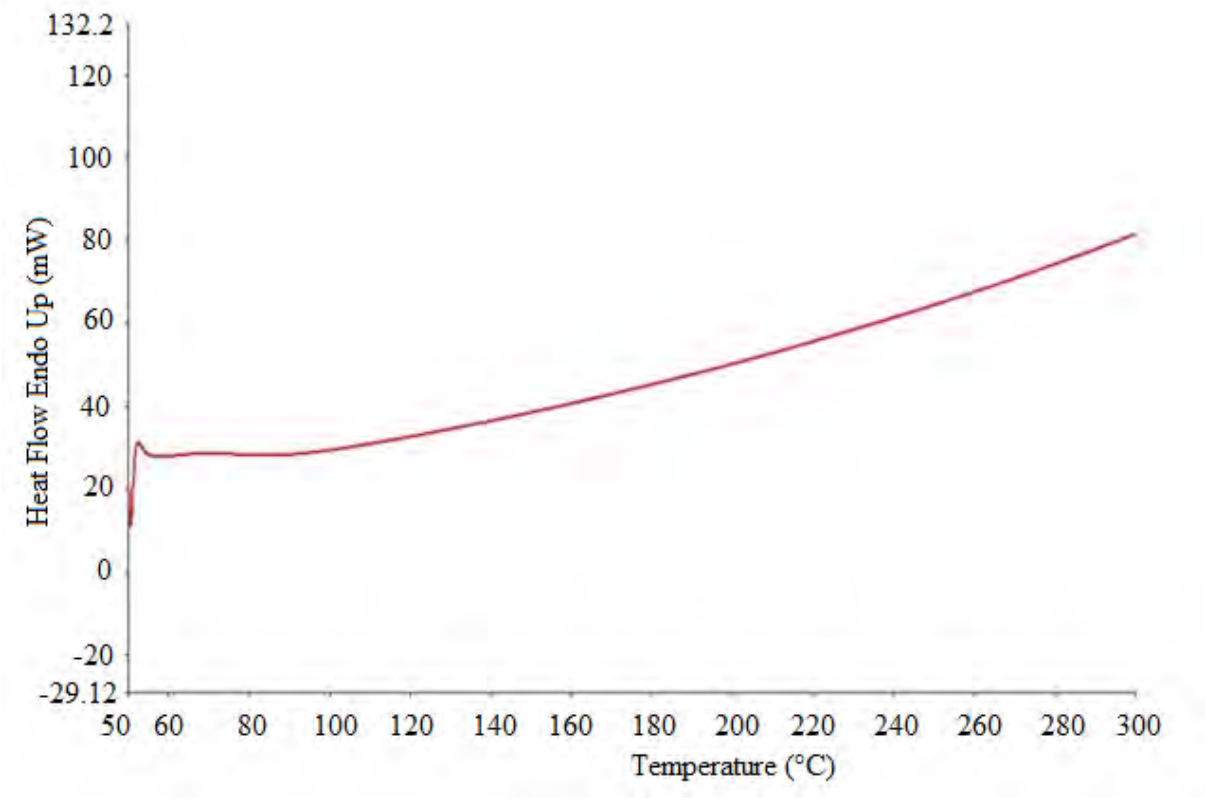

Figure 4.8e. DSC thermogram of Methocel® K4M generated at a heating rate of 10 °C/min.

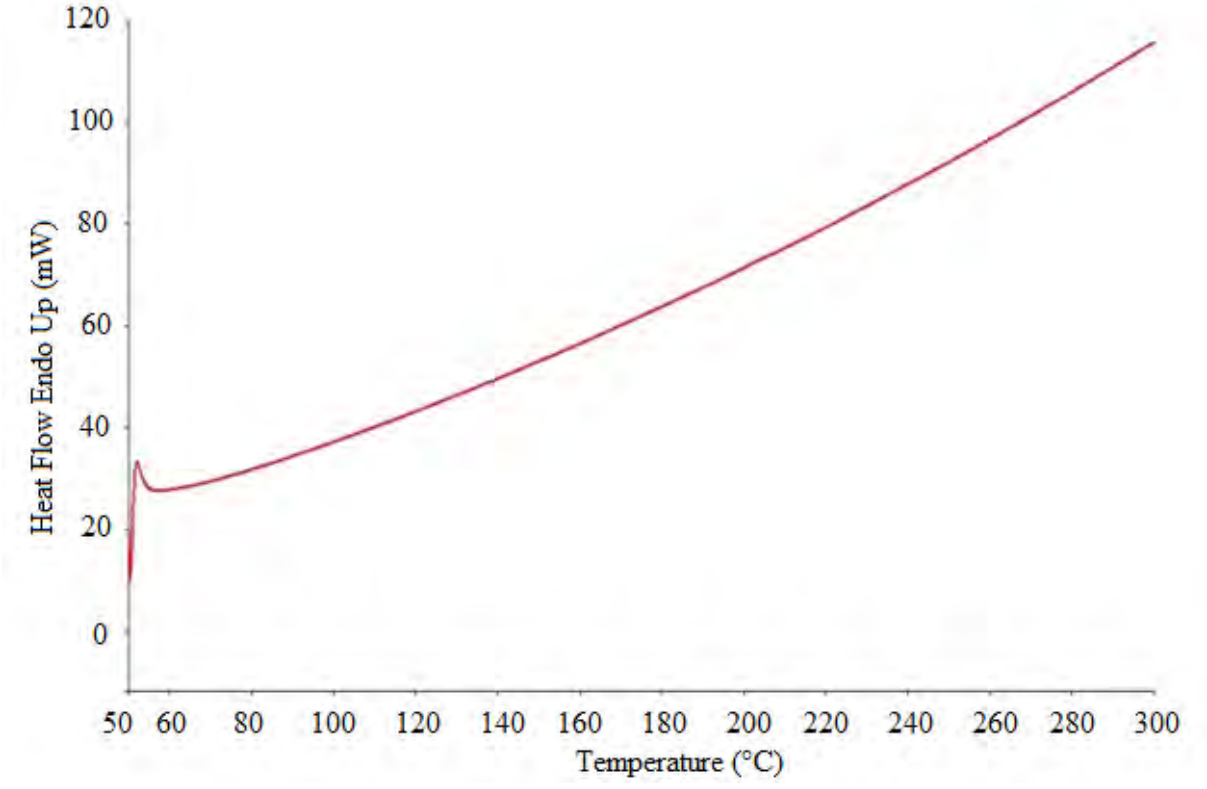

Figure 4.8f. DSC thermogram of talc generated at a heating rate of 10 °C/min.

The DSC thermogram of a 1:1 binary mixture of NVP and Avicel® PH102 revealed the presence of a single sharp and symmetrical endothermic peak at a temperature of 254.00 °C as shown in Figure 4.9 and which is slightly higher than the melting point of NVP. The 4°C increase in the melting point of NVP may be attributed to a shielding effect usually associated with microcrystalline cellulose [278].

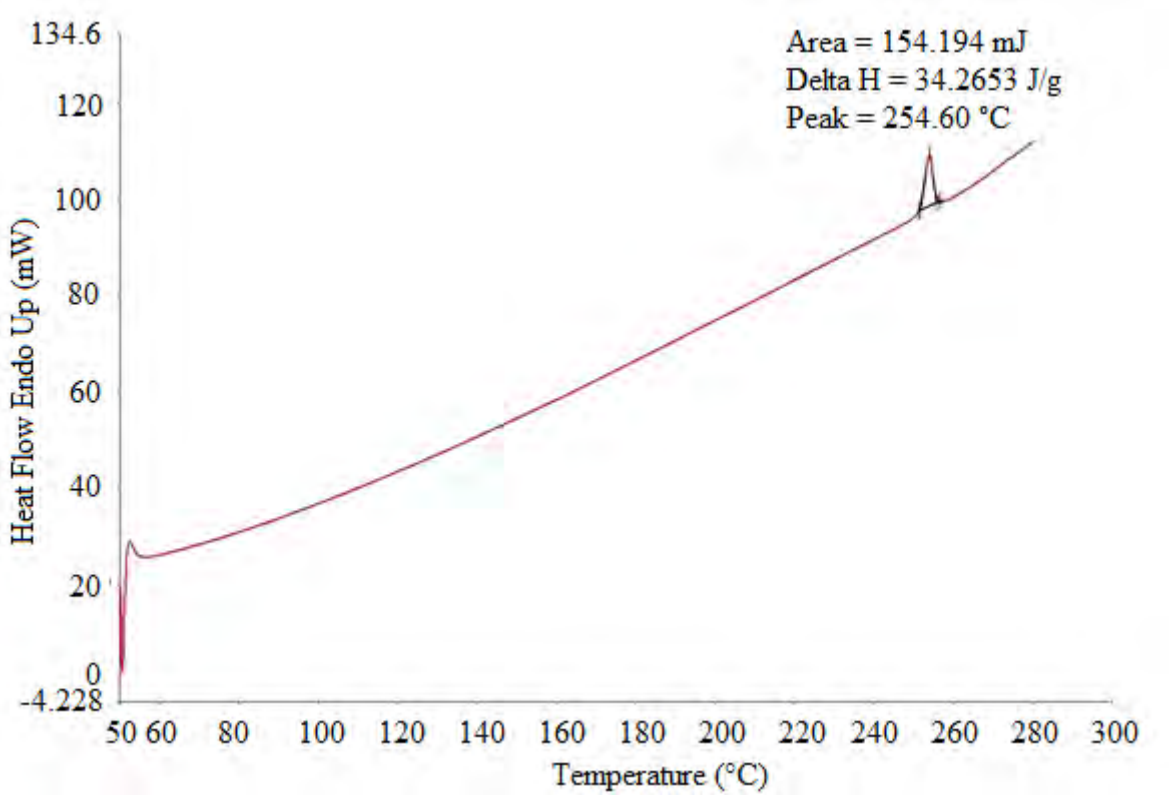

Figure 4.9. DSC thermogram of a 1:1 binary mixture of Avicel® PH102 and NVP generated at a heating rate of 10 °C/min.

The DSC thermograms of 1:1 binary mixtures of NVP and the excipients under investigation exhibited a reduction in the melting point of NVP and the excipients when compared to the values observed for the individual compounds as shown in Figures 4.10-4.14.

The thermograms of the binary mixture of NVP and Mg stearate showed a sharp symmetrical melting endotherm of 245 °C for NVP and 112.17 °C for magnesium stearate as shown in Figure 4.10.

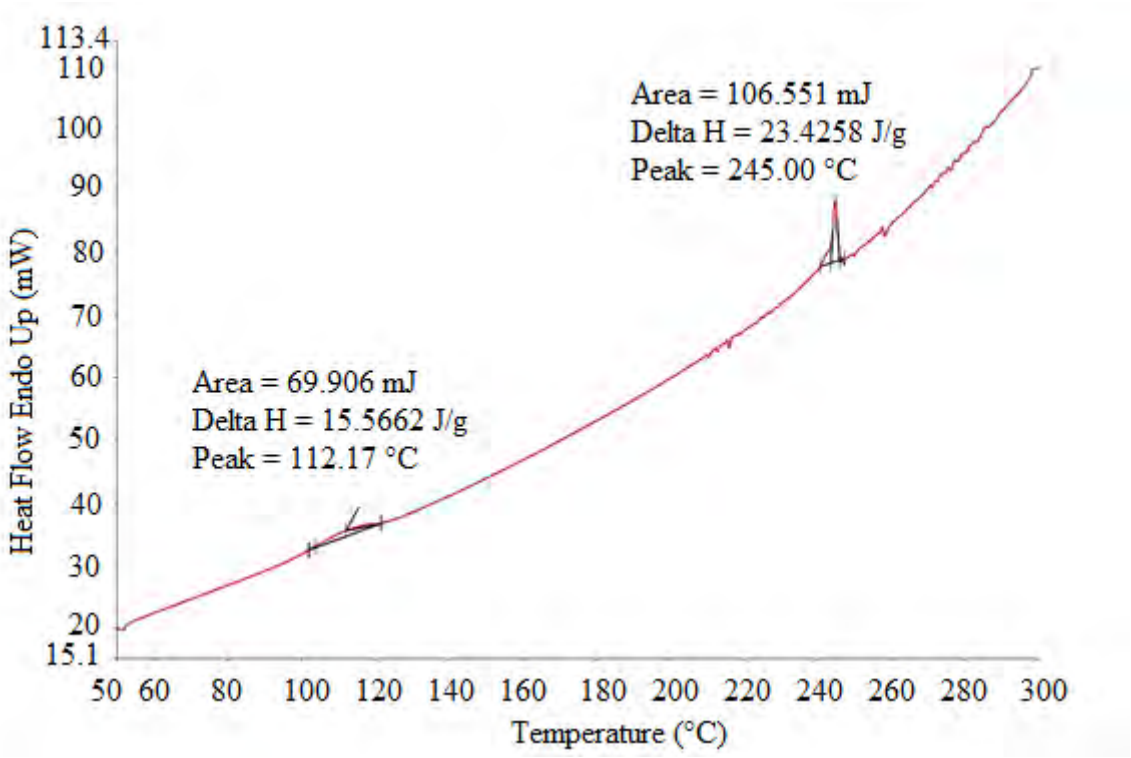

Figure 4.10. DSC thermogram of a 1:1 binary mixture of NVP and Mg stearate generated at a heating rate of 10 °C/min.

The thermogram of a 1:1 binary mixture of NVP and Methocel® K4M yielded a symmetrical peak with a broad base as shown in Figure 4.11, which could be an indication of a change from a crystalline phase to an amorphous phase that may also have an implication for the stability of NVP in HPMC containing dosage forms [278]. The melting endotherm of NVP also decreased to 243.5 °C.

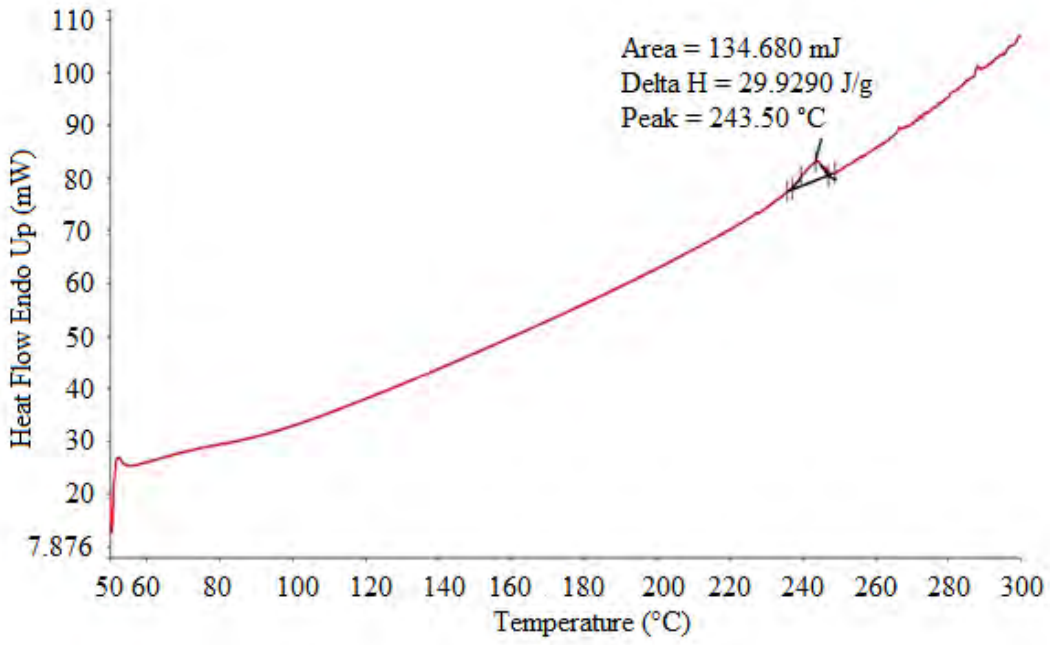

Figure 4.11. DSC thermogram of a 1:1 binary mixture of Methocel® K4M and NVP generated at a heating rate of 10 °C/min.

The DSC thermogram of a 1:1 binary mixture of NVP and DCP showed a decreased sharp and symmetrical melting endotherm of NVP of 245.67 and a broad symmetrical melting endotherm of 193.33 °C for DCP as shown in Figure 4.12.

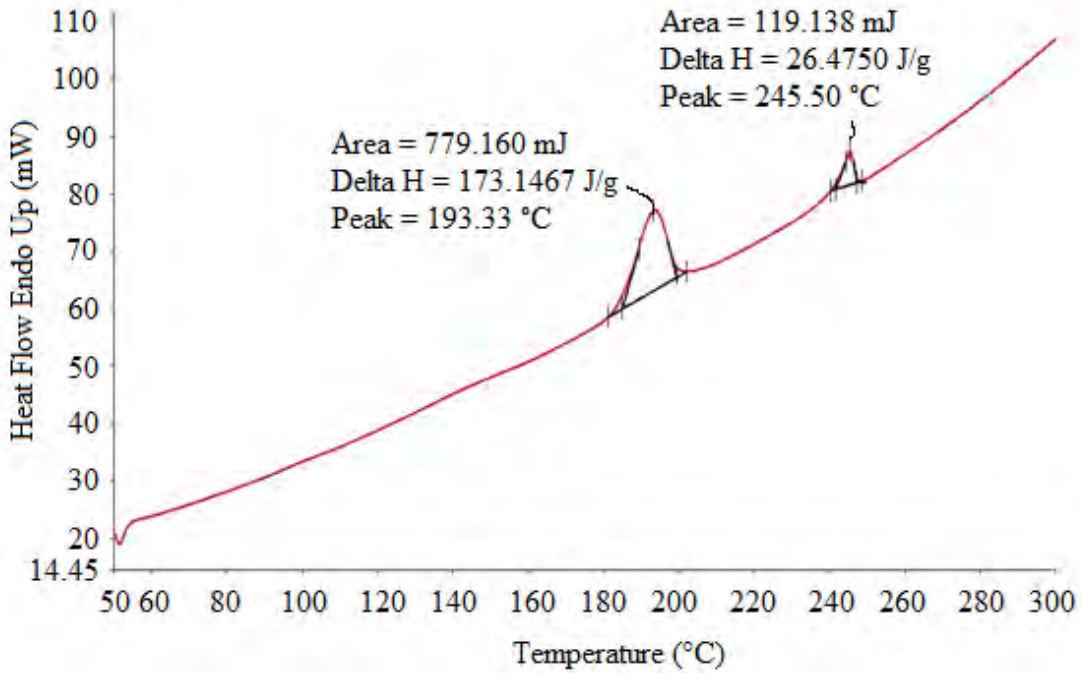

Figure 4.12. DSC thermogram of a 1:1 binary mixture of NVP and DCP generated at a heating rate of 10 °C/min.

The DSC thermogram of a 1:1 binary mixture of NVP and SuperTab® SDL showed a sharp symmetrical melting endotherm of 240 °C for NVP as shown in Figure 4.13, with almost complete disappearance of endothermic peaks attributed to heats of fusion of the α- and β-forms of lactose at 219.33 °C and 230 °C. The reduced peak heights may be an artefact of the quantities of materials used to conduct DSC.

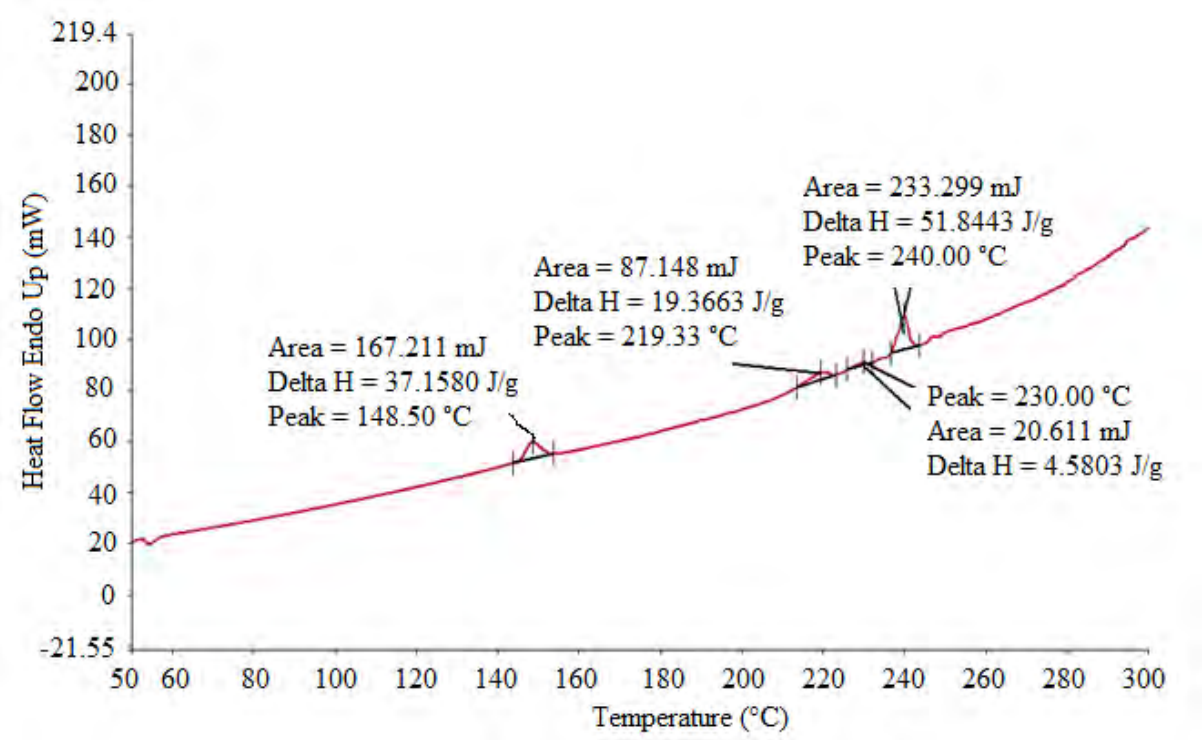

Figure 4.13. DSC thermogram of a 1:1 binary mixture of NVP and SDL generated at a heating rate of 10 °C/min.

The DSC thermogram of a 1:1 binary mixture of NVP and talc showed a sharp and symmetrical endothermic peak of 245.67 °C for NVP as shown in Figure 4.14.

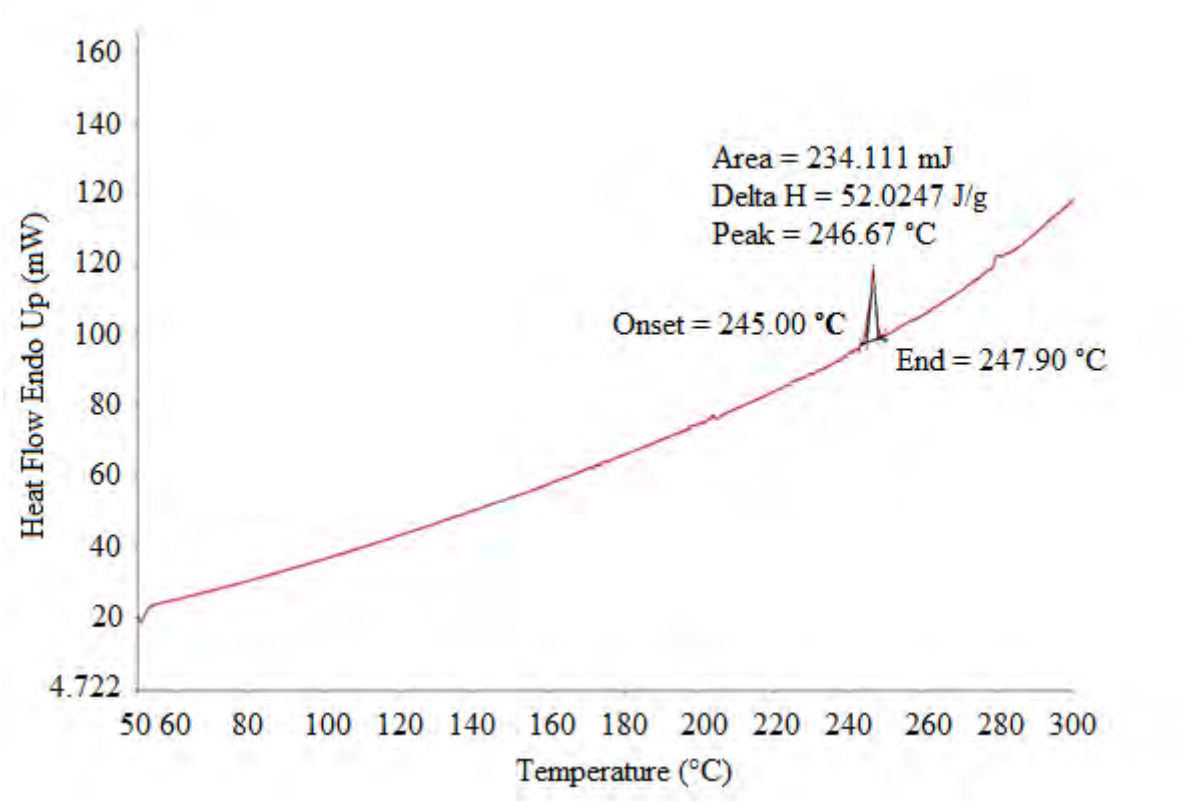

Figure 4.14. DSC thermogram of a 1:1 binary mixture of NVP and talc generated at a heating rate of 10 °C/min.

The decrease in the peak height of the endotherms of NVP and the excipients may be a consequence of the low mass of samples used as this is known to affect the intensity of peaks when using DSC [278].

The dilution effect of excipients on the response generated from an API is a shortcoming of using DSC as a definitive tool to study any possible drug-excipient interactions. However, significant changes in the melting point of an API are indicative of any potential interactions that may warrant further investigation using additional and more specific analytical techniques. The reduced melting point of NVP that was observed in the presence of excipients indicates that it is unlikely that any significant interactions would occur as the shifts in the melting points were < 10 °C. However there is evidence of a potential for a decrease in the thermal stability of NVP [279] and similar studies have shown that Mg stearate [280], MCC, HPMC and silicon dioxide [281] can decrease the thermal stability of an API. Although DSC analysis is used as a preliminary screening tool for compatibility evaluation it does not preclude the need for long term stability studies on manufactured

dosage forms in order to be able to draw meaningful conclusions in respect of the long term stability of products.

4.6.6 IR Spectroscopy

The qualitative aspect of IR spectroscopy is a powerful attribute of this diverse analytical technique. The IR absorption spectrum may be used as fingerprint identification for a molecule and is the result of absorption of electromagnetic radiation at frequencies that correlate to the vibration of specific chemical bonds in a molecule. FT-IR spectroscopy is able to reveal potential interactions at a molecular level as a specific functional group will vibrate at a specific frequency [282].

NVP shows characteristic C-O stretching vibration of cyclic amide at 1646 cm^{-1}, and N-H and C-N stretch of 7-membered ring at 3295-3188 cm^{-1} [11, 270]. The vibrational frequencies of NVP that have been identified following IR spectroscopy studies are summarised in Table 4.7 [11, 270, 283, 284] and the FT-IR spectrum of NVP is depicted in Figure 4.15.

Table 4.7. Assignment of vibrational frequencies for functional groups of NVP

Functional group/Assignment	Vibrational frequency (cm^{-1})
C=O stretching of cyclic amide	1644.36
-C=C-C aromatic ring stretching	1585.82
CH_2 of cyclopropyl ring stretching	1410.32
N-H stretching of 7-membered ring	3183.67
OH in plane bending	1242.21
C-H asymmetric bending	1465.11
C-H symmetric bending	1383.01
Aromatic C-H in plane bending	3061.37
-C=O bending	1288.31
CH_2 rocking	818.18
Ring breathing and deformation	883.97
CH deformation of rings	1210.17
CH_2 twisting	1153.33

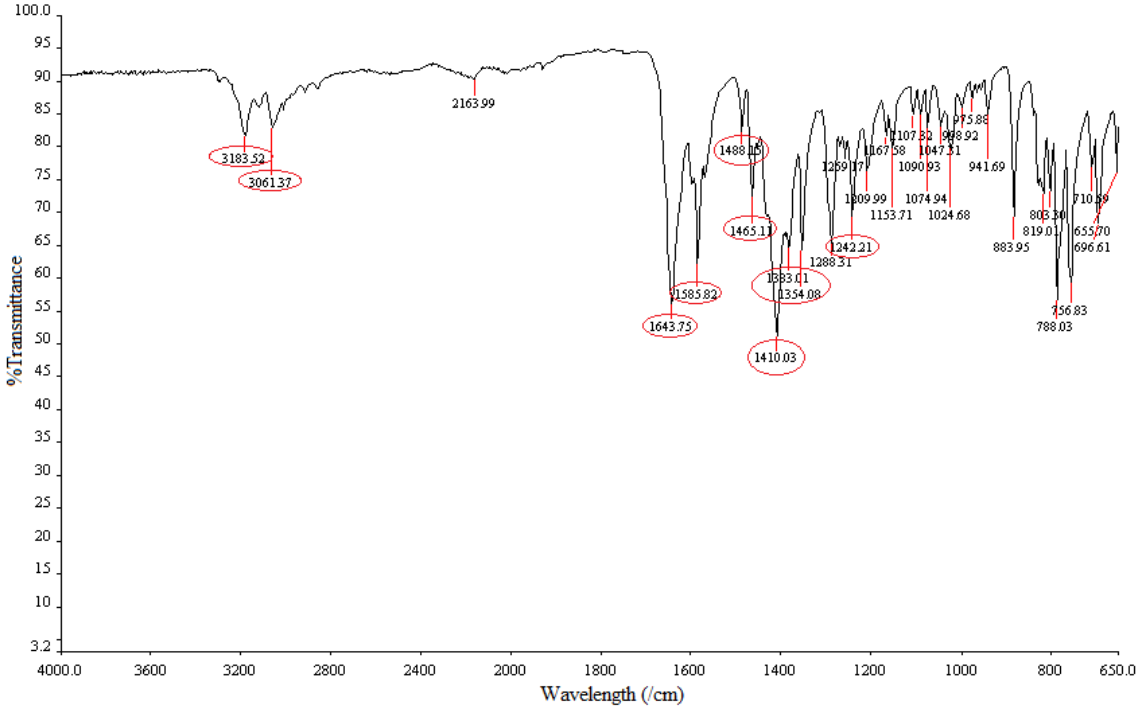

Figure 4.15. FT-IR absorption spectrum of NVP.

All absorption and frequency peaks were observed in 1:1 binary mixtures of NVP and the excipients under consideration and no new or additional peaks were evident. However slight shifts in the frequencies of vibration were evident in the binary mixtures that were tested and may be attributed to hydrogen bonding between the materials as opposed to a chemical interaction. The FT-IR spectra of 1:1 binary mixtures of NVP and excipients are shown in Figures 4.16.

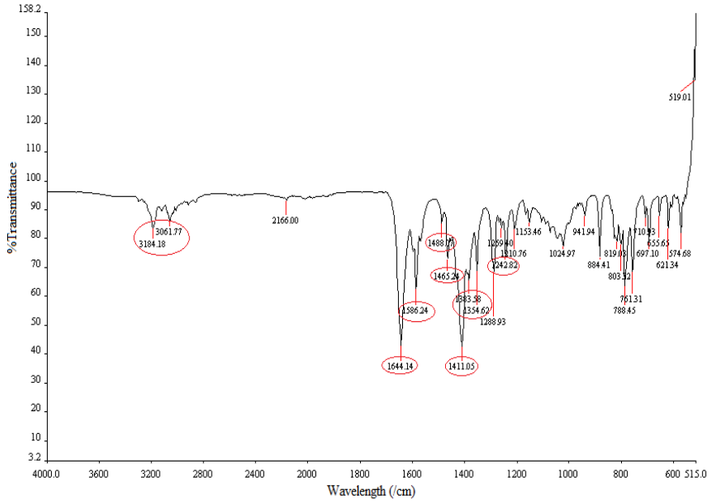

NVP + Methocel® K4M

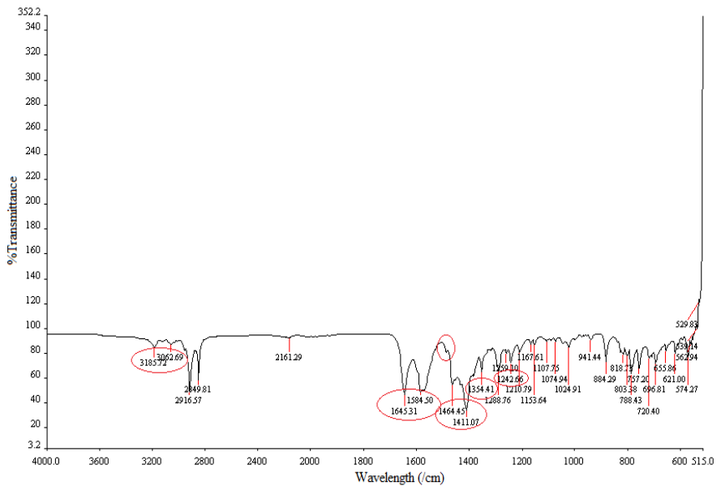

NVP + Mg stearate

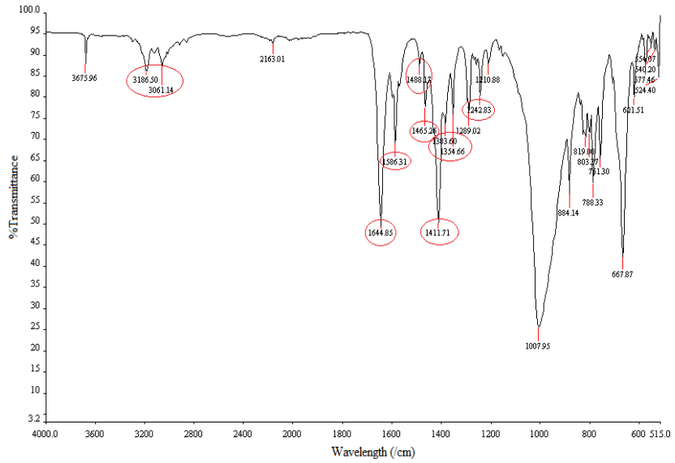

NVP + Talc

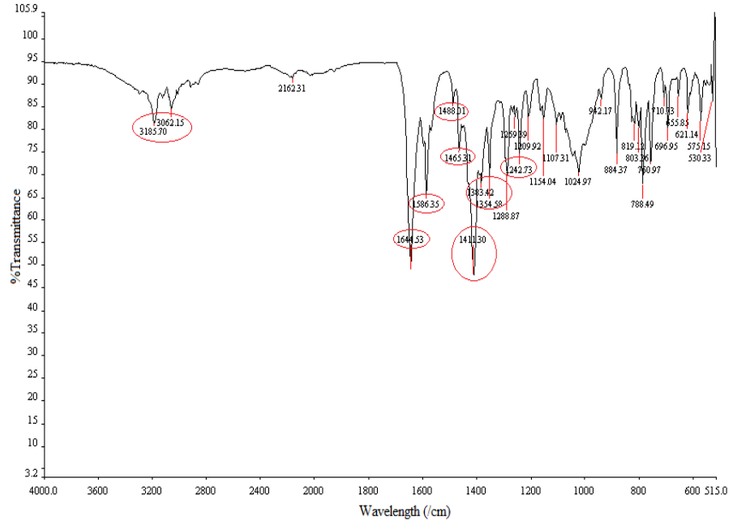

NVP + Avicel® PH102

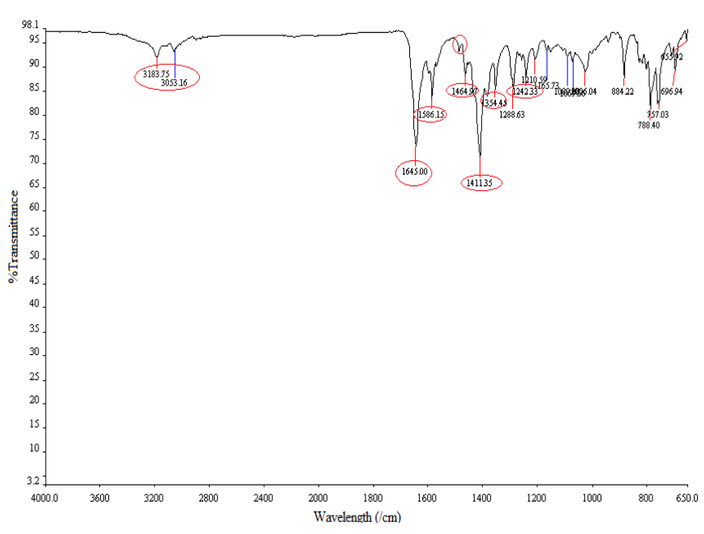

NVP + SuperTab® SDL

Figure 4.16. FT-IR spectra of 1:1 binary mixtures of NVP and excipients.

4.7 CONCLUSIONS

In order to undertake a successful tableting process, it is essential to select components of formulation that will ensure that a tablet of desirable characteristics and quality is produced. Important factors that must be considered when selecting an excipient include consideration of the particle size and shape of material which can impact powder flow and compaction properties, and API-excipient compatibility.

Most often the components of a tablet are available in different particle size and shape as is evident of the results of particle shape and size distribution analysis of the excipients and the NVP used in these studies. The results indicate that there is a possibility of poor flow properties which may result in tablets of inadequate quality. Screening of powder blends with a sieve of a desirable size prior to blending was considered appropriate as this would produce materials of uniform size distribution with a subsequent possible improvement in powder flow properties.

The flow properties of the powder blends for all the batches in formulation development were within the acceptable limits. Although some powder blends had values of AOR, HR and CI slightly above the required values it was anticipated that the values would improve following the addition of a lubricant. These studies showed that the powder blends may be suitable for direct compression tableting without further manipulation and were likely to produce tablets with acceptable quality attributes.

The potential for physical and chemical interactions to occur between an API and excipients is well-documented [285-290]. It was therefore deemed important to conduct NVP-excipient compatibility studies and ascertain which excipients were appropriate for formulation development studies.

DSC was used to study the potential for significant interactions to occur between the excipients under consideration and NVP. The DSC data generated for the different binary mixtures evaluated indicate that the characteristic melting endotherm at 250 °C for NVP was present in all thermograms. The results revealed that that there was a low potential for NVP-excipient interactions despite minor variations in the melting point of excipients and NVP when tested in combination. Whilst DSC is a well-known technique for characterisation of pharmaceutical and polymeric materials, limitations with respect to its practical use exist as it

is unable to provide insight into the changes to thermal events or reactions at a molecular level. Therefore it was essential to combine DSC with other techniques to permit a greater understanding of any changes in the materials to be used and therefore FT-IR studies were also conducted.

The use of FT-IR absorption spectroscopy for studying the potential for interactions between NVP and other materials offer an opportunity to evaluate such interactions at a molecular level. The fingerprint FT-IR generated for NVP and each excipient permitted the study of possible interactions and any shift in IR fingerprint may be indicative of a significant interaction. FT-IR studies did not reveal any interactions as the identified characteristic frequencies of NVP functional groups were present in all FT-IR spectra albeit minor shifts in vibrational frequencies that could be attributed to hydrogen bonding.

The theoretical basis of DSC and FT-IR analysis to study possible drug-excipient interactions has been applied and the results revealed that the probability of detrimental interactions between NVP and the excipients was low.

Since all the excipients appeared to be compatible with NVP, they were all used for formulation development studies.

CHAPTER FIVE

FORMULATION DEVELOPMENT AND ASSESSMENT OF NVP SUSTAINED RELEASE TABLETS

5.1 INTRODUCTION

Sustained release (SR) refers to dosage forms that modulate the rate of drug release and control the rate of drug availability for absorption, thereby achieving desired concentrations of the API in plasma over a prolonged period of time [291]. SR dosage forms have also been referred to as extended release (XR) technologies [219, 291, 292]. In order to optimise therapy for the majority of therapeutic agents, the primary goal is to attempt to achieve constant therapeutic blood levels of the API. However, fluctuations in blood levels are common and may result in therapeutic failure and/or undesirable adverse events. SR technologies provide an effective means of optimising the bioavailability of a compound and can produce predictable concentration-time profiles of an API that would otherwise not be possible [291, 293].

Key physiological factors that affect drug absorption from the GIT include gastric and intestinal secretions, fluid and food intake, bulk fluid and luminal pH, mechanisms of absorption and enterocyte-based metabolism and/or secretion. These factors in conjunction with the physicochemical properties of an API such solubility, ionisation state, stability and lipophilicity can and often do influence the rate and extent of API absorption from the lumen of the GIT [291, 294-297].

A critical assessment of the fundamental physicochemical properties of an API and consideration of the biopharmaceutics of the compound are crucial to the successful design of an oral SR delivery system. The control of API release is dependent on the dosage form design and should not be adversely influenced by the intrinsic physicochemical properties of the API or the physiological constraints of the GIT [291, 296].

Drug candidates exhibiting high permeability across the epithelium of the GIT are considered to be BCS Class I and II compounds and absorption of these API are controlled exclusively by their rate of release from a dosage form [291]. It is only for these compounds that *in vitro* dissolution rates can be used to predict *in vivo* absorption rates and guide formulation development.

Although SR delivery systems offer a number of advantages over conventional drug delivery systems, they do present serious challenges to the patient or clinician due to the variability of GIT transit times between different ethnic groups. The release of an API for absorption may be constant and sustained, however absorption may occur over different time durations. A short transit time would mean that the API may not be available for complete absorption to occur, whereas longer transit times may result in the patient being over exposed to an API and they may potentially exhibit adverse effects [291, 294, 298].

The regional absorption patterns shown by some API in different positions of the GIT may result in reduced bioavailability if the API is best absorbed from the upper parts of the GIT and are formulated into a SR delivery system [298]. Another factor that may result in reduced bioavailability from a SR delivery system is reduced saturable first pass metabolic effects in the liver and/or the gut wall. Saturation of the metabolising capacity of the liver enzymes may readily occur following chronic administration of immediate release dosage forms and this may result in reduced metabolism of the drug as the enzymes are saturated. However, saturation of liver enzymes does not readily occur with SR drug delivery systems as there is a smoother and gradual drug release. This may result in continuous metabolism of the drug and may result in significantly lower systemic levels [298-300].

5.2 SUSTAINED RELEASE DELIVERY SYSTEMS

5.2.1 Matrix Systems

Matrix systems are comprised of an API dispersed, entrapped or dissolved in a polymer and other excipients that are inert, erodible and/or swellable. Matrices have been studied and used for the manufacture of sustained release systems as they are simple and easy to produce [298, 300]. They are relatively safe as there is little chance of dose dumping due to collapse of the delivery system [300]. Inert matrices release API and leave a residual skeleton whereas erodible matrices disintegrate slowly over time. Swellable technologies undergo transformation to produce a gel layer that modulates API release [301].

The characteristics of the polymer used determine whether the matrix is hydrophilic (e.g. HPMC), hydrophobic (e.g. polyethylene oxide) or plastic (e.g. methyl methacrylate) [300]. Hydrophilic and hydrophobic matrix systems are commonly used as drug delivery systems [302].

Matrix systems can be further classified as diffusion/swellable or dissolution controlled systems [300]. API release from diffusion or swellable matrices is preceded by penetration of a solvent into the matrix, resulting in hydration and swelling of the polymeric material, followed by diffusion of the API through the hydrated layer of polymer to the bulk dissolution fluid or gastrointestinal tract contents. Hydration of the polymer due to penetration of a solvent results in relaxation of polymer chains as a result of a decrease in the vitreous transition temperature of the polymer [303]. A zone in which transformation of the polymer from a crystalline to a rubbery state is formed is known as the gel layer. The thickness of the gel layer increases as additional fluid enters the dosage form and the polymer chains located at the surface hydrate and gradually relax until they lose consistency, after which erosion of the polymer occurs [219, 303]. Examples of polymers used in diffusion/swellable matrices include cellulose ethers such as HPMC, methacrylic acid copolymers and carbomers [219, 301, 302].

The thickness of the gel layer is critical to the API release process, and as the gel layer gets thicker the distance that the drug must diffuse through increases. Furthermore API diffusion from matrices have been observed to be affected by the molecular weight [304], solubility [305], API dose [221] and Particle size [221, 304-308]. Other factors that affect API diffusion include polymer type *viz.,* hydrophilic, hydrophobic or plastic, molecular weight [309, 310], polymeric composition, cross-linking and substitution of the polymer side chain, radius of gyration [311], particle size, viscosity, intrinsic viscosity and the amount of polymer used [309-312]. The viscosity of the hydrated polymer and the drug load contributes to the formation of a concentration gradient that has an impact on the diffusion front and positional movement of the API in the gel layer [313].

Dissolution controlled systems achieve sustained drug delivery as a consequence of the control they exert on the dissolution/erosion of a polymeric matrix, which can result in constant drug delivery. Examples of polymers that have been used include HPMC, natural gums such as xanthan and sodium carboxymethylcellulose [314].

The penetration of water into the matrix system results in swelling, erosion of the dosage form and release of the API. The release of the API from such technologies follows the Higuchi model and is dependent on square root of time. The full equation describing the Higuchi model is shown by Equation 5.1.

$$M_t = A\,[D\,(2C_0 - C_s)]\,C_s t \qquad \textbf{Equation 5.1}$$

where,

M_t = cumulative amount of drug released,
t = time,
A = surface area of the controlled release device,
D = drug diffusivity in the polymer carrier,
C_0 = initial drug concentration, and
Cs = solubility of the drug in the polymer.

In diffusion-controlled matrix systems, particles of API on the surface of the dosage form are released initially resulting in the dissolution front receding into the dosage form with a consequent increase in the diffusion distance across which the drug must travel to be released. A continual slowing of API release is observed [302]. A schematic illustration of API release from a non-eroding diffusion-controlled matrix is depicted in Figure 5.1.

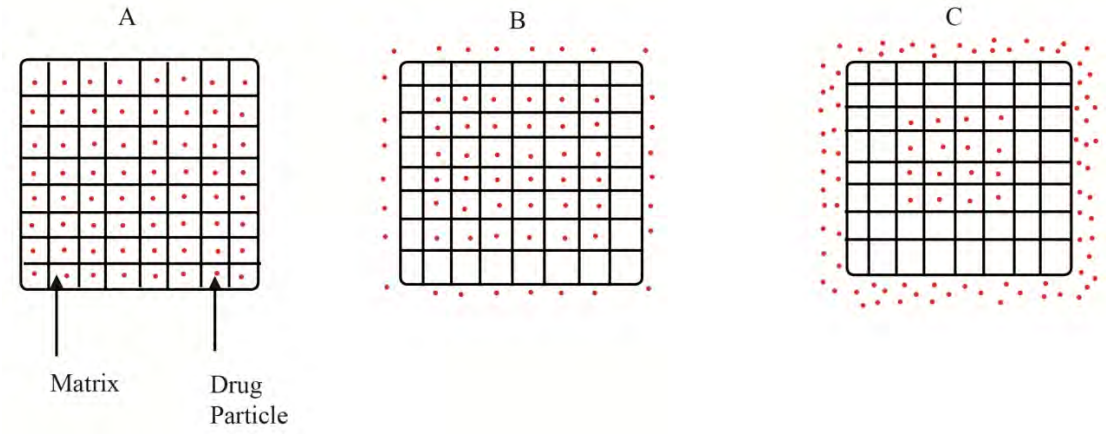

Figure 5.1. Mechanism of drug release from a non-eroding diffusion-controlled matrix. Adapted from [315].

In erosion-controlled matrix systems the rate of release of API is, in part, controlled by dissolution of the matrix, thereby resulting in constant drug delivery. This phenomenon is depicted in Figure 5.2 [302].

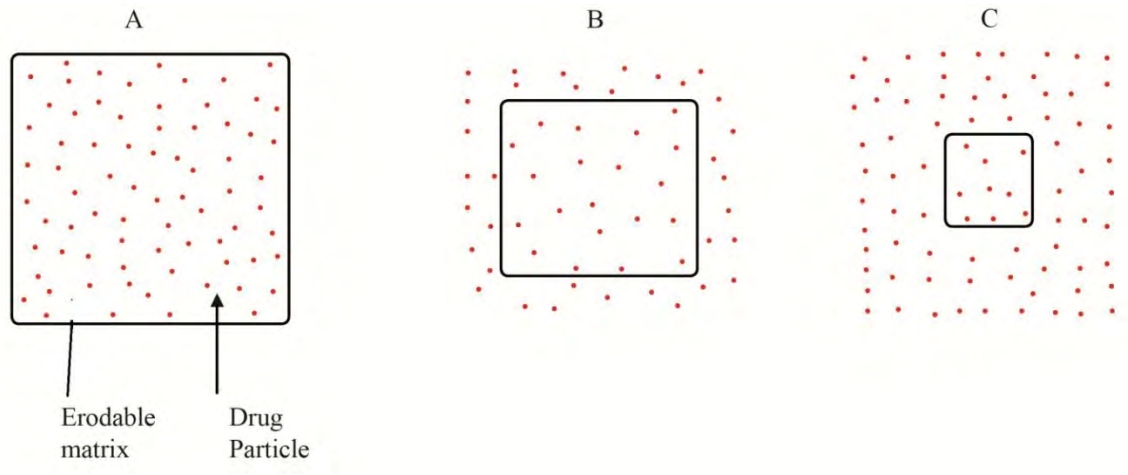

Figure 5.2. Mechanism of drug release from an erosion-controlled matrix [315].

API release from a swelling controlled matrix decreases over time as the resistance to diffusion through the gel layer is greater than the potential increase in API release due to the increase in surface area that is associated with polymer swelling [316].

Formulation factors affecting API release from these systems include the amount of solvent that penetrates the matrix [317], shape and thickness of the device [318], presence of other API and/or excipients [319], micro-environment pH [320], matrix porosity [321], resistance of the device to breakage and artefacts of the manufacturing process [322, 323].

The targeted release rate can be achieved by altering the polymer type, excipients, manufacturing processes and the use of different amounts and viscosity grades of polymers. These are the widely used approaches to the development of sustained release systems and were followed in these studies.

5.2.2 Reservoir Devices

Reservoir devices are technologies in which an API is encapsulated by a polymeric film or coating and from which release rates are dependent on the nature of the film or coating material, thickness and chemistry, amongst other factors. Reservoir devices can be manufactured by film coating or microencapsulation processes [324, 325].

The selection of an appropriate polymeric material to be used for the development of a reservoir dosage form is critical. However, factors such as other excipients, polymer functionality and porosity must also be considered [326]. A schematic representation of drug release from a diffusion based reservoir technologies over time is depicted in Figure 5.3. The

API partitions from the reservoir into the membrane, after which it diffuses across the membrane to the surface of the technology, and it subsequently partitions into the dissolution medium.

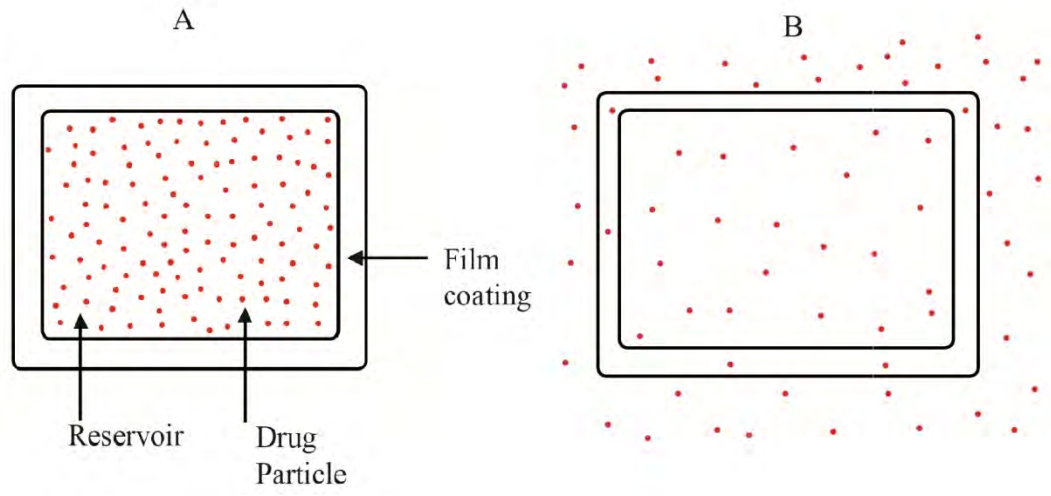

Figure 5.3. Mechanism of drug release from reservoir sustained release system [315].

5.2.3 Osmotic Devices

Osmotic devices are comprised of an osmotic agent that may be the API that is coated with a semi-permeable membrane with a release portal. API release is a function of the osmotic potential and hydrostatic pressure of the system [326, 327]. Water uptake through a semi-permeable membrane coating is facilitated by the presence of a soluble drug or an osmotic propellant. This results in the formation of a saturated aqueous drug solution in the device or propellant compartment and subsequent release of the API from the device through the orifice or portal [328]. The orifice minimises solute diffusion whilst preventing build-up of a hydrostatic head that has the effect of decreasing the osmotic pressure and changing the dimensions of the device [326-330]. The schematic representation of drug release from an osmotic-controlled release delivery system with a single orifice is illustrated in Figure 5.4.

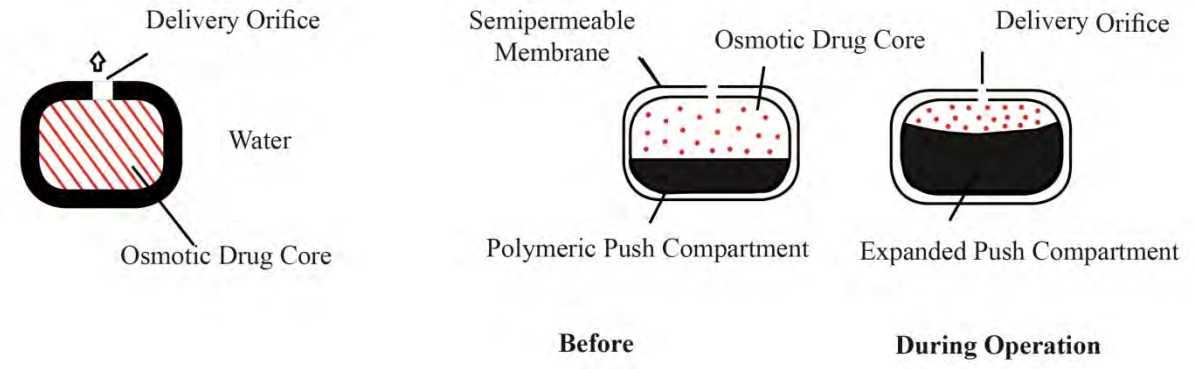

Figure 5.4. Schematic presentation of mechanism of drug release from an osmotic-controlled release system. A = elementary osmotic pump and B = push-pull osmotic pump [251].

Early osmotic-controlled drug delivery systems were only suitable for water soluble API and typically the solubility of the API should be at least 10-15% w/v [326]. Sparingly soluble drugs pose formulation challenges such as unexpected or uncontrolled release and sometimes inefficient dissolution of the API if included in elementary systems. However, the development of push-pull osmotic systems have reduced this challenge significantly [326-330].

The rate at which an API is released from an osmotic system can be described using Equation 5.2.

$$\frac{dm}{dt} = \frac{dv}{dt}\ Cs \qquad \textbf{Equation 5.2}$$

where,

$\frac{dm}{dt}$ = drug flow rate through an orifice,
$\frac{dv}{dt}$ = flow rate of water through an orifice, and
Cs = saturation concentration of the drug.

Osmotic delivery systems release API at a zero order rate until the amount of the osmotically active salt or API in the system decreases to below saturation concentration [326, 328].

5.3 EXPERIMENTAL

5.3.1 Method of Manufacture of NVP Sustained Release Tablets

A direct compression, DC, tableting process was selected and used to manufacture all test formulations. It is a simple and efficient manufacturing process that has a minimum number of unit operations when compared to other manufacturing procedures.

A schematic representation of the manufacturing process that was used is shown in Figure 5.5. NVP and all other excipients except for magnesium stearate and talc were individually weighed using a Model PM top-loading electronic balance (Mettler®, Zurich, Switzerland), screened through a mesh size # 20 (841 μm) and blended in a cube blender rotated at 200 rpm for 30 minutes at an angle of 180°. Mg stearate and talc were weighed, screened through a mesh size # 44 (462 μm) and added to the mixture and the blending process was continued for a further three (3) minutes. The powder blend was compressed on a Manesty® B3B (Manesty®, Knowsley, UK) 16-station rotary press set at 27 rpm and fitted with four 9 mm shallow concave punches. The target weight and hardness of the tablets were set at 300 mg and 100-150 N (10-15 Kp), respectively.

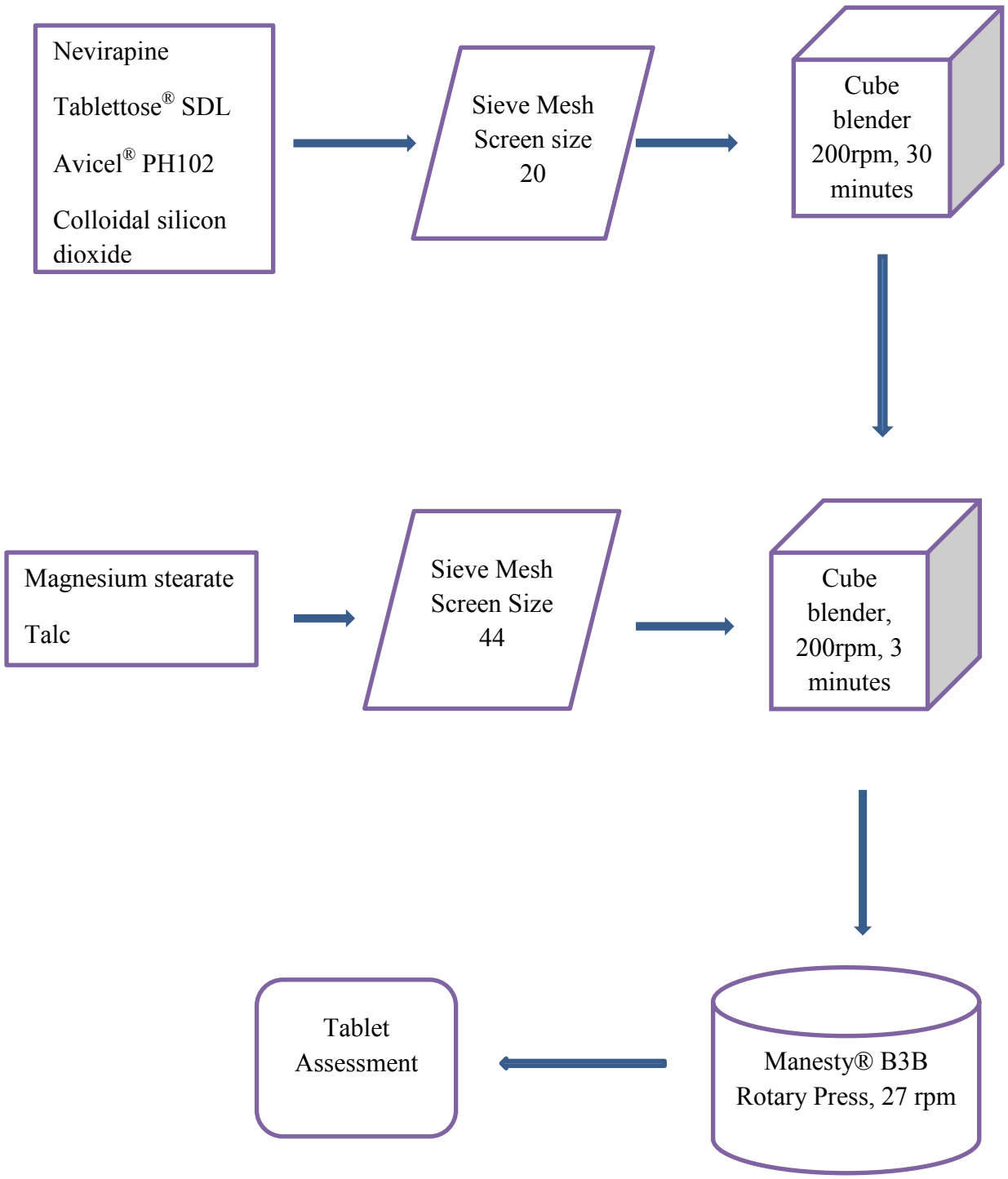

Figure 5.5. Schematic representation of the manufacturing process for NVP tablets.

5.3.2 Formulation

The formulation composition of the tablets that were manufactured during formulation development studies are listed in Table 5.1. The formulations were altered by changing the amount of release rate controlling polymers and diluent used. The amount of NVP and all other components *viz*., Avicel® PH102 (13.5%), magnesium stearate (1.1%), talc (1.0%) and colloidal silicon dioxide (1.1%) which were present in all formulations, were held constant throughout these experiments.

Table 5.1. Formulation composition of experimental batches NVP001 – NVP012

Batch Number	NVP %	Methocel® K4M %	Carbopol® 71GNF %	Eudragit® RSPO %	DCP %	SuperTab® Spray-dried Lactose %
NVP001	33.3	30.0	-	-	10.0	10.0
NVP002	33.3	25.0	-	-	10.0	15.0
NVP003	33.3	20.0	-	-	10.0	20.0
NVP004	33.3	10.0	-	-	-	40.0
NVP005	33.3	20.0	-	-	-	30.0
NVP006	33.3	30.0	-	-	-	20.0
NVP007	33.3	10.0	5.0	-	-	35.0
NVP008	33.3	10.0	10.0	-	-	30.0
NVP009	33.3	10.0	15.0	-	-	25.0
NVP010	33.3	10.0	-	5.0	-	35.0
NVP011	33.3	10.0	-	10.0	-	30.0
NVP012	33.3	10.0	-	15.0	-	25.0

5.3.3 Quality Testing and Desirable Attributes of NVP Tablets

5.3.3.1 Content Uniformity

The content uniformity of tablets may vary due to non-uniform distribution of an API in a powder blend or granules, segregation of powders during the different stages of the manufacturing process or variations in tablet weight. However, tablet weight cannot be used as an indication of potency except when the API content of a formulation is 90-95% of the total weight of the tablets [245].

Ten randomly selected tablets from each manufactured batch were individually weighed and crushed using a mortar and pestle. The powder was then quantitatively transferred to a 100

mL A-grade volumetric flask using methanol. Approximately 50 mL methanol was added and the mixture was sonicated for 10 minutes. The solutions were then made up to the volume with mobile phase and filtered through a 0.45 µm PVDF hydrophilic HVLP Millipore® Millex-HV membrane (Millipore® Corporation, Bedford, USA) prior to analysis using the RP-HPLC described in Chapter 2 *vide infra*.

5.3.3.2 NVP Assay

Twenty randomly selected NVP tablets from each manufactured batch were weighed and crushed using a mortar and pestle. An amount of powder equivalent to 100 mg of NVP was transferred into a 100 mL A-grade volumetric flask. Approximately 50 mL methanol was added and the mixture was sonicated for 10 minutes and then made up to volume with mobile phase. The solution was filtered through a 0.45 µm PVDF Millipore® hydrophilic Millex-HV (Millipore® Corporation, Bedford, USA) membrane prior to analysis using the validated RP-HPLC method described in Chapter 2 *vide infra*.

5.3.3.3 Weight Uniformity

Twenty NVP tablets were randomly selected and weighed individually using a Model AG 135 top-loading balance (Mettler® Toledo, Switzerland) and the average weight of the tablets for each batch calculated.

5.3.3.4 Hardness

Twenty tablets from each batch were randomly selected and the hardness determined using a Model PTB 311 E Hardness Tester (PharmaTest AG®, Hamburg, Germany) after which the average hardness for each batch was established.

5.3.3.5 Tensile Strength

The tensile strength of the tablets for each batch was calculated from the average hardness of 20 tablets using Equation 5.3.

$$\sigma = \frac{2F}{\pi dT} \qquad \textbf{Equation 5.3}$$

where,

σ = maximum radial tensile strength in N/mm^2,
F = crushing strength in N,

d = tablet diameter in mm, and
T = tablet thickness in mm.

5.3.3.6 Friability

Twenty tablets were randomly selected, weighed collectively and then subjected to friability testing for 4 minutes at a rotation speed of 25 rpm using an Erweka® TA3R Friability Tester (Erweka®, GmbH, Heusenstamm, Germany) after which the tablets were de-dusted, weighed and the percent friability calculated.

5.3.3.7 In Vitro API Release Studies

Dissolution studies were performed on all batches of tablets that had been manufactured using the dissolution test method that was developed and validated as described in Chapter 3, *vide infra*.

5.4 RESULTS AND DISCUSSION

5.4.1 Quality Testing and Desirable Attributes of NVP Tablets

5.4.1.1 Content Uniformity

All batches that were tested passed content uniformity testing with all % RSD values for all batches ≤ 5% and as summarised in Table 5.2. These results imply that the manufacturing process was precise and were therefore an indication that the batch-to-batch NVP content uniformity of the ultimate product can be achieved.

Table 5.2. Content uniformity of NVP tablets

Batch Number	Theoretical Amount mg	Actual Amount mg ±SD	%RSD
NVP001	100	98.42±3.12	3.17
NVP002	100	97.86±2.89	2.96
NVP003	100	98.59±2.64	2.68
NVP004	100	97.71±2.46	2.52
NVP005	100	96.88±3.65	3.77
NVP006	100	97.91±1.85	1.89
NVP007	100	98.30±3.38	3.44
NVP008	100	97.22±2.70	2.78
NVP009	100	98.09±2.31	2.35
NVP010	100	97.68±3.506	3.51
NVP011	100	97.67±2.76	2.83
NVP012	100	99.28±3.74	3.77

5.4.1.2 NVP Assay

The NVP content in tablets was within the specifications and ranged from 96.3 ± 2.89 to 101.4 ± 2.72 % as shown in Table 5.3. This further proved that the manufacturing process was precise.

5.4.1.3 Weight Uniformity

The tablets had an average weight ranging from 290.33 ± 2.98 to 300.72 ± 2.72 mg and %RSD values for weight variation analysis were all < 5% as shown in Table 5.3. Although tablets from batch NVP002 and NVP008 had average weights much lower than the target weight, tablets from the rest of the batches had average weight values that were closer to the target showing that the manufacturing process was suitable for further optimisation.

5.4.1.4 Tablet Hardness

The hardness of the tablets ranged from 89.9 ± 5.38 to 129.7 ± 5.81 N and are summarised in Table 5.3. Only tablets from batch NVP011 had an average hardness that was less than the target indicating that the manufacturing process was possibly suitable to produce tablets of appropriate quality.

5.4.1.5 Tensile Strength

The tensile strength of the tablets ranged from 1.18 ± 2.41 to 1.58 ± 4.32 N/mm^2 and these data are summarised in Table 5.3. The tablets were considered sufficiently strong to withstand the abrasion associated with handling, packaging and shipment of such dosage forms.

5.4.1.6 Friability

The friability of the tablets ranged from 0.158 ± 1.22 to 0.172 ± 2.34 % and the data are summarised in Table 5.3. The friability results reveal that the manufacturing process would yield products that would be able to withstand some of the attrition forces that are associated with handling, packaging and transportation of tablets from one location to another.

Table 5.3. Quality attributes of NVP tablets

Batch Number	Thickness Mm	Hardness N	Uniformity of weight, mg	Tensile strength N/mm^2	Assay %	Friability %
NVP001	5.54 ± 1.12	108.4 ± 3.20	297.34 ± 1.77	1.43 ± 2.01	97.4 ± 3.88	0.158 ± 1.22
NVP002	5.53 ± 1.23	117.8 ± 4.11	290.33 ± 2.98	1.56 ± 2.23	99.6 ± 3.07	0.169 ± 2.87
NVP003	5.54 ± 2.15	100.5 ± 6.93	295.57 ± 2.82	1.33 ± 3.12	96.3 ± 2.89	0.172 ± 2.34
NVP004	5.55 ± 2.26	118.3 ± 4.42	296.66 ± 3.93	1.56 ± 3.23	98.7 ± 3.67	0.170 ± 3.41
NVP005	5.53 ± 1.16	129.7 ± 5.81	299.12 ± 3.09	1.72 ± 2.72	97.9 ± 3.66	0.166 ± 3.33
NVP006	5.52 ± 1.24	110.9 ± 3.82	298.22 ± 3.44	1.47 ± 1.91	98.9 ± 2.96	0.169 ± 2.88
NVP007	5.56 ± 1.47	114.5 ± 2.73	297.88 ± 2.37	1.51 ± 2.11	97.8 ± 3.22	0.171 ± 2.71
NVP008	5.57 ± 2.05	120.2 ± 3.86	294.68 ± 3.58	1.58 ± 4.32	96.7 ± 3.82	0.158 ± 3.19
NVP009	5.59 ± 2.33	101.7 ± 3.80	301.47 ± 1.83	1.33 ± 2.82	98.8 ± 1.50	0.171 ± 2.77
NVP010	5.60 ± 3.06	99.8 ± 4.04	299.02 ± 1.79	1.30 ± 1.86	101.4 ± 2.72	0.163 ± 3.56
NVP011	5.59 ± 1.16	89.9 ± 5.38	296.19 ± 3.85	1.18 ± 2.41	96.8 ± 1.87	0.159 ± 2.72
NVP012	5.52 ± 1.33	100.0 ± 3.77	300.72 ± 2.74	1.33 ± 3.72	99.7 ± 3.80	0.171 ± 3.09

All values reported as mean ± %RSD

5.4.2 *In Vitro* API Release Studies

The dissolution profile generated for batch NVP001 revealed that the rate of NVP release was very low and incomplete after 24 hours of testing with only 16.7 % of NVP released as shown in Figure 5.6.

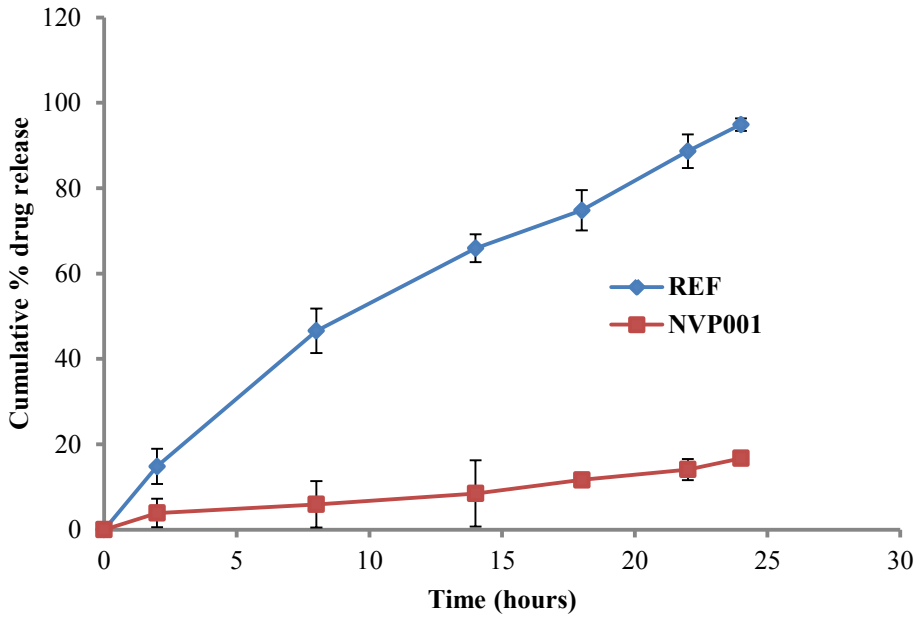

Figure 5.6. Dissolution profile of NVP release from tablets of batch NVP001 and Viramune® XR (n = 6).

The incomplete drug release from the tablets of batch NVP001 was attributed to the use of a high percentage (30%) of HPMC in the formulation. It has been observed that regardless of the physicochemical properties of the polymer and API, drug release generally decreases with an increase in the percent composition of the release controlling polymer used to form the matrix. Large quantities of polymer correspond to low porosity in the matrix resulting in a slower rate and extent of API release [331]. The use of a high proportion of polymer also promotes a greater degree of cross-linking, an increase in the gel layer thickness and tortuosity of the matrix, which are characteristics that impede API diffusion through the gel layer thereby altering API release [332].

The percent HPMC in batch NVP002 was reduced by 5% in an effort to improve the rate and extent of drug release from the tablets, as it has been reported that an increase in the percent polymer from 3.5% to 19.2% resulted in a decrease in the release rate of an API [333]. Therefore, it was anticipated that a decrease in the amount of polymer used in the matrix would result in an increase in NVP release from the tablets. However, the resultant increase in NVP release was minimal and a total of only 19.64% NVP was released after 24 hours of dissolution testing as depicted in Figure 5.7.

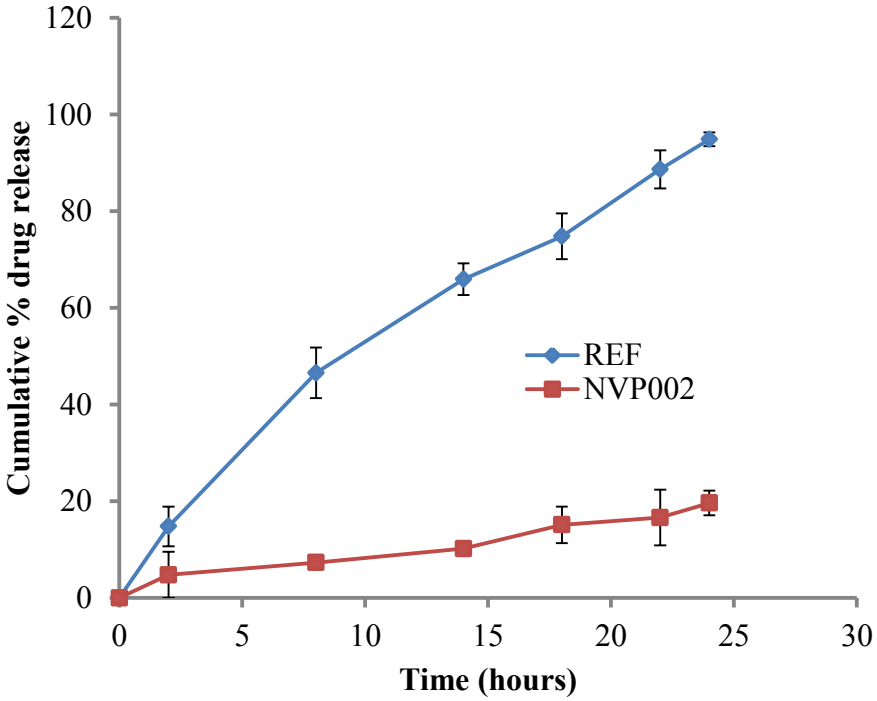

Figure 5.7. Dissolution profile of NVP release from tablets of batch NVP002 and Viramune® XR (n = 6).

The percent HPMC in batch NVP003 was reduced by a further 10 % in an effort to increase the rate and extent of NVP release, however the resultant increase in NVP release was also minimal with only 34.9 % NVP released after 24 hours of dissolution testing as shown in Figure 5.8.

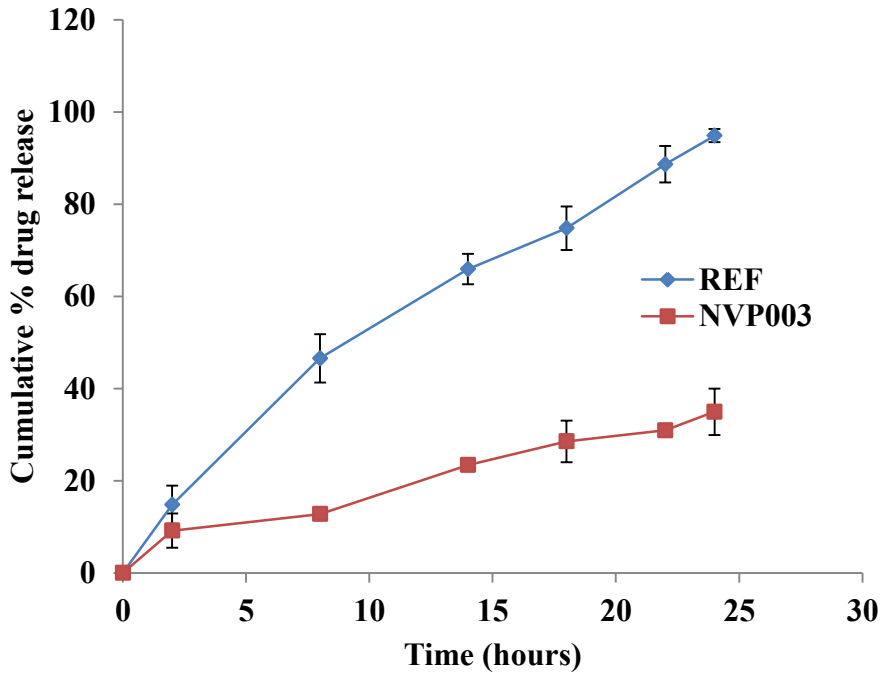

Figure 5.8. Dissolution profile of NVP release from tablets of batch NVP003 and Viramune® XR (n = 6).

The slow rate of release of NVP from tablets of batches NVP002 and NVP003 was attributed to the presence of DCP in the matrices as it is insoluble and has been shown to retard API release from matrix tablets by blocking the diffusion of the API from the matrix and by decreasing the erosion of the polymer matrix [334, 335]. It has been reported that the use of DCP can have a significant impact on API release from matrix formulations, particularly if the API is poorly water soluble, as NVP is. DCP makes the matrix less accessible to water thereby reducing the degree of matrix erosion, which is an important factor in determining the rate and extent of release of poorly water soluble compounds [336]. Consequently DCP was not included in subsequent formulations in an attempt to improve the rate and extent of release of NVP.

In an attempt to improve the rate and extent of NVP release, batch NVP004 was manufactured using 10% w/w HPMC, however the tablets exhibited rapid release and a high extent of NVP release with approximately 98% of the NVP released within two hours of commencing testing as shown in Figure 5.9.

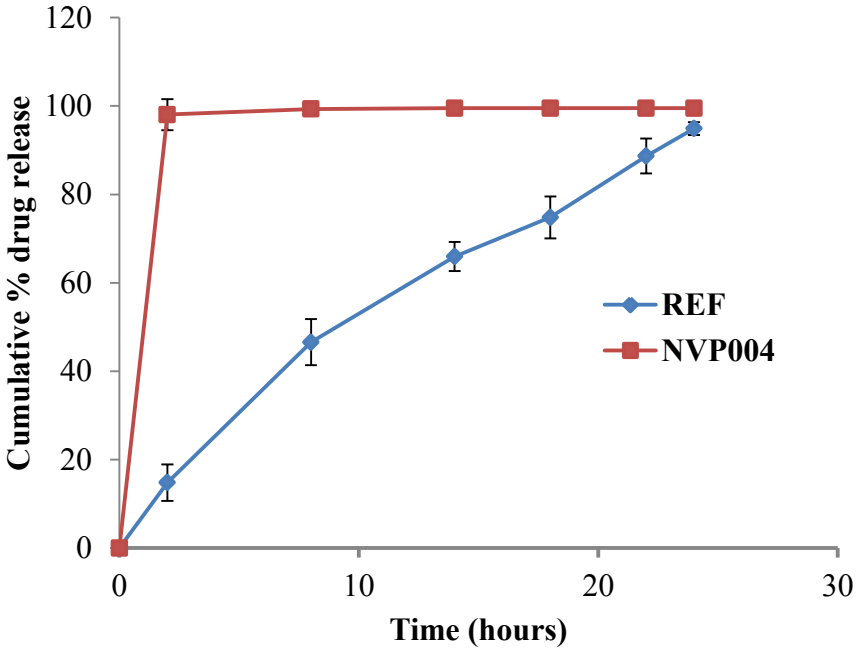

Figure 5.9. Dissolution profile of NVP release from tablets of batch NVP004 and Viramune® XR (n = 6).

The rapid rate of release and high extent of NVP release from tablets of batch NVP004 was more likely due to the fact that DCP was not used in the formulation and insufficient HPMC was included. This resulted in a decrease in the gel strength and a high porosity that favours NVP diffusion out of the matrix [336]. Furthermore the rapid release observed may also be a function of an increase in the amount of lactose used in the formulation. This effect of lactose may be attributed to the dissolution of lactose on hydration of the tablet, which may result in an increase in the porosity and a reduction of the gel strength of the matrix [335].

The formulation of Batch NVP005 was modified by increasing amount of HPMC by 10% and decreasing the amount of lactose by 10 % with a view to decreasing the rate of NVP release from the tablets. The release of NVP decreased appreciably but was still more rapid than that observed for the reference product with approximately 53.5% released within the first two hours of commencing dissolution testing as shown in Figure 5.10.

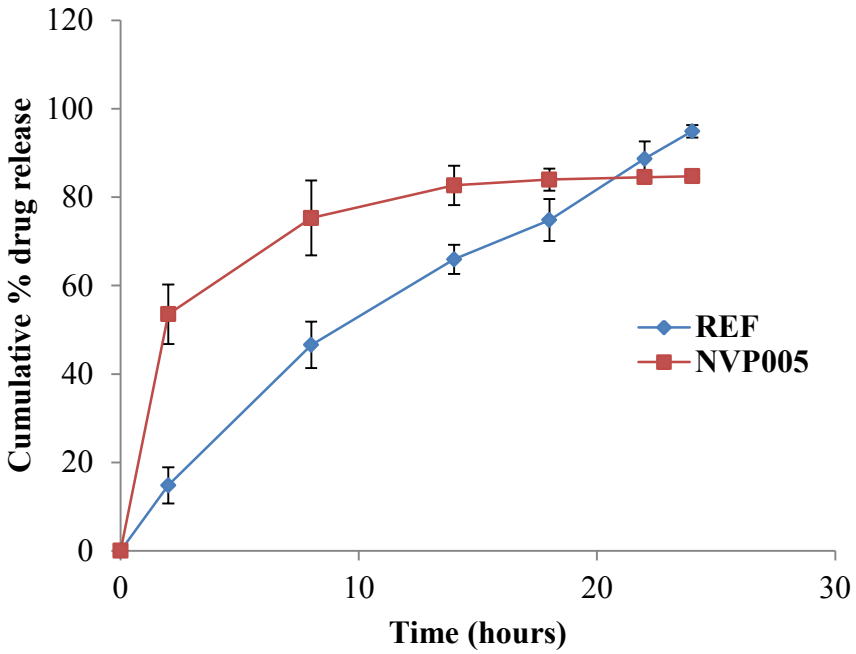

Figure 5.10. Dissolution profile of NVP release from tablets of batch NVP005 and Viramune® XR (n = 5).

The amount of HPMC was then increased by a further 10% and the spray dried lactose content was reduced from 30% to 20% to produce batch NVP006. The rate of release of NVP decreased significantly and the dissolution profile was observed to be similar to that of the reference product as shown in Figure 5.11. Calculation of the f_1 and f_2 values to permit comparison of the dissolution profiles yielded f_1 and f_2 values of 14.1 and 52.1, respectively and indicates that the tablets from batch NVP006 could release NVP similar to the profile observed for the reference tablets. Consequently the formulation for batch NVP006 was selected for further development and optimisation.

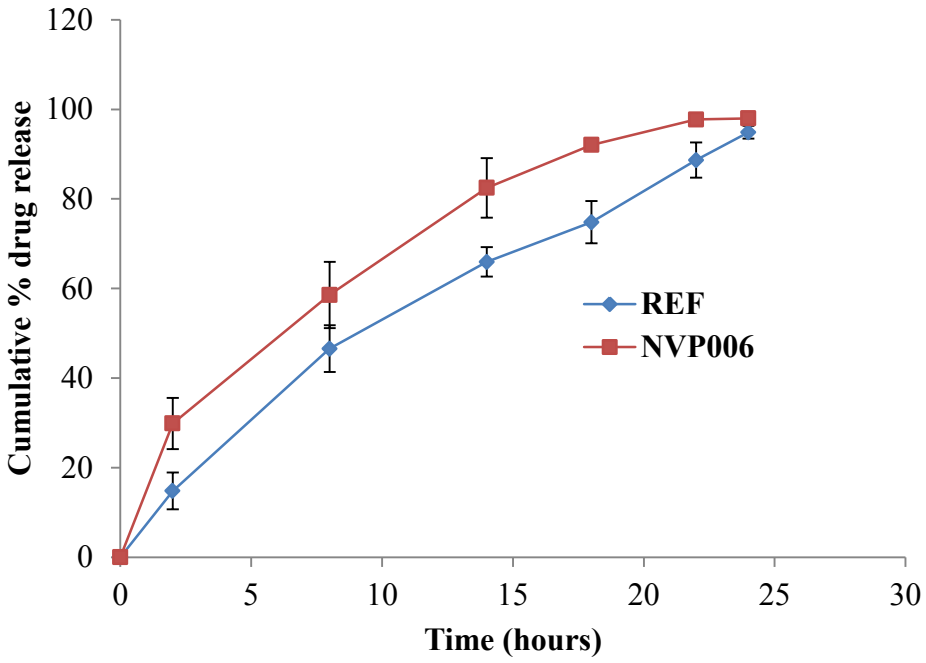

Figure 5.11. Dissolution profile of NVP release from tablets of batch NVP006 and Viramune® XR (n = 6).

A combination of polymers with different chemistries or viscosities can be used to optimise drug release from hydrophilic matrices manufactured using HPMC as the primary release controlling polymer [337, 338] and carbomers to modulate drug release from matrices [339, 340]. This combination has been reported to produce a synergistic increase in the viscosity of a matrix due to strong hydrogen bonding between the carbomer and HPMC [340]. The stronger cross-link between the two polymers produces a more rigid structure through which diffusion must take place and the interaction results in increased stability of API release profiles compared to matrices manufactured with HPMC alone [340].

The combination of anionic polymers and HPMC can influence drug release in basic dissolution media by lowering the micro-environment pH of the matrix and can also decrease API release in acidic media through formation of an insoluble matrix [339, 340].

Batches NVP007, NVP008 and NVP009 were formulated using combinations of Methocel® K4M and Carbopol® 71G NF, with the HPMC content fixed at 10% and the amount of Carbopol® 71G NF ranging between 5% and 15%. Tablets from batch NVP007 produced rapid release of NVP with 100% being released within the first two hours of commencing dissolution testing as shown in Figure 5.12.

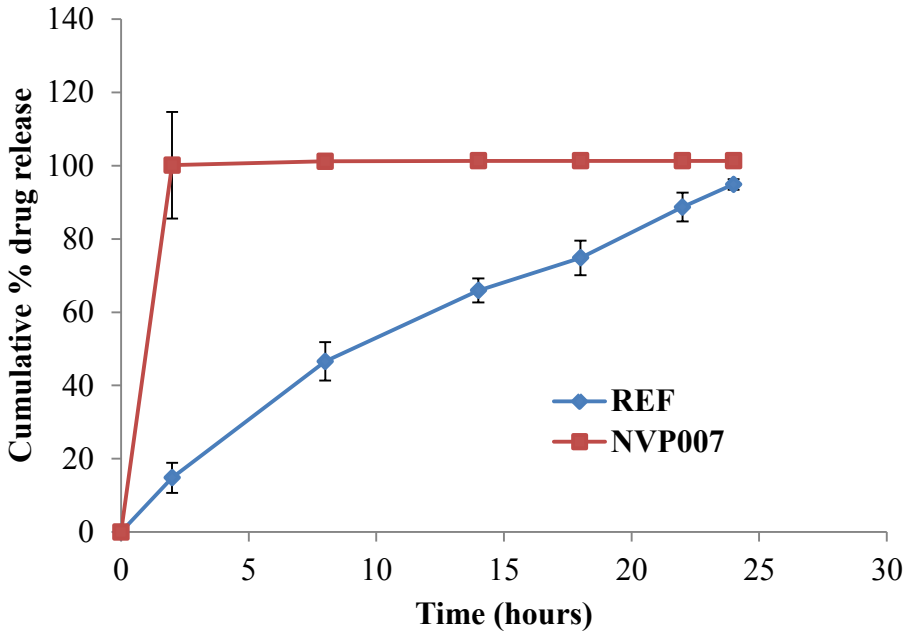

Figure 5.12. Dissolution profile of NVP release from tablets of batch NVP007 and Viramune® XR (n = 6).

Increasing the amount of Carbopol® 71G NF from 5% to 10% and then 20% of the total polymer content resulted in significant retardation of NVP release from the tablets of batch NVP008 as shown in Figure 5.13.

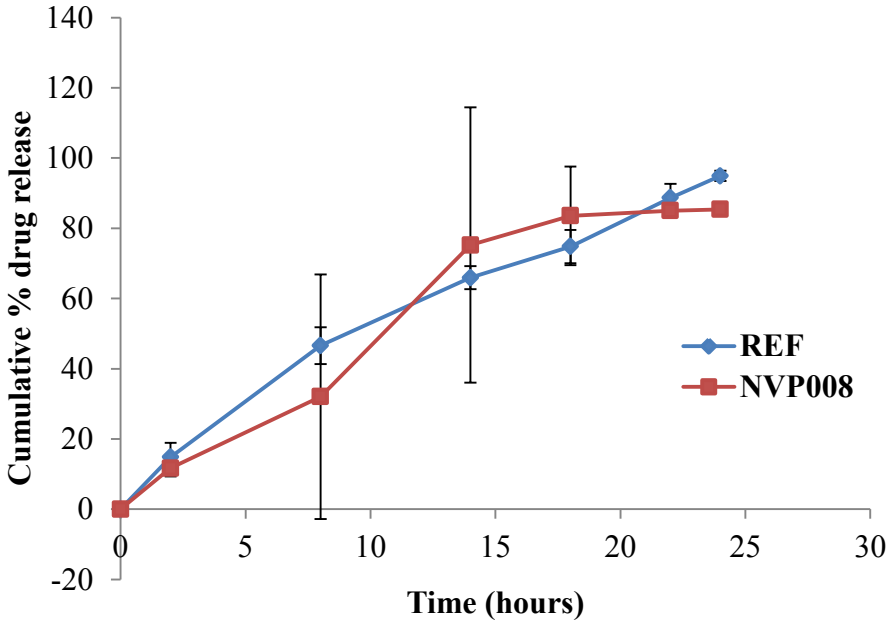

Figure 5.13. Dissolution profile of NVP release from tablets of batch NVP008 and Viramune® XR (n = 8).

Tablets from batch NVP008 had a comparable dissolution profile to that of the reference product and yielded f_1 and f_2 values of 13.5 and 52.4, respectively. However NVP release at selected time points were highly variable and this may well be due to the inclusion of Carbopol® 71G. Performance of carbomers has been reported to be variable with large fluctuations in API release [340] and therefore this formulation was not developed further.

A further increase in the amount of Carbopol® 71G NF to 15% and the total polymer content to 25% resulted in much slower NVP release with a total of only 52.9% of the NVP released after 24 hours of commencing testing as shown in Figure 5.14.

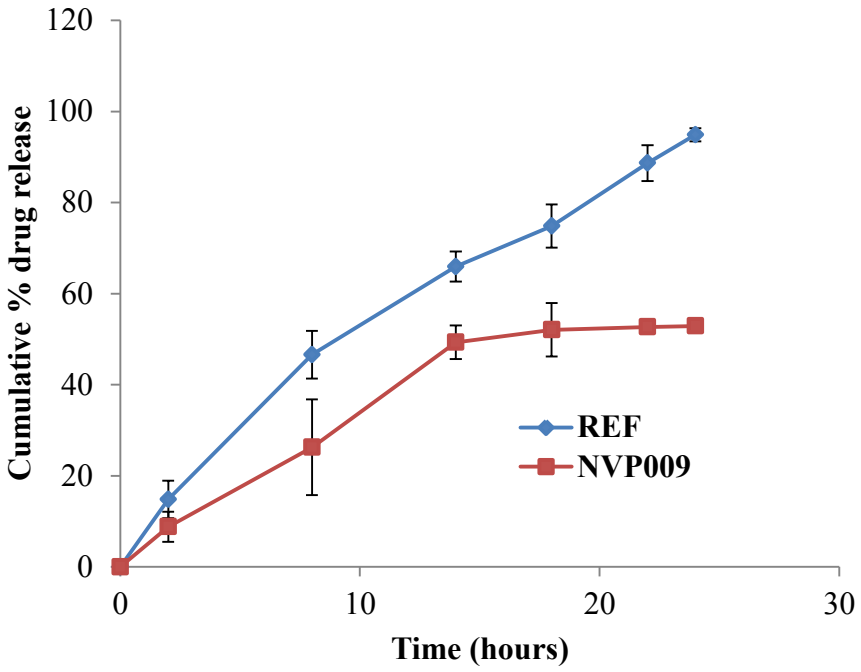

Figure 5.14. Dissolution profile of NVP release from tablets of batch NVP009 and Viramune® XR (n = 6).

These studies indicate that appropriate modulation of NVP release can be readily achieved with a combination of carbomer and HPMC at lower total polymer levels than if the polymers were used individually, which has been observed with other data [338-340].

Combinations of HPMC and methacrylic acid copolymers have been studied extensively and adequate control over drug release rates have been reported with these combinations [341-344]. An attempt to modulate NVP release using a polymer mixture of Methocel® K4M and Eudragit® RS PO was attempted and batches NVP010, NVP011 and NVP012 were produced

using these polymers. This polymer combination did not retard NVP release at the total polymer concentrations used as the tablets released 100% NVP within 2 hours of commencing testing. It was evident that the use of this polymer combination would require large amounts of Eudragit® RS PO which would result in a more expensive product compared to if HPMC or combinations of HPMC and Carbopol® 71G NF were used. Therefore this approach was not pursued further. The dissolution profiles of NVP release from batches NVP010, NVP011, NVP012 and Viramune® XR are shown in Figures 5.15-5.17.

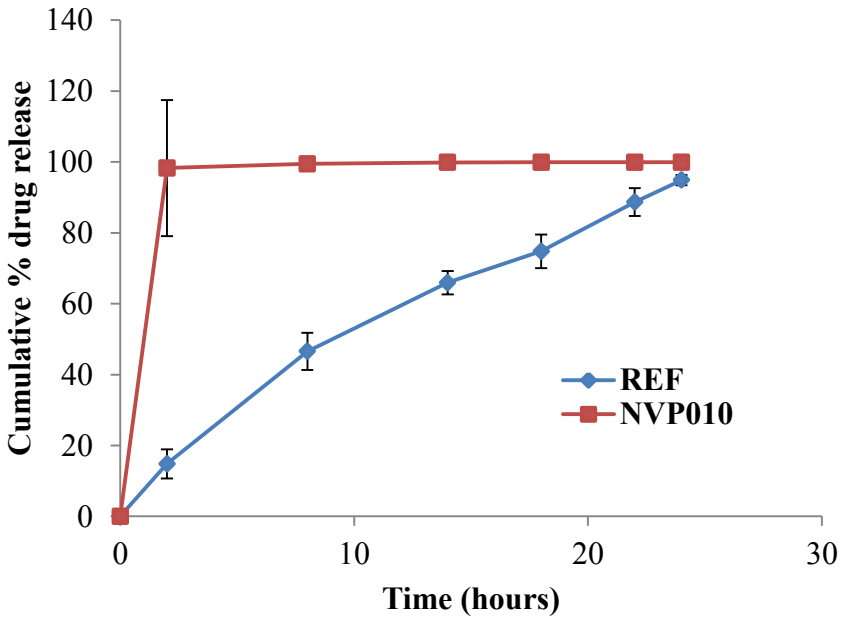

Figure 5.15. Dissolution profile of NVP release from tablets of batch NVP010 and Viramune® XR (n = 6).

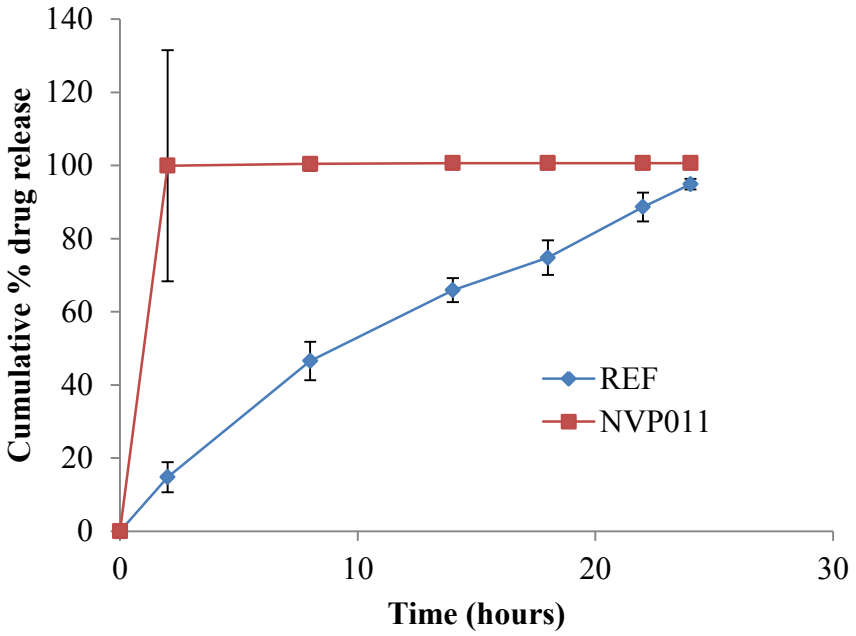

Figure 5.16. Dissolution profile of NVP release from tablets of batch NVP011 and Viramune® XR (n = 6).

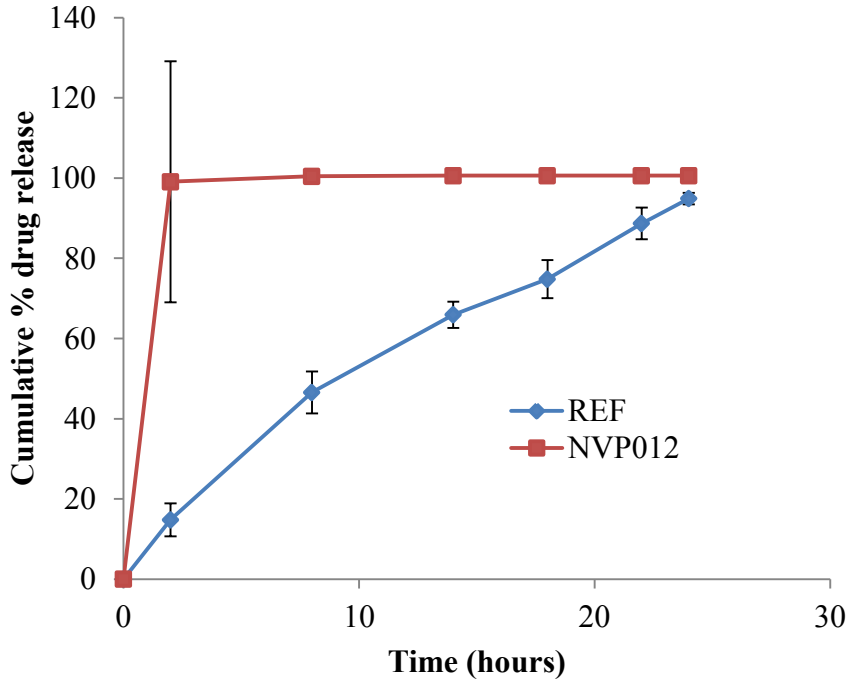

Figure 5.17. Dissolution profile of NVP release from tablets of batch NVP012 and Viramune® XR (n = 6).

5.5 CONCLUSIONS

NVP sustained release tablets with the potential for further optimisation have been developed and manufactured by DC. The tablets satisfied all compedial tests with respect to assay, content uniformity, weight uniformity, hardness, thickness and friability [345]. Modulation of NVP release from the tablets was achieved by altering the amount(s) of release rate controlling polymer. HPMC based matrix tablets were selected for further optimisation as they showed consistent performance of NVP release with acceptable precision at the different times that were monitored.

An increase in amount of HPMC used, resulted in a decrease in the extent of release of NVP from the tablets which is similar to the results observed in other studies [311, 331, 332]. The decrease in NVP release that was observed was attributed to the increased strength and thickness of the gel layer that was formed around the matrix when it was hydrated with dissolution medium [302, 332]. The strength and thickness of the gel layer is the predominant factor that controls API diffusion from a matrix tablet. The decrease in NVP release that was observed with increasing amounts of HPMC has also been attributed to the increase in the tortuosity and reduced porosity of matrices that further retards diffusion of NVP from the tablet core to the dissolution medium [332].

NVP release was best modulated by use of a combination of polymers of different viscosity and chemistry. Methocel® K4M and Carbopol® 71G NF in combination produced slower NVP release rates at lower total polymer amounts than if Methocel® K4M, was used alone. This may be due to the polymer mixture forming a stronger cross-linked structure in the matrix. The tablets manufactured using a combination of HPMC and carbomer yielded promising results and were suitable for further development and optimisation as the dissolution profile was similar to that of the reference drug product with f_1 and f_2 values of 14.1 and 52.4 respectively.

Combinations of Methocel® K4M and Eudragit® RS PO did not result in adequate retardation of NVP release and a higher concentration of polymers than those studied would be required to produce NVP release that was similar to that of the reference product.

Sustained release HPMC based matrix tablets with the potential for use as a once daily dose of NVP have been developed and exhibit dissolution profiles similar to that of the only commercially available NVP modified release formulation, Viramune® XR. The formulation

for batch NVP006 produced a dissolution profile that was similar to the reference product and was deemed suitable for further development and optimisation. The formulation was optimised using RSM and the factors affecting NVP release were further investigated.

CHAPTER SIX

FORMULATION OPTIMISATION

6.1 INTRODUCTION

6.1.1 Use of RSM for Formulation Optimisation

RSM is a common approach for the development and optimisation of drug delivery systems [346-349]. RSM is based on the principles of design of experiments (DOE) and makes use of different types of experimental design, generation of polynomial mathematical relationships and mapping of responses over an experimental domain to identify and select an optimum formulation composition and/or process, to produce the dosage form [346, 350]. Three types of RSM design are commonly used for statistical optimisation of formulations *viz.,* CCD, BBD and D-optimal design [164, 351, 352]. The RSM approach has an advantage over the traditional 'one factor at a time' approach, of reducing the number of experiments that need to be performed to achieve a specific solution and hence requires the use of smaller quantities of reagents and considerably less time in the laboratory. Furthermore, the use of RSM enables the development of mathematical models that can be used to assess the relevance and statistical significance of the impact of the input variables under investigation on a response. In addition, it permits an evaluation of the interaction(s), if any, between the input variables under consideration. The initial step of an optimisation process involves screening the input factors that are to be investigated using a full factorial or fractional factorial design in order to identify the significant effects of these parameters on the performance of a formulation. Thereafter the optimum formulation is identified by using a more complex experimental design approach such as CCD and/or BBD [353, 354].

6.1.2 Box-Behnken Design (BBD)

The BBD is an approach to RSM that is an independent, rotatable or nearly rotatable quadratic design that has treatment combinations at the midpoint of the edges of the process or formulation space [355]. The BBD has been shown to be slightly more efficient than the commonly used CCD approach but is much more efficient than a three-level full factorial design. The efficiency of one experimental design is defined as the number of coefficients in the estimated model divided by the number of experiments. The BBD does not contain experiments of combinations of all factors which are located at their highest or lowest levels

simultaneously and hence avoids conducting experiments under extreme conditions for which unsatisfactory results may be reported [356]. Therefore a BBD was selected for use to optimise the formulation variables identified as important in these studies.

The number of experiments to be performed in the development of a formulation using a BBD can be defined using Equation 6.1.

$$N = 2k\ (k - 1) + C_0 \qquad \textbf{Equation 6.1}$$

where,

k = number of factors,
C_0 = number of central points, and
N = number of experiments.

6.2 EXPERIMENTAL

6.2.1 Experimental Design

A three-factor, three-level BBD was used in these studies as it is a suitable approach for exploring quadratic response surfaces and can produce second order polynomial models that facilitate optimisation with a small number of experiments [356]. When using a BBD four replicated centre points are used in addition to a set of points lying at the midpoint of each edge of a multidimensional cube that defines the region of interest. The model constructed using a BBD can be mathematically represented by Equation 6.2.

$$-Y = a_0+a_1x_1 + a_2x_2 + a_3x_3 + a_4x_1x_2 + a_5x_2x_3 + a_{61}x_3 + a_7x_1^2 + a_8x_2^2 + a_9x_3^2 + \in \qquad \textbf{Equation 6.2}$$

where,

a_0 to a_9 = regression coefficients,
x_1, x_2 and x_3 = input factors studied,
Y = measured response associated with each factor level combination, and
$\in$ = error term.

The input factors and the levels to be used for the optimisation of batch NVP006 developed and reported in Chapter 5 were identified. Out of all the batches produced, batch NVP006 was selected for further optimisation and three independent variables and six responses were used for the optimisation process and are listed in Table 6.1.

Table 6.1. Levels of input variables and responses monitored for BBD

	Levels: Actual [coded]		
Input factor	**Low (%)**	**Medium (%)**	**High (%)**
X_1 = HPMC	25 [-1]	30 [0]	35 [+1]
X_2 = SDL	15 [-1]	20 [0]	25 [+1]
X_3 = MCC	8.5 [-1]	13.5 [0]	18.5 [+1]

Output factor	**Constraints**
Y_1 = % drug release at 2 hrs.	$8\% \leq Y_1 \leq 12\%$
Y_2 = % drug release at 8 hrs.	$40\% \leq Y_2 \leq 50\%$
Y_3 = % drug release at 14 hrs.	$60\% \leq Y_3 \leq 75\%$
Y_4 = % drug release at 24 hrs.	$85\% \leq Y_4 \leq 100\%$
Y_5 = f_2 or similarity factor	$50 \leq Y_5 \leq 100$
Y_6 = diffusion exponent value	$0.5 \leq Y_6 \leq 1.0$

The actual 17 experiments that were conducted with the percent composition of the input variables as well as coded factor levels are listed in Table 6.2. The experiments were conducted in a random manner so as to avoid any bias when analysing the data.

Table 6.2. Actual experiments and coded factor levels for optimisation process

Std Batch Number	**Experiment No.**	**Run**	**Dependent Variable % m/m [coded level]**		
			X_1	**X_2**	**X_3**
NVP013	1	2	35 [1]	15 [-1]	13.5 [0]
NVP014	2	4	35 [1]	25 [1]	13.5 [0]
NVP015	3	14	30 [0]	20 [0]	13.5 [0]
NVP016	4	12	30 [0]	25 [1]	18.5 [1]
NVP017	5	15	30 [0]	20 [0]	13.5 [0]
NVP018	6	16	30 [0]	20 [0]	13.5 [0]
NVP019	7	9	30 [0]	15 [-1]	8.5 [-1]
NVP020	8	1	25 [-1]	15 [-1]	13.5 [0]
NVP021	9	11	30 [0]	15 [-1]	18.5 [+1]
NVP022	10	8	35 [+1]	20 [0]	8.5 [-1]
NVP023	11	5	25 [-1]	20 [0]	8.5 [-1]
NVP024	12	10	30 [0]	25 [+1]	8.5 [-1]
NVP025	13	13	30 [0]	20 [0]	13.5 [0]
NVP026	14	3	25 [-1]	25 [+1]	13.5 [0]
NVP027	15	6	35 [+1]	20 [0]	8.5 [-1]
NVP028	16	17	30 [0]	20 [0]	13.5 [0]

NVP029	17	7	25 [-1]	20 [0]	18.5 [+1]

6.2.2 Manufacture of NVP Tablets

All batches of tablets were manufactured by direct compression using the method described in §5.3.1. Tablets were compressed to a target weight of 300 mg and hardness of 80-100 N. All batches were 300 g each and the target yield was 800 -1000 tablets.

6.2.3 Physical and Chemical Characterisation of NVP Tablets

All batches of tablets were subjected to compendial quality testing for weight uniformity (n = 20), hardness (n = 20), thickness (n = 20), friability (n = 20) and NVP assay (n = 20). Content uniformity was only evaluated for the optimised formulation (n = 10).

6.2.4 *In Vitro* Release Studies

In vitro release studies on all tablets were performed using USP Apparatus 3 and the method described in Chapter 3, *vide infra*. The optimised formulation was tested using dissolution media of pH 1.6 for 2h, 3.4 for 2h, 4.7 for 4h, 6.8 for 6h and 7.2 for 10h in an attempt to mimic human GIT transit conditions. The dissolution profiles for NVP release from the tablets of the 17 batches manufactured were compared to the dissolution profile of NVP release from the reference product, Viramune® XR, using the f_1 and f_2 values.

6.2.5 Water Uptake and Erosion Studies

NVP tablets (n = 3) of the optimised batch were individually weighed using a Model A163 Mettler® electronic top-loading balance (Mettler®, Zurich, Switzerland) and then exposed to 50 mM phosphate buffer of pH 1.6, 3.4, 4.7, 6.8 and 7.2 for 24 hours. The tablets were withdrawn at 2, 4, 8, 14, 18 and 24 hours following exposure and the excess buffer removed using tissue paper. The swollen tablets were weighed and dried in an oven (Memmert, GmbH, Schwabach, Germany) at 70 °C for 12 hours to a constant weight and then allowed to cool to room temperature (22 °C). The measure of water uptake of the tablets, Q was calculated using the percent increase in weight and Equation 6.3 [357].

$$Q = \frac{Mh-Mi}{Mi} X\ 100 \qquad \textbf{Equation 6.3}$$

where,

Mi = mass of tablet before being placed in dissolution media, and

Mh = mass of tablet after placing in dissolution media (hydrated).

The degree of erosion, E, was estimated using Equation 6.4 as described by Efentakis *et al.,* [358].

$$E = \frac{Mi-Mf}{Mi} X100 \qquad \textbf{Equation 6.4}$$

where,

Mf = final dry weight after erosion i.e., when there is no further change in weight, and
Mi = mass of tablet before being placed in dissolution media.

6.2.6 Mathematical Modelling of Drug Release

6.2.6.1 Overview

Mathematical modelling of drug release data derived from SR delivery systems generates important information on mass transport mechanisms and the effects of device design parameters on the kinetics of API release from those systems [172]. API release can also be predicted from formulation parameters such as porosity, thickness of polymeric layer(s) or solubility using mathematical modelling approaches [359].

The choice of an appropriate model to describe API release is dependent on the API, excipients used, composition and *in vitro* behaviour of the delivery system under investigation [360]. The mechanism of release of an API can be diffusion, dissolution or osmotically controlled and from a mathematical modelling point of view, SR systems can be classified according to the physical mechanisms controlling release of the API from these systems. The available approaches to modelling are based on mechanisms of transport and include diffusion-, swelling- and chemically-controlled systems, amongst others [172, 361].

Mathematical models take into consideration the mechanistic aspects of transport processes of a drug delivery system, in addition to structural characteristics of the polymer used in the technology [172]. Model equations may be generated and used to design new SR systems by selection of an optimal geometry, formulation and/or size of a technology [359].

Mathematical modelling can be used to predict and/or design a dissolution profile for a SR system based on an understanding of the release kinetics of the API that are desired and this approach was used for these studies. NVP is a sparingly soluble in aqueous media and NVP

release from a hydrophilic matrix would be primarily governed by a combination of diffusion, swelling and erosion of the polymeric matrix, used to produce the technology. For the purposes of elucidating the kinetics of NVP release, dissolution data were fitted to zero-order, first-order, Higuchi, Hixson-Crowell Cube Root and the Korsmeyer-Peppas models.

6.2.6.2 Zero-Order Model

A zero-order model can be used to describe API dissolution under specific conditions from modified release dosage forms, such as from matrices that contain a poorly water-soluble API, osmotic or film coated systems [362]. The zero-order model is used to describe a dissolution profile for which a constant amount of API is released per unit time and represents the ideal target for API release to achieve prolonged and/or sustained pharmacological effects. Zero-order release can be described mathematically using Equation 6.5.

$$Q_t = Q_0 + K_0 t \qquad \textbf{Equation 6.5}$$

where,

Q_t = amount of drug dissolved in time t,
Q_0 = initial amount of drug in the solution, and
K_0 = zero order release rate constant.

6.2.6.3 First-Order Model

A first order kinetic model can be used to describe the release of most compounds from dosage forms that contain water-soluble molecules dispersed in porous matrices. API release from these dosage forms is directly proportional to the amount of API in the core of the technology, at a particular time and the release rate of the API decreases over time. The release rate is concentration dependent and a plot of the natural logarithm of the amount of API released versus time will result in a straight line [363, 364] and the first-order model can be represented mathematically by Equation 6.6.

$$Ln\ Q_t = Ln\ Q_0 + K_1 t \qquad \textbf{Equation 6.6}$$

where,

Q_t = amount of drug released at time *t,*
Q_0 = initial amount of drug in the solution, and

K_1 = first order release constant.

6.2.6.4 Higuchi Model

A mathematical model that could be used to describe the rate of release of an API from a non-erodible matrix system was first described by Higuchi [365]. The model was initially developed for API release from a semi-solid system and was later revised so as to take into consideration technologies of different geometry and/or characteristics [366-369]. The Higuchi model can be mathematically represented by Equation 6.7.

$$\frac{Qt}{A} = \sqrt{D(2C0 - Cs)Cst} \qquad \textbf{Equation 6.7}$$

where,

Q_t = cumulative absolute amount of drug released at time *t,*
A = surface area of the controlled release device exposed to the release medium,
D = drug diffusivity in the polymer carrier,
C_0 = initial drug concentration, and
C_s = solubility of the drug in the polymer.

According to the Higuchi model, if the release rate of the API is proportional to the reciprocal of the square root of time, the release of the API is controlled by diffusion [172]. When applying the principles of the Higuchi model to dissolution or release data from dosage forms, a number of principles and assumptions must be considered. These include the initial concentration of API in the system that must be significantly higher than the solubility of the API which provides the basis for justification of the applied pseudo-state approach. Furthermore the model holds true if mathematical analysis of the data is based on one dimensional diffusion, if the suspended API particles are much smaller in diameter than the thickness of the entire system, swelling or dissolution of the polymer carrier is negligible, the diffusivity of the API in the polymer is constant and perfect sink conditions are maintained during the experiment [172].

The simplicity of the Higuchi equation enables its use for the analysis of dissolution data to provide a preliminary understanding of the underlying mechanism of release of an API in a specific technology. Additional mathematical analysis should always be undertaken to provide a more conclusive interpretation of the data [336, 369].

6.2.6.5 Korsmeyer-Peppas Model

Korsmeyer and Peppas developed a semi-empirical equation to describe API release from polymeric systems [370, 371] and the Korsmeyer-Peppas model can be described mathematically as shown Equation 6.8.

$$\frac{Qt}{Q_\infty} = kt^n \qquad \textbf{Equation 6.8}$$

where,

Q_t = absolute cumulative amounts of drug released at time *t,*
= absolute cumulative amount of drug released at infinite time,
k = constant, and
n = release exponent and indicates the overall mechanism of drug release.

The Korsmeyer-Peppas model is also called the power law. The Higuchi model represents a special case of the power law where n = 0.5 [370, 371] and API release is controlled by diffusion only. If a value for n = 1 then the release of API is best described by a zero order kinetic process and is independent of time and this is an indication that API release is swelling controlled. A value for n = 0.5 is an indication that API release is a diffusion controlled process whereas when both diffusion and swelling control API release the value for n falls between 0.5 and 1.0 and API release is considered to occur by a process termed anomalous transport. Zero-order API release from thin polymeric films has also been described as Case-II transport in which the relaxation of macromolecules occurs on water uptake into a delivery system and which becomes the rate limiting step in API release [370-373]. The value of n varies according to the geometry of the delivery technology investigated and specific conditions have been derived for slabs, spheres and cylinders and are listed in Table 6.3 [200, 374-376].

Table 6.3. Values for *n* and associated transport mechanisms for films, cylinders and spheres

Release Exponent (n)	Shape	Drug Transport Mechanism	Rate as a function of time
0.43	Sphere	Fickian diffusion	$t^{-0.5}$
0.45	Cylinder		
0.50	Thin film		
0.43 < n < 0.85	Sphere	Anomalous Transport	t^{n-1}
0.45 < n < 0.89	Cylinder		
0.5 < n < 1.0	Thin film		
0.85	Sphere	Case-II transport	Zero-order
0.89	Cylinder		
1.00	Thin film		
> 0.85	Sphere	Super Case-II transport	t^{n-1}
> 0.89	Cylinder		
> 1.0	Thin film		

6.2.6.6 Hixson-Crowell Cube Root Law

The Hixson-Crowell Cube Root Law model describes API release from delivery systems in which there is a change of surface area and diameter of the dosage form, over time. The assumption is that the dissolution rate of the API is the rate limiting factor in release and not diffusion of the API [377]. This model may be useful for describing API release from tablets in which dissolution of the API occurs in a plane(s) that is parallel to the surface of the tablet and where the dimensions of the tablet diminish proportionally over time [200]. The mathematical representation of the Hixson-Crowell model is shown in Equation 6.9.

$$Q_0^{1/3} - Q_t^{1/3} = K_{HC}\, t \qquad \textbf{Equation 6.9}$$

where,

Q_0 = initial amount of drug in the delivery system,
Q_t = amount of drug remaining in the delivery system,
K_{HC} = constant taking into consideration the surface area/volume relationship, and
t = time.

6.2.6.7 Determination of Best Fit Mathematical Model

In order to establish which model the data were best fitted to, the R^2 values generated from regression analysis of plots of cumulative % NVP released versus Time (zero-order model),

the natural logarithm of the cumulative % drug remaining in the matrix versus time (first-order model), cumulative % drug release versus square root of time (Higuchi model), Log cumulative % drug release versus the Log of time (Korsmeyer-Peppas model) and the cube root of drug % remaining in the matrix versus time (Hixson-Crowell Cube Root Law) were compared. The model yielding the highest R^2 values were deemed appropriate as this represents the predominant kinetic model that best described NVP release. The dissolution data were used to calculate the NVP release exponent for the Korsmeyer-Peppas model. The Korsmeyer-Peppas model is only useful to describe processes for up to 60 % API release.

6.3 RESULTS AND DISCUSSION

6.3.1 Box-Behnken Design

The responses that were obtained from the Box-Behnken design experiments are summarised in Table 6.4.

Table 6.4. Responses observed for Box-Behnken design experiments.

Runs	Independent Variables					
	Y_1 %	Y_2 %	Y_3 %	Y_4 %	Y_5 f_2	Y_6 n
NVP013	7.89	33.52	53.83	85.91	54.6	0.9653
NVP014	8.86	33.52	63.12	88.62	61.4	1.0171
NVP015	10.50	38.12	60.48	85.12	59.8	0.9053
NVP016	11.54	44.39	64.95	87.23	81.5	0.8843
NVP017	9.30	47.64	68.57	86.11	62.1	0.8864
NVP018	10.63	46.73	61.88	83.31	61.4	0.9362
NVP019	12.58	40.90	68.39	83.73	61.5	0.8133
NVP020	16.39	52.28	78.73	89.73	50.4	0.7752
NVP021	10.40	43.32	60.02	82.31	58.2	0.925
NVP022	8.74	35.54	53.61	87.02	52.6	0.926
NVP023	15.96	58.56	70.31	83.70	43	0.7933
NVP024	10.52	48.13	62.90	85.20	75.4	0.9527
NVP025	11.29	43.60	60.87	90.45	66.4	0.8889
NVP026	16.48	55.32	70.02	81.57	55.3	0.7522
NVP027	8.83	34.67	55.74	85.63	51.9	0.918
NVP028	10.88	43.64	60.60	82.91	63.4	0.9412
NVP029	15.81	55.78	75.31	89.46	51.6	0.8083

Most batches of tablets that were manufactured had a total % NVP release of ≥ 85% and the highest % NVP released after 24 hours of dissolution testing was 90.5%. A quick theoretical mass balance analysis using assay values showed that the highest amount of NVP released represented approximately 93% NVP release (batch NVP025) and the lowest percent release of approximately 82% (batch NVP026).

All dissolution profiles, except for that of batch NVP011 that had an f_2 value of 43, were found to be similar to that of the reference product, Viramune® XR with f_2 values >50. It was noted that batches with the lowest amount of HPMC *viz.,* 25% w/w were the least similar to the reference product.

The release exponent *n* ranged between 0.79 and 1.01 indicating that an anomalous mechanism was the primary mechanism for NVP release for all batches. This suggests that NVP release from the matrix tablets was controlled by diffusion, swelling and relaxation of the matrix.

The responses generated from batches manufactured using the Box-Behnken approach were statistically analysed using Design-Expert® software and the data were fitted to different quadratic models. The model(s) that best described the data were selected for use in the optimisation process. The best fit model was chosen based on a p-value ≤ 0.05, residuals, PRESS, lack of fit and the correlation coefficient, R^2. ANOVA was used to identify significant factors that affected the responses studied, and response surface plots were produced to study interaction effects of input variables, if any, on all responses. However for the purposes of this discussion only the response surface plots for NVP release at 14 hours (Y_3) will be discussed in detail and all other response surface plots are in Appendix III.

6.3.2 Determination of Regression Models and Statistical Evaluation

6.3.2.1 Evaluation of Model Adequacy

The selection of the best statistical model involving the individual main effects and interaction factors was achieved by comparison of statistical parameters such as multiple R^2 values, adjusted multiple R_a^2 values, lack of fit and PRESS values. The results for model analysis are summarised in Tables 6.5 and 6.6, and the models for which the smallest value of PRESS, p-value, acceptable lack of fit (highest p-value) and highest R^2 values were selected for use in the optimisation process.

Table 6.5. Results of model analysis and lack of fit

Source	Y_1		Y_2		Y_3		Y_4		Y_5		Y_6	
	SS[a]	P > F	SS	P > F	SS	P > F	SS	P > F	SS	P > F	SS	P > F
Model Analysis												
Mean vs. total	2273.0		35012.68		69801.68		$1.248E^{5}$		1.98		13.61	
Linear vs. mean	115.3	<0.0001	835.05	< 0.0001	580.64	0.0006	7.17	0.8160	0.024	0.4325	0.063	0.0045
2FI[b] vs. linear	2.75	0.6053	3.42	0.4503	20.94	0.0364	34.32	0.2185	$8.564E^{-3}$	0.8266	$9.52E^{-3}$	0.3967
Quadratic vs. 2FI	10.97	0.0127	12.63	0.5034	35.23	0.3328	7.48	0.8225	0.081	0.0035	0.014	0.1798
Cubic vs. Quadratic	1.09	0.6230	8.45	0.7380	13.22	0.7794	21.07	0.5683	0.012	0.0800	$6.312E^{-3}$	0.4920
Residual	2.23		25.69		47.54		36.52		$3.280E^{-3}$		$8.743E^{-3}$	
Total	2405.4		35907.91		70599.24		$1.249E^{5}$		2.11		13.71	
Lack of fit												
Linear	14.82	0.1549	34.50	0.7614	169.39	0.3475	6.86	0.6622	0.01	0.0113		
2FI	12.06	0.1176	21.08	0.7577	48.45	0.6803	28.55	0.7734	0.093	0.0067		
Quadratic	1.09	0.6230	8.45	0.7380	13.22	0.7794	21.07	0.5683	0.012	0.0800		
Cubic	0.000		0.000		0.000		0.000		0.000			
Pure Error	2.23		25.69		47.54		36.52					

[a] Sum of Squares, [b] Two-Factor Interaction, dark red = significant parameters.

Table 6.6. Summary of analysis of coefficients of correlation, R^2

		Model			
Response	**Parameter**	**Linear**	**2FI**	**Quadratic**	**Cubic**
Y_1	R^2	0.871	0.892	0.975	0.983
	R_a^2	0.842	0.827	0.943	0.933
	PRESS	28.29	42.68	20.91	ND
Y_2	R^2	0.933	0.948	0.962	0.971
	R_a^2	0.917	0.916	0.913	0.885
	PRESS	98.00	124.0	175.3	ND
Y_3	R^2	0.728	0.880	0.924	0.940
	R_a^2	0.665	0.807	0.826	0.762
	PRESS	396.0	251.5	285.8	ND
Y_4	R^2	0.067	0.389	0.460	0.657
	R_a^2	-0.148	0.023	-0.235	-0.371
	PRESS	172.8	187.7	394.1	ND
Y_5	R^2	0.266	0.294	0.920	0.982
	R_a^2	0.097	-0.129	0.816	0.929
	PRESS	2053.5	4718.5	1423.8	ND
Y_6	R^2	0.622	0.715	0.852	0.914
	R_a^2	0.534	0.5441	0.6624	0.6569
	PRESS	0.064	0.081	0.110	ND

ND = PRESS statistic parameter not defined, R_a^2 = adjusted R^2, dark red = significant parameters.

Analysis of results in Tables 6.5 and 6.6 showed that linear and quadratic models were both significant for response Y_1. However, the quadratic model had a smaller PRESS value and a greater p-value for lack of fit, and the adjusted R^2 value was close to the R^2 value implying that the quadratic model would better describe response Y_1 and was therefore selected. Similar analysis was applied in the selection of models for other responses and these analyses revealed responses Y_2 and Y_6 were best described by the linear model, responses Y_3 and Y_4 by the 2-factor interaction (2FI) model and response Y_5 by the quadratic model.

6.3.2.2 ANOVA for Responses

ANOVA revealed that the amount of HPMC in the tablets had a significant effect on the cumulative % NVP released at 2 hours which is in agreement with other studies that reported that the amount of HPMC used in a formulation has a significant effect on API release from matrix technologies [321, 343]. An increase in the amount of HPMC in the formulation resulted in decrease in the cumulative % NVP released at 2 hours.

Furthermore, the cumulative % NVP released at 8 hours and 14 hours was also significantly affected by the amount of HPMC in the formulation in addition to the ratio of HPMC to

lactose. These results are similar to previously reported results that suggest that lactose has an effect on API release, which has been attributed to the dissolution of lactose creating pores in the matrix through which API molecules can diffuse [302, 308, 334, 343]. Increasing the amount of lactose in a formulation resulted in an increase in the rate of NVP release from these tablets.

No other input variables had a significant impact on drug release at 24 hours and whilst no single factor could be identified, the agitation rate used during dissolution testing was thought to be a contributing factor. The agitation rate could have had a more pronounced effect on the integrity of the matrix and NVP release at the end of testing rather than the formulation variables.

The f_2 factor was significantly affected by the amount of HPMC and lactose used and it was observed that formulations that had the lowest amount of HPMC and lactose exhibited f_2 values closer to 50.

The amount of HPMC used in the formulation had a significant effect on the Korsmeyer-Peppas release exponent implying that the mechanism of NVP release could be modulated or altered by changing the composition of the rate retarding polymer in the formulation.

Increasing the amount of MCC in the tablets resulted in a reduced rate of NVP release but the effect was not found to be significant, which may be a consequence of the low amount of MCC used in the test formulations. Other studies in which MCC was used in higher amounts have reported that MCC can have a significant effect on API release rates from dosage forms [334, 343, 378].

A summary of the models describing all observed responses in addition to the significant factors and mathematical equations describing the responses in relation to the independent variables is shown in Table 6.7. The equations show that responses Y_1 was significantly affected by an antagonistic contribution of model term X_1 as indicated by the negative sign in the equation. Response Y_2 was significantly affected by an antagonistic linear contribution of X_1, and a synergistic linear contribution of X_2 as indicated by the positive sign in the equation. Response Y_3 was significantly affected by an antagonistic linear contribution of X_1 in addition to a synergistic linear interaction contribution of model terms X_1X_2 and X_2X_3. No factor significantly affected response Y_4 and response Y_5 was significantly affected by a

synergistic linear contribution of X_2 and quadratic interactions of model terms X_1^2 and X_2^2. Response Y_6 was significantly affected by a synergistic linear contribution of X_1.

To illustrate how ANOVA was used to study the independent and dependent variables, ANOVA, diagnostic plots and response surface model graphs for response Y_3 will be discussed in further detail.

Table 6.7. Summary of best fit models, significant factors and equations describing input variables and responses

Response	Fitting model	Significant factors	Equation
Y_1	Quadratic	HPMC	$Y_1 = 10.52 - 3.79X_1 + 0.020X_2 - 0.18X_3 + 0.23X_1X_2 - 0.014X_1X_3 + 0.80X_2X_3 - 1.48X_1^2 + 0.40X_2^2 + 0.34X_3^2$
Y_2	Linear	HPMC, SDL	$Y_2 = 45.38 - 10.08X_1 + 1.99X_2 - 0.40X_3$
Y_3	2FI	HPMC, SDL	$Y_3 = 64.08 - 8.51X_1 + 0.001875X_2 - 0.43X_3 + 4.50X_1X_2 - 1.78X_1X_3 + 2.61X_2X_3$
Y_4	2FI	None	$Y_4 = 85.77 - 0.34X_1 + 0.12X_2 + 0.97X_3 + 2.71X_1X_2 - 1.09X_1X_3 + 0.86X_2X_3$
Y_5	Quadratic	HPMC, SDL	$Y_5 = 62.62 + 2.53X_1 + 6.11X_2 + 1.51X_3 + 0.47X_1X_2 - 1.98X_1X_3 + 2.35X_2X_3 - 13.29X_1^2 + 6.09X_2^2 + 0.44X_3^2$
Y_6	Linear	HPMC	$Y_6 = 0.89 + 0.087X_1 + 0.016X_2 + 0.008288X_3$

6.3.2.3 ANOVA for Response Y_3

A summary of the ANOVA analysis for the cumulative percent NVP released at 14 hours following the commencement of dissolution testing is listed in Table 6.8. Parameters with a p-value < 0.05 were considered significant and as can be observed the model selected was deemed significant with a reported p-value of 0.0004. The parameters that were found to affect the responses significantly were linear contributions of A (HPMC) and linear interactions of two factors A and B (HPMC: SDL) with reported p-values of <0.0001 and 0.0157, respectively. Insignificant model terms included linear contributions of B (SDL), linear contributions of C (MCC), linear contributions of the interactive effects between A and C and between B and C with p-values > 0.05 and the lack of fit was also insignificant with a reported p-value = 0.6803, which is the desired condition.

Table 6.8. ANOVA for the response surface 2FI model [partial sum of squares – type III] for response Y_3

Source	Sum of squares	Df	Mean square	F value	P-value P > F	Comment
Model	701.58	6	116.93	12.18	0.0004	Significant
A = HPMC	579.14	1	579.14	60.33	< 0.0001	Significant
B = SDL	$2.521E^{-005}$	1	$2.521E^{-005}$	$2.626E^{-006}$	0.9987	Not significant
C=Avicel PH102	1.49	1	1.49	0.16	0.7016	Not significant
AB	81.09	1	81.09	8.45	0.0157	Significant
AC	12.67	1	12.67	1.32	0.2773	Not significant
BC	27.18	1	27.18	2.83	0.1233	Not significant
Residual	95.99	10	9.60	PND	PND	
Lack of fit	48.45	6	8.07	0.68	0.6803	Not significant
Pure Error	47.54	4	11.88	PND	PND	
Total	797.57	16				

PND = Parameter not defined, dark red = significant parameters.

6.3.2.4 Diagnostic Plots for Response Y_3

In order to establish how well the statistical models selected described the relationship between input variables and the output responses, different diagnostic plots were constructed. These included a normal probability plot of residuals, a plot of residuals versus predicted responses and a Box-Cox plot. The diagnostic plots are shown in Figures 6.1-6.4 and fulfil the criteria for model adequacy, *viz.* the points on the plot of normal probability versus residuals should fall on or close to a straight line, the points on the plot of residuals versus predicted responses should be structureless and no transformations on the Box-Cox plots should be required.

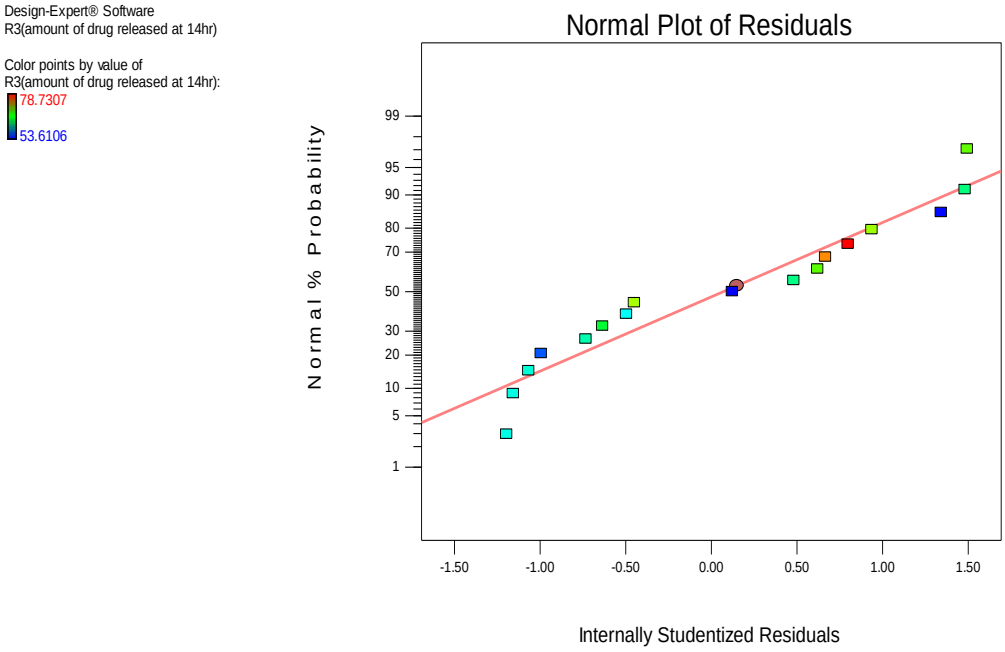

Figure 6.1. Plot of normal probability versus residuals for NVP release at 14 hours.

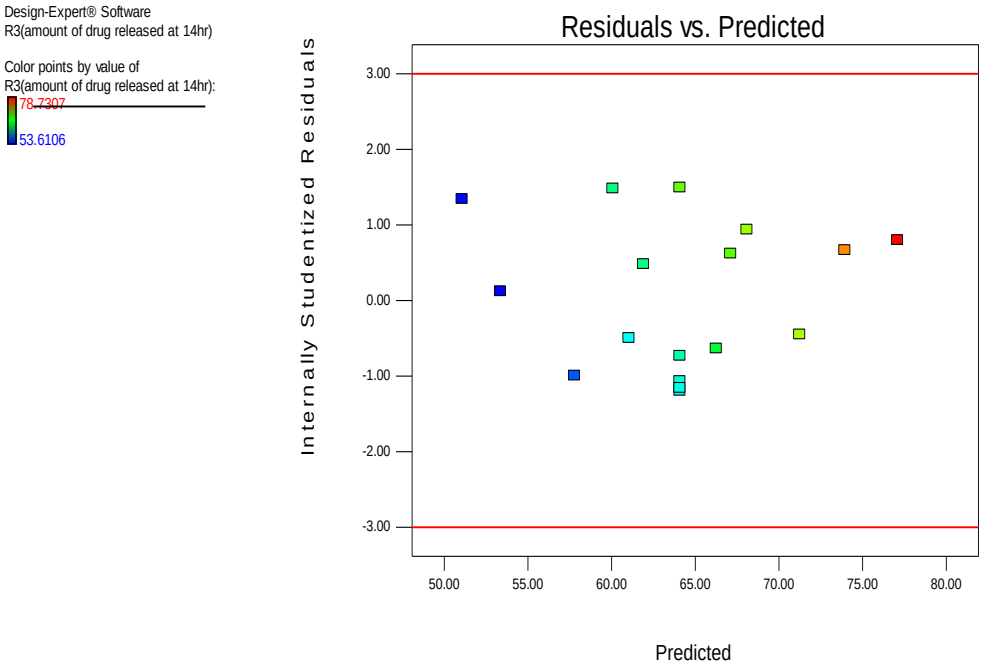

Figure 6.2. Plot of residuals versus predicted responses for NVP release at 14 hours.

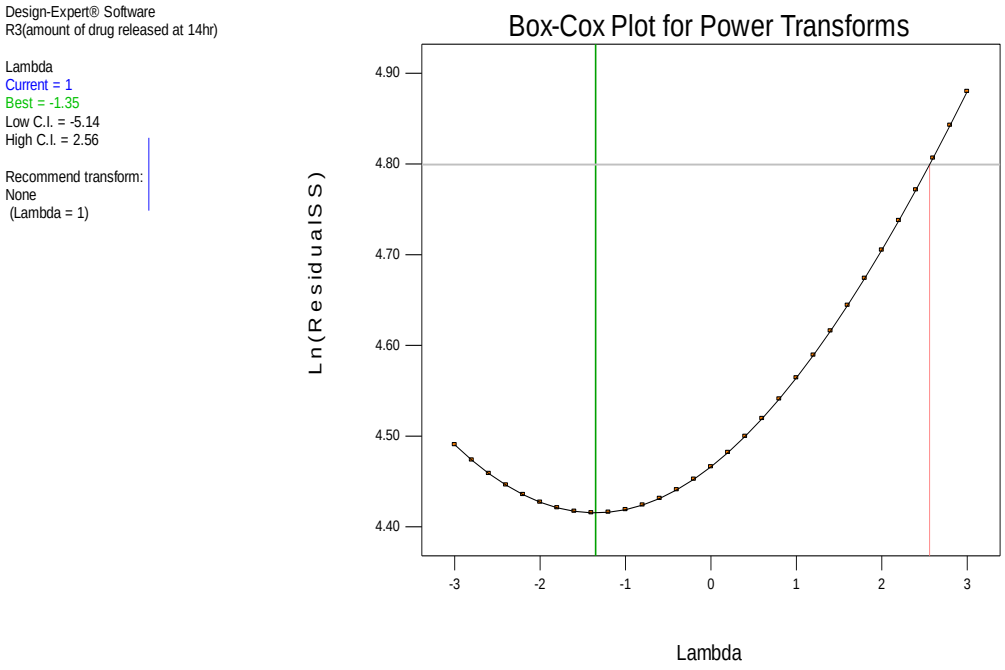

Figure 6.3. Box-Cox plot for power transformation for NVP release at 14 hours.

6.3.3.5 Response Surface Model Plot for Response Y_3

The relationship between the input variables and the cumulative NVP released at 14 hours following the commencement of dissolution testing was visualised by use of three dimensional (3-D) and contour plots. Increasing the amount of HPMC while keeping MCC constant resulted in a decrease in the amount of NVP released whereas increasing the amount of MCC while keeping HPMC constant in the formulation did not appear to have a significant effect on NVP release as depicted in a contour plot in Figure 6.4.

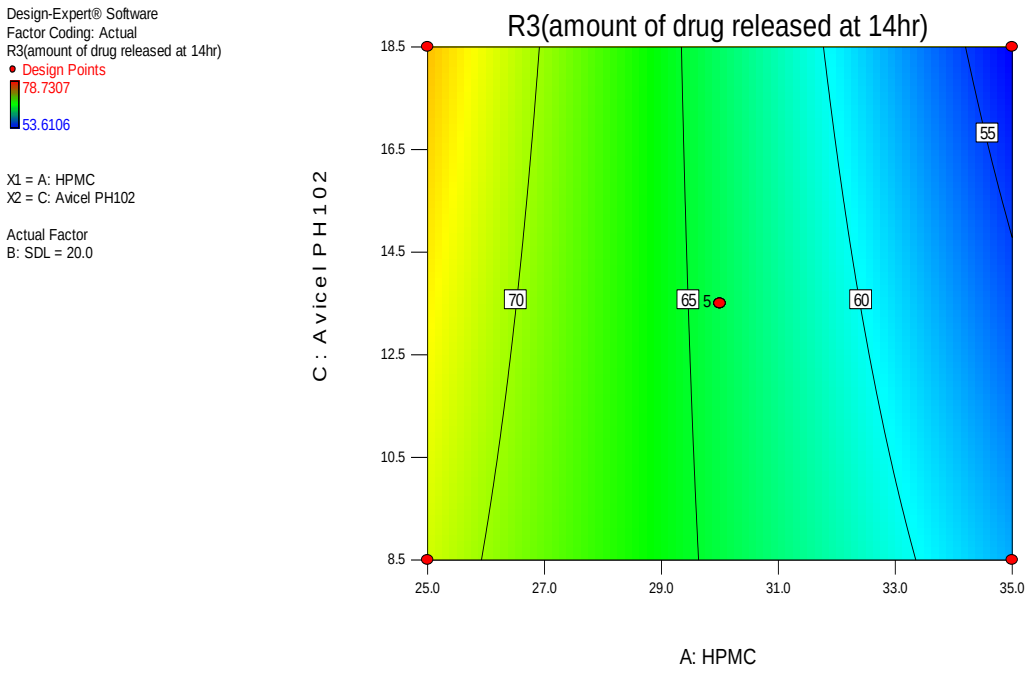

Figure 6.4. Contour plot of the effect of HPMC and MCC on percent NVP released at 14 hours.

The 3-D plot depicted in Figure 6.5 reveals that the amount of NVP released was highest when a low amount of HPMC and high amount of MCC was used as compared to when a high amount of HPMC and low amount of MCC was used. Consequently when the amount of HPMC used is constant, a change in the amount of MCC did not affect NVP release significantly. Maintaining the level of MCC constant and altering the amount of HPMC in the formulation had a significant impact on NVP release.

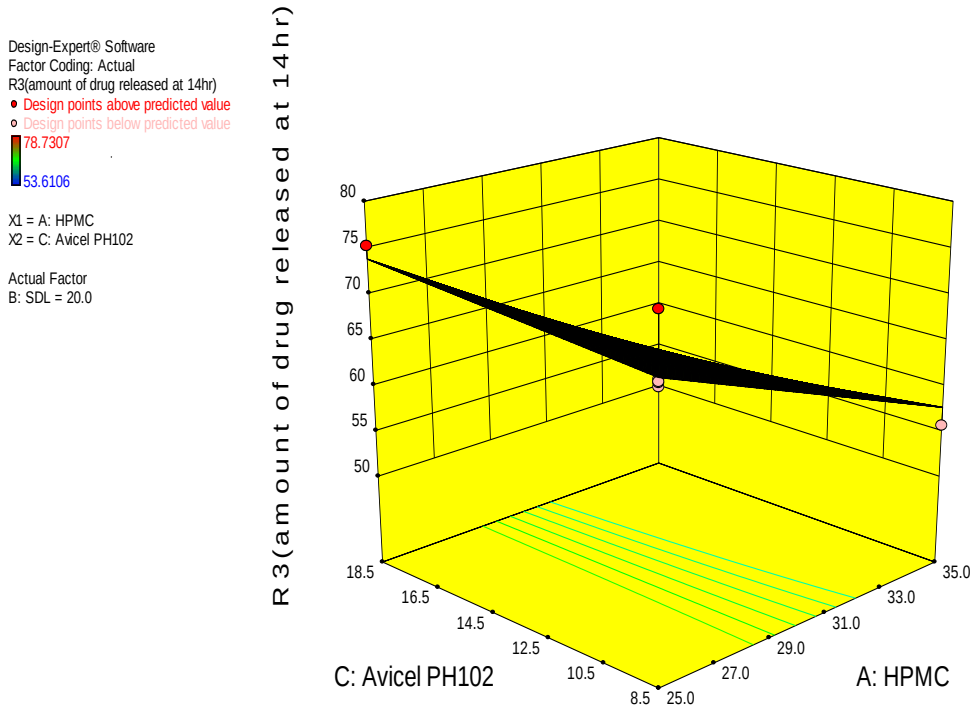

Figure 6.5. 3-D plot of the effect of HPMC and MCC on percent NVP released at 14 hours.

A study of the effects of SDL and HPMC revealed that increasing the amount of SDL while keeping HPMC constant did not have a significant effect on NVP release whereas increasing the amount of HPMC and keeping the levels of SDL constant resulted in a significant decrease in NVP released as observed in the contour plot depicted in Figure 6.6.

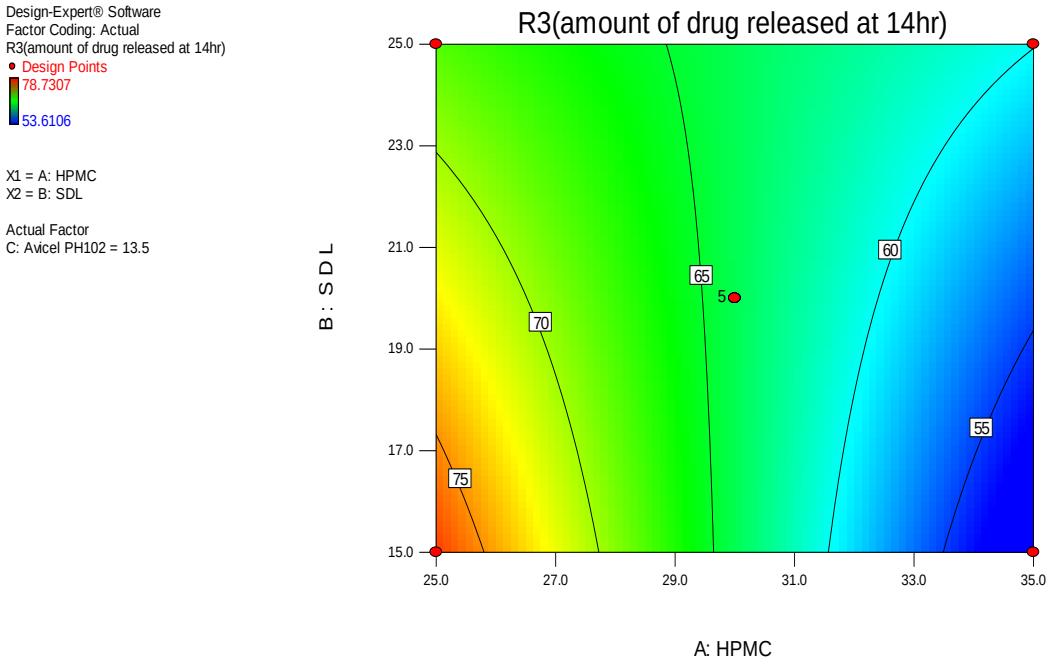

Figure 6.6. Contour plot of the effect of HPMC and SDL on percent NVP released at 14 hours.

The 3-D plot depicted in Figure 6.7 reveal that the highest amount of NVP was released when high amounts of SDL and low amounts of HPMC were used in the formulation.

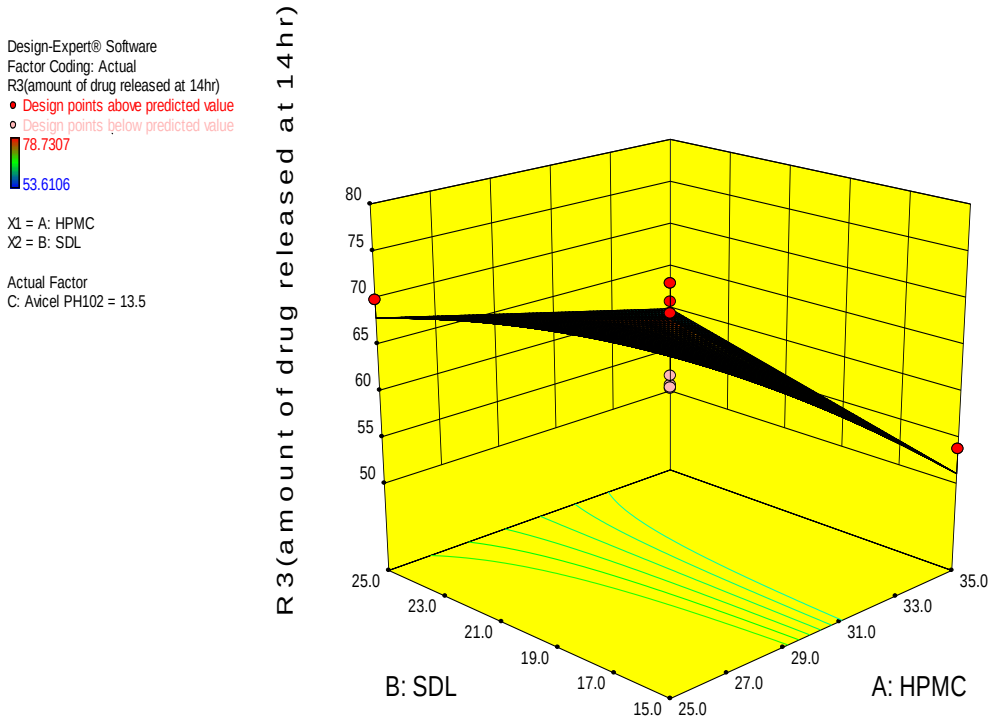

Figure 6.7. 3-D plot of the effects of HPMC and SDL on percent NVP released at 14 hours.

A contour plot of the effect of SDL and MCC on NVP released at 14 hours also showed that these two formulation components did not have a significant effect on the release characteristics of the tablets as shown in a contour plot in Figure 6.8 and the 3-D plot in Figure 6.9. Consequently when the amount of SDL used is constant a change in the amount of MCC resulted in slight but not significant changes in NVP release, and maintaining the levels of MCC constant and altering the amount of SDL in the formulation also had a slight but not significant effect on NVP release.

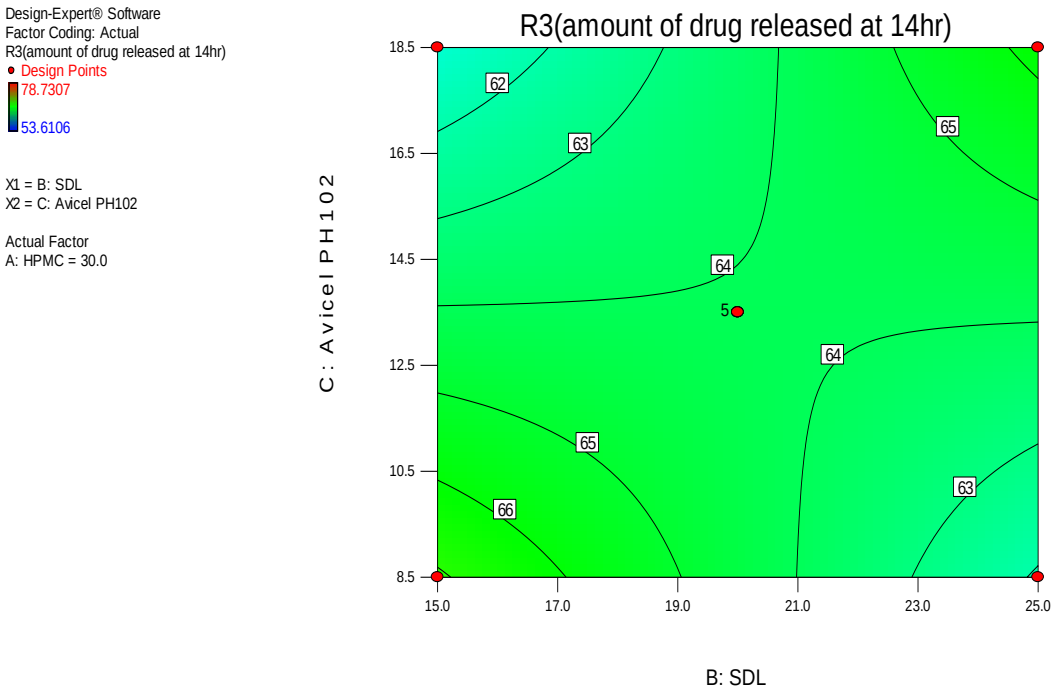

Figure 6.8. Contour plot of the effects of SDL and MCC on percent NVP released at 14 hours.

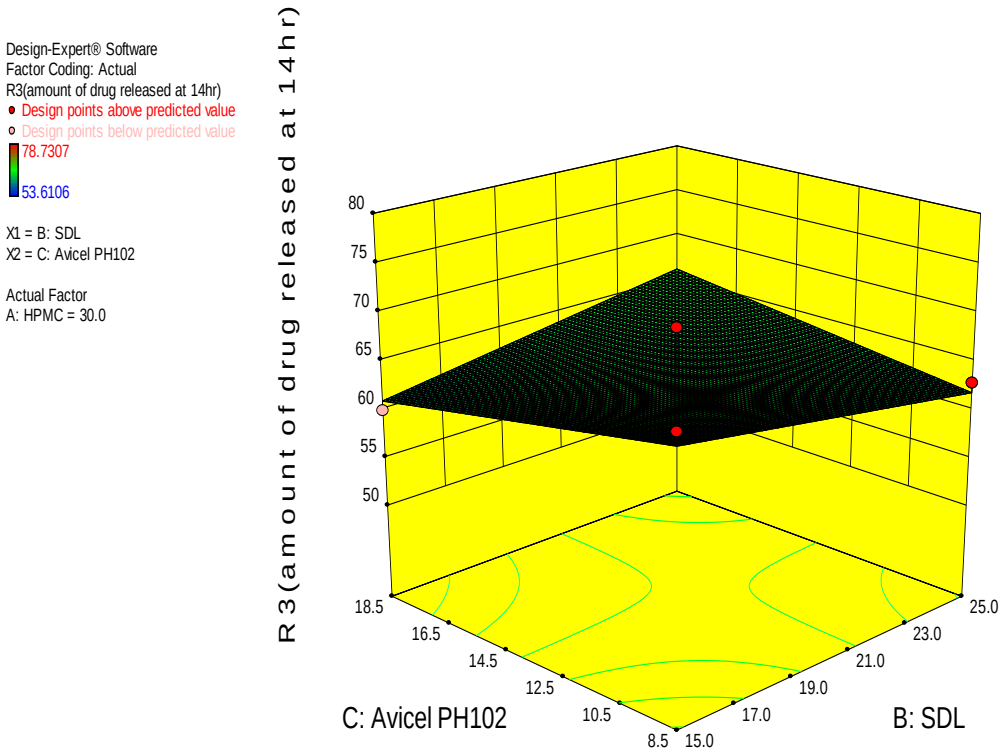

Figure 6.9. 3-D plot of the effects of SDL and MCC on percent NVP released at 14 hours.

6.3.3 Physical and Chemical Characteristics of the Tablets

The tablets from all 17 batches showed variable trends in terms of their characteristics. Tablets from batches NVP016, NVP021 and NVP028 failed the assay test. The tablets from batches NVP013 and NVP014 did not meet the set specifications for hardness. However, tablets from all batches passed the friability test indicating they were strong enough to withstand the abrasion and attrition that might occur during handling, packaging and transportation. Batches NVP020, NVP026 and NVP029 exhibited suitable physical and chemical characteristics with a NVP content > 96 %, and a hardness value close to the limit of 100 N set in addition to weight uniformity. The diverse responses observed using the BBD experimental data further emphasises the advantage of using a DOE approach for formulation optimisation. The results for all quality control tests *viz.,* weight uniformity, thickness, hardness, friability and assay for NVP are summarised in Table 6.9.

Table 6.9. Physical and chemical characteristics of tablets from Box-Behnken design (values reported as mean ± SD)

Batch	Thickness Mm	Weight Uniformity Mg	Hardness N	NVP content Mg	Friability %
NVP013	5.52±0.06	296.45±2.69	67.8 ±11.5	94.7 ± 0.94	0.171
NVP014	5.52±0.05	292.19±3.79	70.4 ± 8.65	100.2±0.51	0.175
NVP015	5.56±0.06	297.86±1.54	80.4 ± 11.4	94.9 ± 0.43	0.169
NVP016	5.57±0.07	299.29±1.07	83.7 ± 9.70	93.6 ± 2.74	0.171
NVP017	5.54±0.03	298.98±2.81	81.9 ± 8.53	97.4 ± 0.42	0.170
NVP018	5.53±0.07	299.16±1.66	85.2 ± 13.9	97.7 ± 1.99	0.172
NVP019	5.55±0.04	295.69±3.26	83.7 ± 6.99	96.5 ± 0.29	0.166
NVP020	5.67±0.04	300.44±1.93	94.9 ± 8.92	100.9 ± 0.37	0.167
NVP021	5.58±0.05	297.75±3.78	87.3 ± 7.20	94.1 ± 0.20	0.169
NVP022	5.57±0.05	297.67±2.85	92.1 ± 8.37	96.2 ± 0.31	0.171
NVP023	5.61±0.05	293.48±4.15	84.7 ± 8.64	96.7 ± 0.31	0.166
NVP024	5.62±0.06	303.91±1.37	92.0 ± 8.36	96.1 ± 0.20	0.341
NVP025	5.62±0.06	295.71±4.81	81.8 ± 8.17	97.5 ± 0.18	0.168
NVP026	5.62±0.06	302.21±1.71	79.6 ± 5.56	99.8 ± 0.28	0.174
NVP027	5.64±0.05	295.15±3.41	95.4±7.91	96.8 ± 0.07	0.169
NVP028	5.66±0.23	293.77±4.64	80.9 ± 7.22	94.7 ± 1.34	0.169
NVP029	5.61±0.05	296.18±3.32	81.5 ± 5.11	98.8 ± 0.94	0.169

6.3.4 Kinetics of NVP Release

The dissolution data from all 17 formulations were fitted to mathematical models and the results of modelling for the BBD are summarised in Table 6.10. NVP release from most batches was best fitted to the Korsmeyer-Peppas model, as this produced the highest average R^2 value of 0.9793 ± 0.11. The data were also well fitted to the Higuchi model. The R^2 values derived from fitting data to the Hixson-Crowell model revealed that there was a significant change in the surface area of the dosage form over time, implying that erosion and swelling of the matrix may be significant contributing factors in NVP release. The values of the release exponent *n*, for tablets from all the batches also confirmed that polymer dissolution also had an impact on NVP release. Consequently NVP release from these hydrophilic matrix tablets involve multiple factors including diffusion, swelling and erosion of the HPMC and constitute a complex release process.

Table 6.10. Summary of NVP release kinetics for BBD formulations

Batch	R^2						Rate Constant *K*	Diffusion Exponent n
	Zero-order	First-order	Higuchi	Power Law	Hixson-Crowell	Mechanism		
NVP013	0.8630	0.9451	0.9493	0.9588	0.9255	Peppas	0.7522	1.0045
NVP014	0.9607	0.8142	0.9959	0.9836	0.9919	Higuchi	0.9250	0.7527
NVP015	0.9614	0.9882	0.9962	0.9850	0.9924	Higuchi	0.9053	0.7771
NVP016	0.9813	0.9543	0.9957	0.9922	0.9847	Higuchi	0.8864	0.7978
NVP017	0.9466	0.9881	0.9917	0.9753	0.9886	Higuchi	0.9362	0.7625
NVP018	0.8851	0.9423	0.9576	0.9733	0.9494	Peppas	0.7752	0.9874
NVP019	0.9630	0.9855	0.9969	0.9880	0.9946	Higuchi	0.8843	0.8073
NVP020	0.9882	0.9257	0.9797	0.9964	0.9618	Peppas	0.9180	0.6818
NVP021	0.9306	0.9860	0.9864	0.9668	0.9846	Higuchi	1.0089	0.6871
NVP022	0.8902	0.9694	0.9650	0.9796	0.9568	Peppas	0.8083	0.9657
NVP023	0.9900	0.9192	0.9765	0.9964	0.9577	Peppas	0.9653	0.6187
NVP024	0.9420	0.9763	0.9856	0.9689	0.9821	Higuchi	0.9412	0.7614
NVP025	0.9905	0.9180	0.9781	0.9963	0.9579	Peppas	0.9260	0.6759
NVP026	0.8525	0.9420	0.9414	0.9499	0.9223	Peppas	0.7933	0.9800
NVP027	0.9487	0.9852	0.9867	0.9889	0.9836	Peppas	0.8133	0.8599
NVP028	0.9769	0.9292	0.9862	0.9910	0.9655	Peppas	1.0170	0.6462
NVP029	0.9446	0.9853	0.9905	0.9730	0.9882	Higuchi	0.9527	0.7547
Viramune® XR	0.9816	0.9010	0.9964	0.9954	0.9660	Higuchi	0.7739	0.9439

6.3.5 Optimisation of Variables and Validation of the Experimental Model

The polynomial equations relating the dependent and independent variables that were generated were used to optimise the formulation variables for all responses. The responses were optimised by introducing constraints and searching for levels of independent variables that would produce the targeted responses (Table 6.1) and yield a dissolution profile similar to that of Viramune® XR tablets. The polynomial equations generated theoretical or predicted values for the responses that were then compared to the responses observed for all batches of tablets that were manufactured. The optimised formulation variables that were suggested by Design Expert® software were compared to the variables of the starting formula. The results are shown in Table 6.11, and the variables were selected on the basis of desirability. The results generated using the BBD in addition to evaluation of the statistical and mathematical data generated during data analysis facilitated this decision.

Table 6.11. Formulation variables for starting formula and optimised batch

	Amount % w/w	
Excipient	**Starting batch (NVP006)**	**Optimised batch (NVP030)**
NVP	33.33	33.33
Methocel® K4M	30.00	33.12
SuperTab® SDL	20.00	25.00
Avicel® PH102	13.50	15.32
Magnesium stearate	1.10	1.10
Talc	1.10	1.10
Colloidal silicon dioxide	1.00	1.00

The prediction accuracy of the process was then established by calculating the residual and percent prediction errors (%P.E.) of three formulations that were manufactured using the optimised independent variables. The results are summarised in Table 6.12. The residuals and %P.E. for the responses were < 5%, except for response Y_2 in batches NVP030 and NVP031, in which the %P.E was > 5% and was <5% in batch NVP032, indicating that the prediction process was more precise for other responses than for response Y_2. These results showed that the experimental model used has the potential for improvement and further optimisation.

Table 6.12. Validation of experimental model: predicted and observed responses

Batch	Response	Predicted value	Observed value	Residual	% P.E.
NVP030	Y_1	9.53	10.41	0.87	9.161
	Y_2	40.0	34.01	5.99	14.97
	Y_3	63.11	61.65	1.46	2.32
	Y_4	88.05	88.81	0.76	0.87
	Y_5	72.41	69.70	2.71	3.74
	Y_6	0.9644	0.9753	0.011	1.141
NVP031	Y_1	9.53	9.89	0.36	3.80
	Y_2	40.0	36.78	3.22	8.05
	Y_3	63.11	60.68	2.43	3.85
	Y_4	88.05	88.94	0.89	1.01
	Y_5	72.41	70.80	1.610	2.223
	Y_6	0.9644	0.9688	0.0044	0.456
NVP032	Y_1	9.53	9.92	0.39	4.07
	Y_2	40.0	38.33	1.67	4.17
	Y_3	63.11	62.81	0.30	0.47
	Y_4	88.05	87.87	0.19	0.21
	Y_5	72.41	70.62	1.79	2.47
	Y_6	0.9644	0.9749	0.011	1.58

Tablets manufactured using the optimised formulation variables, *viz*., batch NVP030 were assessed in terms of their physical characteristics, content uniformity, and water uptake and erosion indices. The quality attributes of the tablets were all within Pharmacopoeial limits [345]. The % RSD for content uniformity was 3.26% revealing that the production process was adequate and resulted in the production of tablets with an even distribution of NVP. The results for assay revealed that the tablets contained an average of 97.5 ± 0.3% NVP and had a tensile strength of 1.45 ± 0.064 N/mm^2.

The dissolution profiles of NVP release generated using USP Apparatus III and media of pH 1.2 (2h) and 7.2 (22h), sampling times shown in Table 3.8, for the tablets from batch NVP030 and Viramune® XR, are depicted Figure 6.10. Comparison of the dissolution profiles of NVP release from the optimised formulation and Viramune® XR yielded f_1 and f_2 values of 7.9 and 69.7 respectively, indicating that the profiles were similar. The f_1 and f_2 factors obtained for the tablets from batch NVP030 were better than the values obtained for the starting formulation, batch NVP006, indicating that the optimisation process resulted in an improved formulation.

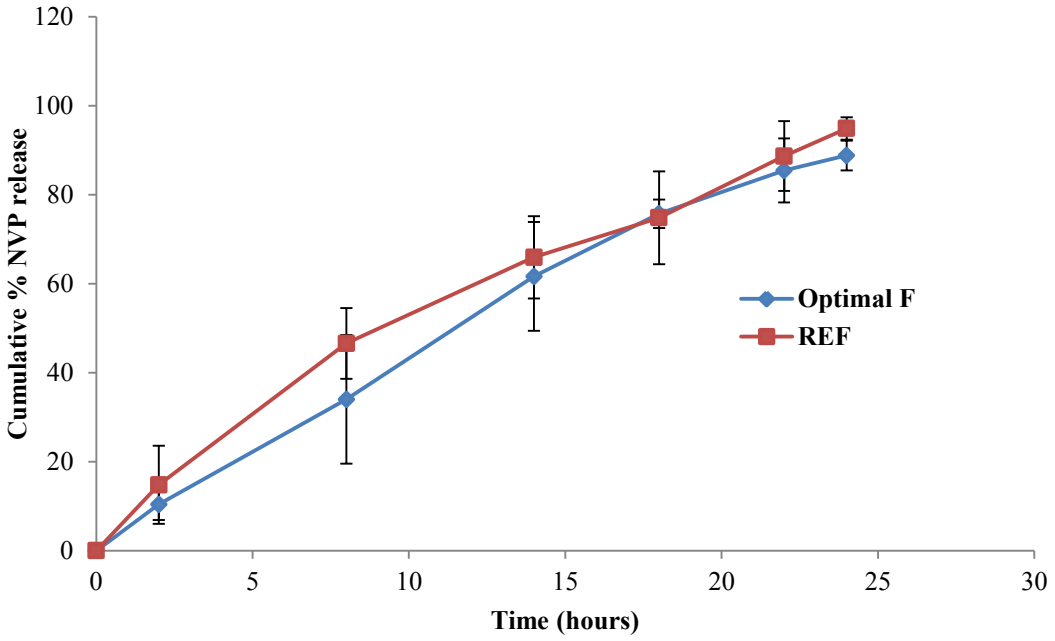

Figure 6.10. Dissolution profiles of NVP from batch NVP030 and Viramune® XR [n = 6, pH 1.2 (2h) and 7.2 (22h)].

It has been suggested that < 20% of an API should be released within the first 2 hours of commencing dissolution testing as a dosage form would be in the stomach and dose dumping should be avoided [379]. However, most of the API should be released and made available for absorption whilst the dosage form is resident in the GIT and specifically the small intestine if that is the site of absorption. The dissolution profile generated by performing dissolution testing to mimic GIT pH conditions (§ 3.3.2.1, Tables 3.2 and 3.8) are depicted in Figure 6.11 and reveals that most of the drug would be made available for absorption within 14 hours of administration, which is the expected residence time of a dosage form in the GIT [379].

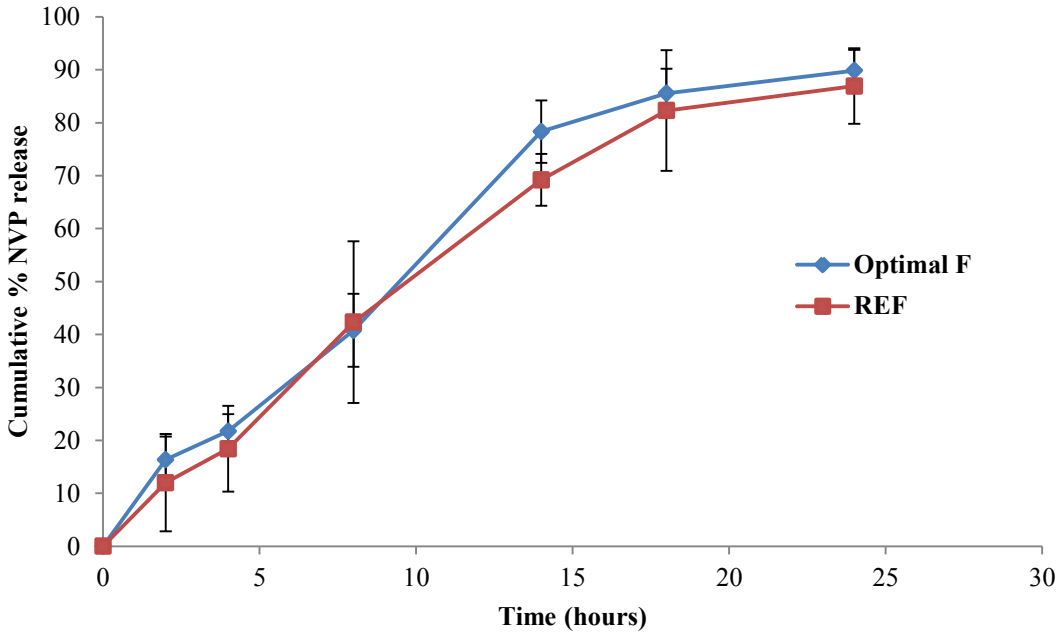

Figure 6.11. Dissolution profile of NVP release from batch NVP030 and Viramune® XR in media of different pH (pH 1.6 = 2h, pH 3.4 = 2h, pH 4.5 = 4h, pH 6.8 = 6h, pH7.2 = 10h) (n = 6).

NVP release from tablets of batch NVP NVP030 exhibited a diffusion release exponent of 0.9753 compared to that of 0.9644 for the reference product Viramune® XR. The release exponent values are similar suggesting that the mechanism of NVP release from the optimised batch was similar to that of the reference product. The R^2 values generated following fitting of dissolution data to different kinetic models are shown in Table 6.13. The values also suggest there is close similarity in the mechanism of NVP release from the test and reference formulations. Furthermore this approach has indicated that mathematical modelling can be used to design dosage forms with targeted and desired dissolution characteristics.

Table 6.13. Comparison of drug release kinetics of batch NVP030 and Viramune® XR

	R^2 value	
Kinetic model	**Optimal F**	**Viramune® XR**
Zero-order	0.9438	0.9246
First-order	0.9788	0.9593
Higuchi	0.9848	0.9799
Korsmeyer-Peppas	0.9823	0.9844
Hixson-Crowell	0.9789	0.9714
Diffusion exponent	0.9644	0.9753

6.3.6 Water Uptake and Erosion Studies

The release of an API from hydrophilic matrices is influenced by polymer swelling, front movement, dissolution and diffusion of an API and erosion of the matrix [321]. The release of poorly soluble drugs such as NVP will likely be controlled by polymer relaxation or dissolution. The kinetics of this phenomenon that takes place when HPMC based matrix tablets come into contact with an aqueous dissolution medium were analysed by determining the swelling and erosion indices for these dosage forms. The swelling of NVP tablets over the time period of dissolution testing is depicted in Figure 6.12. The ratio of wet weight to the initial weight increases gradually during the initial stages of testing and then starts to decrease over time during the later stages of testing. This could be due to erosion that may take place simultaneously with swelling, and results in lower wet weights for the dosage form, when compared to the initial weight after 14 hours of dissolution testing.

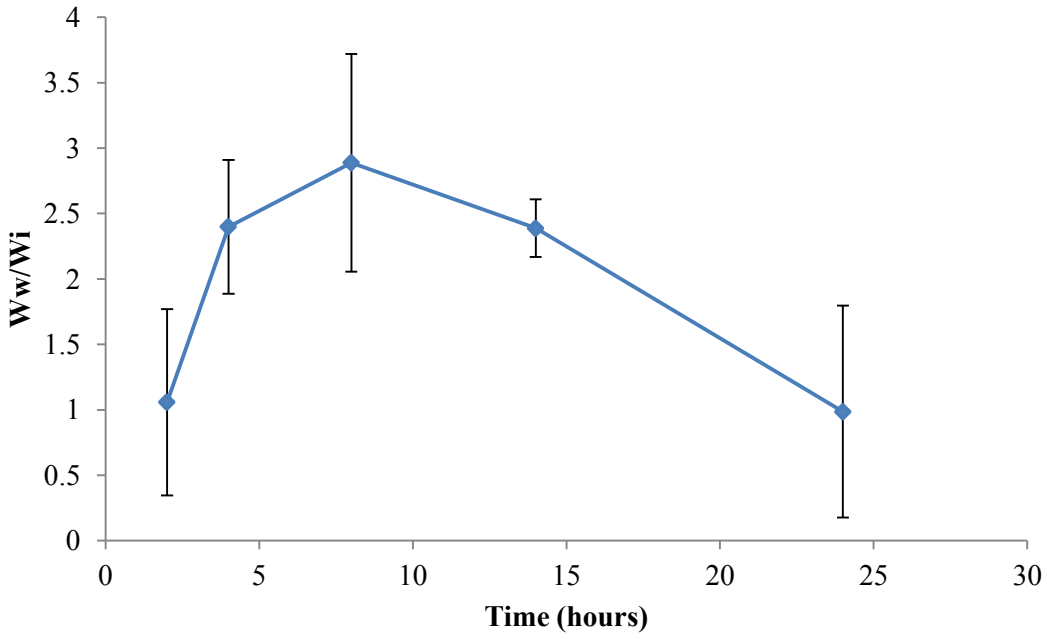

Figure 6.12. Change in weight of tablet at different times during dissolution testing (n = 3) in 50 mM phosphate buffer of pH 1.6 (2h), 3.4 (2h), 4.7 (4h), 6.8 (6h) and 7.2 (10h).

During the initial stages of dissolution, polymer chains of HPMC are not yet relaxed and therefore swelling is not pronounced. The NVP that was released was likely located on the outer surface of the matrix, which may also account for the initial burst release that is commonly associated with HPMC matrices. Following hydration there is a rapid increase in

the swelling of the dosage form over the first two hours which implies that polymer swelling is predominant as additional dissolution medium enters the matrix system. The higher degree of swelling observed during this time results in a decrease in the amount of NVP release. This is because the diffusional distance that the NVP must traverse from the core of the matrix to the dissolution medium increases. Swelling of the polymer matrix continues to increase for approximately 8 hours after commencing dissolution testing, albeit at a slower but constant rate. This could be due to an insignificant contribution of the dissolution medium to polymer swelling as the water holding capacity of the polymer decreases, or as a result of erosion and swelling rates being the same [380]. The dissolution medium then moves into and out of the polymer matrix at a constant rate and the swelling of the matrix then becomes a function of the mobility of the polymer only [381]. To establish the rate of dissolution medium uptake, the values for dissolution medium uptake over the period of testing were fitted to Equation 6.11.

$$\frac{Wt-Wi}{Wi} = K_{mu}(t^{0.5}) \qquad \textbf{Equation 6.11}$$

where,

W_i = initial weight of the tablet,
W_t = weight of the tablet after time t, and
K_{mu} = the rate constant of medium uptake.

The rate of dissolution uptake was determined for all phases of the dissolution test *viz.,* 0 - 2 h, 2 h - 4 h, 4 h - 8 h, 8 h - 14 h and 14 h - 24 h and a summary of the rates of dissolution media uptake for the time phases studied are shown in Table 6.14.

Table 6.14. Rate of dissolution medium uptake for the different time phases of testing

Time Phase (hours)	Initial Weight (mg)	Final weight (mg)	Rate of medium uptake ($h^{-0.5}$)
0 – 2	328.6	347.8	7×10^{-18}
2 – 4	325.4	780.4	3.175
4 – 8	328.3	948.0	0.295
8 – 14	325.3	1101.4	0.3299
14 – 24	326.8	1256.5	0.3869

The data revealed that the rate of medium uptake in the first 2 hours of dissolution testing was very slow but increased during the 2 – 4 hour period. The rate of medium uptake then decreased but at a fairly constant rate for the remainder of the testing period. This data

implies that swelling was expected to significantly affect NVP release during the 2 – 4 hour period when the swelling rate of the matrix is high.

The erosion of a matrix can be described by the Hixson-Crowell Cube Root Law [382]. The values of the ratio of dried weight following dissolution medium exposure to initial weight were fitted to the Hixson-Crowell Cube Root relationship as shown in Figure 6.13 and the apparent polymer erosion rate constant was calculated using Equation 6.12.

$$\frac{Wd}{Wi} = \sqrt[3]{(1 - K_{er}t)} \qquad \textbf{Equation 6.12}$$

where,

W_d = final dry weight of the tablet,
W_i = initial weight, and
K_{er} = erosion rate constant at time t.

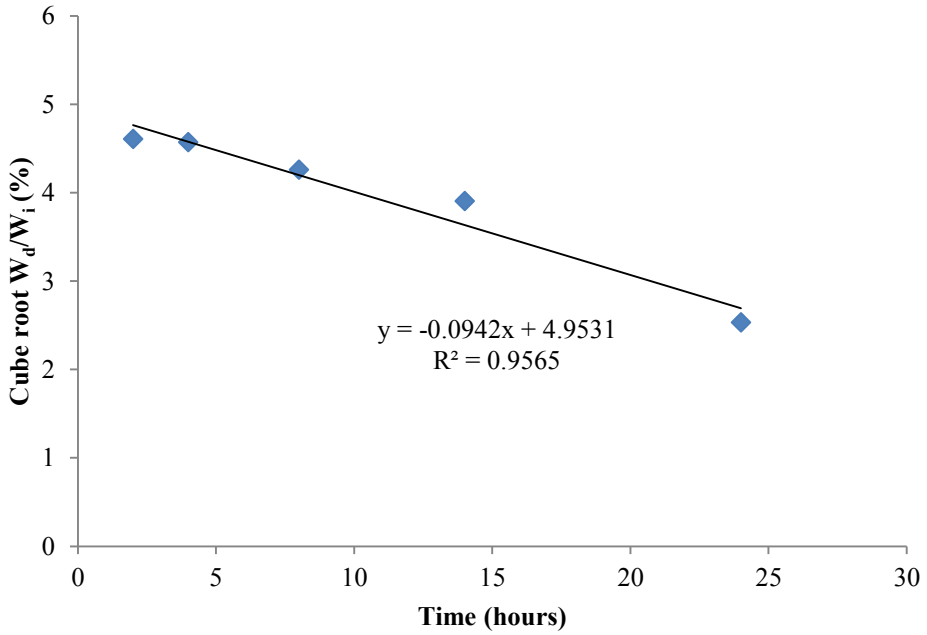

Figure 6.13. Linear regression analysis of the ratio of dry weight to initial weight using Hixson-Crowell Cube Root Law.

Analysis of the data depicted in Figure 6.13 yields an erosion rate constant of 4.953 h^{-1}. The rate of erosion was minimal during the initial stages of dissolution testing and increased over time. This was possibly due to the dissolution of lactose resulting in the development of pores

in the tablet, through which dissolution medium can diffuse into and out of the matrix thereby facilitating an increase in the rate of erosion.

6.3.6.1 Effect of pH on Swelling and Erosion of NVP Tablets

The effect of dissolution medium pH on the swelling and erosion of NVP tablets (NVP030) was studied by exposing the tablets to 50 mM phosphate buffer of pH 1.6, 4.7 and 6.8 for 18 hours in each pH environment. The effect of pH on swelling and erosion of these matrix tablets is depicted in Figure 6.14.

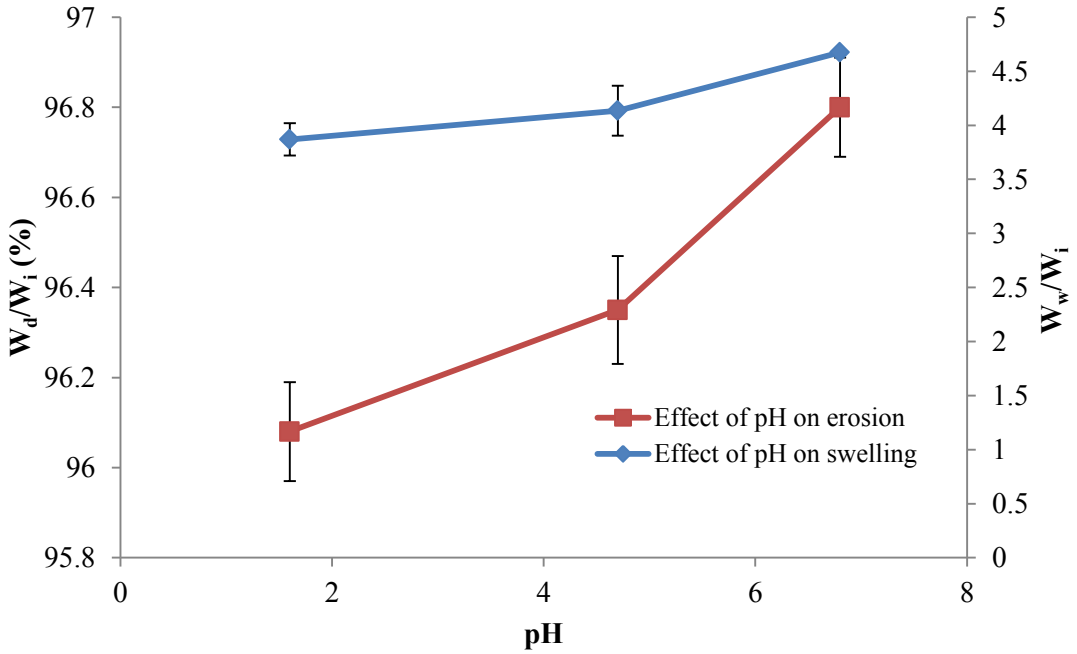

Figure 6.14. Effect of pH on swelling and erosion of NVP tablets. Ratio of dry weight (W_d) to initial weight (W_i) and wet weight (W_w) to the initial weight following exposure to media of different pH (n =3).

The pH of the dissolution medium was found to have a significant effect on the swelling of these matrix systems. An increase in pH resulted in an increase in the degree of swelling of the matrix and the data are similar to previously reported studies [383]. Erosion was found to be slightly higher in media of low pH. The difference in erosion indices in different pH media was not significant as HPMC is a non-ionic polymer.

6.3.6.2 Effect of Buffer Molarity on Swelling and Erosion

The effect of buffer molarity on water uptake and erosion characteristics of this formulation was studied by exposing tablets to 25 mM, 50 mM and 75 mM phosphate buffers of pH 6.8 for 18 h. The effect of buffer molarity on swelling and erosion characteristics is depicted in Figure 6.15.

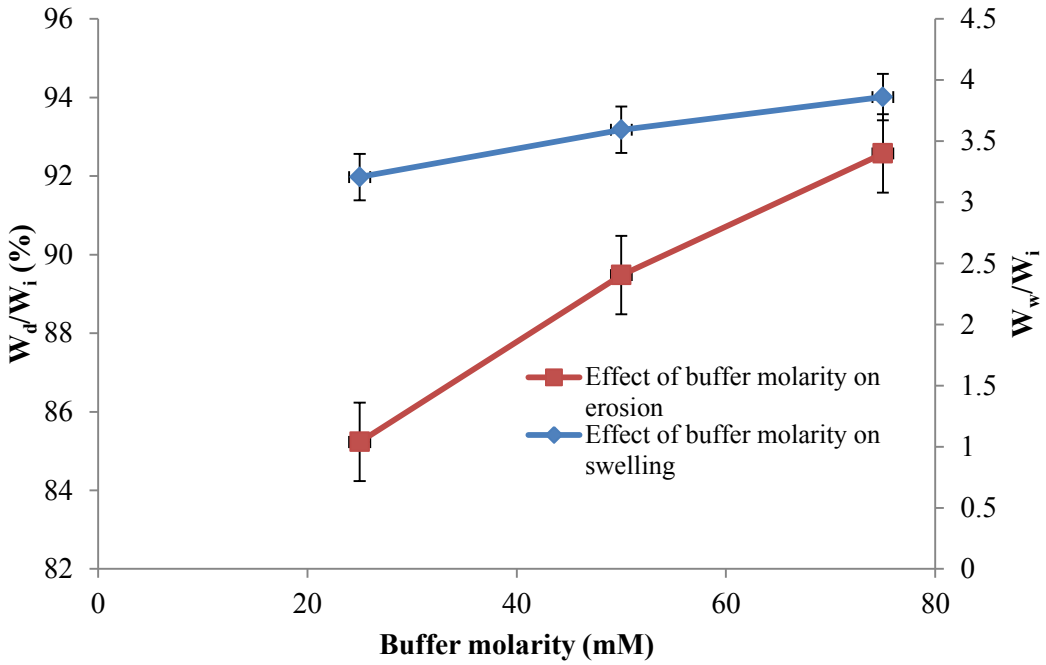

Figure 6.15. Effect of pH on swelling and erosion of NVP tablets. Ratio of dry weight (W_d) to initial weight (W_i) and wet weight (W_w) to the initial weight following exposure to media of different molarity strengths at pH 6.8 (n =3).

The results depicted in Figure 6.15 indicate that that rate of swelling of the HPMC based tablets increased slightly as the molarity of the buffer increases, whereas the rate of erosion decreased with an increase in buffer molarity. Similar observations have been reported and the decrease in erosion rate with increase in ionic strength has been attributed to 'salting out' effect of the polymer by inorganic ions present in the dissolution medium [380]. An increase in the ionic strength of a solution results in polymer chains losing water of hydration [216], however, the polymer still forms a protective gel layer around the core but does not disintegrate [380, 384]. A high ionic strength has been reported to facilitate competition between inorganic ions for available water of hydration with polymer chains [198, 380]. The rate of erosion decreases with an increase in molarity which may be attributed to an increase

in the number of phosphate ions in the buffer that compete for the water of hydration and subsequently reduce the amount of water that is able to enter into and diffuse out of the matrix tablets [380, 384].

6.4 EFFECT OF FORMULATION COMPOSITION ON NVP RELEASE, SWELLING AND EROSION

In order to determine the effect(s) of formulation composition of the optimised formulation on the dissolution rate of NVP, tablets containing different grades of HPMC, different particle sizes of MCC and different types of lactose were manufactured. A summary of the batches that were manufactured is shown in Table 6.15.

Table 6.15. Formulae for tablets using different grades of HPMC, MCC and lactose

	Batch					
Excipient (%)	**NVP033**	**NVP034**	**NVP035**	**NVP036**	**NVP037**	**NVP038**
K4M	-	-	33.16	33.16	33.16	33.16
K15M	33.16	-	-	-	-	-
K100M	-	33.16	-	-	-	-
PH101	-	-	15.32	-	-	-
PH102	15.32	15.32	-	-	15.32	15.32
PH200	-	-	-	15.32	-	-
SuperTab® SDL	25	25	25	25	-	-
Tablettose® 100	-	-	-	-	25	-
FlowLac® SDL	-	-	-	-	-	25

NB: NVP, Mg stearate, talc and colloidal silicon dioxide as for batch NVP030.

The grades of HPMC that were used were Methocel® K4M, K15M and K100M, MCC were Avicel® PH101, PH102 and PH200 and lactose were SuperTab® spray dried lactose (Lactose New Zealand), Tablettose® 100 agglomerated lactose for DC and FlowLac® 90 spray dried lactose. The dissolution data for NVP for these batches were compared using f_1 and f_2 analysis. The effects of HPMC grade on swelling and erosion were investigated.

6.4.1 Effect of HPMC Grade on Dissolution Rate of NVP

An increase in the viscosity of HPMC resulted in a decrease in the rate of NVP release. The use of Methocel® K100M resulted in significant reduction of NVP release with only 42% of the total NVP being released after 24 hours in comparison to approximately 63% and 88% for tablets containing Methocel® K15M and K4M, respectively. These results are similar to those

reported by many other authors [306, 307, 385-387]. The dissolution profiles of NVP for tablets containing different grades of HPMC are shown in Figure 6.16 and a comparison of these results show that HPMC grade had an effect on the rate and extent of NVP release from the tablets. The greater the difference in HPMC grade the greater the difference in the rate and extent of NVP dissolution.

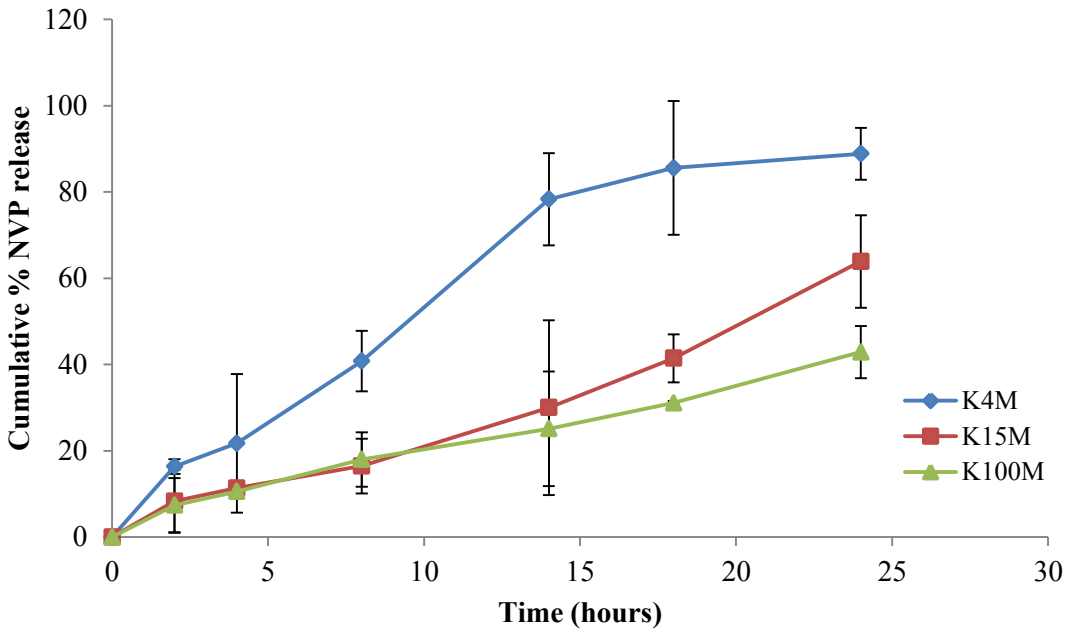

Figure 6.16. Dissolution profiles of NVP from tablets manufactured using different grades of HPMC (n =6).

It has been suggested that the higher viscosity grades of HPMC swell rapidly to form a strong gel that decreases the rate of API release. The rapid swelling is due to rapid expansion of the side chains of the high viscosity grade HPMC and blocks the pores into which water and the API can diffuse [386]. The f_1 and f_2 factors obtained following comparison of dissolution profiles of NVP from tablets with HPMC of different grades are listed in Table 6.16.

Table 6.16. Comparison of f_1 and f_2 for NVP release from formulations with HPMC of different molecular weights

Formulations compared	f_1	f_2
K4M vs. K15M	27.7	47.3
K4M vs. K100M	43.1	35.8
K15M vs. K100M	23.0	50.3

Red = out of specification.

6.4.1.1 Effect of HPMC Grade on Swelling of NVP Tablets

Water uptake studies were performed on tablets containing different grades of HPMC to assess the impact of molecular weight on the rate of uptake of the dissolution medium. The extent of medium uptake data was fitted to the Higuchi model and the dissolution medium uptake rate constant calculated. The rate of uptake of the dissolution medium was found to be non-linear and decreased with time which is consistent with previously reported data [380]. The rate of dissolution medium uptake was found to increase slightly with an increase in the molecular weight of HPMC as shown in Figure 6.17.

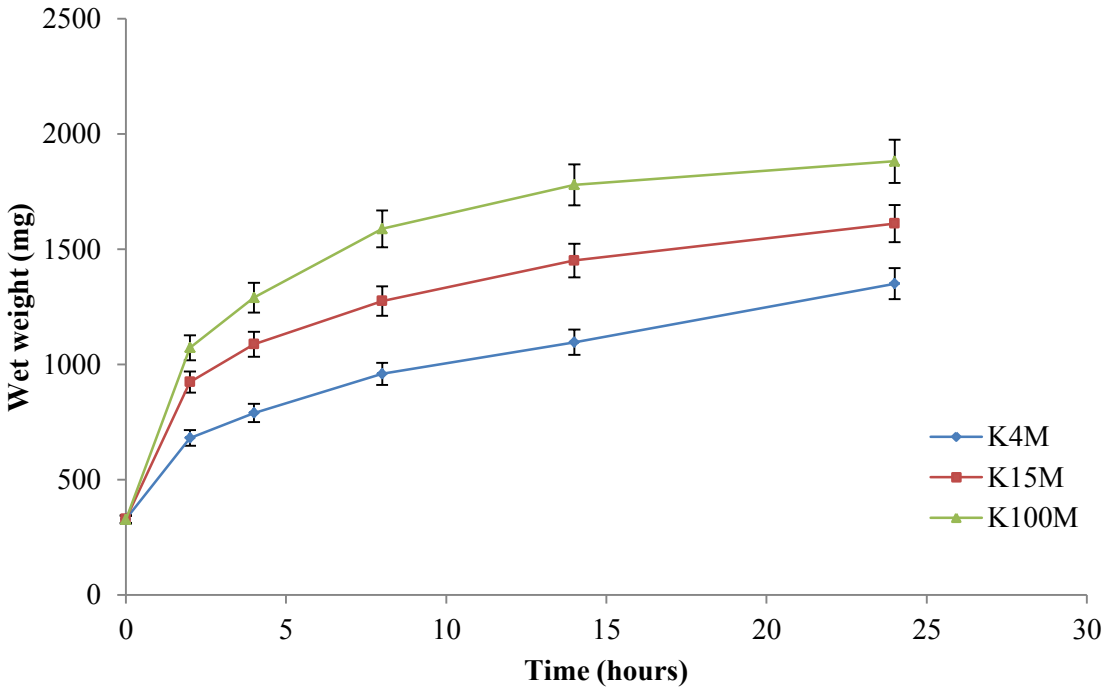

Figure 6.17. Wet weight of tablets manufactured with different molecular weight HPMC (n=3).

Fitting of the data from medium uptake studies to the Higuchi model permitted the calculation of rate constants for dissolution medium uptake that were observed to increase as the molecular weight of the polymer increased as shown in Table 6.17.

Table 6.17. Rate constants of dissolution medium uptake for tablets manufactured using HPMC of different molecular weight

Polymer	Rate constant (K_{mu}, $h^{-0.5}$)	R^2 value
K4M	3.1759 ± 0.025	0.9969 ± 0.012
K15M	3.4816 ± 0.013	0.9833 ± 0.005
K100M	3.6061 ± 0.021	0.9307 ± 0.041

These data reveal that tablets manufactured with a high molecular weight HPMC are more likely to release NVP at lower rates. This is due to a high degree of swelling, which increases the distance NVP has to diffuse to the surface of the matrix, as well as the increased viscosity and strength of the HPMC gel layer.

6.4.1.3 Effect of HPMC Grade on Erosion

The rate of erosion of HPMC tablets decreased with an increase in molecular weight of HPMC and the data are consistent with previously reported results [307, 379]. This has been attributed to the formation of a stronger gel layer when high molecular weight HPMC polymers are used. A plot of erosion data versus time is shown in Figure 6.18.

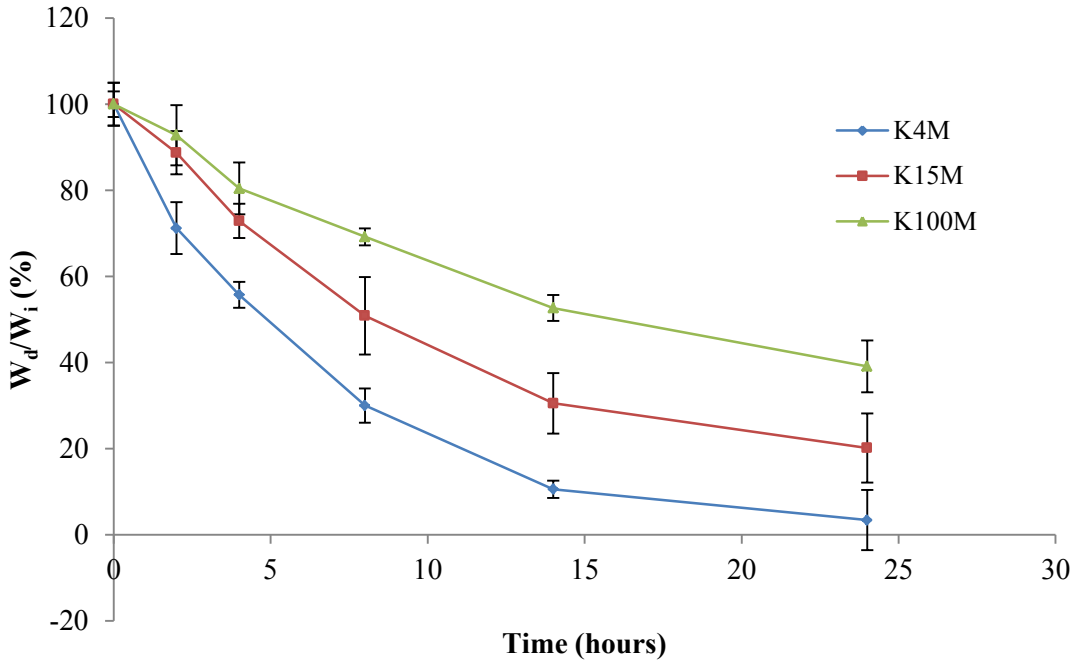

Figure 6.18. Percent erosion of tablets manufactured with different molecular weight HPMC (n = 3).

The rate constants of erosion obtained after fitting erosion data to the Hixson-Crowell Cube Root Law are summarised in Table 6.18 and reveal that the degree of erosion decreases with an increase in the molecular weight of the HPMC polymer that was used to produce the tablets.

Table 6.18. Erosion rate constants of tablets manufactured with different molecular weight HPMC (n = 3)

Polymer	Rate constant, K_{er} h^{-1}	R^2
K4M	4.5413 ± 0.032	0.9747 ± 0.043
K15M	4.4571 ± 0.041	0.9432 ± 0.022
K100M	4.2190 ± 0.045	0.9584 ± 0.019

The swelling and erosion of HPMC matrices is entirely dependent on the viscosity of the polymer. The degree of swelling increases as the viscosity of the polymer increases whereas the percent erosion decreases with an increase in polymer viscosity [388]. This observation is relevant for formulations in which a sparingly water soluble API, such as NVP is to be included and the use of a low viscosity grade HPMC for which erosion predominates may therefore be preferred. This was confirmed by observations for the optimised batch (NVP030) in which a low molecular weight HPMC was used and the extent of NVP release was > 88 %.

The relationship between NVP dissolution, swelling and erosion can be visualised in Figures 6.19 - 6.21 for the tablets that were manufactured with Methocel® K4M, K15 and K100M, respectively.

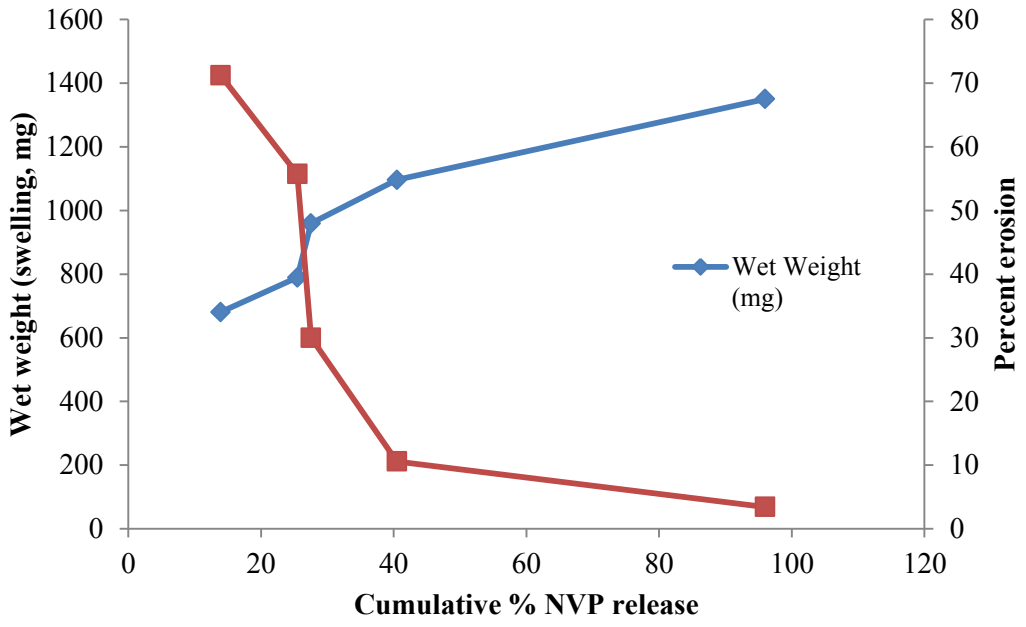

Figure 6.19. The relationship between swelling, erosion and NVP release from tablets containing Methocel® K4M.

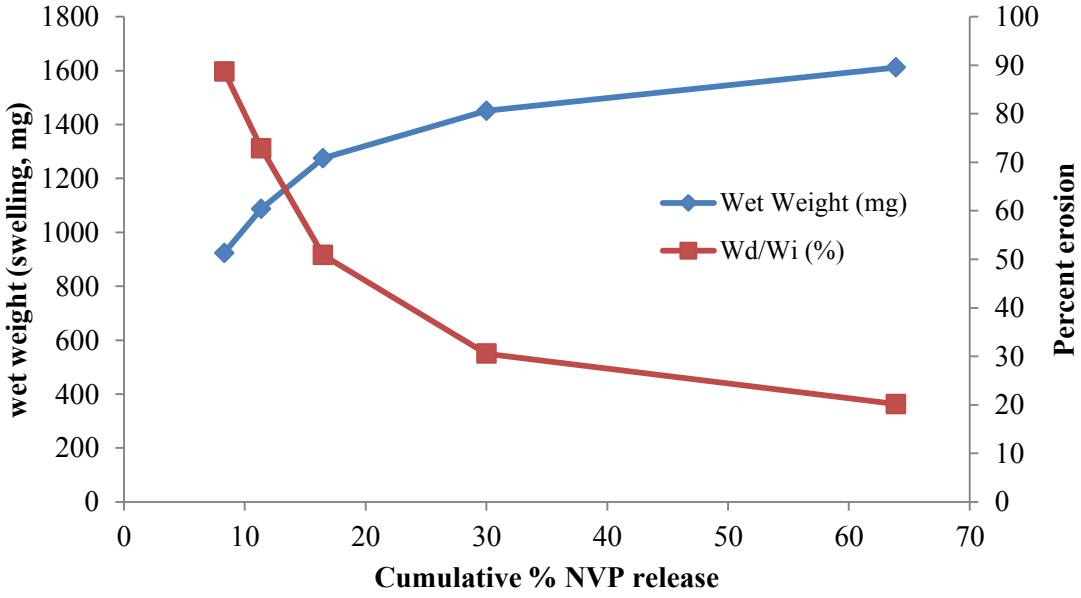

Figure 6.20. The relationship between swelling, erosion and NVP release from tablets containing Methocel® K15M.

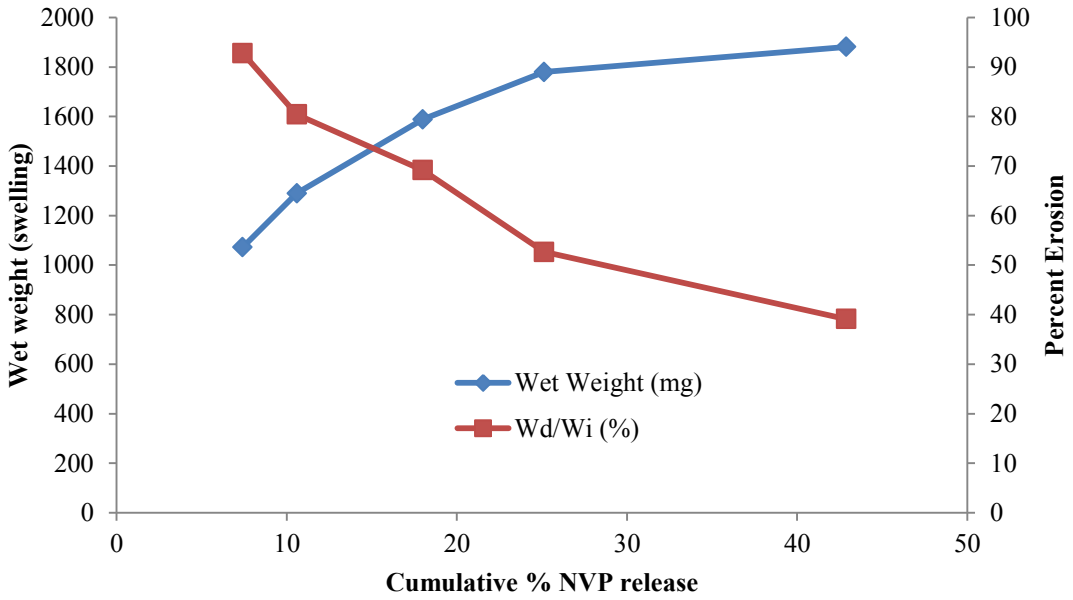

Figure 6.21. The relationship between swelling, erosion and NVP release from tablets containing Methocel® K100M.

An increase in the rate of dissolution medium uptake in conjunction with a decrease in the rate of erosion with an increase in molecular weight of HPMC used explains why the rate of NVP release from the tablets decreases when polymers of higher viscosity grade were used in the formulation. These figures graphically depict the fact that the higher the molecular weight of HPMC used, the greater the degree of swelling and the lower the extent of erosion. These factors when operating together result in a decrease in the rate and extent of NVP release from these matrices.

6.4.2 Effect of Grade of MCC on Dissolution of NVP

An investigation into the effect of particle size of MCC on the dissolution of a self-nanoemulsified solid dosage form of ubiquinone revealed that the rate of dissolution of the nanoemulsion from the tablets increased with increasing particle size of MCC [389]. In another study a decrease in the dissolution rate of API was observed with a decrease in the particle size of MCC. This was attributed to a decrease in the porosity of the dosage form due to the smaller particle size of the MCC [390].

A comparison of the MCC grades used in these studies is shown in Table 6.19.

Table 6.19. Physical characteristics of MCC grades [217].

MCC grade	Nominal Mean Particle Size µm	Bulk density g/cm^3	Tapped density g/cm^3	True density g/cm^3
PH101	50	0.32	0.45	1.512 – 1.668
PH102	100	0.337	0.478	1.420 – 1.460
PH200	180	0.337	0.478	1.512 – 1.668

In these studies the grade of MCC did not appear to have a significant effect on the dissolution rate of NVP. Similar results have been observed where there were no significant differences in dissolution profiles reported when MCC PH101 and PH102 were used to manufacture liquid-solid compacts [391]. The f_1 and f_2 factors obtained from comparisons of dissolution data from tablets with different MCC grades used in this study are shown in Table 6.20.

Table 6.20. Similarity and difference factors of dissolution profiles from tablets with different MCC grades

Formulations compared	f_1	f_2
PH101 vs. PH102	9.3	66.6
PH101 vs. PH200	15.7	57.8
PH102 vs. PH200	12.2	59.3

Red = out of specification

However a comparison of NVP release rates from tablets manufactured with MCC PH101 and PH200 revealed a difference with an f_1 value of 15.7. NVP release from tablets containing MCC PH101 was slightly faster than the release rate from tablets containing MCC PH200 during the initial stages of testing, and this could be as a result of smaller particle size of PH101 which increases the surface area and thus allow greater exposure of the matrix to the dissolution medium for NVP release during this early phase. However, over time the release rate of NVP from tablets containing PH200 was higher and the extent more complete than that observed for tablets containing PH101. This may be due to the tablets containing MCC PH200 having a greater porosity thereby facilitating the release of NVP from the core of the tablet.

Comparison of the dissolution profiles of NVP release from tablets containing MCC PH102 and PH200 revealed that there was no significant difference between the two formulations despite expectations that the larger particle size grade MCC PH200 would yield tablets with a high dissolution rate due to an increase in the porosity of the matrix system. This could be as

consequence of the significant effects of HPMC and lactose on NVP which might have overshadowed the effects of MCC.

The dissolution profiles for NVP from tablets manufactured using different grades of MCC are shown in Figure 6.22.

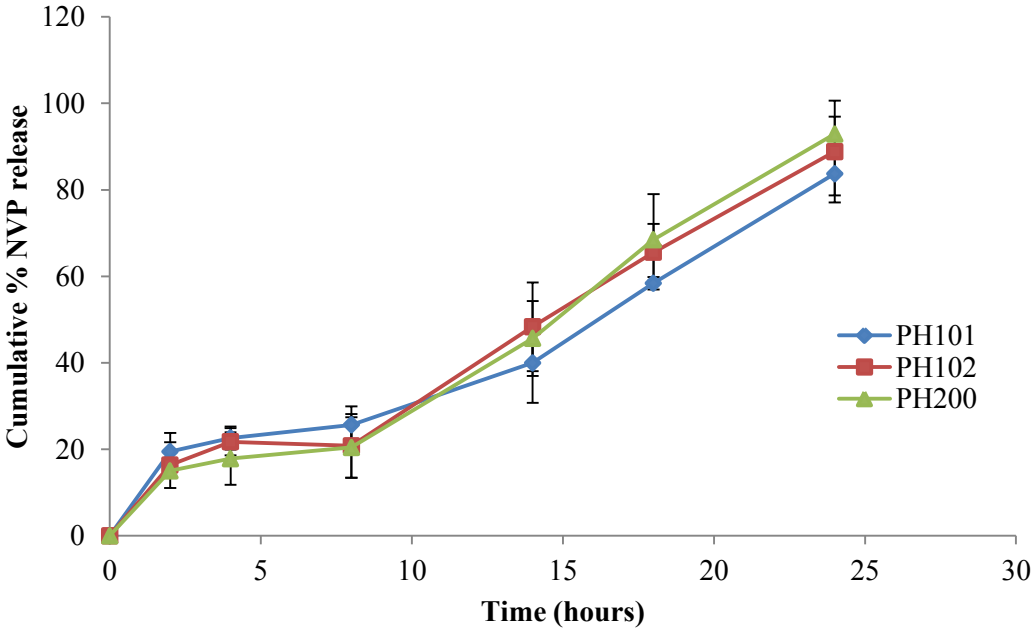

Figure 6.22. Dissolution profiles of NVP release from tablets manufactured with different grades of MCC (n = 6, pH = 6.8).

The profiles reveal that minimal NVP is released between 4 and 8 hours and it can possibly be attributed to significant swelling and a low degree of erosion of the matrices during this period. The low level of NVP release observed may also be a consequence of the low solubility of NVP in the buffer (pH 6.8) as the solubility of NVP may be lower at this pH, however further investigations are required.

6.4.3 Effect of Lactose Type on Dissolution of NVP

Several types of lactose are commercially available and have different physical characteristics such as particle size distribution and flow characteristics. Modified forms of lactose for use as filler-binder for the production of tablets by direct compression are now also available. Three types of modified lactose for DC were tested to investigate if a change in type of lactose would affect the dissolution performance of the NVP SR tablets. The differences between the types of lactose used are summarised in Table 6.21.

Table 6.21. Physical characteristic of lactose used in these studies

Lactose grade	Particle size distribution µm	Bulk density g/cm^3	Tapped density g/cm^3	Source
SuperTab® SDL	< 45, NMT 15% < 100, 30-60% < 250, NLT 98%	0.600	0.710	Lactose New Zealand
Tablettose® 100 AL	< 63, NMT 25% < 250, 60-90% <500, NLT 96%	0.540	0.690	Meggle Excipients and Technology, Wasserberg, Germany
FlowLac® SDL	< 32, NMT 5% <100, 25-40% < 200, NLT 85%	0.600	0.660	Meggle Excipients and Technology, Wasserberg, Germany

AL = agglomerated lactose, NMT = not more than, NLT = not less than.

The f_1 and f_2 factors obtained following dissolution testing of tablets manufactured using different grades of lactose are shown in Table 6.22 and reveal that the profiles were similar in all cases if using f_2 only for the comparison.

Table 6.22. Comparison of dissolution profiles from tablets manufactured using different grades of lactose

Lactose grade	f_1	f_2
SuperTab® SDL vs. Tablettose® 100 AL	17.7	57.0
SuperTab® SDL vs. FlowLac® SDL	10.2	65.0
Tablettose® 100 AL vs. FlowLac® SDL	10.1	66.2

Red = out of specifications.

The dissolution profiles of NVP release from tablets containing different types of lactose are shown in Figure 6.23.

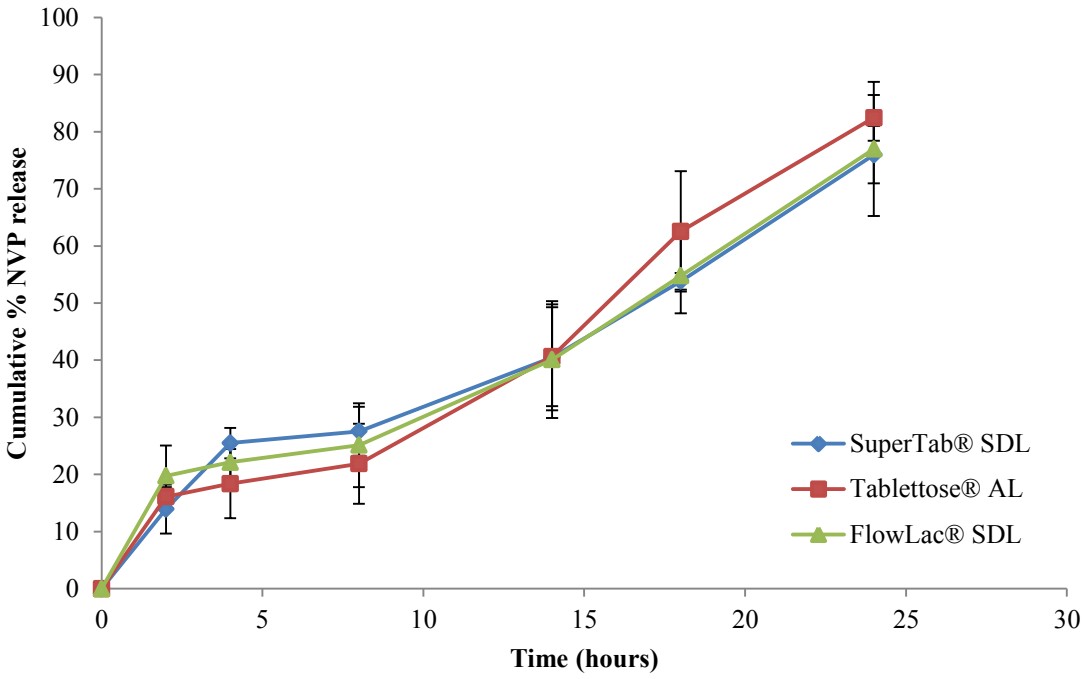

Figure 6.23. Dissolution profiles of NVP from tablets manufactured using different types of lactose (n = 6, pH = 6.8).

These observations are similar to previously reported data that indicate that the performance of tablets manufactured from granules made by extrusion granulation and high shear granulation using different grades of lactose were similar [392]. However the rate of NVP release from tablets manufactured with SuperTab® spray dried lactose was slightly slower than the rate observed for tablets manufactured using Tablettose® 100 and this may be attributed to differences in particle size of the lactose. Smaller particle sizes of SuperTab® spray dried lactose were suspected to reduce the porosity of the matrix tablets.

6.5 CONCLUSIONS

The use of statistical experimental design has become useful for the development of dosage forms. This approach permits the successful development of dosage forms with fewer experiments than the traditional "one factor at a time" approach. In this study the primary objective was to optimise a NVP sustained release tablet formulation to be manufactured as described in Chapter 5 *vide infra,* using a BBD. The BBD approach is useful as it enables a comprehensive study of quadratic interactions of the variables under investigation with fewer experiments required than when using a CCD approach.

The tablets manufactured following the optimisation process passed all Pharmacopoeial tests [345] and the dissolution profile for the NVP tablets was similar to that of Viramune® XR. These results demonstrate that optimum NVP release can be achieved using a response surface methodological approach for the development of a multi-source product. The prediction accuracy of the model was regarded as good as the difference between the predicted and the observed responses, in addition to the % P.E. were 4.07, 2.17, 0.47, 0.21, 2.47 and 1.58 % for responses Y_1, Y_2, Y_3, Y_4, Y_5 and Y_6, respectively and were all within the pre-set limit of < 5%.

Mathematical modelling was used to design the dosage form with a specific release mechanism for NVP such that it mimicked that of the reference product, Viramune® XR. The diffusion release exponent for the optimised formulation closely matched that of the reference product and is evidence that this approach can be used to design a formulation that would release NVP by a specific mechanism.

Response surface studies confirmed earlier observations that NVP release from these tablets was significantly affected by the amount of HPMC and SDL used in the formulation. The amount of MCC used did not have a significant impact on NVP release and this may in part be attributed to the low amount of this excipient used in these studies.

The behaviour of HPMC when exposed to dissolution media has been extensively studied and the polymer swells on penetration of the media and forms a gel layer around the tablet core, through which diffusion of NVP must occur. The strength and thickness of the gel layer formed has a significant effect on the rate and extent of API release from a matrix. Consequently the factors that affect gel formation and thickness will affect the rate of API dissolution. The diffusion of the medium into and out of the matrix also results in subsequent erosion of the polymer. Swelling and erosion of the polymer occur simultaneously and contribute to the release of NVP, from this matrix.

Whether it is swelling or erosion that limits API dissolution depends on the solubility of the API. Water soluble API release is limited by polymer swelling whereas for a poorly water soluble API such as NVP, polymer erosion has an impact on API release. Therefore the factors that affect swelling and erosion of the dosage forms developed in this study will have an impact on the dissolution process.

Parameters related to dissolution media that are likely to have an effect on swelling and erosion of a polymer, may include the pH and molarity of the buffer used to make the media. The swelling of HPMC was found to increase with an increase in pH of the medium and erosion was not significantly affected by a change in pH. These findings may explain the slightly higher NVP release in media of low pH as compared to that observed for media of higher pH. However, it should be noted that NVP is weakly basic and increased release of weakly basic compounds in a medium of low pH values has been reported [393]. Therefore the basic nature of NVP may have more of an effect on release in media of low pH as opposed to the effect of pH on the swelling and erosion of the matrix, since HPMC is non-ionic. An increase in the molarity of the dissolution medium resulted in slight increase in the degree of swelling and a decrease in erosion of the HPMC matrices.

The viscosity grade of HPMC had an effect on the rate of swelling and erosion of NVP with an increase in polymer molecular weight resulting in an increase in swelling and a reduction of erosion. Consequently, dissolution rate of NVP was affected by grade of HPMC with K100M and K15M releasing 42% and 63% respectively after 24 hours of exposure. A comparison of tablets from batches formulated using different polymer grades of HPMC yielded f_1 and f_2 factors that were out of specification. These findings further emphasise the significance of selecting low molecular weight HPMC grades when formulating sustained release dosage forms with sparingly soluble API molecules such as NVP.

The studies to investigate the effects of grades of MCC and types of lactose on NVP release from the matrices showed that these two excipients did not have a significant effect on NVP release. This observation was further solidified by the values for f_1 and f_2 values that were within the <15 and >50 range, respectively. However, there are some indications that the particle size of these excipients may have an effect on dissolution and must be further investigated.

Sustained release matrix tablets of NVP have been successfully developed and optimised. The NVP tablets are of high quality and exhibit NVP release that is similar to that of Viramune® XR. The optimised formulation has the potential for further development, and stability and *in vivo* bioequivalence studies would form part of the future development of this product. This formulation is relatively simple to manufacture and its use may reduce the cost of HIV therapy and enhance adherence to treatment.

CHAPTER SEVEN

CONCLUSIONS

The objectives of these studies were to develop, manufacture and assess sustained release matrix formulations of NVP. Sustained release drug delivery systems have an advantage over conventional technologies as they provide a means to deliver a constant amount of therapeutic agent to the GIT, which facilitates controlled absorption. The controlled absorption avoids large peak to trough fluctuations in plasma concentrations of an API. The formulation of a NVP sustained release delivery system may ensure predictable bioavailability and a reduction in dose dependent side effects associated with the use of this molecule. A sustained release formulation for once daily dosing would also help in improving patient convenience by reducing the frequency of dosing, which might have a positive impact on long term adherence to the medication. Therefore, the development of a generic or multisource sustained release dosage form of NVP that has similar dissolution characteristics to the commercially available sustained release product, Viramune® XR (Boehringer Ingelheim Pharmaceuticals Ltd, Ridgefield, USA) was undertaken.

An isocratic RP-HPLC method was developed and validated for the analysis of NVP in tablets and to assess the performance of the dosage forms that were developed and manufactured. The analytical method was developed and optimised using DOE and a Central Composite Design approach, a form of quadratic response surface method design was used. ANOVA was used to study the significant factors affecting the retention time and resolution factor to arrive at chromatographic conditions that would result in an appropriate separation. The quadratic model that was used to describe the relationship between input variables and output responses revealed that the retention time of NVP was significantly affected by antagonistic linear contributions of the organic solvent composition and mobile phase flow rate, linear interactions between organic solvent concentration and flow rate, in addition to antagonistic quadratic contributions of the organic solvent and flow rate. ANOVA showed that the resolution factor was affected by the antagonistic linear contributions of the organic solvent concentration, column temperature, linear interactions between organic solvent content and temperature, linear interactions between organic solvent concentration and flow rate, in addition to antagonistic quadratic contributions of the organic solvent content, column temperature and flow rate. The relationships established, were confirmed by response surface plots, *viz.,* contour and 3-dimensional plots. Optimum chromatographic conditions were

selected based on desirability and the experimental model used to predict output variables was found to be precise with % P.E. of 6.98 and 3.0 % for the retention time of NVP and resolution factor, respectively. The optimised method was validated using ICH guidelines and was found to be selective, sensitive, precise and accurate for use in the assessment of NVP dosage forms. Stability indicating studies did not produce any degradation peaks, however NVP was found to degrade in 30 % v/v H_2O_2 (11.72%), 0.1 M HCl (7.11%), and 0.1 M NaOH (4.83%) after 8 hours of refluxing at 90 °C. NVP was stable under neutral hydrolytic conditions at 90 °C in addition to exposure to light of 500 w/m^2 at 27 °C for 8 hours.

A dissolution method for NVP SR dosage forms based on USP Apparatus 3 was developed and validated. USP Apparatus 3 has an advantage with regard to the ease with which media change can be achieved and readily allows for simulation of the GIT pH environment, compared to the commonly used USP Apparatus 1 and 2 where change of media during dissolution testing is tedious and time consuming. The exposure of dosage forms to fresh dissolution media of different pH at predetermined times, prevents saturation conditions being attained and enables better discrimination between API release from dosage forms of different composition. USP Apparatus 3 is also suitable for dosage forms containing poorly water soluble API such as NVP. The dissolution method was developed by assessing the factors that affect NVP dissolution from Viramune® XR. The conditions investigated included agitation rate, mesh size, buffer molarity and surfactant addition. The effects of these factors on NVP release were studied and the dissolution profiles generated were compared using the FDA recommended model independent method for curve comparison by use of the difference (f_1) and similarity (f_2) factors. Different reciprocating rates of USP Apparatus 3 were tested to establish the effect of agitation rate on NVP release and to determine what rate would produce an equivalent response to that observed when NVP tablets were tested using USP Apparatus 2 at 50 rpm. A low reciprocation rate of 5 – 10 dpm was found to produce dissolution profiles that were similar to the dissolution profiles generated using USP Apparatus 2 set at 50 rpm. Furthermore, at these dip rates the dissolution method permitted discrimination of the responses which was not possible when a high agitation rate was used. Close investigation of the data revealed that a reciprocation rate of 8 dpm produced a NVP dissolution profile that was closely related to the profile generated using USP Apparatus 2 and therefore, all dissolution studies were performed at a reciprocation rate of 8 dpm. NVP release increased with an increase in mesh screen pore size but was not significant. An increase in the molarity of the dissolution medium was found to

increase the rate of NVP release slightly. However, for each of the molarities tested the percent NVP released was above 85 %. Increasing the amount of SLS in the dissolution medium resulted in an increase in the dissolution rate of the NVP from the tablets. The dissolution method was validated using ICH guidelines and was found to be precise, accurate and discriminatory for dissolution testing of NVP tablets. ANOVA single factor analysis at $\alpha = 0.05$ for the stability of NVP in 50 mM phosphate buffer of pH 1.6, 4.7 and 7.2 stored at 2 - 8 °C, 22 °C and 37 °C, as well as % recovery of NVP in 50 mM phosphate buffer of pH 1.6, 3.4, 4.7, 6.8 and 7.2 stored at the same temperatures, revealed that NVP was stable for 48 hours for all conditions, indicating that dissolution samples could be stored for that duration in the dissolution medium, prior to analysis.

Preformulation studies that were undertaken included an assessment of particle size and shape of NVP and excipients, powder flow and compressibility assessment of individual powders and blends, TGA and DSC analysis in addition to FT-IR spectroscopy. TGA analysis revealed that NVP is stable up to a temperature of approximately 244 °C after which almost complete decomposition of the compound (> 90%) occurs at 250 °C, which is also the melting point of NVP. The results observed suggest that it is unlikely that NVP would decompose under normal tableting and storage conditions during which temperatures rarely exceed 100 °C.

DSC thermograms revealed no significant shifts in the melting point of NVP when it was combined with excipients that were to be used for tablet manufacture. Furthermore FT-IR did not reveal any significant shifts in the absorption bands of NVP in the presence of the excipients. Therefore it was concluded that the excipients that were selected for use would facilitate the production of a NVP dosage form for which dissolution and stability would unlikely be affected by incompatibility reactions. However, long term stability studies must be undertaken to ensure that this is indeed, the case.

The results of particle size and shape analysis indicated that there was a possibility of poor flow which may result in the production of tablets of inadequate quality. Screening of powder blends with a sieve of an appropriate size was considered necessary as this would facilitate the production of powder blends of uniform particle size distribution in addition to an improvement in powder flow properties. The flow properties of the powder blends for all the batches produced during formulation development studies were within acceptable limits, and although some powder blends had values of AOR, HR and CI slightly above the optimum

levels these studies revealed that the powder blends were suitable for use in a direct compression tableting process and was likely to produce tablets of with acceptable quality attributes.

All batches of tablets manufactured in these studies were produced by direct compression. Preliminary formulations were developed using different proportions of polymers and diluent to identify a suitable polymer or combination thereof that would produce a dissolution profile that was similar to that of Viramune® XR. Tablets manufactured using HPMC as a rate retarding polymer showed more consistent modulation of NVP release at the time points used for dissolution testing when compared to tablets manufactured using combinations of HPMC and Carbopol® 71G NF or Eudragit® RSPO. Therefore HPMC based matrix tablets were selected for further development and optimisation.

A Box-Behnken Design was used for the optimisation process as it has been shown to be slightly more effective than the commonly used Central Composite Design approach. Three formulation variables that were considered critical included the amount of HPMC, lactose and MCC used. The responses that were monitored were the amount of NVP released at 2 h in order to ensure dose dumping had been controlled, 8 h and 14 h to facilitate a study of the release kinetics of NVP and 24 h to establish the total amount of NVP released. Other responses that were monitored included the Korsmeyer-Peppas diffusion exponent, n and f_1 and f_2 values. The diffusion exponent was used as it permits an assessment of the overall mechanism of NVP release from these dosage forms. All responses were constrained to ensure that they met specifications that had been established during preliminary formulation development studies. The tablets passed Pharmacopoeial tests for content uniformity, assay, weight variation and friability indicating that the manufacturing process was suitable to produce a product with good quality attributes.

The responses generated during Box-Behnken design experiments were then analysed using Design-Expert® software. The data were fitted to different statistical models to determine which model was best able to describe the relationship between the input variables and responses observed. The interactions of the terms of the model for excipients were studied and the significant factors affecting the responses observed were determined. The relationship(s) established between the input variables and the output responses were used to identify an optimal formulation composition.

ANOVA revealed that drug release at 2 h was significantly affected by the antagonistic linear contribution of HPMC, with an increase in the amount of HPMC resulting in a decrease in amount of NVP released. Increasing the amount of lactose in the formulation resulted in an increase in the amount of NVP released, however, this effect was only significant after 8 h of dissolution testing with the model showing a synergistic linear contribution of lactose in addition to an antagonistic linear contribution of HPMC at 8 h. NVP release at 14 h was significantly affected by antagonistic linear contributions of HPMC and synergistic linear interactions between HPMC and lactose content. No single factor was significant for the amount of NVP released at 24 h and this was thought to be a consequence of the hydrodynamic forces the dosage form was exposed to having a greater effect on NVP release than formulation variables during the latter stages of dissolution testing. The ratio of HPMC to lactose used was found to be the most significant factor affecting the value for f_2. This implied that the formulation composition to be used to produce a dosage from with a dissolution profile similar to that of Viramune® XR could be achieved by alteration of the amounts of HMPC and lactose used in the formulation. The overall mechanism of drug release determined by evaluation of the Korsmeyer-Peppas diffusion exponent was also significantly affected by the amount of HPMC used to manufacture the NVP tablets.

The prediction accuracy of the statistical methods used in the optimisation process was assessed by manufacturing three batches of the optimised formulation and comparing the predicted and observed responses for these batches. The method was judged to be precise with a % P. E of 4.07% for Y_1, 4.17% for Y_2, 0.47% for Y_3, 0.21% for Y_4, 2.47% for Y_5 and 1.58% for Y_6 obtained with batch NVP032. The % P.E for batches NVP030 and NVP031 were also within acceptable limits. Therefore use of the Box-Behnken approach and the optimisation method were adequate for the design of sustained release NVP matrix tablets.

Fitting of the dissolution data from NVP tablets manufactured using the Box-Behnken design approach to different kinetic models revealed that drug release from most batches followed the Korsmeyer-Peppas and Higuchi models indicating that diffusion was the predominant mechanism of NVP release from the tablets. Further inspection of the R^2 values from these data revealed that the correlation to the Hixson-Crowell model was also high suggesting that there may have been a significant change in the surface area of the matrix tablets that can be attributed to swelling and constant erosion of these matrices that may impact NVP release.

The dissolution data generated for the optimised formulation were fitted to the 'power law' as described by Peppas *et al.,* in order to describe NVP release for the entire dissolution profile and the observed value for *n* suggests that an anomalous mechanism is best used to describe NVP release. Consequently diffusion, polymer swelling and relaxation in addition to erosion all contributed to the release of NVP observed for these tablets.

The objective to use NVP release kinetics to design SR matrix tablets of NVP that would have release kinetics similar to that of Viramune® XR was achieved. The overall mechanism of NVP release based on Korsmeyer-Peppas exponent value *n* of the two formulations were similar, *viz.,* 0.9644 and 0.9753 for the optimised formulation and Viramune® XR tablets, respectively. Inspection of the R^2 values for other kinetic models also showed that the release kinetics of NVP from the two formulations were almost similar.

A comparison of the dissolution profiles for the optimised formulation and Viramune XR tablets revealed that the dissolution profiles were similar, with f_1 and f_2 values falling within the limits of < 15 for f_1 and > 50 f_2. The similarity in *in vitro* release characteristics of the two products also suggests that the two formulations may be bioequivalent since NVP is BCS Class II compound, for which dissolution is the rate limiting step for absorption.

Water uptake and erosion studies were undertaken to assess the swelling and erosion characteristics of the optimised formulation. The factors that were likely to affect swelling and erosion of the tablets were investigated. An increase in pH of the media resulted in an increase in swelling of the matrix tablets whereas an increase in the molarity resulted in a decrease in tablet swelling which has been attributed to 'salting out' effect of polymer by inorganic ions in the medium. Erosion of the tablet matrices was not significantly affected by a change in pH which was attributed to the non-ionic nature of HPMC. However, an increase in molarity resulted in a decrease in erosion which was attributed to an increase in the amount of phosphate ions competing for water of hydration and reducing the amount of water entering or leaving the matrix system.

A study of the effect of HPMC grade on NVP release revealed that an increase in the viscosity of the polymer grade used, had a negative impact on NVP release from the tablets. This was confirmed by evaluation of the values for f_1 and f_2 derived following evaluation of the dissolution profiles of tablets containing Methocel® K4M, K15M and K100M. An assessment of the effect of HPMC grade on swelling and erosion characteristics revealed that the degree of swelling increased with higher viscosity grades of HPMC whereas erosion

decreased. The decrease in the extent of erosion provides a basis for explaining the decrease in NVP release as erosion of a hydrophilic matrix is crucial for the release of a sparingly soluble API such as NVP.

The grade of MCC and type of lactose type did not appear to have a significant effect of the release of NVP from the manufactured tablets. However the results suggest that the particle size of MCC and lactose might have an effect on NVP release with increased release rates for larger particle sizes of excipients observed from subtle differences in the dissolution profiles generated from dosage forms that were produced with diluents of different particle size.

Sustained release matrix tablets of NVP have been successfully developed, manufactured and optimised. The availability of a generic drug delivery system of NVP will reduce the cost of chronic therapy in addition to possibly improving patient adherence to therapy.

Further development and assessment of the NVP sustained release tablets produced in these studies are required. Additional studies will establish whether further enhancement of the *in vitro* performance of the technology, such as releasing NVP *via* a zero-order process is possible. Further development studies of the technology would necessarily include an assessment of stability of the technology in order to establish long term stability and a shelf life for the optimised formulation. Thereafter scale-up manufacture and *in vivo* studies can be undertaken prior to commercialisation of this product.

REFERENCES

1. WHO/UNAIDS/UNICEF. Global HIV/AIDS Response: Epidemic Update and Health Sector Progress towards Universal Access 2011. http://www.who.int/hiv/pub/progress_report2011/en/index.html. Accessed11/02/2012.

2. Kaiser Family Foundation/UNAIDS. Report on the Global AIDS Epidemic. Statistics: Worldwide 2011. http://www.thebodypro.com/index/whatis/global_statistics.html. Accessed 11/02/2012.

3. E. Ojewole, I. Mackraj, P. Naidoo and T. Govender. Exploring the use of Novel Drug Delivery Systems for Antiretrovial Drugs. *European Journal of Pharmaceutics and Biopharmaceutics*, Vol. 70, No. 3, 2008, pp. 697-710.

4. K.V. Allam, G. P. Kumar, V. Cheruku, A. Jannu and C. K. Bairi. Controlled and Sustained Release Approaches in Developing Suitable Dosage Forms for the Antiretroviral Drug Lamivudine. *International Journal of Pharmaceutical Sciences Review and Research*, Vol. 8, No. 1, 2011, pp. 21-27.

5. R. Mondol, S. Paul, S. Ray and S. Maiti. Polymeric Nanocarriers: A Promising Research Avenue for the Delivery of Anti-HIV Drugs. *International Journal of Applied Pharmaceutics*, Vol. 2, No. 2, 2010, pp. 1-5.

6. Boehringer Ingelheim International. Viramune Summary of Product Characteristics. 2001. http://www.rxlist.com/viramune-drug.htm. Accessed 12/012/2012.

7. British Pharmacopoeia Commission Office, *British Pharmacopoeia*, London, 2002, Vol. 2, Pg. 1530.

8. C. Flexner. Antiretroviral Agents and Treatment of HIV infection. In Goodman & Gilman (Editor), *Goodman & Gilman's The Pharmacological Basis of Therapeutics*. New York, McGraw-Hill, 2011.

9. A. Datta, N. S. Ghosh, S. Ghosh, T. Samanta and R. C. Das. Enhancement of Solubility and Dissolution Profile of Nevirapine by Solid Dispersion Technique. *International Journal of Chemistry Research*, Vol. 2, No. 3, 2011, pp. 53-58.

10. K. M. Lokamatha, S. S. M. Kumar and R. N. Rama. Enhancement of Solubility and Dissolution Rate of Nevirapine by Solid Dispersion Technique using Dextran: Preparation and *In Vitro* Evaluation. *International Journal of Pharmaceutical Research and Development-Online*, Vol. 2, No. 12, 2011, pp. 1-8.

11. M. Sarkar, O. P. Perumal and R. Panchangnula. Solid-State Characterisation of Nevirapine. *Indian Journal of Pharmaceutical Sciences*, Vol. 70, No. 5, 2008, pp. 619-630.

12. C. H. R. Prasada, J. V. L. N. R. Seshagiri, K. Ashok, K. R. Mallikarjuna and G. A. Lakshmi. Simple Spectrophotometric Estimation of Nevirapine in Bulk Drug and Tablet Formulation. *The Journal of Pharmacy*, Vol. 1, No. 2, 2011, pp. 1-3.

13. V. Amudhavalli and K. S. Lakshmi. Derivative Spectrophotometric Estimation of Nevirapine in Pharmaceutical Dosage Forms. *Journal of Chemical and Pharmaceutical Research*, Vol. 2, No. 5, 2010, pp. 502-505.

14. S. Macha, C. Yong, T. Darrington, M. S. Davies, T. R. MacGregor, M. Castles and S. L. Krill. *In Vitro - In Vivo* Correlation of Nevirapine Extended Release Tablets. *Biopharmaceutics and Drug Disposition*, Vol. 30, No. 9, 2009, pp. 542-550.

15. *United States Pharmacopoeia Incorporating "The national Formulary 29."* United States Pharmacopoeial Convention, Maryland, USA, 34th Edition, Vol. 3, 2011, pp. 3645-3649.

16. B. R. Ahire, B. R. Rane, S. R. Bakliwal and S. P. Pawar. Solubility Enhancement of Poorly Water Soluble Drug by Solid Dispersion Techniques. *International Journal of Pharmaceutical Technology Research*, Vol. 2, No. 3, 2010, pp. 2007-2015.

17. N. A. Kasim, M. Whitehouse, C. Ramachandran, M. Bermejo, H. Lennernas, A. S. Hussain, H. E. Junginger, S. A. Stavchansky, K. K. Midha, V. P. Shah, G. L. Amidon. Molecular Properties of WHO Essential Drugs and Provisional Biopharmaceutical Classification. *Molecular Pharmacology*, Vol. 1, No. 1, 2004, pp. 85-96.

18. J. W. Pav, L. S. Rowland and D. J. Korpalski. HPLC-UV Method for the Quantitation of Nevirapine in Biological Matrices following Solid Phase Extraction. *Journal of Pharmaceutical and Biomedical Analysis*, Vol. 20, No. 1 and 2, 1999, pp. 91-98.

19. R. M. F. Hollanders, E.W.J van Ewijk-Beneken Kolmer, D. M. Burger, E. W. Wuis, P. P. Koopmans, and Y. A. Hekster. Determination of Nevirapine, an HIV-1 Non-Nucleoside Reverse Transcriptase Inhibitor, in Human Plasma by Reversed-Phase High-Performance Liquid Chromatography. *Journal of Chromatography B: Biomedical Sciences and Applications,* Vol. 744, No. 1, 2000, pp. 65-71.

20. B. S. Kappelhoff, H. Rosing, A. D. R. Huitema and J. H. Beijnen. Simple and Rapid Method for the Simultaneous Determination of the Non-Nucleoside Reverse Transcriptase Inhibitors Efavirenz and Nevirapine in Human Plasma using Liquid Chromatography. *Journal of Chromatography B*, Vol. 792, 2003, pp. 353-362.

21. R. P. G van Heeswijk, R. M. W. Hoetelmans, P. L. Meenhorst, J. W. Mulder, and J. H. Beijnen. Rapid Determination of Nevirapine in Human Plasma by Ion-Pair Reversed-Phase High Performance Liquid Chromatography with Ultraviolet Detection. *Journal of Chromatography B: Biomedical Sciences and Applications*, Vol. 713, No. 2, 1998, pp. 395-399.

22. V. Kabra, V. Agrahari, C. Karthikeyan and P. Trivedi. Simultaneous Quantitative Determination of Zidovudine and Nevirapine in Human Plasma using Isocratic Reversed-Phase High Performance Liquid Chromatography. *Tropical Journal of Pharmaceutical Research*, Vol. 8, No. 1, 2009, pp. 79-86.

23. N. Kaul, H. Agrawal, A. R. Paradkar and K. R. Mahadik. Effect of System Variables Involved in Packed Column SFC of Nevirapine as Model Analyte using Response Surface Methodology: Application to Retention Thermodynamics, Solute Transfer

Kinetic Study and Binary Diffusion Coefficient Determination. *Journal of Biochemical and Biophysical Methods*, Vol. 64, No. 2, 2005, pp. 121-141.

24. European Medicines Agency. CHMP Assessment Report for Nevirapine Teva. 2009, http://www.ema.europa.eu/docs/en_GB/document_library/EPAR-Public_assessment_report/human/001119/WC500041901.pdf. Accessed 15/02/2012.

25. L. A. Z. Filho, C. R. Galdez, C. A. Silva, M. F. M. Tavares, D. M. Costa, and M. S. Aurora-Prado. Development and Validation of a Simple and Rapid Capillary Zone Electrophoresis Method for Determination of NNRTI Nevirapine in Pharmaceutical Formulations. *Journal of the Brazilian Chemical Society*, Vol. 22, No. 10, 2011, pp. 2005-2012.

26. Ch. Dharmaraju, P. Hiranmayi, K. V. Himavani, R. Mishra and J. S. Srinivas. Spectrophotometric Determination of Nevirapine in Bulk Drugs and its Forced Degradation Studies. *Journal of Pharmacy Research*, Vol. 4, No. 9, 2011, pp. 2910-2912.

27. Q. C. Li, T. Tougas, K. Cohen, R. Lee, P. Meagan, M. Corson, T. Muchnick. Validation of a High Performance Liquid Chromatography Method for the Assay of and Determination of Related Organic Impurities in Nevirapine Drug Substance. *Journal of Chromatographic Science*, Vol. 38, No. 6, 2000, pp. 246-254.

28. B. G. Pereira, F. D. Fonte-Boa, J. A. L. C. Resende, C. B. Pinheiro, N. G. Fernandes, M. I. Yoshida and C. D. Vianna-Soares. Pseudopolymorphs and Intrinsic Dissolution of Nevirapine. *Crystal Growth and Design*, Vol. **7,** No. 10, 2007, pp. 2016-2023.

29. R. F. Boswell, B. F. Gupton and Y. S. Lo. Method for Making Nevirapine: United States Patent 6680383. Boehringer Ingelheim Chemicals, Inc Petersburg VA, 2004.

30. M. Lv and H. Xu. Dipyridodiazepinone Analogs as Human Immunodeficiency Virus Type 1 Specific Non-Nucleoside Reverse Transcriptase Inhibitors: An Overview. *Current Medicinal Chemistry*, Vol. 17, No. 18, 2010, pp. 1874-1898.

31. R. L. LaFemina and American Society for Microbiology. *Antiviral Research: Strategies in Antiviral Drug Discovery*. ASM Press, 2009, pp. 35-49.

32. M-P.de Bethune. Non-nucleoside Reverse Transcriptase Inhibitors (NNRTIs), their Discovery, Development, and Use in the Treatment of HIV-1 Infection: A Review of the Last 20 years (1989–2009). *Antiviral Research*, Vol. 85, No. 1, 2010, pp. 75-90.

33. E. Arrive, M. L. Newell, D. K. Ekouevi, R. Thiebaut, B. Masquelier, V. Leroy, P. V. Perre, C. Rouzioux, F. Dabis and Gent Group on HIV in Women and Children. Prevalence of Resistance to Nevirapine in Mothers and Children after Single-Dose Exposure to Prevent Vertical Transmission of HIV-1: A Meta-Analysis. *International Journal of Epidemiology*, Vol. 36, No. 5, 2007, pp. 1009-1021.

34. J. W. Mellors and J. Y. Chow. Single-Dose Nevirapine to Prevent Mother-to-Child Transmission of HIV Type 1: Balancing the Benefits and Risks. *Clinical Infectious Diseases*, Vol. 48, No. 4, 2009, pp. 473-475.

35. C. Y. Chang and T. D. Schiano. Review Article: Drug Hepatotoxicity. *Alimentary Pharmacology & Therapeutics,* Vol. 25, No. 10, 2007, pp.1135-1151.

36. Department of Health and Human Services. Guidelines for the Use of Antiretroviral Agents in HIV-1 Infected Adults and Adolescents. http://aidsinfo.nih.gov/contentFiles/AdultandAdolescentGL.pdf. Accessed 3/01/2013.

37. M. S. Rhee and D. J. Greenblatt. Pharmacologic Consideration for the Use of Antiretroviral Agents in the Elderly. *Journal of Clinical Pharmacology*, Vol. 48, No. 10, 2008, pp. 1212-1225.

38. I. Shah. Adverse Effects of Antiretroviral Therapy in HIV-1 Infected Children. *Journal of Tropical Paediatrics*, Vol. 52, No. 4, 2006, pp. 244-248.

39. U. Natarajan, A. Pym, C. McDonald, P. Velisetty, S. G. Edwards, P. Hay, J. Welch, A. de Ruiter, G. P. Taylor and J. Anderson. Safety of Nevirapine in Pregnancy. *HIV Medicine*, Vol. 8, No. 1, 2007, pp. 64-69.

40. J. Deepthi, A. T. Francesca., R. Rudolph, K. S. C. Robert, H. H. Michael and G. G. John. Antiviral Therapy for HIV Patients with Renal Insufficiency. *Journal of Acquired Immune Deficiency Syndromes*, Vol. 21, No. 5, 1999, pp. 384-395.

41. N. Franceschini, S. Napravnik, J. J. Eron, L. A. Szczech. Incidence and Etiology of Acute Renal Failure among Ambulatory HIV-Infected Patients. *Kidney International*, Vol. 67, No. 4, 2005, pp. 1526-1531.

42. P. J. Peters, N. Polle, C. Zeh, R. Masaba, C. B. Borkowf, B. Oyaro, P. Omolo, P. Ogindo, R. Ndivo, F. Angira, R. Lando, M. G. Fowler, P. J. Weidle, T. K. Thomas. Nevirapine-Associated Hepatotoxicity and Rash among HIV-Infected Pregnant Women in Kenya. *Journal of the International Association of Physicians in AIDS Care (JIAPAC),* Vol. 11, No. 2, 2012, pp. 142-149.

43. E. Martinez, J. L. Blanco, J. A. Arnaiz, J. B. Perez-Cuevas, A. Mocroft, A. Cruceta, M. A. Marcos, A. Milinkovic, M. A. Garcia-Viejo, J. Mallolas, X. Carne, A. Phillips and J. M. Gatell. Hepatotoxicity in HIV-1-Infected Patients Receiving Nevirapine-Containing Antiretroviral Therapy. *Journal of Acquired Immune Deficiency Syndromes,* Vol. 15, No. 10, 2001, pp. 1261-1268.

44. F. Lyons, S. Hopkins, B. Kelleher, A. McGeary, G. Sheehan, J. Geoghegan, C. Bergin, F. M. Mulcahy and P. A. McCormick. Maternal Hepatotoxicity with Nevirapine as part of Combination Antiretroviral Therapy in Pregnancy. *HIV Medicine*, Vol. **7,** No. 4, 2006, pp. 255-260.

45. H. Knobel, A. Guelar, M. Montero, A. Carmona, S. Luque, N. Berenguer and A. Gonzalez. Risk of Side Effects Associated with the Use of Nevirapine in Treatment of Naive Patients, with Respect to Gender and CD4 Cell Count. *HIV Medicine*, Vol. 9, No. 1, 2008, pp. 14-18.

46. I. Sanne, H. Mommeja-Marin, J. Hinkle, J. A. Bartlett, M. M. Lederman, G. Maartens, C. Wakeford, A. Shaw, J. Quinn, R. G. Gish and F. Rousseau. Severe Hepatotoxicity Associated with Nevirapine Use in HIV-Infected Subjects. *Journal of Infectious Diseases*, Vol. 191, No. 6, 2005, pp. 825-829.

47. P. Riska, M. Lamson, T. MacGregor, J. Sabo, S. Hattox, J. Pav and J. Keirns. Disposition and Biotransformation of Antiretroviral Drug Nevirapine in Humans. *Drug Metabolism and Disposition,* Vol. 28, No. 8, 1999, pp. 895-901.

48. D. Back, S. Gibbons and S. Khoo. Pharmacokinetic Drug Interactions with Nevirapine. *Journal of Acquired Immune Deficiency Syndromes*, Vol. 34, 2003, pp. S8-S14.

49. D. Mildvan, R. Yarrish, A. Marshak, H. W. Hutman, M. McDonough, M. Lamson, P. Robinson. Pharmacokinetic Interaction between Nevirapine and Ethinyl Estradiol/Norethindrone When Administered Concurrently to HIV-Infected Women. *Journal of Acquired Immune Deficiency Syndromes,* Vol. 29, No. 5, 2002, pp. 471-477.

50. A. E. Herve, L. Loue, and J. P. Tillement. Systemic Antifungal Agents: Drug Interactions of Clinical Significance. *Drug safety*, Vol. 18, No. 2, 1998, pp. 83-97.

51. F. L. Altice, G. H. Friedland and E. L. Cooney. Nevirapine Induced Opiate Withdrawal among Injection Drug Users with HIV Infection Receiving Methadone. *Journal of Acquired Immune Deficiency Syndromes*, Vol. 13, No. 8, 1999, pp. 957-962.

52. E. Ribera, L. Pou, R. M. Lopez, M. Crespo, V. Falco, O. Imma, I. Ruiz and A. Pahisa. Pharmacokinetic Interaction between Nevirapine and Rifampicin in HIV-Infected Patients with Tuberculosis. *Journal of Acquired Immune Deficiency Syndromes*, Vol. 28, No. 5, 2001, pp. 450-453.

53. H. McIlleron, G. Meintjes, W. J. Burman and G. Maartens. Complications of Antiretroviral Therapy in Patients with Tuberculosis: Drug Interactions, Toxicity, and Immune Reconstitution Inflammatory Syndrome. *Journal of Infectious Diseases*, Vol. 196, Supp. 1, 2007, pp. S63-S75.

54. U. S. Justesen, N. Andersen, N. A. Klitgaard NA, K. Bransen K, J. Gerstoft and C. Pedersen. Pharmacokinetic Interaction between Rifampin and the Combination of Indinavir and Low-Dose Ritonavir in HIV-Infected Patients. *Clinical Infectious Diseases*, Vol. 38, No. 3, 2004, pp. 426-429.

55. E. Ribera, C. Azuaje C, R. M. Lopez, P. Domingo, A. Curran, M. Feijoo, L. Pou, P. Sanchez, M. A. Sambeat, J. Colomer and J. L. Lopez-Colomes. Pharmacokinetic Interaction between Rifampicin and the Once-Daily Combination of Saquinavir and Low-Dose Ritonavir in HIV-Infected Patients with Tuberculosis. *Journal of Antimicrobial Chemotherapy*, Vol. 59, No. 4, 2007, pp. 690-697.

56. M. M. R. de Maat, R. M. W. Hoetelmans, R. A. A. Mathew, E. C. M. van Gorp, P. L. Meenhorst, J. W. Mulder and J. H. Beijnen. Drug interaction between St John's Wort and Nevirapine. *Acquired Immune Deficiency Syndrome*, Vol. 15, No. 3, 2001, pp. 420-421.

57. M. S. Baylor and R. Johann-Liang. Hepatotoxicity Associated With Nevirapine Use. *Journal of Acquired Immune Deficiency Syndromes,* Vol. 35, No. 5, 2004, pp. 538-539.

58. J. P. Fagot, M. Mockenhaupt, J. N. Bouwes-Bavinck, L. Naldi, C. Viboud and J. C. Roujeau. Nevirapine and the Risk of Stevens-Johnson Syndrome or Toxic Epidermal Necrolysis. *Journal of Acquired Immune Deficiency Syndromes,* Vol. 15, No. 14, 2001, pp. 1843-1848.

59. G. D. de Requena, N. Marina, J-N. Inmaculada and S. Vincen. Liver toxicity Caused by Nevirapine. *Acquired Immune Deficiency Syndrome*, Vol. 16, No. 2, 2002, pp. 290-291.

60. A. D. A. M. Rotunda. Severe Cutaneous Reactions Associated with the Use of Human Immunodeficiency Virus Medications. *Acta Dermato-Venereologica,* Vol. 83, No. 1, 2003, pp. 1-9.

61. L. Jay and G. J. Marshall. Dermatological Adverse Effects of Antiretroviral Therapy: Recognition and Management. *American Journal of Clinical Dermatology*, Vol. 8, No. 4, 2007, pp. 221-233.

62. S. M. Patel, S. Johnson, S. M. Belknap, J. Chan, B. E. Sha and C. Bennett. Serious Adverse Cutaneous and Hepatic Toxicities Associated With Nevirapine Use by Non-HIV-Infected Individuals. *Journal of Acquired Immune Deficiency Syndromes*, Vol. 35, No. 2, 2004, pp. 120-125.

63. A. Calmy, B. Hirschel, D. A. Cooper and A. Carr. A New Era of Antiretroviral Drug Toxicity. *Antiviral Therapy*, Vol. 14, No. 2, 2009, pp. 165-179.

64. M. Esteban, C. Ignacio, L. Luisa, C. Rosert and G. M. Jose. Reversion of Metabolic Abnormalities after Switching from HIV-1 Protease Inhibitors to Nevirapine. *Journal of Acquired Immune Deficiency Syndromes*, Vol. 13, No. 7, 1999, pp. 805-810.

65. V. Montessori, N. Press, M. Harris, L. Akagi and J. S. G. Montaner. Adverse Effects of Antiretroviral Therapy for HIV Infection. *Canadian Medical Association Journal*, Vol. 170, No. 2, 2004, pp. 229-238.

66. R. Subbaraman, S. K. Chaguturu, K. H. Mayer, T. P. Flanigan and N. Kumarasamy. Adverse Effects of Highly Active Antiretroviral Therapy in Developing Countries. *Clinical Infectious Diseases*, Vol. 45, No. 8, 2007, pp. 1093-1101.

67. T. E. Taha, N. Kumwenda, A. Gibbons, D. Hoover, V. Lema, S. Fiscus, J. Mukiibi, G. Liomba and R. Broadhead. Effect of HIV-1 Antiretroviral Prophylaxis on Hepatic and Hematological Parameters of African Infants. *Acquired Immune Deficiency Syndrome,* Vol. 16, No. 6, 2002, pp. 851-858.

68. R. B. Pollard, P. Robinson and K. Dransfield. Safety profile of Nevirapine, a Non-Nucleoside Reverse Transcriptase Inhibitor for the Treatment of Human Immunodeficiency Virus Infection. *Clinical Therapeutics*, Vol. 20, No. 6, 1998, pp. 1071-1092.

69. P. Reiss and M. D. de Jong. Antiviral drugs. In: *Side Effects of Drugs Annual*, J.K. Ronson (Editor), Elsevier, 1995, pp. 273-281.

70. M. S. Hirsch, H. F. Gunthard, J. M. Schapiro, F. B. Vezinet, B. Clotet, S. M. Hammer, V. A. Johnson, D. R. Kuritzkes, J. W. Mellors, D. Pillay, P. G. Yeni, D. M.

Jacobsen and D. D. Richman. Antiretroviral Drug Resistance Testing in Adult HIV-1 Infection: 2008 Recommendations of an International AIDS Society-USA Panel. *Clinical Infectious Diseases*, Vol. 47, No. 2, 2008, pp. 266-285.

71. G. Maga, M. Amacker, N. Ruel, U. Hubscher and S. Spadari. Resistance to Nevirapine of HIV-1 Reverse Transcriptase Mutants: Loss of Stabilizing Interactions and Thermodynamic or Steric Barriers are Induced by Different Single Amino Acid Substitutions. *Journal of Molecular Biology*, Vol. 274, No. 5, 1997, pp. 738-747.

72. D. D. Richman, D. Havlir, J. Corbeil, D. Looney, C. Ignacio, S. A. Spector, J. Sullivan, S. Cheeseman, K. Barringer and D. Pauletti. Nevirapine Resistance Mutations of Human Immunodeficiency Virus Type 1 Selected during Therapy. *Journal of Virology*, Vol. 68, No. 3, 1994, pp. 1660-1666.

73. J. Molto, V. Marta, M. Cristina, C. Samandhy, J. Miranda, J. R. Santos, E. Negredo, J. Vilaro, J. Costa and B. Clotet. Once- or Twice-Daily Dosing of Nevirapine in HIV-Infected Adults: A Population Pharmacokinetics Approach. *Journal of Antimicrobial Chemotherapy*, Vol. 62, No. 4, 2008, pp. 784-792.

74. A. Bardsley-Elliot and C. M. Perry. Nevirapine: A Review of its Use in the Prevention and Treatment of Paediatric HIV Infection. *Paediatric Drugs*, Vol. 2, No. 5, 2000, pp. 373-405.

75. K. Luzuriaga, Y. Bryson, G. McSherry, J. Robinson, B. Stechenberg, G. Scott, M. Lamson, S. Cort, J. L. Sullivan. Pharmacokinetics, Safety, and Activity of Nevirapine in Human Immunodeficiency Virus Type 1-Infected Children. *Journal of Infectious Diseases,* Vol. 174, No. 4, 1996, pp. 713-721.

76. S. K. Gupta, J. A. Eustace, J. A. Winston, I. I. Boydstun, T. S. Ahuja, R. A. Rodriguez, K. T Tashima, M. Roland, N. Franceschini and F. J. Palella. Guidelines for the Management of Chronic Kidney Disease in HIV-Infected Patients: Recommendations of the HIV Medicine Association of the Infectious Diseases Society of America. *Clinical Infectious Diseases*, Vol. 40, No. 11, 2005, pp. 1559-1585.

77. D. Jayasekara, F. T. Aweeka, R. Rodriguez, S. C. Kalayjian, M. H. Humphreys and J. G. Gambertoglio. Antiviral Therapy for HIV Patients with Renal Insufficiency. *Journal of Acquired Immune Deficiency Syndromes*, Vol. 21, No. 5, 1999, pp. 384-395.

78. T. Gabler, B. Yudelowitz and A. Mahomed. Overdose with HAART: Are We Managing these Patients Adequately? *South African Medical Journal*, Vol. 101, 2011, pp. 520-521.

79. M. E. Jan Wise. Neuropsychiatric Complications of Nevirapine Treatment. *British Medical Journal*, Vol. 324, pp. 879.

80. M. J. Lamson, J. P. Sabo, T. R. MacGregor, J. W. Pav, L. S. Rowland, A. Hawi, M. Cappola and P. Robinson. Single Dose Pharmacokinetics and Bioavailability of Nevirapine in Healthy Volunteers. *Biopharmaceutics & Drug Disposition*, Vol. 20, No. 6, 1999, pp. 285-291.

81. S. Macha, C. L. Yong, T. R. MacGregor, M. Castles, A. M. Quinson, N. Rouyrre, and I. Wilding. Assessment of Nevirapine Bioavailability from Targeted Sites in the Human Gastrointestinal Tract. *The Journal of Clinical Pharmacology*, Vol. 49, No. 12, 2009, pp. 1417-1425.

82. S. H. Cheeseman, S. E. Hattox, J. W. Pav, M. M. Mclaughlin, R. A. Koup, C. Andrews, C. A. Bova, T. Roy, J. L. Sullivan and J. J. Keirns. Pharmacokinetics of Nevirapine: Initial Single-Rising-Dose Study in Humans. *Antimicrobial Agents and Chemotherapy,* Vol. 37, No. 2, 1993, pp. 178-182.

83. P. F. Smith, R. Di Cenzo and G. D. Morse. Clinical Pharmacokinetics of Non-Nucleoside Reverse Transcriptase Inhibitors. *Clinical Pharmacokinetics*, Vol. 40, No. 12, 2012, pp. 893-905.

84. M. Lamson, T. MacGregor, P. Priska, D. Erickson, P. Maxfield, L. Rowland, M. Gigliotti, P. Robinson, S. Azzam and J. Keirns. Nevirapine Induces both CYP3A4 and CYP2B6 Metabolic Pathways. *Clinical Pharmacology and Therapeutics,* Vol. 65, No. 2, 1999, pp. 137.

85. D. L. Wyles, and J. G. Gerber. Antiretroviral Drug Pharmacokinetics in Hepatitis with Hepatic Dysfunction. *Clinical Infectious Diseases,* Vol. 40, No. 1, 2005, pp. 174-181.

86. I. Ofotokun, S. K. Chuck, and J. E. Hitti. Antiretroviral Pharmacokinetic Profile: A Review of Sex Differences. *Gender Medicine,* Vol. 4, No. 2, 2007, pp. 106-119.

87. M. Rotger, C. Csajka, A. Telenti. Genetic, Ethnic, and Gender Differences in the Pharmacokinetics of Antiretroviral Agents. *Gender Medicine*, Vol. 4, No. 2, 2007, pp. 106-119.

88. M. Mirochnick, D. F. Clarke, A. Dorenbaum. Nevirapine: Pharmacokinetic Considerations in Children and Pregnant Women. *Clinical Pharmacokinetics*, vol. 39**,** No. 4, 2000, pp. 281-293.

89. *Introduction to High Performance Liquid Chromatography,* R. J. Hamilton and P. A. Sewell, Chapman and Hall, London, UK, 2nd Edition, 1982, pp. 1-78.

90. *Liquid Chromatography in Pharmaceutical Development: An Introduction,* I. W. Wainer, Aster Publishing Corporation, Oregon, USA, 1995, pp. 149-175.

91. M. E. Swartz. Ultra Performance Liquid Chromatography (UPLC): An Introduction. *Separation Science Redefined*, 2005, http://www.chromatographyonline.com/lcgc/data/articlestandard/lcgc/242005/164621/article.pdf. Accessed 03/01/2013.

92. *High Performance Liquid Chromatography.* J. H. Knox, J. N. Done, A. F. Fell, A. Pryde, R. A. Wall, Edinburgh University Press, Edinburgh, Scotland, 1978, pp. 1-138.

93. *Practical Skills in Chemistry.* J. R. Dean, A. M. Jones, D. Holmes, R. Reed, J. Weyers, A. Jones, Pearson Education Ltd Publishers, Essex, UK, 2002, pp. 205-208.

94. *Pharmaceutical Analysis*. D. G. Watson, Churchill Livingstone, London, 1999, pp. 239-276.

95. *Maintaining and Troubleshooting HPLC Systems*. D. J. Rusner, New York, USA: John Wiley and Sons, New York, USA, 1981, pp. 4-95.

96. *Practical HPLC*. C. F. Simpson, Heyden and Sons Ltd (Editors), London, UK: The Whitefriars Press, London, UK, 1976, pp. 624-641.

97. *Practical HPLC Method Development*. L. R. Snyder, J. J. Kirkland, J. L. Glajch. New York, USA: John Wiley and Sons, New York, USA, 2nd Edition, 1997, pp. 3-296.

98. R. J. M. Vervoort, A. J. J. Debets, H. A. Claessens, C. A. Cramers, and G. J. de Jong. Optimisation and Characterisation of Silica-based Reversed-Phase Liquid Chromatographic Systems for the Analysis of Basic Pharmaceuticals. *Journal of Chromatography A,* Vol. 897, No. 1-2, 2000, pp. 1-22.

99. *Techniques for the Automated Optimisation of HPLC Separation*. J. C. Berridge, New York, USA: John Wiley and Sons, New York, USA, 1985, pp. 1-25.

100. *Analytical Chemistry by Open Learning: High Performance Liquid Chromatography,* S. Lindsay, John Wiley and Sons, New York, 1987, pp. 1-207.

101. T. D Wilson and D. M. Simmons. A Particle size Distribution Analysis of Used HPLC Column Packing Material. *Chromatographia,* Vol. 35, No. 5, 1993, pp. 295-301.

102. C. S. Young and R. J. Weigand. An Efficient Approach to Column Selection in HPLC Method Development. *Liquid Chromatography-Gas Chromatography North America,* Vol. 20, No. 5*,* 2002, pp. 465-473.

103. R. E. Majors. Recent Advances in High Performance Liquid Chromatography Packings and Columns. *Journal of Chromatographic Science,* Vol. 15, No. 9, 1977, pp. 334-351.

104. J. J. Kirkland. HPLC Method Development: Practical Aspects of Increasing Analysis Speed While Maintaining Separation Resolution. *Journal of Chromatographic Science,* Vol. 31, No. 12, 1993, pp. 493-497.

105. J. Kohler and J. J. Kirkland. Improved Silica-based Column Packings for High-Performance Liquid Chromatography. *Journal of Chromatography A,* Vol. 385, No. 1-2, 1987, pp. 125-150.

106. H. A. Claessens, M. A. van Straten and J. J. Kirkland. Effect of Buffers on Silica-based Column Stability in Reversed-Phase High-Performance Liquid Chromatography. *Journal of Chromatography A,* Vol. 728, No. 1-2, 1996, pp. 259-270.

107. J. J. Kirkland, J. W. Henderson, J. J. De Stefano, M. A. van Straten and H. A. Claessens. Stability of Silica-based, End-capped Columns with pH 7 and 11 Mobile Phases for Reversed-Phase High-Performance Liquid Chromatography. *Journal of Chromatography A,* Vol. 762, No. 1-2, 1997, pp. 97-112.

108. J. D. Sunseri, W. T. Cooper and J. G. Dorsey. Reducing Residual Silanol Interactions in Reversed-Phase Liquid Chromatography: Thermal treatment of Silica before Derivatization. *Journal of Chromatography A,* Vol. 1011, No. 1-2, 2003, pp. 23-29.

109. R. Kaliszan, M. P. Marszall, M. J. Markuszewski, T. Baczek and J. Pernak. Suppression of Deleterious Effects of Free Silanols in Liquid Chromatography by Imidazolium Tetrafluoborate Ionic Liquids. *Journal of Chromatography A,* Vol. 1030, No. 1-2, 2004, pp. 263-271.

110. J. Kohler, D. B. Chase, R. D. Farlee, A. J. Vega and J. J. Kirkland. Comprehensive Characterisation of some Silica-based Stationary Phase for High-Performance Liquid Chromatography. *Journal of Chromatography A,* Vol. 352, No. 1-2, 1986, pp. 275-305.

111. A. Tchapla, S. Heron., E. Lesellier and H. Colin. General View of Molecular Interaction Mechanisms in Reversed-Phase Liquid Chromatography. *Journal of Chromatography A,* Vol. 656, No. 1-2, 1993, pp. 81-112.

112. M. Ringo and C. Evans. Effect of Mobile Phase Composition on Pressure Induced Shifts in Solute Retention for LC Separations Using α- cyclodextrin Stationary Phase. *Journal of Microcolumn Separations,* Vol. 10, No. 8, 1998, pp. 647-652.

113. T. Wilson. Liquid Chromatographic Methods Validation for Pharmaceutical Products. *Journal of Pharmaceutical and Biomedical Analysis,* Vol. 8, No. 5, 1990, pp. 389-400.

114. N. Torrealday, L. Gonzalez, R. M. Alonso, R. M. Jiminez and E. O. Lastra. Experimental Design Approach for the Optimisation of a HPLC-Fluorimetric Method for the Quantitation of Angiotensin II Receptor Antagonist Telmisartan in Urine. *Journal of Pharmaceutical and Biomedical Analysis,* Vol. 32, No. 4-5, 2003, pp. 847-857.

115. S. M. M. Khamanga, R. B. Walker. The Use of Experimental Design in the Development of an HPLC-ECD Method for the Analysis of Captopril. *Talanta*, Vol. 83, No. 3, 2011, pp. 1037-1049.

116. V. Morris, J. Hughes and P. Marriott. Spherical Coordinate Representations of Solvent Composition for Liquid Chromatography Method Development Using Experimental Design. *Journal of Chromatography A,* Vol. 1008, No. 1-2, 2003, pp. 43-56.

117. W. J. Hill, W. G. Hunter. A Review of Response Surface Methodology: A Literature Survey. *Technometrics,* Vol. 8, No. 4, 1966, pp. 571-590.

118. A. I. Khuri and S. Mukhopadhyay. Response Surface Methodology. *Wiley Interdisciplinary Reviews*: *Computational Statistics*, Vol. 2, No. 2, 2010, pp. 128-149.

119. *Response Surface Methodology: Process and Product Optimisation Using Designed Experiments,* R. H. Myers, D. C. Montgomery and C. M. Anderson-Cook, John Wiley and Sons, New York, USA, 2009, pp. 1-600.

120. A. B. Eldin, A. A. Shalaby and M. El-Tohamy. Development and Validation of a HPLC Method for the Determination of Montelukast and its Degradation Products in Pharmaceutical Formulation using an Experimental Design. *Acta Pharmaceutica Sciencia,* Vol. 53, 2011, pp. 45-56.

121. E. Cagigal, L. Gonzalez, R. M. Alonso and R. M. Jiminez. Experimental Design Methodologies to Optimise the Spectroflourimetic Determination of Losartan and Valsartan in Human Urine. *Talanta,* Vol. 54, No. 6, 2001, pp. 1121-1133.

122. G. Iriarte, N. Ferreiros, I. Ibarrondo, R. M. Alonso, M. I. Maguregi and L. Gonzalez. Optimisation via Experimental Design of an SPE-HPLC-UV-Flourescence Method for the Determination of Valsartan and its Metabolite in Human Plasma Samples. *Journal of Separation Science,* Vol. 29, No. 15, 2006, pp. 2265-2283.

123. L. M. Osborne and T. W. Miyakawa. Use of Experimental Design in the Optimisation of HPLC Methodology for the Separation of Stereoisomers. *Journal of Liquid Chromatography and Related Technologies,* Vol. 20, No. 4, 1997, pp. 501-509.

124. M. Kiendrebeogo, L. Choisnard, C. E. Lamien, A. Meda, D. Wouessidjewe and O. G. Nacoulma. Experimental Design Optimisation for Screening Relevant Free Phenolic Acids from Various Preparations used in Burkina Faso Folk Medicine. *The African Journal of Traditional, Complementary and Alternative Medicine,* Vol. 3, No. 1, 2006, pp. 115-128.

125. P. Barmpalexis, F. I. Kanaze, E. Georgarakis. Developing and Optimising a Validated Iscocratic Reversed-Phase High-Performance Liquid Chromatography Separation of Nimodipine and Impurities in Tablets Using Experimental Design Methodology. *Journal of Pharmaceutical and Biomedical Analysis,* Vol. 49, No. 5, 2009, pp. 1192-1202.

126. D. B. Hibbert. Experimental Design in Chromatography: A Tutorial Review. *Journal of Chromatography B,* Vol. 910, No. 1, 2012, pp. 2-13.

127. C. H. V. Kumar, D. A. Kumar and J. V. L. N. R. Seshagiri. A New Validated RP-HPLC Method for The Determination of Nevirapine in Human Plasma. *E-Journal of Chemistry,* Vol. 7, No. 3, 2010, pp. 821-826.

128. P. D. Hamrapurkar, M. D. Phale and N. Shah. Quantitative Estimation of Nevirapine by High Performance Thin Layer Chromatography. *Journal of Pharmaceutical Research and Health Care,* Vol. 1. No. 2, 2009, pp. 197-216.

129. P. D. Hamrapurkar, M. D. Phale, P. Patil and N. Shah. Determination of Nevirapine in Human Plasma by High Performance Liquid Chromatography with Ultraviolet Detection. *International Journal of PharmTech Research,* Vol. 2, No. 2, 2010, pp. 1316-1324.

130. P. Mohanraji, D. K.Sarkar, T. Chouldhury and K. Gauthaman. A simple and Rapid RP-HPLC Method for the Estimation of Nevirapine in Bulk and Pharmaceutical Dosage Forms. *E-Journal of Chemistry,* Vol. 5. No. S2, 2008, pp. 1081-1086.

131. E. Dailly, L. Thomas, M. F. Kergueris, P. Jolliet, M. Bourin. High-Performance Liquid Chromatographic Assay to Determine the Plasma Levels of HIV-protease

Inhibitors (Amprenavir, Indinavir, Nelfinavir, Ritonavir and Saquinavir) and the Non-Nucleoside Reverse Transcriptase Inhibitor (Nevirapine) after Liquid–Liquid Extraction. *Journal of Chromatography B,* Vol. 758, No. 2, 2001, pp. 129-135.

132. M. Vogel, N. Bertram, J. C. Wasmuth, J. Emmelkamp, J. K. Rockstroh and C. Reichel. Determination of Nevirapine in Plasma by GC-MC. *Journal of Chromatographic Science,* Vol. 48, No. 2, 2010, pp. 91-94.

133. P. Langmann, D. Schirmer, T. Vath, S. Desch, M. Zilly, H. Klinker. Rapid Determination of Nevirapine in Human Plasma by Gas Chromatography. *Journal of Chromatography B, Analytical Technologies in the Biomedical and Life Sciences,* Vol. 767, No. 1, 2002, pp. 69-74.

134. C. F. Silverthorn and T. L. Parsons. A Validated New Method for Nevirapine Quantitation in Human Plasma via High Performance Liquid Chromatography. *Biomedical Chromatography,* Vol. 20, No. 1, 2006, pp. 23-27.

135. P. C. H. Rao, K. P. Channabasavaraj and L. G. Aswini. Development and Validation of RP-HPLC Method for the Estimation of Nevirapine in Bulk Drug and Tablets. *Journal of Pharmaceutical Sciences and Research,* Vol. 1, No. 2, 2009, pp. 78-82.

136. P. P. Manisha, B. V. Dhiraj, K. L. Ashish, J. P. Sapna and Y. G. Pramod. Simultaneous Determination of Lamivudine, Stavudine and Nevirapine in Combined Dosage form by RP- HPLC. *International Research Journal of Pharmacy,* Vol. 2, No. 4, 2011, pp. 169-176.

137. P. Rohini, I. Madhusudhanareddy, A. Gupta, V. B. Lokeswara and G. Sudharani. Method Development and Validation for Estimation of Nevirapine from Tablets by RP-HPLC. *International Journal of Pharmacy,* Vol. 1, No. 1, 2011, pp. 29-33.

138. T. L. Laurito, V. Santagada, G. Caliendo, C. H. Oliveira, R. E. Barrientos-Astigarraga and G. De Nucci. Nevirapine Quantification in Human Plasma by HPLC Coupled to Electrospray Tandem Mass Spectrometry: Application to Bioequivalence Study. *Journal of Mass Spectrometry,* Vol. 37, No. 4, 2002, pp. 434-441.

139. J. Lindholm, M. Johansson, T. Foenstedt. Guidelines for Analytical Method Development and Validation of Biotechnological Synthesis of Drugs Production of a Hydroxyprogesterone as Model. *Journal of Chromatography B,* Vol. 791, No. 1-2, 2003, pp. 323-336.

140. K. Hammarstrand. Internal Standard in Gas Chromatography. *Varian Instrument Applications,* Vol. 10. No. 1, 1976, pp. 10-11.

141. F. Vanhaecke, H. Vanhoe, R. Dams and C. Vandecasteele. The Use of Internal Standards in ICP-MS. *Talanta,* Vol. 39. No. 7, 1992, pp. 737-742.

142. K. Kuo, R. Still, S. Cale, I. McDowell. Standardisation (External and Internal) of HPLC Assay for Plasma Homocysteine. *Clinical Chemistry,* Vol. 43, No. 9, 1997, pp. 1653-1655.

143. K. Worbel, G. Cruz-Jiminez and F. Ngulo-Romelo. Application of Internal Standard for Micro-Extraction-Spectrophotometric Determination of Copper in Serum and in Natural Waters. *Analytica Chimica Acta,* Vol. 387, No. 2, 1999, pp. 17-224.

144. Y. Vander Heyden, A. Nijhuis, J. Smeyers-Verbeke, B. G. M. Vandeginste and D. L. Massart. Guidance for Robustness/Ruggedness Tests in Method Validation. *Journal of Pharmaceutical and Biomedical Analysis,* Vol. 24, No. 5-6, 2001, pp. 723-753.

145. E. L. Inman, J. K. Frischmann, P. J. Jimenez, G. D. Winkel, M. L. Persinger and B. S. Rutherford. General Method Validation Guidelines for Pharmaceutical Samples. *Journal of Chromatography Science*, Vol. 25, No. 6, 1987, pp.252-256.

146. J. M. Green. Peer Reviewed: A Practical Guide to Analytical Method Validation. *Analytical Chemistry,* Vol. 68, No. 9, 1996, pp. 305A-309A.

147. International Conference on Harmonisation. ICH Harmonised Tripartite Guidelines: Validation of Analytical Methods, Definitions and Terminology. *ICH Topic Q 2 A*, London, 1995.

148. US Department of Health and Human Services, Food and Drug Administration, Center for Drug Evaluation and Research, Center for Veterinary Medicine. Guidance for Industry: Bioanalytical Methods Validation. Rockville, 2001.

149. G. A. Shabir. Validation of High Performance Liquid Chromatography Methods for Pharmaceutical Analysis: Understanding the Differences and Similarities between Validation Requirements of the US Food and Drug Administration, the US Pharmacopoeia and the International Conference on Harmonisation. *Journal of Chromatography A,* Vol. 987, No. 1-2, 2003, pp. 57-66.

150. A. G. Causey, H. M. Hills and L. J. Phillips. Evaluation of Criteria for the Acceptance of Bioanalytical Data. *Journal of Pharmaceutical and Biomedical Analysis,* Vol. 8, No. 8-12, 1990, pp. 625-628.

151. R. Wood. How to Validate Analytical Methods. *Trends in Analytical Chemistry,* Vol. 18, No. 9-10, 1999, pp. 624-632.

152. W. L. Paul. USP Perspectives on Analytical Methods Validation. *Pharmaceutical Technology,* Vol. 15, No. 3, 1991, pp. 130-141.

153. G. C. Clarke. The Validation and of Analytical Methods for Drug Substances and Drug Products in UK Pharmaceutical Laboratories. *Journal of Pharmacy and Biomedical Analysis,* Vol. 12, No. 5, 1994, pp. 643-652.

154. G. C. Hokanson. A life Cycle Approach to the Development of Analytical Methods during Pharmaceutical Product Development Part I: The Initial Method Validation Process. *Pharmaceutical Technology,* Vol. 18, No. 9, 1994, pp. 118-130.

155. T. C. Paino and A. D. Moore. Determination of the LOD and LOQ of an HPLC Method using Four Different Techniques. *Pharmaceutical Technology,* Vol. 23, 1999, pp. 86-92.

156. H. Rosing, W. Y. Man, E. Doyle, A. Bult and J. H. Beijnen. Bioanalytical Liquid Chromatographic Method Validation: A Review of Current Practices and Procedures. *Journal of Liquid Chromatography and Related Technologies,* Vol. 23. No. 3, 2000, pp. 329-354.

157. J. Vessman. Selectivity or Specificity? Validation of Analytical Methods from the Perspective of an Analytical Chemist in the Pharmaceutical Industry. *Journal of Pharmacy and Biomedical Analysis,* Vol. 14, No. 8-10, 1996, pp. 867-869.

158. M. Bakshi and S. Singh. Development of Validated Stability Indicating Assay Methods: Critical Review. *Journal of Pharmaceutical and Biomedical Analysis,* Vol. 28, No. 6, 2002, pp. 1011-1040.

159. European Medicines Agency. International Conference on Harmonisation of Technical Requirements for Registration of Pharmaceuticals for Human Use, Stability Testing of New Drug Substance and Product Q1A R2, London, 2006.

160. M. Y. Noordin, V. C. Venkatesh, S. Sharif, S. Elting and A. Abdullah. Application of Response Surface Methodology in Describing the Performance of Coated Carbide Tools when Turning AISI 1045 Steel. *Journal of Materials Processing Technology,* Vol. 145, No. 1, 2004, pp. 46-58.

161. T. B. L. Kirkwood. Geometric Means and Measures of Dispersion. *Biometrics,* Vol. 35, No. 4, 1979, pp. 908-909.

162. W. A. Hendricks and K. W. Robey. The Sampling Distribution of the Coefficient of Variation. *Annals of Mathematical Statistics,* Vol. 7, No. 3, 1936, pp. 129-132.

163. P. Barmpalexis, F. I. Kanaze and E.Ojewole. Developing and Optimising a Validated Isocratic Reversed Phase HPLC Separation of Nimodipine and Impurities in Tablets using Experimental Design Methodology. *Journal of Pharmaceutical and Biomedical Analysis,* Vol. 49, No. 4, 2009, pp. 1192-1202.

164. G. E. P. Box and K. B. Wilson. On the Experimental Attainment of Optimum Multifactorial Conditions. *Royal Statistics Society,* Vol. 13, 1951, pp. 1-12.

165. J. F. Wheeler, T. L. Beck, S. J. Klatte, L. A. Cole and J. G. Dorsey. Phase Transitions of Reversed-Phase Stationary Phases: Cause and Effects in the Mechanism of Retention. *Journal of Chromatography A,* Vol. 656, No. 1-2, 1993, pp. 317-333.

166. Z. Hao, B. Xiao and N. Weng. Impact of Column Temperature and Mobile Phase Components on Selectivity of Hydrophilic Interaction Chromatography (HILIC). *Journal of Separation Science,* Vol. 31, No. 9, 2008, pp. 1449-1464.

167. N. Kaul, H. Agrawal, A. R. Paradkar and K. R. Mahadik. HPTLC Method for Determination of Nevirapine in Pharmaceutical Dosage Form. *Talanta,* Vol. 62, No. 4, 2004, pp. 843-852.

168. A. H. Kibbe. Theory of Dissolution. In *Dissolution Theory, Methodology, and Testing.* A. Palmieri III (Editor), Dissolution Technologies Incorporated, Hockessin, USA, 2007, pp. 1-12.

169. U. V. Banakar. Pharmaceutical Dissolution Testing. In *Drugs and the Pharmaceutical Sciences, Vol. 49*, J. Swarbrick, (Editor), Informa Healthcare, New York, USA, 1991, pp. 1-10.

170. P. Costa and J. M. S. Lobo. Influence of Dissolution Medium Agitation on Release Profiles of Sustained Release Tablets. *Drug Development and Industrial Pharmacy,* Vol. 27, No. 8, 2001, pp. 811-817.

171. A. A. Noyes and W. R. Whitney. The Rate of Dissolution of Solid Substances in their own Solution. *Journal of the American Chemical Society,* Vol. 19, No. 12, 1897, pp. 930-934.

172. R. O. Williams III and J. N. Brown. Dissolution of Modified-Release Oral Dosage Forms. In *Dissolution Theory, Methodology, and Testing*, A. Palmieri III (Editor), Dissolution Technologies, Inc., Hockessin, 2007, pp. 196-231.

173. I. Borst, S. Ugwu and A. H. Bekett. New and Extended Application for USP Drug Release Apparatus 3. *Dissolution Technology,* Vol. 4, No. 1, 1997, pp.11-16.

174. J. M. Aiache, N. Aoyagi, H. Blune, J. Dressman, H. D. Friedel, L. T. Grady and V. Gray. FIP Guidance for Dissolution Testing of Solid Oral Products. *Dissolution Technology,* Vol. 4, No. 4, 1997, pp. 5-14.

175. *United States Pharmacopoeia "Incorporating National Formulary*." United States Pharmacopoeia Convention, Rockville, USA, 34th Edition, Vol. 1, 2011, pp. 609-630.

176. S. Azarmi, W. Roa and R. Lobenberg. Current Perspectives in Dissolution Testing of Conventional and Novel Dosage Forms. *International Journal of Pharmaceutics,* Vol. 328, No. 1, 2007, pp. 12-21.

177. K. R. Reddy, S. Mutalik and S. Reddy. Once-Daily Sustained-Release Matrix Tablets of Nicorandil: Formulation and *In Vitro* Evaluation. *AAPS Pharmaceutical Science and Technology,* Vol. 4, No. 4, 2003, pp. 480-488.

178. D. C. Baun, and G. C. Walker. Apparatus for Determining the Rate of Drug Release from Solid Dosage Forms. *Journal of Pharmaceutical Sciences,* Vol. 58, No. 5, 1969, pp. 611-616.

179. E. C. Gil, I. A. Colarte, B. Bataille, J. L. Pedraz, F. Rodriguez and J. Heinamaki. Development and Optimisation of a Novel Sustained-Release Dextran Tablet Formulation for Propranolol Hydrochloride. *International Journal of Pharmaceutics,* Vol. 317, No. 1, 2006, pp. 32-39.

180. M. M. Crowley, B. Schroeder, A. Fredersdorf, S. Obara, M. Talarico, S. Kucera and J. W. McGinity. Physicochemical Properties and Mechanism of Drug Release from Ethyl Cellulose Matrix Tablets Prepared by Direct Compression and Hot-Melt Extrusion. *International Journal of Pharmaceutics,* Vol. 296, No. 2, 2004, pp. 509-522.

181. T. Komuro, C. Yomota and T. Kimura. *In Vitro* Dissolution Properties of Indomethacin Extended Release Capsules. *Journal of Pharmacy and Pharmacology,* Vol. 43, No. 2, 1991, pp. 79-82.

182. International Pharmaceutical Federation (FIP). Guidelines for Dissolution Testing of Solid Oral Products. *Drug Information Journal,* Vol. 30, No. 4, 1996, pp. 1071-1084.

183. S. A. Qurashi and I. J. McGilveray. Typical Variability in Drug Dissolution Testing: Study with USP and FDA Calibrator Tablets and a Marketed Drug (Glibenclamide) Product. *European Journal of Pharmaceutical Sciences,* Vol. 7, No. 3, 1999, pp. 249-258.

184. M. Ansari, M. Kazemipour and J. Talebnia. The Development and Validation of a Dissolution Method for Chlorpheniramine Solid Dosage Forms. *Dissolution Technologies,* Vol. 8, 2004, pp. 16-24.

185. S. J. Burns, D. Corness, G. Hay, S. Higginbottom, I. Whelan, D. Attwood and S. G. Barnwell. Development and Validation of an *In Vitro* Dissolution Method for a Floating Dosage Form with Biphasic Release Characteristics. *International Journal of Pharmaceutics,* Vol. 121, No. 1, 1995, pp. 37-44.

186. R. C. Rossi, C. L. Dias, E. M. Donato, L. A. Martins, A. M. Bergold and P. E. Froehlich. Development and Validation of Dissolution Test for Ritonavir Soft Gelatin Capsules Based on *In Vivo* Data. *International Journal of Pharmaceutics,* Vol. 338, No. 1-2, 2007, pp. 119-124.

187. J. W. Skoug, G. W. Halstead, D. L. Theis, J. E. Freeman, D. T. Fagan and B. R. Rohrs. Strategy for the Development and Validation of Dissolution Tests for Solid Oral Dosage Forms. *Pharmaceutical Technology,* Vol. 20, No. 5, 1996, pp. 58-72.

188. A. R. Breier, C. S. Paim, M. Steppe and E. E. S. Schapoval. Development and Validation of Dissolution Tests for Fexofenadine Hydrochloride Capsules and Coated Tablets. *Journal of Pharmacy and Pharmaceutical Sciences,* Vol. 8, No. 2, 2005, pp. 289-298.

189. T. Komuro, C. Yomota and T. Kimura. *In Vitro* Dissolution Properties of Indomethacin Extended Release Capsules. *Journal of Pharmacy and Pharmacology,* Vol. 43, No. 2, 1991, pp. 79-82.

190. N. D. Eddington, P. Marroum, R. Uppoor, A. Hussain. Development and Internal Validation of an *In Vitro In Vivo* Correlation for a Hydrophilic Metoprolol Tartrate Extended Release Tablet Formulation. *Pharmaceutical Research,* Vol. 15, No. 3, 1998, pp. 466-473.

191. M. L. Cappola, S. Sienkiewicz, G. C. Snow and F. J. Chen. Extended Release Formulation of Nevirapine. *Boehringer Ingelheim International GmbH*, USA patent 12/523226, 2009.

192. J. Li, L. Yang, S. M. Ferguson, T. J. Hudson, S. Watanabe, M. Katsuma, and J. A. Fix. *In Vitro* Evaluation of Dissolution Behaviour for a Colon-Specific Drug Delivery System (CODES) in Multi-pH Media using USP Apparatus II and III. *AAPS Pharmaceutical Science and Technology,* Vol. 3. No.4, 2002, article 33.

193. T. A. Schauble. Comparison of Various Sampling Methods for Tablet Release Tests using the Stirrer Methods (USP Apparatus 1 & 2). *Dissolution Technology,* Vol. 3, No. 2, 1996, pp. 11-15.

194. V. Pillay and R. Fassihi. Unconventional Dissolution Methodologies. *Journal of Pharmaceutical Sciences,* Vol. 88, No. 9, 1999, pp. 843-851.

195. B. R. Rohrs. Dissolution Method Development for Poorly Soluble Compounds. *Dissolution Technologies,* Vol. 8, No. 3, 2001, pp. 1-5.

196. US Department of Health and Human Services, Food and Drug Administration, Centre for Drug Evaluation and Research. Guidance for Industry: SUPAC-MR: Modified Release Solid Oral Dosage Forms, Rockville, USA, 1997.

197. B. R. Rohrs, D. L. Burch-Clark, M. J. Witt and D. J. Stelzer. USP Dissolution Apparatus 3 (Reciprocating Cylinder): Instrument Parameter Effects on Drug Release from Sustained Release Formulations. *Journal of Pharmaceutical Sciences,* Vol. 84, No. 8, 1995, pp. 922-926.

198. S. M. M. Khamanga and R. B. Walker. The Effect of Buffer Molarity, Agitation Rate, and Mesh Size on Verapamil Release from Modified-Release Mini-Tablets Using USP Apparatus 3. *Dissolution Technology,* Vol. 14, No. 2, 2007, pp. 19-23.

199. J. W. Moore and H. H. Flanner. Mathematical Comparison of Dissolution Profiles. *Pharmaceutical Technology,* Vol. 20, No. 6, 1996, pp. 64-74.

200. P. Costa, J. Manuel and S. Lobo. Modelling and Comparison of Dissolution Profiles. *European Journal of Pharmaceutical Sciences,* Vol. 13, No. 2, 2001, pp. 123-133.

201. N. Yuksel, A. E. Kanik and T. Baykara. Comparison of *In Vitro* Dissolution Profiles by ANOVA-based, Model-Dependent and -Independent Methods. *International Journal of Pharmaceutics,* Vol. 209, No. 1-2, 2000, pp. 57-67.

202. V. P. Shah, Y. Tsong, P. Sathe and J-P. Liu. *In Vitro* Dissolution Profile Comparison - Statistics and Analysis of the Similarity Factor, f_2. *Pharmaceutical Research,* Vol. 15. No. 6, 1998, pp. 889-896.

203. M. Z. I. Khan. Dissolution Testing for Sustained or Controlled Release Oral Dosage Forms and Correlation with *In Vivo* Data: Challenges and Opportunities. *International Journal of Pharmaceutics,* Vol. 140, No. 2, 1996, pp. 131-143.

204. C. K. Brown, H. P. Chokshi, B. Nicherson, R. A. Reed, B. R. Rohrs and P. A. Shah. Acceptable Analytical Practices in Dissolution Testing of Poorly Soluble Compounds. *Pharmaceutical Technology,* Vol. 28, No. 12, 2004, pp. 56-65.

205. V. P. Shah, J. J. Konecny, R. L. Everret, B. McCullough, A. C. Noorizadeh and J. P. Skelly. *In Vitro* Dissolution Profile of Water-Insoluble Drug Dosage Forms in the Presence of Solubilisers. *Pharmaceutical Research,* Vol. 6, 1989, pp. 612-618.

206. International Pharmaceutical Federation (FIP). Joint Report of the Section for Control Laboratories and Industrial Pharmacists: Guidelines for Dissolution Testing of Solid Oral Products. *Pharmaceutical Industry*, Vol. 43, 1981, pp. 334-343.

207. B. J. Lee. Pharmaceutical Preformulation: Physicochemical Properties of Excipients and Powders and Tablet Characterisation. In *Pharmaceutical Manufacturing*

Handbook- Production and Processes, S. C. Gad (Editor), John Wiley and Sons, Cary, USA, 2008, pp. 881-1087.

208. L. X. Yu. Pharmaceutical Quality by Design: Product and Process Development, Understanding, and Control. *Pharmaceutical Research,* Vol.25 No.4, 2008, pp. 781-791.

209. N. H. Huda, Y. M. Jhanker and R. Uddin. First Step in the Assessment of Mechanical Properties of Pure API: Production of Tablet with Minimum Addition of Excipient. *Journal of Applied Pharmaceutical Science,* Vol. 1, No. 6, 2011, pp. 96-98.

210. International Conference on Harmonisation. ICH of Technical Requirements for Registration of Pharmaceuticals for Human Use. ICH Harmonised Tripartite Guideline, Pharmaceutical Development Q8 (R2), 2009.

211. U. S. Department of Health and Human Services, Food and Drug Administration, Center for Drug Evaluation and Research (CDER), Center for Biologics Evaluation and Research (CBER). Guidance for Industry: Nonclinical Studies for the Safety Evaluation of Pharmaceutical Excipients, 2005.

212. *Excipient Development for Pharmaceutical, Biotechnology and Drug Delivery Systems*, A. Katdare, M. Chaubal (Editors), Informa Healthcare, New York, USA, 2006, pp. 1-150.

213. C. Moreton. Functionality and Performance of Excipients in a Quality by-Design World: Part IV. *American Pharmaceutical Review*, Supp., 2010, pp. 18-21.

214. G. S. Clarke. The Validation of Analytical Methods for Drug Substances and Drug Products in UK Pharmaceutical Laboratories. *Journal of Pharmaceutical and Biomedical Analysis,* Vol. 12, No.5, 1994, pp. 643-652.

215. *Excipients and Delivery Systems for Pharmaceutical Formulations.* D. R. Karsa and R. A. Stephenson (Editors). The Royal Society of Chemistry, Cambridge, UK, 1995, pp. 1-192.

216. D. A. Alderman. A Review of Cellulose Ethers in Hydrophilic Matrices for Oral Controlled-Release Dosage Forms. *International Journal of Pharmaceutical Technology and Product Manufacture,* Vol. 5, No. 3, 1984, pp. 1-9.

217. *The Handbook of Pharmaceutical Excipients*. R. C. Rowe, P. J. Sheskey, M. E. Quinn, Pharmaceutical Press, London, UK, 6th Edition, 2009, pp. 94-98, 110-113, 129-132, 186-188, 326-329, 376-378, 404-406, 728-730.

218. S. M. Samani, H. Montaseri and A. Kazemi. The Effect of Polymer Blends on Release Profiles of Diclofenac Sodium. *European Journal of Pharmaceutics and Biopharmaceutics,* Vol. 55, No. 3, 2003, pp. 351-355.

219. S. Kiil, K and Dam-Johansen. Controlled Drug Delivery from Swellable HPMC Matrices: Model Based Analysis of Observed Radial Front Movements. *Journal of Controlled Release,* Vol. 90, No. 1, 2003, pp. 1-21.

220. J. T. McConville, A. C. Ross, A. R. Chambers, G. Smith, A. J. Florence and H. N. E. Stevens. The Effect of Wet Granulation on the Erosion Behaviour of an HPMC-Lactose, used as a Rate-Controlling Component in a Pulsatile Drug Delivery Capsule Formulation. *European Journal of Pharmaceutics and Biopharmaceutics,* Vol. 57, No. 3, 2004, pp. 541-549.

221. P. Gao, J. W. Skoug, P. R. Nixon, T. R. Ju, N. L. Stemm, K. C. Sung. Swelling of Hydroxypropylmethylcellulose Matrix Tablets. 2. Mechanistic Study of the Influence of Formulation Variables on Matrix Performance and Drug Release. *Journal of Pharmaceutical Sciences,* Vol. 85, No.7, 1996, pp. 732-740.

222. R. Bettini, P. L. Catellani, P. Santi, G. Massimo, N. A. Peppas and P. Colombo. Translocation of Drug Particles in HPMC Drug Matrix Layer: Effect of Drug Solubility and Influence on Drug Release. *Journal of Controlled Release,* Vol. 70, No. 3, 2001, pp. 383-391.

223. X. Huang and C. S. Brazel. On the Importance and Mechanisms of Burst Release in Matrix Controlled Drug Delivery Systems. *Journal of Controlled Release,* Vol. 73, No. 2-3, 2001, pp. 121-136.

224. S. Goto, M. Kawata, M. Nakamura, K. Maekawa and T. Aoyama. Eudragit® RS and Eudragit® RL (Acrylic Resins) Microcapsules as pH Insensitive and Sustained Release Preparations of Ketoprofen. *Journal of Microencapsulation,* Vol. 3, No. 4, 1986, pp. 293-304.

225. S. Azarmi, J. Farid, A. Nokhodchi, S. M. B. Saravi and H.Valizadeh. Thermal Treating as a Tool for Sustained-Release of Indomethacin from Eudragit® RS and RL Matrices. *International Journal of Pharmaceutics,* Vol. 246, No. 1, 2002, pp. 171-177.

226. E. A. Arno, P. Anand, K. Bhaskar, S. Ramachandran, M. Saravanan and R. Vinod. Eudragit NE 30D Based Metformin/Gliclazide Extended Release Tablets: Formulation, Characterisation and *In Vitro* Release Studies. *Chemical and Pharmaceutical Bulletin,* Vol. 50, No. 11, 2002, pp. 1495-1498.

227. R. Chauvin. Carbomers. I. A General Concept of Expanded Molecules. *Tetrahedron Letters,* Vol. 36, No. 3, 1995, pp. 397-400.

228. P. Jelena, Z. Djuric, M. Jovanovic, S. Ibric, V. Kilibarda, D. Jovanovic and I. K. Evic. Biopharmaceutical Characterisation of Sustained Release Matrix Tablets Based on Novel Carbomer Polymers: Formulation and *In Vivo* Investigation. *European Journal of Drug Metabolism and Pharmacokinetics,* Vol. 30, No. 1-2, 2005, pp. 99-104.

229. M. H. Fayed, G. M. Mahrous, M. A. Ibrahim and A. Sakr. Influence of Carbopol 71G-NF on the Release of Dextromethorphan Hydrobromide from Extended-Release Matrix Tablets. *Pharmaceutical Development and Technology,* 2011, pp. 1-11.

230. *Oral Controlled Release Formulation Design and Drug Delivery: Theory to Practice.* H. Wen and K. Park. John Wiley and Sons, New York, USA, 2011, pp. 21-337.

231. J. T. Carstensen and C. Ertell. Physical and Chemical Properties of Calcium Phosphates for Solid State Pharmaceutical Formulations. *Drug Development and Industrial Pharmacy,* Vol. 16, No. 7, 1990, pp. 1121-1133.

232. M. Jivraj, L. G. Martini and C. M. Thomson. An Overview of the Different Excipients Useful for the Direct Compression of Tablets. *Pharmaceutical Science and Technology Today,* Vol. 3, No. 2, 2000, pp. 58-63.

233. V. H. Holsinger. Physical and Chemical Properties of Lactose. *Advanced Dairy Chemistry,* Vol. 3, 1997, pp. 1-38.

234. G. K. Bolhuis, C. F. Lerk, J. R. Moes and C. W. A. Mulder. Comparative Evaluation of Excipients for Direct Compression. *Pharmacy World and Science,* Vol.1, No. 1, 1979, pp. 1223-1233.

235. Y. Gonnissen, J. P. Remon and C. Vervaet. Development of Directly Compressible Powders via Co-Spray Drying. *European Journal of Pharmaceutics and Biopharmaceutics,* Vol. 67, No. 1, 2007, pp. 220-226.

236. K. D. Ertel, J.T .Carstensen. Chemical, Physical, and Lubricant Properties of Magnesium Stearate. *Journal of Pharmaceutical Science,* Vol. 77, No. 7, 1988, pp. 625-629.

237. K. D. Ertel and J. T. Carstensen. An Examination of the Physical Properties of Pure Magnesium Stearate. *International Journal of Pharmaceutics,* Vol. 42, No. 1, 1988, pp. 171-180.

238. U. I. Leinonen, H. U. Jalonen, P. A. Vihervaara and E. S. U. Laine. Physical and Lubrication Properties of Magnesium Stearate. *Journal of Pharmaceutical Science,* Vol. 81, No. 12, 1992, pp. 1194-1198.

239. T. Durig and R. Fassihi. Mechanistic Evaluation of Binary Effects of Magnesium Stearate and Talc as Dissolution Retardants at 85% Drug Loading in an Experimental Extended Release Formulation. *Journal of Pharmaceutical Sciences,* Vol. 86, No. 10, 1997, pp. 1092-1098.

240. R. Zazenski, W. H. Ashton, D. Briggs, M. Chudkowski, J. W. Kelse, L. MacEachern, E. F. McCarthy, M. A. Nordhauser, M. T. Roddy and N. M. Teetsel. Talc: Occurrence, Characterisation, and Consumer Applications. *Regulatory Toxicology and Pharmacology,* Vol. 21, No. 2, 1995, pp. 218-229.

241. E. H. Kerns and L. Di. Physicochemical Profiling in Drug Discovery. *Drug Discovery Today,* Vol. 8, No. 7, 2003, pp. 273-285.

242. K. R. Morris, U. J. Griesser, C. J. Eckhardt and J. G. Stowell. Theoretical Approaches to Physical Transformations of Active Pharmaceutical Ingredients during Manufacturing Process. *Advanced Drug Delivery Review,* Vol. 48, No. 1, 2001, pp. 91-114.

243. G. Cornaire, J. Woodley, P. Hermann, A. Cloarec, C. Arellano and G. Hoin. Impact of Excipients on the Absorption of p-glycoprotein Substrates *In Vitro* and *In Vivo*. *International Journal of Pharmaceutics,* Vol. 278, No. 1, 2004, pp. 119-131.

244. R. J. Mountfield, S. Senepin, M. Schleimer, I. Walter and B. Bittner. Potential Inhibitory Effects of Formulation Ingredients on Intestinal Cytochrome P450. *International Journal of Pharmaceutics,* Vol. 211, No. 1, 2000, pp. 89-92.

245. *Pharmaceutical Manufacturing Handbook: Production and Processes*. S. C. Gad (Editor), John Wiley and Sons, Cary, USA, 2008, pp. 881-1222.

246. T. Baxter, R. Barnum and J. K Prescott. Flow: General Principles of Bulk Solids Handling. In *Pharmaceutical Dosage forms: Tablets*, L. L. Augsburger, S. W. Hoang (Editors), Informa Healthcare, Baltimore, USA, 3rd Edition, 2008, pp. 75-109.

247. S. W. Hoang and L. Han-Pin. Particle and Powder Bed Properties. In *Pharmaceutical Dosage Forms: Tablets*, L. L. Augsburger, S. W. Hoang (Editors), Informa Healthcare, Baltimore, USA, 3rd Edition, 2008, pp. 17-71.

248. *Pharmaceutical Preformulation and Formulation: A Practical Guide from Candidate Drug Selection to Commercial Dosage Form.* M. Gibson (Editor), Informa Healthcare, New York, USA, 2nd Edition, 2009, pp. 1-367.

249. H. Patel, A. Stalcup, R. Dansereau and A. Sakr. The Effect of Excipients on the Stability of Levothyroxine Sodium Pentahydrate Tablets. *International Journal of Pharmacy*, Vol. 264, No. 1, 2003, pp. 35-43.

250. K. Jackson, D. Young and S. Pant. Drug-Excipient Interactions and their Effect on Absorption. *Journal of Proteotoxic Stress Targeted Therapy,* Vol. 3, No. 10, 2000, pp. 336-345.

251. R. K. Verma, D. M. Krishna and S. Garg. Formulation Aspects in the Development of Osmotically Controlled Oral Drug Delivery System. *Journal of Controlled Release,* Vol. 79, No. 1-3, 2002, pp. 7-27.

252. T. J. Di Feo. Drug Product Development: A Technical Review of Chemistry, Manufacturing, and Controls Information for the Support of Pharmaceutical Compound Licensing Activities. *Drug Development and Industrial Pharmacy,* Vol. 29, No. 9, 2003, pp. 939-958.

253. N. Fathima, T. Mamatha, H. K. Qureshi, N. Anitha and J. V. Rao. Drug-Excipient Interaction and its Importance in Dosage Form Development. *Journal of Applied Pharmaceutical Science,* Vol. 1, No. 6, 2011, pp. 66-71.

254. M. Z. Ahmad, V. Kumar, A. Kumar and S. Akhter. Drug-Excipient(s) Interactions and Compatibility Study: A Review. *Journal of Pharmacy Research,* Vol. 3, No. 9, 2010, pp. 2092-2095.

255. K. Mizutari. Photo-Enhanced Modification of Human Skin Elastin in Actinic Elastosis by N-(Carboxymethyl)lysine, One of the Glycoxidation Products of the Maillard Reaction. *Journal of Investigative Dermatology,* Vol. 108, 1997, pp. 792-802.

256. K. Okimoto and M. Miyake. Design and Evaluation of an Osmotic Pump Tablet for Prednisolone, a Poorly Water Soluble Drug using (SBE)7M-b-CD. *Pharmaceutical Research,* Vol. 15, No. 10, 1998, pp. 1562-1568.

257. A. T. M. Serajuddin, A. B. Thakur, R. N. Ghoshal, M. G. Fakes, S. A. Ranadive, K. R. Morris, S. A. Varia. Selection of Solid Dosage Form Composition through Drug-Excipient Compatibility Testing. *Journal of Pharmaceutical Sciences,* Vol. 88, No. 7, 1999, pp. 696-704.

258. T. Durig and R. Fassihi. Mechanistic Evaluation of Binary Effects of Magnesium Stearate and Talc as Dissolution Retardants at 85% Drug Loading in an Experimental Extended-Release Formulation. *Journal of Pharmaceutical Sciences,* Vol. 86, No. 10, 1997, pp. 1092-1098.

259. R. Michael, E. Richards, J. Z. Xing and K. M. B. Mackay. Excipients Interaction with Cetylpiridinium Chloride Activity in Tablet Based Lozenges. *Pharmaceutical Research,* Vol. 13, No. 8, 1996, pp. 1258-1264.

260. J. Czaja and J. B. Mielck. Solid State Degradation Kinetics of Nitrazepam in the Presence of Colloidal Silica. *Pharm Acta,* Vol. 57, No. 5-6, 1982, pp. 153-155.

261. P. Singh, J. K. Guillory, T. D. Sokoloski, L. Z. Benet and V. N. Bhatia. Effect of Inert Tablet Ingredients on Drug absorption, I. Effect of PEG-400 on Intestinal Absorption of Four Barbiturates. *Journal of Pharmaceutical Science,* Vol. 85, No. 1, 1996, pp. 63-68.

262. S. S. P. Rege, L. H. Block. Use of Chitosan in Compressed Tablets of Diclofenac Sodium: Inhibition of Drug Release in an Acidic Environment. *Journal of Pharmaceutical Development and Technology,* Vol. 2, No. 3, 1997, pp. 243-255.

263. D. Ritter. Effect of Silica Gel on Stability and Biological Availability of Ascorbic Acid. *Journal of Pharmaceutical Science,* Vol. 59, No. 2, 1970, pp. 229-232.

264. C. Powers. A New Roundness Scale for Sedimentary Particles. *Sedimentary Petrol,* Vol. 23, No. 2, 1953, pp. 117-119.

265. X. Fu, D. Huck, L. Makein, B. Armstrong, U. Willen and T. Freeman. Effect of Particle Shape and Size on Flow Properties of Lactose Powders. *Particuology,* Vol. 10, No. 2, 2012, pp. 203-208.

266. P. W. Cleary. The Effect of Particle Shape on Simple Shear Flows. *Powder Technology,* Vol. 179, No.3, 2008, pp. 144-163.

267. A. Guo, J. K. Beddow and A. F. Vetter. A Simple Relationship Between Particle Shape Effects and Density, Flow Rate and Hausner Ratio. *Powder Technology,* Vol. 43, No. 3, 1985, pp. 279-284.

268. N. Pilpel and C. A. Walton. The Effect of Particle Size and Shape on the Flow and Failure Properties of Procaine Penicillin Powders. *Journal of Pharmacy and Pharmacology,* Vol. 26, No. S1, 1974, 1P-10P.

269. G. Gold, R. N. Duvall, B. T. Palermo and J. G. Slater. Powder Flow Studies III. Factors Affecting the Flow of Lactose Granules. *Journal of Pharmaceutical Science,* Vol. 57, No. 4, 1968, pp. 667-671.

270. R. Chadha, P. Arora, A. Saini and D. S. Jain. Solvated Crystalline Forms of Nevirapine: Thermoanalytical and Spectroscopic Studies. *Pharmaceutical Science Technology,* Vol. 11, No. 3, 2010, pp. 1328-1339.

271. F. Balestrieri, A. D. Magri, A. L. Magri, D. Marini and A. Sacchini. Application of Differential Scanning Calorimetry to the Study of Drug-Excipient Compatibility. *Thermochimica Acta,* Vol. 285, No. 2, 1996, pp. 337-345.

272. M. J. Hardly. Drug-Excipient Compatibility Prediction by DSC. *Analytical Proceedings,* Vol. 19, No. 12, 1982, pp. 556-557.

273. D. Kiss, R. Zelko, C. Novaik and Z. Ehen. Application of DSC and NIRS to Study the Compatibility of Metronidazole with Different Pharmaceutical Excipients. *Journal of Thermal Analysis and Calorimetry,* Vol. 84, No. 2, 2006, pp. 447-451.

274. A. Nokhodchi, O. N. Okwudarue, H. Valizadeh and M. N. Momin. Cogrinding as a Tool to Produce Sustained Release Behaviour for Theophylline Particles Containing Magnesium Stearate. *AAPS Pharmaceutical Science and Technology*, Vol. 10, No. 4, 2009, pp. 1243-1251.

275. A. V. Singh and L. K. Nath. Evaluation of Compatibility of Lamivudine with Tablet Excipients and a Novel Synthesised Polymer. *Journal of Materials and Environmental Science,* Vol. 2, No. 3, 2011, pp. 243-240.

276. M. Angberg. Lactose and Thermal Analysis with Special Emphasis on Microcalorimetry. *Thermochimica Acta,* Vol. 248, 1995, pp. 161-176.

277. R. Price and P. M. Young. Visualisation of the Crystallisation of Lactose from the Amorphous State. *Journal of Pharmaceutical Sciences,* Vol. 93, No.1, 2004, pp. 155-164.

278. D. Kiss, R. Zelko, C. Novaik and Z. Ehen. Application of DSC and NIRS to Study the Compatibility of Metronidazole with Different Pharmaceutical Excipients. *Journal of Thermal Analysis and Calorimetry,* Vol. 84, No. 2, 2006, pp. 447-451.

279. S. S. Bharate, S. B. Bharate and A. N. Bajaj. Interactions and Incompatibilities of Pharmaceutical Excipients with Active Pharmaceutical Ingredients: A Comprehensive Review. *Journal of Excipients and Food Chemicals,* Vol. 1, No. 3, 2010, pp. 3-25.

280. T. A. Miller and P. York. Pharmaceutical Tablet Lubrication. *International Journal of Pharmaceutics,* Vol. 41, No. 1-2, 1988, pp. 1-19.

281. R. L. O. Rezende, M. I. R. M. Santoro and J. R. Matos. Stability and Compatibility Study of Enalapril Maleate using Thermoanalytical Techniques. *Journal of Thermal Analysis and Calorimetry,* Vol. 93, No. 3, 2008, pp. 881-886.

282. S. B. Sonali, B. B. Sandip, N. B. Amrita. Incompatibilities of Pharmaceutical Excipients with Active Pharmaceutical Ingredients: A Comprehensive Review. *Journal of Excipients and Food Chemicals,* Vol. 1, No. 3, 2010, pp. 3-26.

283. A. P. Ayala, H. W. Siesler, S. M. S. V. Wardell, N. Boechat, V. Dabbene and S. L. Cuffini. Vibrational Spectra and Quantum Mechanical Calculations of Antiretroviral

Drugs: Nevirapine. *Journal of Molecular Structure,* Vol.828, No. 1-3, 2007, pp. 201-210.

284. J. Coates. Interpretation of Infrared Spectra: A practical Approach. In *Encyclopedia of Analytical Chemistry*, R. A. Meyers (Editor), John Wiley and Sons, Chichester, UK, 2000, pp. 10815-10837.

285. G. R. Hollenbeck, K. T. Mitrevej and C. A. Fan. Estimation of the Extent of Drug–Excipient Interactions Involving Croscarmellose Sodium. *Journal of Pharmaceutical Science,* Vol. 72, No. 3, 1983, pp. 325-327.

286. G. Bruni, L. Amici, V. Berbenni, A. Marini and A. Orlandi. Drug-Excipient Compatibility Studies. Search of Interaction Indicators. *Journal of Thermal Analysis and Calorimetry,* Vol. 68, No. 2, 2002, pp. 561-573.

287. M. L. Cotton, D. W. Wu and E. B. Vadas. Drug-Excipient Interaction Study of Enalapril Maleate Using Thermal Analysis and Scanning Electron Microscopy. *International Journal of Pharmaceutics,* Vol. 40, N0. 1-2, 1987, pp. 129-142.

288. S. A. Botha, A. P. Lotter and J. L. Du Preez. DSC Screening for Drug-Excipient and Excipient -Excipient Interactions in Polypharmaceuticals Intended for the Alleviation of the Symptoms of Colds and FLU. III. *Drug Development and Industrial Pharmacy,* Vol. 13, No. 7, 1987, pp. 1197-1215.

289. M. J. Akers. Excipient–Drug Interactions in Parenteral Formulations. *Journal of Pharmaceutical Science,* Vol. 91, No. 11, 2002, pp. 2283-2300.

290. S. A. Schildcrout, D. S. Risley and R. L. Kleemann. Drug-Excipient Interactions of Seproxetine Maleate Hemi-Hydrate: Isothermal Stress Methods. *Drug Development and Industrial Pharmacy,* Vol. 19, No. 10, 1993, pp. 1113-1130.

291. S. A. Charman and W. N. Charman. Modified-Release Drug Delivery Technology. In *Drugs and the Pharmaceutical Sciences Vol. 126*, M. J. Rathbone, J. Hadgraft, M. S. Roberts (Editors), Marcel Dekker, Inc., New York, USA, 2003, pp. 1-10.

292. S. B. Tiwari and A. R. Rajab-Siahboomi. Applications of Complimentary Polymers in HPMC Hydrophilic Extended Release Matrices. *Drug Delivery Technology,* Vol. 9, No. 7, 2009, pp. 20-27.

293. R. B. Walker. Modified-Release Delivery Systems for Oral Use. *In Drugs and the Pharmaceutical Sciences Vol. 183: Modified-Release Drug Delivery Technology.* M. J. Rathbone, J. Hadgraft, M. S. Roberts, M. E. Lane (Editors), Informa Healthcare, New York, USA, 2nd Edition, Vol. 1, 2008, pp. 131-138.

294. M. Jamei, D. Turner, J. Yang, S. Neuhoff, S. Polak, A. Rostami-Hodjegan and G. Tucker. Population-Based Mechanistic Prediction of Oral Drug Absorption. *American Association of Pharmaceutical Scientists Journal,* Vol. 11, No. 2, 2009, pp. 225-237.

295. A. MacAdam. The Effect of Gastro-Intestinal Mucus on Drug Absorption. *Advanced Drug Delivery Reviews,* Vol. 11, No. 3, 1993, pp. 201-220.

296. *Absorption and Drug Development: Solubility, Permeability, and Charge State*. A. Avdeef, John Wiley & Sons, New York, USA, 2012, pp. 1-578.

297. H. Sun, K. S. Pang. Physiological Modeling to Understand the Impact of Enzymes and Transporters on Drug and Metabolite Data and Bioavailability Estimates. *Pharmaceutical Research,* Vol. 27, No. 7, 2010, pp. 237-1254.

298. J. Siepmann, F. Siepmann and M. M. Anelli. Modified-Drug Delivery Technology. In *Drugs and the Pharmaceutical Sciences Vol. 184,* M. J. Rathbone, J. Hadgraft, M. S. Roberts, M. E. Lane (Editors), Informa Healthcare, New York, USA, 2nd Edition, Vol. 2, 2008, pp. 17-47. 2008.

299. T. Salsa, F. Veiga and M. E. Pina. Oral Controlled-Release Dosage Forms. I. Cellulose Ether Polymers in Hydrophilic Matrices. *Drug Development and Industrial Pharmacy,* Vol. 23, No. 9, 1997, pp. 929-938.

300. P. Haan and C. F. Lerk. Oral Controlled Release Dosage Forms: A Review. *Pharmaceutisch Weekblad Scientific Edition,* Vol. 6. No. 2, 1984, pp. 57-67.

301. P. Colombo and P. Santi. Swellable and Rigid Matrices: Controlled Release Matrices with Cellulose Ethers. In *Pharmaceutical Dosage Forms: Tablets,* L. L. Augsburger, S. W. Hoang (Editors), Informa Healthcare, Baltimore, USA, 2008, pp. 433-462.

302. C. Maderuelo, A. Zarzuelo and J. M. Lanao. Critical Factors in the Release of Drugs from Sustained Release Hydrophilic Matrices. *Journal of Controlled Release,* Vol. 154, No. 1, 2011, pp. 2-19.

303. J. Adler, A. Jayan and C. D. Melia. A Method for Quantifying Differential Expansion within Hydrating Hydrophilic Matrixes by Tracking Embedded Fluorescent Microspheres. *Journal of Pharmaceutical Sciences,* Vol. 88, No. 3, 1999, pp. 371-377.

304. E. Efentakis and M. Vlachou. Evaluation of High molecular Weight Poly(oxyethylene) (polyox) Polymer: Studies of Flow Properties and Release Rates of Furosemide and Captopril from Controlled-Release Hard Gelatin Capsules. *Pharmaceutical Development and Technology,* Vol. 5, No. 3, 2000, pp. 339-346.

305. J. L. Ford, M. H. Rubinstein, F. McCaul, J. E. Hogan and P. J. Edgar. Importance of Drug Type, Tablet Shape and added Diluents on Drug Release Kinetics from HPMC Matrix Tablets. *International Journal of Pharmaceutics,* Vol. 40, No. 3, 1987, pp. 223-234.

306. M. M. Taludkar, A. Michoel, P. Rombaut and R. Kinget. Comparative Study on Xanthan Gum and Hydroxypropylmethylcellulose as Matrices for Controlled Release Drug Delivery. Compaction and *In Vitro* Release Behaviour. *International Journal of Pharmaceutics,* Vol. 129, No. 1-2, 1996, pp. 233-241.

307. P. S. Hiremath and R. N. Saha. Oral Controlled Release Formulations of Rifampicin. Part II: Effect of Formulation Variables and Process Parameters on *In Vitro* Release. *Drug Delivery,* Vol. 15, No. 3, 2008, pp. 159-168.

308. T. D. Reynolds, S. A. Mitchell and K. M. Balwinski. Investigation of the Effect of Tablet Surface Area/Volume on Drug release from HPMC Controlled-Release Matrix Tablets. *Drug Development and Industrial Pharmacy,* Vol. 28, No. 4, 2002, pp. 457-466.

309. A. Viriden, B. Wittgren and A. Larsson. Investigation of Critical Polymer Properties for Polymer Release and Swelling of HPMC Matrix Tablets. *European Journal of Pharmaceutical Sciences,* Vol. 36, No. 2-3, 2009, pp. 297-309.

310. F. A. Chaibva, S. M. Khamanga and R. B. Walker. Swelling, Erosion and Drug Release Characteristics of Salbutamol Sulfate from Hydroxypropylmethylcellulose-based Matrix Tablets. *Drug Development and Industrial Pharmacy,* Vol. 36, No. 12, 2010, pp. 1497-1510.

311. M. E. Campos-Aldrete and L. Villafuerte-Robles. Influence of the Viscosity Grade and the Particle Size of HPMC on Metronidazole Release from Matrix Tablets. *European Journal of Pharmaceutics and Biopharmaceutics,* Vol. 43, No. 2, 1997, pp. 173-178.

312. M. S. Reza, M. A. Quadir and S. S. Haider. Comparative Evaluation of Plastic, Hydrophobic and Hydrophilic Polymers as Matrices for Controlled-Release Drug Delivery. *Journal of Pharmaceutical Science,* Vol. 6, No. 2, 2003, pp. 282-291.

313. A. T. Pham and P. I. Lee. Probing the Mechanism of Drug Release from Hydroxypropylmethyl Cellulose Matrices. *Journal of Pharmaceutical Research,* Vol. 11, No. 10, 1994, pp. 1379-1384.

314. U. S. Toti and T. M. Aminabhavi. Modified Guar-Gum Matrix Tablet for Controlled-Release of Diltiazem Hydrochloride. *Journal of Controlled Release,* Vol. 95, No. 3, 2004, pp. 567-57722.

315. M. E. Aulton (Editor). Pharmaceutics: The Science of Dosage Form Design. Churchill Livingstone, London, UK, 2nd Edition, 2002, pp. 413-439.

316. K. V. R. Rao and K. P. Devi. Swelling Controlled Release Systems: Recent Developments and Applications. *International Journal of Pharmacy,* Vol. 48, No. 1-3, 1988, pp. 1-13.

317. P. Colombo, R. Bettini, P. Sant, D. Ascentiis and N. A. Peppas. Analysis of the Swelling and Release Mechanisms from Drug Delivery Systems with Emphasis on Drug Solubility and Water Transport. *Journal of Controlled Release,* Vol. 39, No. 2-3, 1996, pp. 231-237.

318. J. W. Skoug, M. T. Borin, J. C. Fleishaker and A. M. Cooper. *In Vitro* and *In Vivo* Evaluation of Whole and Half Tablets of Sustained-Release Adinazolam Mesylate. *Pharmaceutical Research,* Vol. 8, No. 12, 1991, pp. 1482-1488.

319. N. K. Ebube, A. H. Hikal, C. M. Wyandt, D. C. Beer, L. G. Miller and A. B. Jones. Sustained Release of Acetaminophen from Heterogeneous Matrix Tablets: Influence of Polymer Ratio, Polymer Loading, and Co-Active on Drug Release. *Pharmaceutical Development and Technology,* Vol. 2, No. 2, 1997, pp. 161-170.

320. S. Siepe, B. Luecke, A. Kramer, A. Ries and R. Gurny. Strategies for the Design of Hydrophilic Matrix Tablets with Controlled Microenvironmental pH. *International Journal of Pharmaceutics,* Vol. 316, No. 1-2, 2006, pp. 14-20.

321. S. Jamzad, L. Tutunji and R. Fassihi. Analysis of Macromolecular Changes and Drug Release from Hydrophilic Matrix Systems. *International Journal of Pharmaceutics,* Vol. 291, No. 1-2, 2005, pp. 75-85.

322. C. Gustafsson, M. C. Bonferoni, C. Caramella, H. Lennholm and C. Nyström. Characterisation of Particle Properties and Compaction Behaviour of Hydroxypropyl Methylcellulose with Different Degrees of Methoxy/Hydroxypropyl Substitution. *European Journal of Pharmaceutical Sciences,* Vol. 9, No. 2, 1999, pp. 171-184.

323. P. York. A Consideration of Experimental Variables in the Analysis of Powder Compaction Behaviour. *Journal of Pharmaceutics and Pharmacology,* Vol. 31, No. 4, 1979, pp. 244-246.

324. F. Sadeghi, J. L. Ford and A. R. Siahboomi. The Influence of Drug Type on the Release Profiles from Surelease-Coated Pellets. *International Journal of Pharmaceutics,* Vol. 254, No. 2, 2003, pp. 123-135.

325. M. J. Habib and R. Mesue. Development of Controlled-Release Formulations of Ketoprofen for Oral Use. *Drug Development and Industrial Pharmacy,* Vol. 21, No. 12, 1995, pp. 1463-1472.

326. A. G. Thombre, G. M. Zentner and K. J. Himmelstein. Mechanism of Water Transport in Controlled Porosity Osmotic Devices. *Journal of Membrane Science*, Vol. 40, No. 3, 1989, pp. 279-310.

327. F. Theeumes. Elementary Osmotic Pump. *Journal of Pharmaceutical Sciences,* Vol. 64, No. 12, 1975, pp. 1987-1991.

328. D. Prabakaran, P. Singh, P. Kanaujia and S. P. Vyas. Effect of Hydrophilic Polymers on the Release of Diltiazem Hydrochloride from Elementary Osmotic Pumps. *International Journal of Pharmaceutics,* Vol. 259, No. 1, 2003, pp. 173-179.

329. L. Liu, G. Khang, J. M. Rhee and H. B. Lee. Monolithic Osmotic Tablet Systems for Nifedipine Delivery. *Journal of Controlled Release,* Vol. 67, No. 1-3, 2000, pp. 309-322.

330. X. Li, W. Pan, S. Nie and L. Wu. Studies on Controlled-Release Effervescent Osmotic Pump Tablets from Traditional Chinese Medicine Compound Recipe. *Journal of Controlled Release,* Vol. 96, No. 3, 2004, pp. 359-367.

331. M. S. Reza, M. A. Quadir and S. S. Haider. Comparative Evaluation of Plastic, Hydrophobic and Hydrophilic Polymers as Matrices for Controlled-Release Drug Delivery. *Journal of Pharmacy and Pharmaceutical Sciences,* Vol. 6, No. 2, 2003, pp. 282-291.

332. K. Mitchell, J. L. Ford, D. J. Armstrong, P. N. C. Elliott, C. Rostron and J. E. Hogan. The Influence of Concentration on the Release of Drugs from Gels and Matrices

Containing Methocel®. *International Journal of Pharmaceutics,* Vol. 100, No. 1-3, 1993, pp. 155-163.

333. N. K. Ebube and A. B. Jones. Sustained Release of Acetaminophen from a Heterogeneous Mixture of Two Hydrophilic Non-Ionic Cellulose Ether Polymers. *International Journal of Pharmaceutics,* Vol. 272, No. 1-2, 2004, pp. 19-27.

334. R. L. C. Sasidhar. Effect of Diluents on the Release Rate of Venlafaxine HCl from Matrix Tablets. *Journal of Pharmacy Research,* Vol. 4, No. 1, 2011, pp. 153.

335. G. S. Rekh, R. V. Nellore, A. S. Hussain, L. G. Tillman, H. J. Malinowski and L. L. Augsburger. Identification of Critical Formulation and Processing Variables for Metoprolol Tartrate Extended-Release (ER) Matrix Tablets. *Journal of Controlled Release,* Vol. 59, No. 3, 1999, pp. 327-342.

336. R. O. Williams, T. D. Reynolds, T. D. Cabelka, M. A. Sykora and V. Mahaguna. Investigation of Excipient Type and Level on Drug Release from Controlled Release Tablets Containing HPMC. *Journal of Pharmaceutical Development and Technology,* Vol. 7, No. 2, 2002, pp. 181-193.

337. S. K. Baveja, K. V. Ranga Rao, D. K. Padmalatha. Zero-Order Release Hydrophilic Matrix Tablets of β-Adrenergic Blockers. *International Journal of Pharmaceutics,* Vol. 39, No. 1-2, 1987, pp. 39-45.

338. M. Harihara. Optimisation of Sustained-Release Tablet Formulations: A Four-Component Mixture Experiment. *Pharmaceutical Development and Technology,* Vol. 4, No. 4, 1999, pp. 39.

339. B. Perez-Marcos, J. L. Ford, D. J. Armstrong, P. N. Elliott, C. Rostron and J. E. Hogan. Influence of pH on the Release of Propranolol Hydrochloride from Matrices Containing Hydroxypropylmethylcellulose K4M and Carbopol 974. *Journal of Pharmaceutical Sciences,* Vol. 85, No. 3, 1996, pp. 330-334.

340. S. M. Samani, H. Montaseri and A. Kazemi. The Effect of Polymer Blends on Release Profiles of Diclofenac Sodium from Matrices. *European Journal of Pharmaceutics and Biopharmaceutics,* Vol. 55, No. 3, 2003, pp. 351-355.

341. N. M. Harish, N. Mathew, R. N. Charyulu and P. Prabhu. Improved Bioavailability of Pefloxacin using Controlled Release Ocular Inserts. *International Journal of Pharmacy and Pharmaceutical Sciences,* Vol. 1, 2009, pp. 71-77.

342. M. M. Rahman, H. M. Sayeed, A. Ashiqul, R. Sumon, K. J. Mithilesh, M. A. Qamrul Ahsan and M. H. Rahman. Formulation and Evaluation of Ranolazine Sustained Release Matrix Tablets Using Eudragit and HPMC. *International Journal of Pharmaceutical and Biomedical Research,* Vol. 2, No. 1, 2011, pp. 7-12.

343. B. G. Prajapati and K. R. Patel. Once-Daily Sustained-Release Matrix Tablets of Losartan Potassium: Formulation and *In Vitro* Evaluation. *International Journal of Medical and Clinical Research,* Vol. 1, No. 1, 2010, pp. 1-7.

344. S. K. Swain, Ch. P. Niranjan, J. Sruti and M. E. R. Bhanoji. Design and Evaluation of Sustained Release Dispersions of Verapamil Hydrochloride. *International Journal of Pharmaceutical Sciences and Nanotechnology,* Vol. 3, No. 4, 2011, pp. 1252-1262.

345. *United States Pharmacopoeia Incorporating 'The National Formulary.'* United States Pharmacopoeial Convention, Washington, USA, 34th Edition, Vol. 1, 2011, pp. 33-415.

346. A. A. Karnachi and M. A. Khan. Box-Behnken Design for the Optimisation of Formulation Variables of Indomethacin Coprecipitates with Polymer Mixtures. *International Journal of Pharmaceutics,* Vol. 131, No. 1, 1996, pp. 9-17.

347. A. Abd Elbary, A. A. Aboelwafa and I. M. Al Sharabi. Once Daily, High-Dose Meselazine Controlled-Release Tablet for Colonic Delivery: Optimisation of Formulation Variables Using Box-Behnken Design. *Pharmaceutical Science and Technology,* Vol. 12, No. 4, 2011, pp. 1454-1464.

348. C. K. Ghandi, T. J. Mehta, M. R. Patel, K. R. Patel and N. M. Patel. Box-Behnken Design for Optimisation of Formulation Variables of Tramadol HCl Sustained Release Matrix Tablets. *International Journal for Pharmaceutical Research Scholars,* Vol. 1, No. 2, 2012, pp. 99-114.

349. L. Prabakaran and M. Vishalin. Hydrophilic Polymers Matrix Systems of Nifedipine Sustained Release Matrix Tablets: Formulation Optimisation by Response Surface Methodology. *Der Pharmacia Sinica,* Vol. 1, No. 1, 2010, pp. 147-165.

350. S. K. Singh, J. Dodge, M. J. Durrani and M. A. Khan. Optimisation and Characterisation of Controlled Release Pellets Coated with an Experimental Latex: I. Anionic drug. *International Journal of Pharmaceutics,* Vol. 125, No. 2, 1995, pp. 243-255.

351. A. Palamakula, M. T. H. Nutan and M. A. Khan. Response Surface Methodology for Optimisation and Characterisation of Limonene-based Coenzyme Q10 Self-Nanoemulsified Capsule Dosage Form. *Pharmaceutical Science and Technology,* Vol. 5, No. 4, 2004, pp. 114-121.

352. A. Boza, Y. Cruz, G. Jordan, U. Jauregui-Haza, A. Aleman and I. Caraballo. Statistical Optimisation of a Sustained-Release Matrix Tablet of Lobenzarit Disodium. *Drug Development and Industrial Pharmacy,* Vol. 26, No. 12, 2000, pp. 1303-1307.

353. *Statistics for Experiments: Design, Innovation and Discovery.* G. E. P. Box, J. S. Hunter and W. G. Hunter, Wiley-Interscience, New York, USA, 2nd Edition, 2005, pp. 10-359.

354. *Statistical Design-Chemometrics.* R. E. Bruns, I. S. Scarminio and B. B. Neto. Elsevier, Amsterdam, Netherlands, Vol. 25, 2006, pp. 1-412.

355. S. Govender, V. Pillay, D. J. Chetty, S. Y. Essack, C. M. Dangor and T. Govender. Optimisation and Characterisation of Bioadhesive Controlled Release Tetracycline Microspheres. *International Journal of Pharmaceutics,* Vol. 306, No. 1-2, 2005, pp. 24-40.

356. S. L. C. Ferreira, R. E. Bruns, H. S. Ferreira, G. D. Matos, J. M. David, G. C. Brandao, E. G. P. da Silva, L. A. Portugal, P. S. dos Reis, A. S. Souza and W. N. L. dos Santos. Box-Behnken Design: An Alternative for the Optimisation of Analytical Methods. *Analytica Chimica Acta,* Vol. 597, No. 2, 2007, pp. 179-186.

357. K. J. Wadher, R. B. Kakde and M. J. Umekar. Development of a Sustained-Release Tablet of Metformin Hydrochloride Containing Hydrophilic Eudragit® and Ethylcellulose Polymer. *International Journal of Comprehensive Pharmacy*, Vol. 02, No.05, 2011, pp. 1-6.

358. M. Efentakis, A. Koutlis, and M. Vlachou. Development and Evaluation of Oral Multiple-Unit and Single-Unit Hydrophilic Controlled-Release Systems. *Pharmaceutical Science and Technology,* Vol. 1, No. 4, 2000, pp. 1-9.

359. B. Narasimhan, S. Mallapragada and N. Peppas. Release Kinetics - Data Interpretation. *Encyclopedia of Controlled Drug Delivery*, E. Mathiowitz (Editor), John Wiley and Sons, New York, 1999, pp. 921-935.

360. S. Dash, P. N. Murthy, L. Nath and P. Chowdhury. Kinetic Modelling on Drug Release from Controlled Delivery Systems. *Acta Paloniae Pharmaceutica- Drug Research,* Vol. 67, No. 3, 2010, pp. 217-223.

361. R. Langer and N. Peppas. Chemical and Physical Structure of Polymers as Carriers for Controlled Release of Bioactive Agents- A Review. *Journal of Macromolecular Science - Reviews in Macromolecular Chemistry and Physics,* Vol. C23, No. 1, 1983, pp. 61-126.

362. C. G. Varelas, D. G. Dixon and C. A. Steiner. Zero-Order Release from Biphasic Polymer Hydrogels. *Journal of Controlled Release,* Vol. 34, No. 3, 1995, pp. 185-192.

363. A. Sood and R. Panchangnula. Drug Release Evaluation of Diltiazem CR Preparations. *International Journal of Pharmaceutics,* Vol. 175, No. 1, 1998, pp. 95-107.

364. M. Gibalde and S. Feldman. Establishment of Sink Conditions in Dissolution Rate Determinations- Theoretical Considerations and Applications. *Journal of Pharmaceutical Science,* Vol. 56, No. 10, 1967, pp. 1238-1242.

365. T. Higuchi. Rate of Release of Medicaments from Ointment Bases Containing Drugs in Suspensions. *Journal of Pharmaceutical Science,* Vol. 50, 1961, pp. 874-875.

366. H. Lapidus and N. G. Lordi. Drug Release from Compressed Hydrophilic Matrices. *Journal of Pharmaceutical Science,* Vol. 57, No. 8, 1968, pp. 1292-1301.

367. S. J. Desai, A. P. Simonelli, and W. I. Higuchi. Investigation of Factors Influencing Release of Solid Drug Dispersed in Inert Matrices. *Journal of Pharmaceutical Science,* Vol. 54, No. 10, 1965, pp. 1459-1464.

368. S. J. Desai, A. P. Simonelli, W.I. Higuchi. Investigation of Factors Influencing Release of Solid Drug Dispersed in Inert Matrices, II. *Journal of Pharmaceutical Science,* Vol. 55, No. 11, 1965, pp. 1224-1229.

369. T. Higuchi. Mechanism of Sustained Action Medication. *Journal of Pharmaceutical Science,* Vol. 52, No. 12, 1963, pp. 1145-1149.

370. N. A. Peppas. Analysis of Fickian and non-Fickian Drug Release from Polymers. *Pharmaceutica Acta Helvetiae,* Vol. 60, No. 4, 1985, pp. 110-111.

371. N. Peppas and R. W. Korsmeyer. Dynamically Swelling Hydrogels in Controlled Release Applications. *Hydrogels in Medicine and Pharmacy*, Vol. 15, 1986, pp. 109-110.

372. K. F. Chou, C. C. Han and S. Lee. Buffer Transport in Hydroxyethyl Methacrylate Copolymer Irradiated by Gamma Rays. *Polymer,* Vol. 42, No. 11, 2001, pp. 4989-4996.

373. T. T. Wang, T. K. Kwei and H. L. Frisch. Diffusion in Glassy Polymers, III. *Journal of Polymer Science,* Vol. 7, No. 12, 1968, pp. 2019-2028.

374. J. Siepmann and N. Peppas. Modelling of Drug Release from Delivery Systems Based on Hydroxypropylmethylcellulose (HPMC). *Advanced Drug Delivery Review,* Vol. 48, No. 1, 2001, pp. 139-157.

375. P. L. Rigter and N. Peppas. A Simple Equation for the Description of Solute release: I. Fickian and non-Fickian Release from Non Swellable Devices in the Form of Slabs, Spheres, Cylinders or Discs. *Journal of Controlled Release,* Vol. 5, 1987, pp. 23-36.

376. P. L. Rigter and N. Peppas. A Simple Equation for Description of Solute Release: II. Fickian and Anomalous Release from Swellable Devices. *Journal of Controlled Release,* Vol. 5, 1987, pp. 37-42.

377. P. J. Niebergall, G. Milosovich and J. E. Goyan. Dissolution Rate Studies. II. Dissolution of Particles under Conditions of Rapid Agitation. *Journal of Pharmaceutical Science,* Vol. 52, No. 3, 1963, pp. 236-241.

378. R. Bushra, M. H. Shoaib, N. Aslam, D. Hashmat and M. U. Rehman. Formulation Development and Optimisation of Ibuprofen Tablets by Direct Compression Method. *Journal of Pharmaceutical Science,* Vol. 21, No. 2, 2008, pp. 113-12041.

379. S. Chandran, K. S. Sanjay and L. F. Ali Asghar. Microspheres with pH Modulated Release: Design and Characterisation of Formulation Variables for Colonic Delivery. *Journal of Microencapsulation,* Vol. 26, No. 5, 2009, pp. 420-431.

380. N. Kavanagh and O. I. Corrigan. Swelling and Erosion Properties of Hydroxypropylmethylcellulose Matrices- Influence of Agitation Rate and Dissolution Medium Composition. *International Journal of Pharmaceutics,* Vol. 279, No. 1-2, 2004, pp. 141-152.

381. K. Tahara, K. Yamamoto and T. Nishihata. Overall Mechanism behind Matrix Sustained Release (SR) Tablets Prepared with Hydroxypropylmethylcellulose 2910. *Journal of Controlled Release,* Vol. 35, No. 1, 1995, pp. 59-66.

382. T. D. Reynolds, S. H. Gehrke, A. S. Hussain and L. S. Shenouda. Polymer Erosion and Drug Release Characterisation of Hydroxypropylmethylcellulose Matrices. *Journal of Pharmaceutical Sciences,* Vol. 87, No. 9, 1998, pp. 1115-1123.

383. B. M. Al-Taani and B. M. Tashtoush. Effect of Microenvironment pH of Swellable and Erodible Buffered Matrices on the Release Characteristics of Diclofenac Sodium. *Pharmaceutical Science and Technology,* Vol. 4, No. 3. 2003, Article 43.

384. K. Mitchell, J. L. Ford, D. J. Armstrong, P. N. C. Elliott, C. Rostron and J. E. Hogan. The Influence of Additives on the Cloud Point, Disintegration and Dissolution of Hydroxypropylethylcellulose Gels and Matrix Tablets. *International Journal of Pharmaceutics,* Vol. 66, 1990, pp. 233-242.

385. B. J. Lee, S. G. Ryu and J. H. Cui. Formulation and Release Characteristics of Hydroxypropyl Methylcellulose Matrix Tablet Containing Melatonin. *Drug Development and Industrial Pharmacy,* Vol. 25, No. 4, 1999, pp. 493-501.

386. L. S. C. Wan, P. W. S. Heng and L. F. Wong. The Effect of Hydroxypropylmethyl Cellulose on Water Penetration into Matrix System. *International Journal of Pharmaceutics,* Vol. 73, No. 2, 1991, pp. 111-116.

387. N. Sarkar. Thermal Gelation Properties of Methyl and Hydroxypropylmethyl Cellulose. *Journal of Applied Polymer Science and Symposium,* Vol. 24, No. 4, 1979, pp. 1073-1087.

388. P. R. Ravi, S. Ganga and R. N. Saha. Design and *In Vitro* Evaluation of Zidovudine Oral Controlled Release Tablets Prepared using Hydroxypropylmethyl Cellulose. *Chemical and Pharmaceutical Bulletin,* Vol. 56, No. 4, 2008, pp. 518-524.

389. S. Nazzal, Z. Abdel-Azim and M. A. Khan. Effect of Extragranular Microcrystalline Cellulose on Compaction, Surface Roughness, and *In Vitro* Dissolution of a Self-Nanoemulsified Solid Dosage Form of Ubiquinone. *Pharmaceutical Technology,* Vol. 65, 2002, pp. 86-98.

390. D. Sixsmith. Effect of Compression on Some Physical Properties of Microcrystalline Cellulose Powders. *Journal of Pharmacy and Pharmacology,* Vol. 29, No. 1, 1977, pp. 33-36.

391. Y. Javadzadeh, H. Shariati and E. Movahhed-Danesh. Effect of Some Commercial Grades of Microcrystalline Cellulose on Flowability, Compressibility, and Dissolution Profile of Piroxicam Liquisolid Compacts. *Drug Development and Industrial Pharmacy,* Vol. 35, No. 2, 2009, pp. 243-251.

392. E. I. Keleb, A. Vermeire, C. Vervaet and J. P. Remon. Extrusion Granulation and High Shear Granulation of Different Grades of Lactose and Highly Dosed Drugs: A Comparative Study. *Drug Development and Industrial Pharmacy,* Vol. 30, No. 6, 2004, pp. 679-691.

393. A. Streubel, J. Siepmann, A. Dashevsky and R. Bodmeir. pH-Independent Release of a Weakly Basic Drug from Water-Insoluble and Soluble Matrix Tablets. *Journal of Controlled Release,* Vol. 67, No. 1, 2000, pp. 101-110.

APPENDIX ONE

BATCH PRODUCTION RECORD-NVP001

LABORATORY SCALE MANUFACTURE

A sample batch production record for Batch NVP001, a laboratory scale tablet formulation is shown. The batch production records for the other batches are available on request.

RHODES UNIVERSITY, FACULTY OF PHARMACY

GRAHAMSTOWN, 6140, SOUTH AFRICA

BATCH PRODUCTION RECORD

Product name: **Nevirapine tablets**	**Page 1 0f 3**
Batch number: **NVP001**	**Batch size: 400 g**
Batch record issued by:	**Date:**
Batch record verified by:	**Date:**

SIGNATURE AND INITIAL REFERENCE			
Full name (Print)	Signature	Initials	Date

RHODES UNIVERSITY, FACULTY OF PHARMACY

GRAHAMSTOWN, 6140, SOTH AFRICA

BATCH PRODUCTION RECORD

Product name: Nevirapine tablets **Page 2 of 3**
Batch number: NVP001 **Batch size: 400 g**

BATCH FORMULA					
Material	Rhodes No.	Quantity (% w/w)	Amount dispensed	Dispensed by	Checked by
NVP	RM000260	33.3	133.2		
Methocel® K4M	RM000060	30.0	120.0		
SuperTab® SDL	RM000161	10.0	40.0		
Avicel® PH102	RM000038	13.5	54.0		
Emcompress®	RM000059	10.0	40.0		
Mg stearate	RM000304	1.10	4.4		
Talc	RM000050	1.00	4.0		
Colloidal silicon dioxide	RM000305	1.10	4.4		

EQUIPMENT VERIFICATION			
Description	Type	Verified by	Confirmed by
Weighing balance	Model 500C PJ Precisa®		
Cube blender			
Sieve	# 20 and 44 mesh size		
Tableting machine	Manesty B3B Rotary Press		

RHODES UNIVERSITY, FACULTY OF PHARMACY

GRAHAMSTOWN, 6140, SOUTH AFRICA

BATCH PRODUCTION RECORD

Product name: Nevirapine tablets **Page 3 of 3**
Batch number : NVP001 **Batch size: 400 g**

MANUFACTURING PROCEDURE			
Steps	**Procedure**	**Done by**	**Checked by**
1	Screen all Weighed materials through #20 mesh screen (except mg stearate and talc). Use # 44 mesh screen for mg stearate and talc.		
2	Blend the excipients screened using #20 mesh screen in a cube blender rotating at 200 rpm for 30 minutes		
3	Add mg stearate and talc to 2 and blend for further 3 minutes		
4	Assess powder characteristics; angle of repose, bulk density, tapped density		
5	Tablet the powder blends on Manesty B3B Rotary press manually to set weight and hardness		
6	Set the machine to automatic mode and check for weight and hardness of the tablets every minute		
7	Calculate % yield		

	when process is complete		
8	Pack the tablets in self-sealing plastic bags for analysis		

APPENDIX TWO

BATCH SUMMARY

BATCH SUMMARY – NVP001

Faculty of Pharmacy, Rhodes University

Formulator:	Chiluba Mwila	**Batch size:**	400 g
Product:	Nevirapine tablets	**Blending Time (start):**	17h00 pm
Batch Number:	NVP001	**(end):**	17h45 pm
Blending Date:	07-03-2012	**Tableting Time (start):**	20h45 pm
Tableting Date:	07-03-2012	**(end):**	21h15 pm

Formula

Material	%w/w	Amount added (g)	Rhodes #
NVP	33.3	133.2	RM000260
Methocel® K4M	30.0	120.0	RM000060
SuperTab®	10.0	40.0	RM000161
Avicel® PH102	13.5	54.0	RM000038
DCP	10.0	40.0	RM000059
Mg stearate	1.1	4.4	RM000304
Talc	1.1	4.0	RM000050
Colloidal silicon dioxide	1.0	4.4	RM000305

Dissolution profile

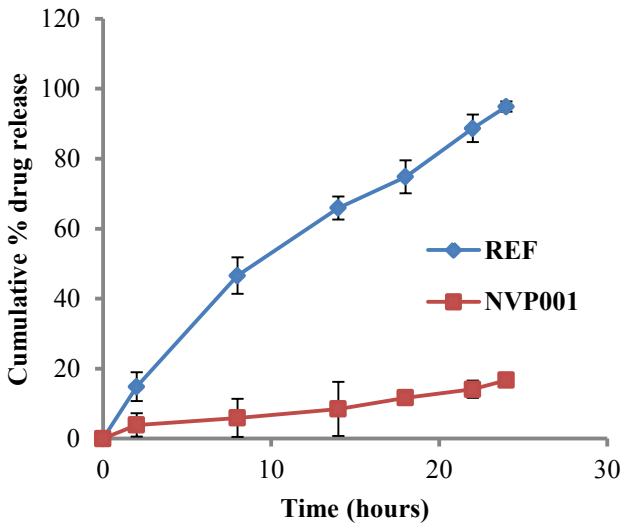

Target weight: 300 mg
Actual weight: 297.3±1.77
Target hardness: 100 – 150 N
Actual hardness:108.4±3.20
Tensile Strength: 1.43±2.01
Friability: 0.158±1.22
%Assay: 97.4±2.88
Temperature: 23.8°C
Humidity: 60.0 %
Yield: 77.3 %

Comments

-No sticking
-No edge splitting
-No capping
-Smooth surface finish

BATCH SUMMARY – NVP002

Faculty of Pharmacy, Rhodes University

Formulator:	Chiluba Mwila	**Batch size:**	400 g
Product:	Nevirapine tablets	**Blending Time (start):**	18h25 pm
Batch Number:	NVP002	**(end):**	19h20 pm
Blending Date:	07-03-2012	**Tableting Time (start):**	21h25 pm
Tableting Date:	07-03-2012	**(end):**	21h50 pm

Formula

Material	%w/w	Amount added (g)	Rhodes #
NVP	33.3	133.2	RM000260
Methocel® K4M	25.0	100.0	RM000060
SuperTab®	15.0	60.0	RM000161
Avicel® PH102	13.5	54.0	RM000038
DCP	10.0	40.0	RM000059
Mg stearate	1.1	4.4	RM000304
Talc	1.0	4.0	RM000050
Colloidal silicon dioxide	1.1	4.4	RM000305

Dissolution profile

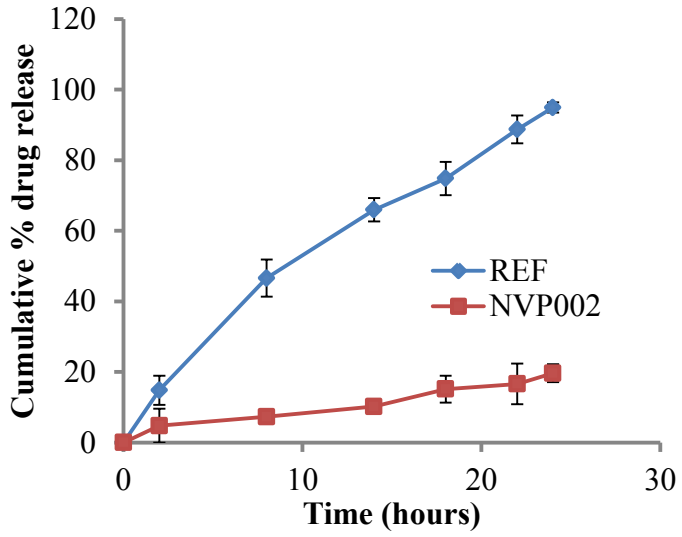

Target weight: 300 mg
Actual weight: 290.3±2.88
Target hardness: 100 – 150 N
Actual hardness:117.8±4.11
Tensile Strength: 1.56±2.23
Friability: 0.169±2.87
%Assay: 99.6±3.07
Temperature: 23.8°C
Humidity: 60.0 %
Yield: 77.3 %

Comments

-No sticking
-No edge splitting
-No capping
-Smooth surface finish

BATCH SUMMARY – NVP003

Faculty of Pharmacy, Rhodes University

Formulator:	Chiluba Mwila	**Batch size:**	400 g
Product:	Nevirapine tablets	**Blending Time (start):**	19h45 pm
Batch Number:	NVP003	**(end):**	20h35 pm
Blending Date:	07-03-2012	**Tableting Time (start):**	22h00 pm
Tableting Date:	07-03-2012	**(end):**	22h35 pm

Formula

Material	%w/w	Amount added (g)	Rhodes #
NVP	33.3	133.2	RM000260
Methocel® K4M	20.0	80.0	RM000060
SuperTab®	20.0	80.0	RM000161
Avicel® PH102	13.5	54.0	RM000038
DCP	10.0	40.0	RM000059
Mg stearate	1.1	4.4	RM000304
Talc	1.0	4.0	RM000050
Colloidal silicon dioxide	1.1	4.4	RM000305

Dissolution profile

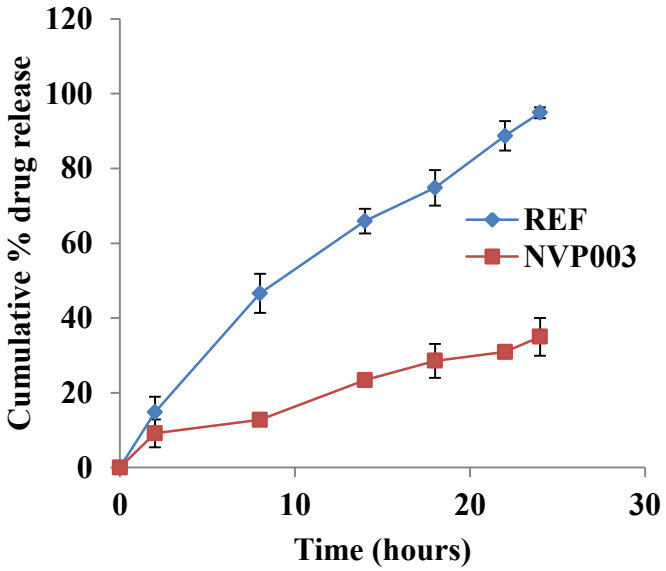

Target weight: 300 mg
Actual weight: 295.6±2.82
Target hardness: 100 – 150 N
Actual hardness:100.5±6.93
Tensile Strength: 1.33±3.12
Friability: 0.171±2.34
%Assay: 96.3±2.89
Temperature: 23.8°C
Humidity: 60.0 %
Yield: 77.3 %

Comments

-No sticking
-No edge splitting
-No capping
-Smooth surface finish

BATCH SUMMARY – NVP004

Faculty of Pharmacy, Rhodes University

Formulator:	Chiluba Mwila	**Batch size:**	300 g
Product:	Nevirapine tablets	**Blending Time (start):**	12h30 pm
Batch Number:	NVP004	**(end):**	13h08 pm
Blending Date:	12-03-2012	**Tableting Time (start):**	14h55 pm
Tableting Date:	12-03-2012	**(end):**	15h20 pm

Formula

Material	%w/w	Amount added (g)	Rhodes #
NVP	33.3	100.0	RM000260
Methocel® K4M	10.0	30.0	RM000060
SuperTab® Spray dried lactose	40.0	120.0	RM000161
Avicel® PH102	13.5	40.5	RM000038
Mg stearate	1.1	3.3	RM000304
Talc	1.0	3.0	RM000050
Colloidal silicon dioxide	1.1	3.3	RM000305

Dissolution profile

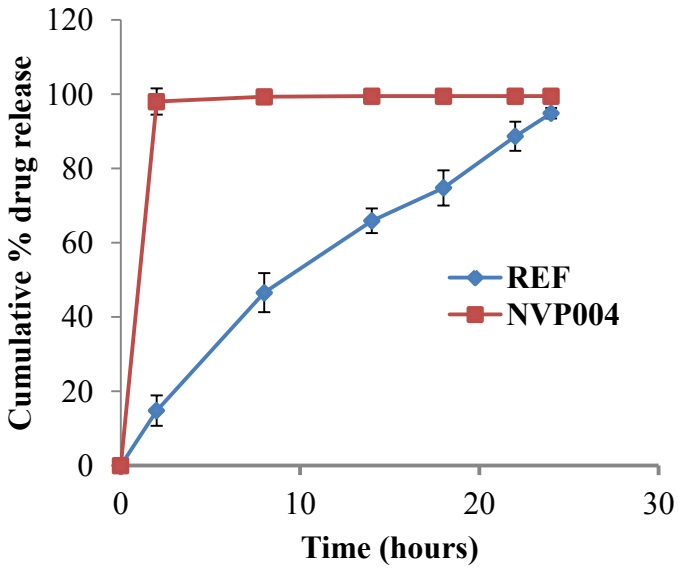

Target weight: 300 mg
Actual weight: 295.6±2.82
Target hardness: 100 – 150 N
Actual hardness:118.3±4.42
Tensile Strength: 1.56±3.23
Friability: 0.166 ±3.33
%Assay: 98.7±3.67
Temperature: 24.1°C
Humidity: 56.0 %
Yield: 79.4 %

Comments

-No sticking
-No edge splitting
-No capping
-Smooth surface finish

BATCH SUMMARY – NVP005

Faculty of Pharmacy, Rhodes University

Formulator:	Chiluba Mwila	**Batch size:**	300 g
Product:	Nevirapine tablets	**Blending Time (start):**	13h12 pm
Batch Number:	NVP005	**(end):**	13h40 pm
Blending Date:	12-03-2012	**Tableting Time (start):**	15h48 pm
Tableting Date:	12-03-2012	**(end):**	16h05 pm

Formula

Material	%w/w	Amount added (g)	Rhodes #
NVP	33.3	100.0	RM000260
Methocel® K4M	20.0	60.0	RM000060
SuperTab® Spray dried lactose	30.0	90.0	RM000161
Avicel® PH102	13.5	40.5	RM000038
Mg stearate	1.1	3.3	RM000304
Talc	1.0	3.0	RM000050
Colloidal silicon dioxide	1.1	3.3	RM000305

Dissolution profile

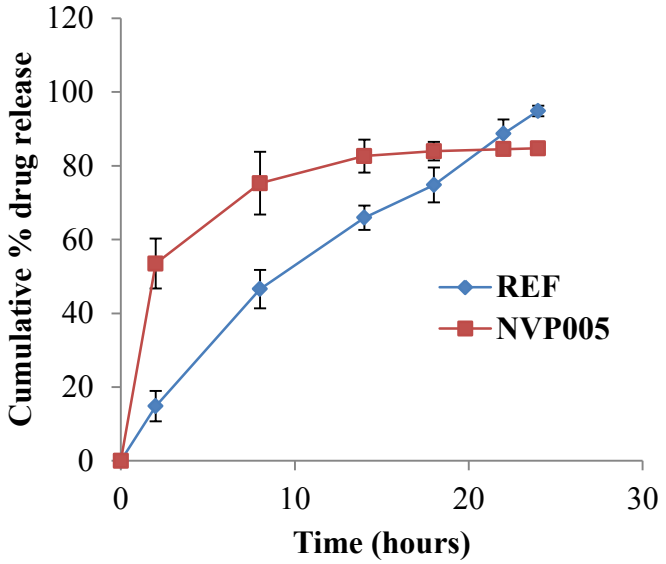

Target weight: 300 mg
Actual weight: 299.2±3.03
Target hardness: 100 – 150 N
Actual hardness:129.7±5.81
Tensile Strength: 1.71±2.72
Friability: 0.166±3.33
%Assay: 97.9±3.66
Temperature: 24.1°C
Humidity: 56.0 %
Yield: 89.7 %

Comments
-No sticking
-No edge splitting
-No capping
-Smooth surface finish

BATCH SUMMARY – NVP006

Faculty of Pharmacy, Rhodes University

Formulator:	Chiluba Mwila	**Batch size:**	300 g
Product:	Nevirapine tablets	**Blending Time (start):**	13h45 pm
Batch Number:	NVP006	**(end):**	14h19 pm
Blending Date:	12-03-2012	**Tableting Time (start):**	16h19 pm
Tableting Date:	12-03-2012	**(end):**	16h33 pm

Formula

Material	%w/w	Amount added (g)	Rhodes #
NVP	33.3	100	RM000260
Methocel® K4M	30.0	90.0	RM000060
SuperTab® Spray dried lactose	20.0	60.0	RM000161
Avicel® PH102	13.5	40.5	RM000038
Mg stearate	1.1	3.3	RM000304
Talc	1.0	3.0	RM000050
Colloidal silicon dioxide	1.1	3.3	RM000305

Dissolution profile

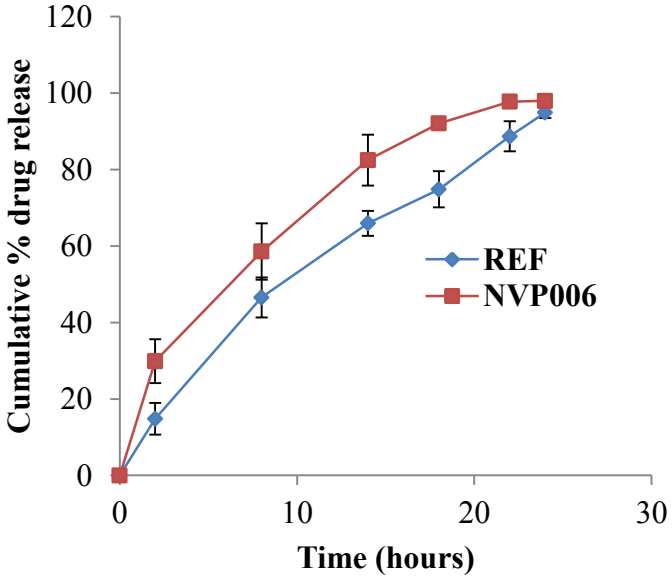

Target weight: 300 mg
Actual weight: 298.2±3.44
Target hardness: 100 – 150 N
Actual hardness:110.9±3.82
Tensile Strength: 1.47±1.91
Friability: 0.169±2.88
%Assay: 98.9±2.96
Temperature: 24.1°C
Humidity: 56.0 %
Yield: 77.9 %

Comments

-No sticking
-No edge splitting
-No capping
-Smooth surface finish

BATCH SUMMARY – NVP007

Faculty of Pharmacy, Rhodes University

Formulator:	Chiluba Mwila	**Batch size:**	300 g
Product:	Nevirapine tablets	**Blending Time (start):**	14h00 pm
Batch Number:	NVP007	**(end):**	14h40 pm
Blending Date:	17-03-2012	**Tableting Time (start):**	18h45 pm
Tableting Date:	17-03-2012	**(end):**	19h10 pm

Formula

Material	%w/w	Amount added (g)	Rhodes #
NVP	33.3	100	RM000260
Methocel® K4M	10.0	30.0	RM000060
SuperTab® Spray dried lactose	35.0	105.0	RM000161
Avicel® PH102	13.5	40.5	RM000038
Carbopol® 71G NF	5.0	15.0	RM000119
Mg stearate	1.1	3.3	RM000304
Talc	1.0	3.0	RM000050
Colloidal silicon dioxide	1.1	3.3	RM000305

Dissolution profile

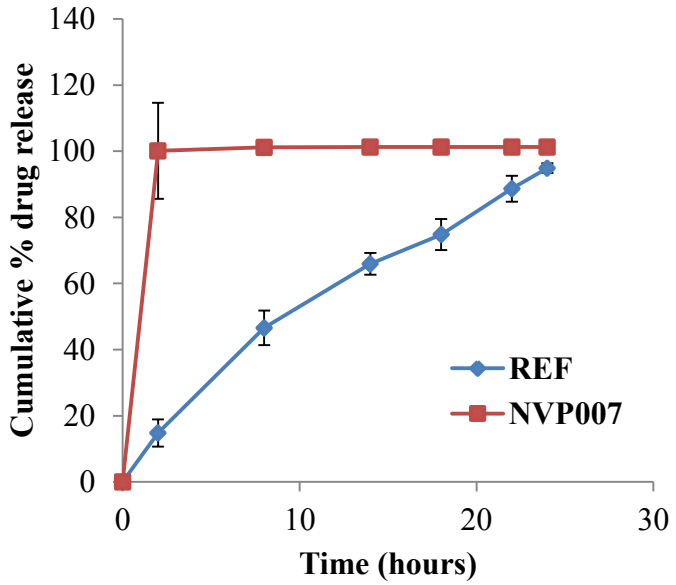

Target weight: 300 mg
Actual weight: 297.9±2.37
Target hardness: 100 – 150 N
Actual hardness:114.5±2.73
Tensile Strength: 1.51±2.11
Friability: 0.171±2.71
%Assay: 97.8±3.22
Temperature: 23.8°C
Humidity: 43.0 %
Yield: 69.7 %

Comments

-No sticking
-No edge splitting
-No capping
-Smooth surface finish

BATCH SUMMARY – NVP008

Faculty of Pharmacy, Rhodes University

Formulator:	Chiluba Mwila	**Batch size:**	300 g
Product:	Nevirapine tablets	**Blending Time (start):**	14h45 pm
Batch Number:	NVP008	**(end):**	15h25 pm
Blending Date:	17-03-2012	**Tableting Time (start):**	19h45 pm
Tableting Date:	17-03-2012	**(end):**	20h20 pm

Formula

Material	%w/w	Amount added (g)	Rhodes #
NVP	33.3	100	RM000260
Methocel® K4M	10.0	30.0	RM000060
SuperTab® Spray dried lactose	30.0	90.0	RM000161
Avicel® PH102	13.5	40.5	RM000038
Carbopol® 71G NF	10.0	30.0	RM000119
Mg stearate	1.1	3.3	RM000305
Talc	1.0	3.0	RM000050
Colloidal silicon dioxide	1.1	3.3	RM000305

Dissolution profile

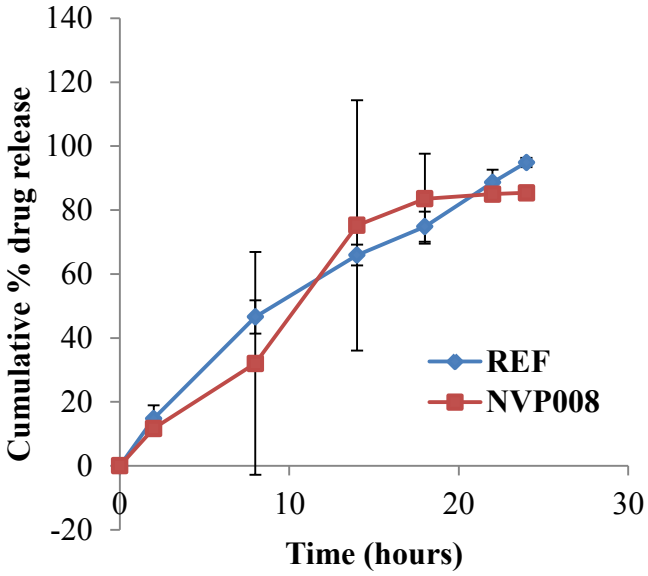

Target weight: 300 mg
Actual weight: 294.7±3.58
Target hardness: 100 – 150 N
Actual hardness:120.2±3.86
Tensile Strength: 1.58±3.12
Friability: 0.171±4.32
%Assay: 96.7±3.82
Temperature: 23.8°C
Humidity: 43.0 %
Yield: 60.4 %

Comments

-No sticking
-No edge splitting
-No capping
-Smooth surface finish

BATCH SUMMARY – NVP009

Faculty of Pharmacy, Rhodes University

Formulator:	Chiluba Mwila	**Batch size:**	300 g
Product:	Nevirapine tablets	**Blending Time (start):**	15h30 pm
Batch Number:	NVP009	**(end):**	16h05 pm
Blending Date:	17-03-2012	**Tableting Time (start):**	20h28 pm
Tableting Date:	17-03-2012	**(end):**	20h58 pm

Formula

Material	%w/w	Amount added (g)	Rhodes #
NVP	33.3	100	RM000260
Methocel® K4M	10.0	30.0	RM000060
SuperTab® Spray dried lactose	25.0	75.0	RM000161
Avicel® PH102	13.5	40.5	RM000038
Carbopol® 71G NF	15.0	45.0	RM000119
Mg stearate	1.1	3.3	RM000304
Talc	1.0	3.0	RM000050
Colloidal silicon dioxide	1.1	3.3	RM000305

Dissolution profile

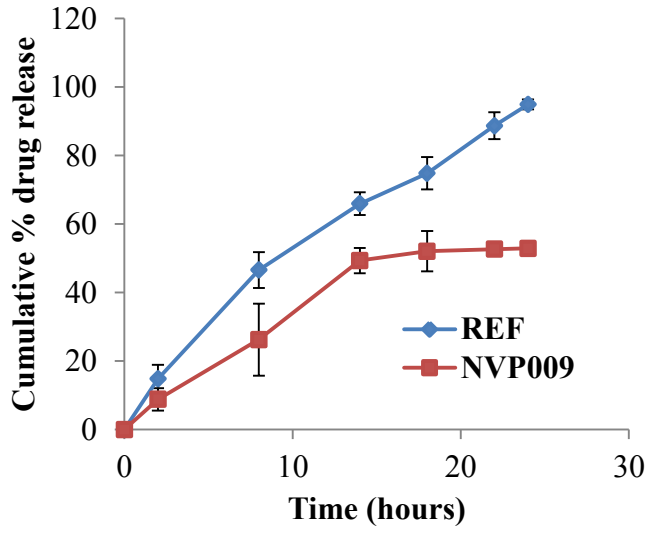

Target weight: 300 mg
Actual weight: 301.5±1.83
Target hardness: 100 – 150 N
Actual hardness:101.7±3.80
Tensile Strength: 1.33±2.82
Friability: 0.171±2.77
%Assay: 98.8±150
Temperature: 23.8°C
Humidity: 43.0 %
Yield: 64.8 %

Comments

-No sticking
-No edge splitting
-No capping
-Smooth surface finish

BATCH SUMMARY – NVP010

Faculty of Pharmacy, Rhodes University

Formulator:	Chiluba Mwila	**Batch size:**	300 g
Product:	Nevirapine tablets	**Blending Time (start):**	16h10 pm
Batch Number:	NVP010	**(end):**	16h45 pm
Blending Date:	17-03-2012	**Tableting Time (start):**	21h10 pm
Tableting Date:	17-03-2012	**(end):**	21h35 pm

Formula

Material	%w/w	Amount added (g)	Rhodes #
NVP	33.3	100	RM000260
Methocel® K4M	10.0	30.0	RM000060
SuperTab® Spray dried lactose	35.0	105.0	RM000161
Avicel® PH102	13.5	40.5	RM000038
Eudragit® RSPO	5.0	15.0	RM000023
Mg stearate	1.1	3.3	RM000304
Talc	1.0	3.0	RM000050
Colloidal silicon dioxide	1.1	3.3	RM000305

Dissolution profile

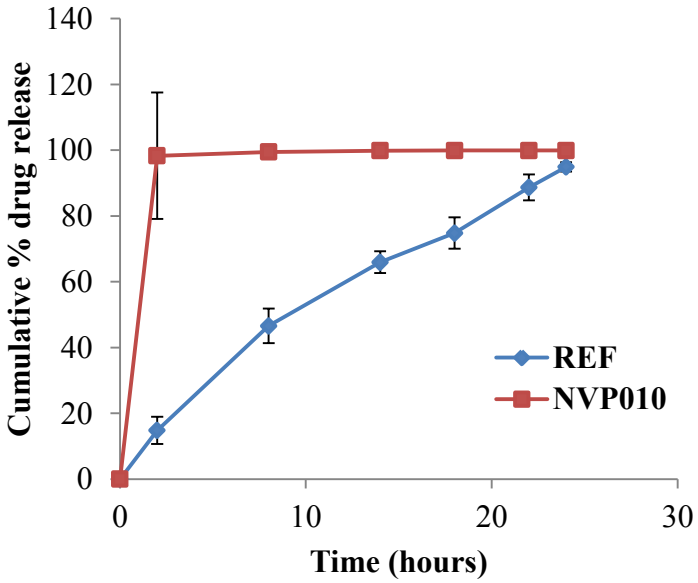

Target weight: 300 mg
Actual weight: 299.0±1.79
Target hardness: 100 – 150 N
Actual hardness:99.8±4.04
Tensile Strength: 1.30±1.86
Friability: 0.163±3.56
%Assay: 101.4±2.72
Temperature: 24.1°C
Humidity: 56.0 %
Yield: 66.6 %

Comments

-No sticking
-No edge splitting
-No capping
-Smooth surface finish

BATCH SUMMARY – NVP011

Faculty of Pharmacy, Rhodes University

Formulator:	Chiluba Mwila	**Batch size:**	300 g
Product:	Nevirapine tablets	**Blending Time (start):**	14h00 pm
Batch Number:	NVP011	**(end):**	14h35 pm
Blending Date:	19-03-2012	**Tableting Time (start):**	17h51 pm
Tableting Date:	19-03-2012	**(end):**	18h21 pm

Formula

Material	%w/w	Amount added (g)	Rhodes #
NVP	33.3	100	RM000260
Methocel® K4M	10.0	30.0	RM000060
SuperTab® Spray dried lactose	30.0	90.0	RM000161
Avicel® PH102	13.5	40.5	RM000038
Eudragit® RSPO	10.0	30.0	RM000023
Mg stearate	1.1	3.3	RM000304
Talc	1.0	3.0	RM000050
Colloidal silicon dioxide	1.1	3.3	RM000305

Dissolution profile

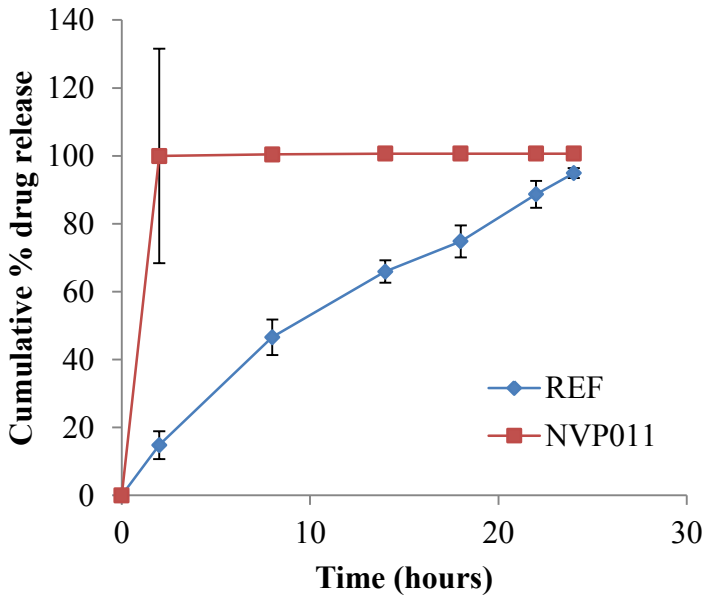

Target weight: 300 mg
Actual weight: 296.2±3.85
Target hardness: 100 – 150 N
Actual hardness:89.9±5.38
Tensile Strength: 1.18±2.41
Friability: 0.159±2.72
%Assay: 96.8±1.87
Temperature: 23.6°C
Humidity: 61.0 %
Yield: 65.3 %

Comments
-No sticking
-No edge splitting
-No capping
-Smooth surface finish

BATCH SUMMARY – NVP012

Faculty of Pharmacy, Rhodes University

Formulator:	Chiluba Mwila	**Batch size:**	300 g
Product:	Nevirapine tablets	**Blending Time (start):**	14h45 pm
Batch Number:	NVP012	**(end):**	15h19 pm
Blending Date:	19-03-2012	**Tableting Time (start):**	18h26 pm
Tableting Date:	19-03-2012	**(end):**	18h50 pm

Formula

Material	%w/w	Amount added (g)	Rhodes #
NVP	33.3	100	RM000260
Methocel® K4M	10.0	30.0	RM000060
SuperTab® Spray dried lactose	25.0	75.0	RM000161
Avicel® PH102	13.5	40.5	RM000038
Eudragit® RSPO	15.0	45.0	RM000023
Mg stearate	1.1	3.3	RM000304
Talc	1.0	3.0	RM000050
Colloidal silicon dioxide	1.	3.3	RM000305

Dissolution profile

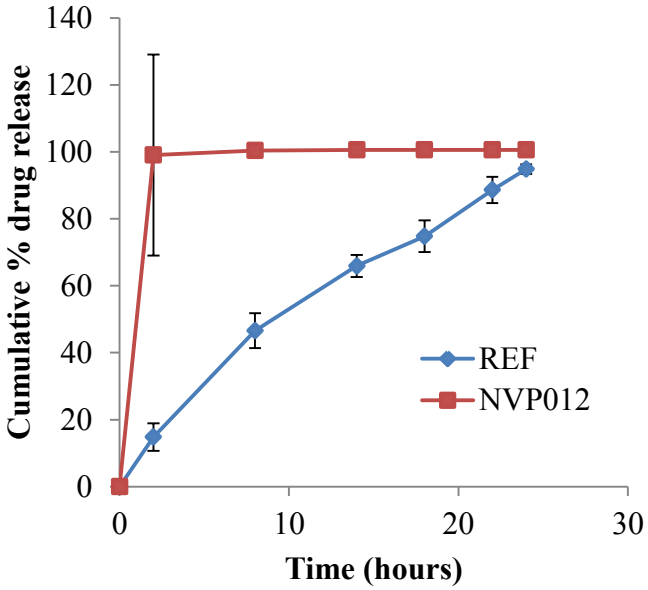

Target weight: 300 mg
Actual weight: 300.7±2.74
Target hardness: 100 – 150 N
Actual hardness:100.0±3.77
Tensile Strength: 1.33±3.72
Friability: 0.171±2.34
%Assay: 99.7±3.80
Temperature: 23.6°C
Humidity: 61.0 %
Yield: 70.8 %

Comments

-No sticking
-No edge splitting
-No capping
-Smooth surface finish

BATCH SUMMARY – NVP013

Faculty of Pharmacy, Rhodes University

Formulator:	Chiluba Mwila	**Batch size:**	300 g
Product:	Nevirapine tablets	**Blending Time (start):**	09h30 am
Batch Number:	NVP013	**(end):**	10h10 am
Blending Date:	17-04-2012	**Tableting Time (start):**	12h30 pm
Tableting Date:	17-04-2012	**(end):**	12h50 pm

Formula

Material	%w/w	Amount added (g)	Rhodes #
NVP	33.3	100	RM000260
Methocel® K4M	25.0	75	RM000060
SuperTab® Spray dried lactose	25.0	75	RM000161
Avicel® PH102	13.5	40.5	RM000038
Mg stearate	1.1	3.3	RM000304
Talc	1.1	3.3	RM000050
Colloidal silicon dioxide	1.0	3.0	RM000305

Dissolution profile

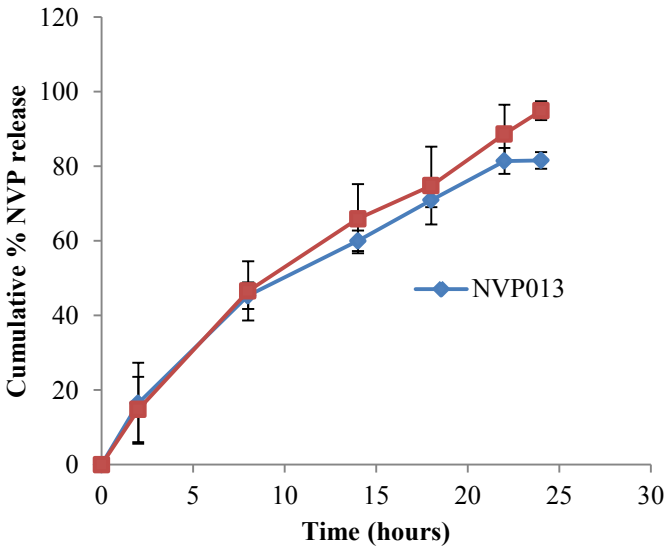

Target weight: 300 mg
Actual weight: 296.5±2.69
Target hardness: 80 – 100 N
Actual hardness:67.8±11.5
Friability: 0.171
%Assay: 94.7±0.94
Temperature: 23.8°C
Humidity: 60.0 %
Yield: 77.3 %

Comments

-No sticking
-No edge splitting
-No capping
-Smooth surface finish

BATCH SUMMARY – NVP014

Faculty of Pharmacy, Rhodes University

Formulator:	Chiluba Mwila	**Batch size:**	300 g
Product:	Nevirapine tablets	**Blending Time (start):**	10h30 am
Batch Number:	NVP014	**(end):**	11h10 am
Blending Date:	17-04-2012	**Tableting Time (start):**	13h00 pm
Tableting Date:	17-04-2012	**(end):**	13h27 pm

Formula

Material	%w/w	Amount added (g)	Rhodes #
NVP	33.3	100	RM000260
Methocel® K4M	30.0	90	RM000060
SuperTab® Spray dried lactose	15.0	45	RM000161
Avicel® PH102	18.5	55.5	RM000038
Mg stearate	1.1	3.3	RM000304
Talc	1.1	3.3	RM000050
Colloidal silicon dioxide	1.0	3.0	RM000305

Dissolution profile

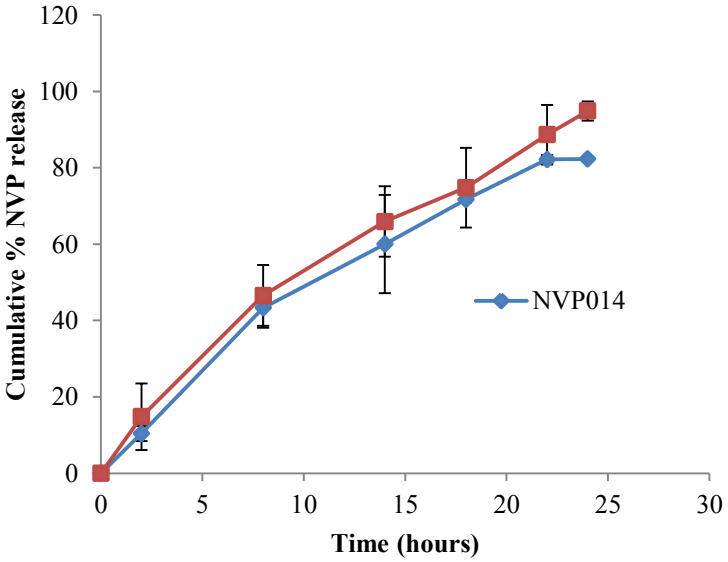

Target weight: 300 mg
Actual weight: 292.2±3.79
Target hardness: 80 – 100 N
Actual hardness:70.4±8.65
Friability: 0.175
%Assay: 100.2±0.51
Temperature: 23.8°C
Humidity: 60.0 %
Yield: 77.3 %

Comments

-No sticking
-No edge splitting
-No capping
-Smooth surface finish

BATCH SUMMARY – NVP015

Faculty of Pharmacy, Rhodes University

Formulator:	Chiluba Mwila	**Batch size:**	300 g
Product:	Nevirapine tablets	**Blending Time (start):**	11h30 am
Batch Number:	NVP015	**(end):**	12h20 pm
Blending Date:	17-04-2012	**Tableting Time (start):**	13h40 pm
Tableting Date:	17-04-2012	**(end):**	14h23 pm

Formula

Material	%w/w	Amount added (g)	Rhodes #
NVP	33.3	100	RM000260
Methocel® K4M	30.0	90	RM000060
SuperTab® Spray dried lactose	20.0	60	RM000161
Avicel® PH102	13.5	40.5	RM000038
Mg stearate	1.1	3.3	RM000304
Talc	1.1	3.3	RM000050
Colloidal silicon dioxide	1.0	3.0	RM000305

Dissolution profile

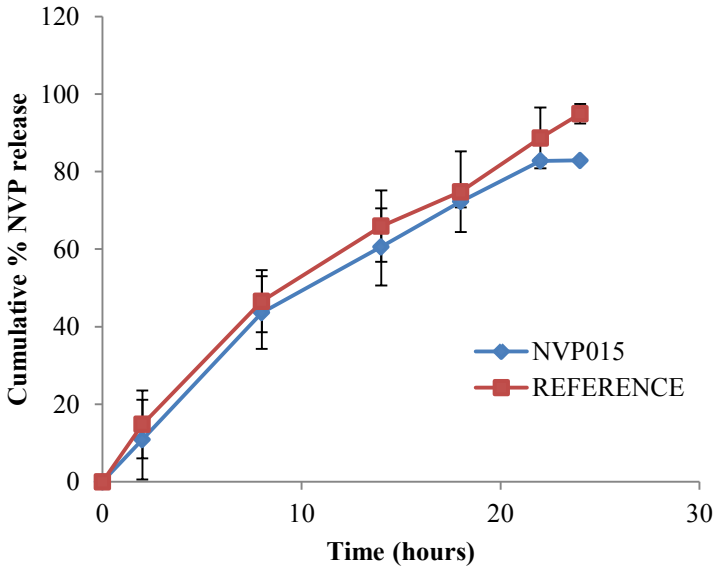

Target weight: 300 mg
Actual weight: 297.9±3.79
Target hardness: 80 – 100 N
Actual hardness:80.4±11.4
Friability: 0.169
%Assay: 94.9±0.43
Temperature: 23.8°C
Humidity: 60.0 %
Yield: 77.0 %

Comments

-No sticking
-No edge splitting
-No capping
-Smooth surface finish

BATCH SUMMARY – NVP016

Faculty of Pharmacy, Rhodes University

Formulator:	Chiluba Mwila	**Batch size:**	300 g
Product:	Nevirapine tablets	**Blending Time (start):**	08h45 am
Batch Number:	NVP016	**(end):**	09h31 am
Blending Date:	18-04-2012	**Tableting Time (start):**	10h45 pm
Tableting Date:	18-04-2012	**(end):**	11h00 pm

Formula

Material	%w/w	Amount added (g)	Rhodes #
NVP	33.3	100	RM000260
Methocel® K4M	30.0	90	RM000060
SuperTab® Spray dried lactose	20.0	60	RM000161
Avicel® PH102	13.5	40.5	RM000038
Mg stearate	1.1	3.3	RM000304
Talc	1.1	3.3	RM000050
Colloidal silicon dioxide	1.0	3.0	RM000305

Dissolution profile

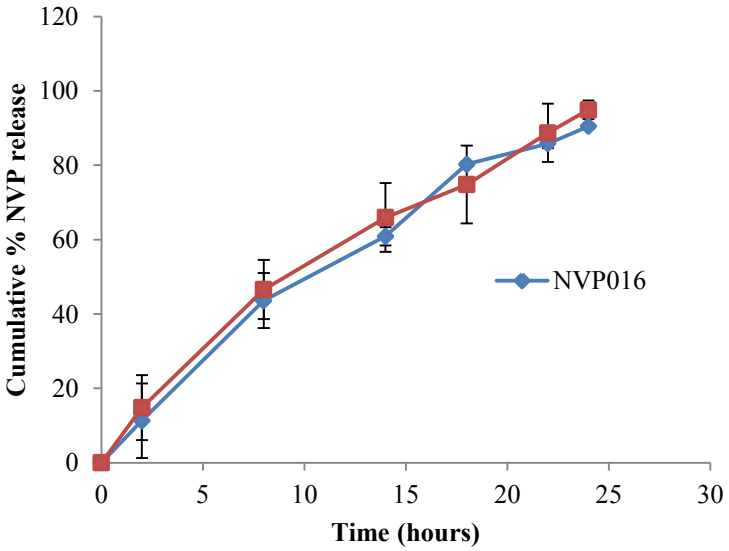

Target weight: 300 mg
Actual weight: 299.3±1.07
Target hardness: 80 – 100 N
Actual hardness:83.7±9.70
Friability: 0.171
%Assay: 93.6±2.74
Temperature: 22.9°C
Humidity: 54.0 %
Yield: 70.4 %

Comments

-No sticking
-No edge splitting
-No capping
-Smooth surface finish

BATCH SUMMARY – NVP017

Faculty of Pharmacy, Rhodes University

Formulator:	Chiluba Mwila	**Batch size:**	300 g
Product:	Nevirapine tablets	**Blending Time (start):**	09h40 am
Batch Number:	NVP017	**(end):**	10h15 am
Blending Date:	18-04-2012	**Tableting Time (start):**	11h10 pm
Tableting Date:	18-04-2012	**(end):**	11h33 pm

Formula

Material	%w/w	Amount added (g)	Rhodes #
NVP	33.3	100	RM000260
Methocel® K4M	30.0	90	RM000060
SuperTab® Spray dried lactose	20.0	60	RM000161
Avicel® PH102	13.5	40.5	RM000038
Mg stearate	1.1	3.3	RM000304
Talc	1.1	3.3	RM000050
Colloidal silicon dioxide	1.0	3.0	RM000305

Dissolution profile

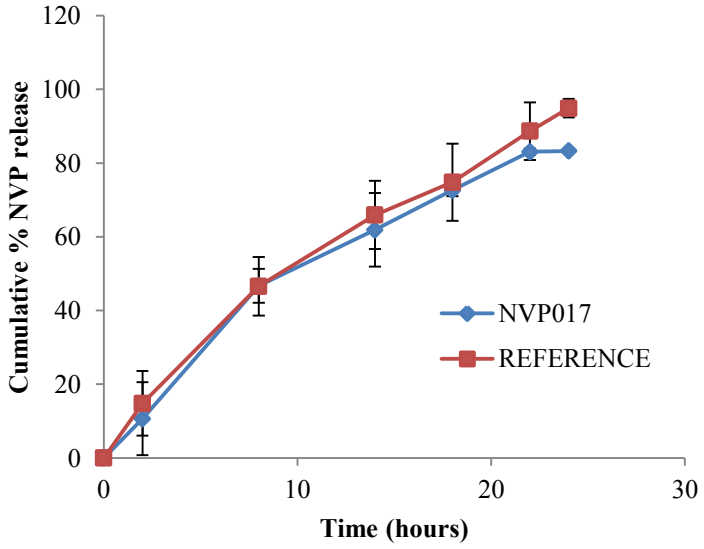

Target weight: 300 mg
Actual weight: 299.0±2.81
Target hardness: 80 – 100 N
Actual hardness:81.9±8.53
Friability: 0.170
%Assay: 97.4±0.42
Temperature: 22.9°C
Humidity: 54.0 %
Yield: 67.4 %

Comments

-No sticking
-No edge splitting
-No capping
-Smooth surface finish

BATCH SUMMARY – NVP018

Faculty of Pharmacy, Rhodes University

Formulator:	Chiluba Mwila	**Batch size:**	300 g
Product:	Nevirapine tablets	**Blending Time (start):**	10h20 am
Batch Number:	NVP018	**(end):**	11h05 am
Blending Date:	18-04-2012	**Tableting Time (start):**	11h40 pm
Tableting Date:	18-04-2012	**(end):**	12h06 pm

Formula

Material	%w/w	Amount added (g)	Rhodes #
NVP	33.3	111	RM000260
Methocel® K4M	25.0	83.33	RM000060
SuperTab® Spray dried lactose	15.0	50	RM000161
Avicel® PH102	13.5	45	RM000038
Mg stearate	1.1	3.67	RM000304
Talc	1.1	3.67	RM000050
Colloidal silicon dioxide	1.0	3.33	RM000305

Dissolution profile

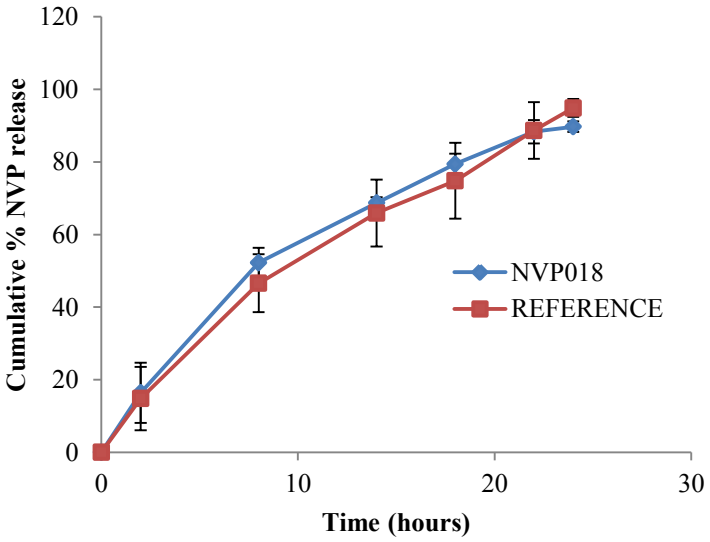

Target weight: 300 mg
Actual weight: 299.2±1.66
Target hardness: 80 – 100 N
Actual hardness:85.2±13.9
Friability: 0.172
%Assay: 97.7±1.99
Temperature: 22.9°C
Humidity: 54.0 %
Yield: 80.0 %

Comments

-No sticking
-No edge splitting
-No capping
-Smooth surface finish

BATCH SUMMARY – NVP019

Faculty of Pharmacy, Rhodes University

Formulator:	Chiluba Mwila	**Batch size:**	300 g
Product:	Nevirapine tablets	**Blending Time (start):**	14h45 pm
Batch Number:	NVP019	**(end):**	15h20 pm
Blending Date:	23-04-2012	**Tableting Time (start):**	16h00 pm
Tableting Date:	23-04-2012	**(end):**	16h20 pm

Formula

Material	%w/w	Amount added (g)	Rhodes #
NVP	33.3	90.82	RM000260
Methocel® K4M	30.0	81.82	RM000060
SuperTab® Spray dried lactose	25.0	68.18	RM000161
Avicel® PH102	18.5	50.45	RM000038
Mg stearate	1.1	3.0	RM000304
Talc	1.1	3.0	RM000050
Colloidal silicon dioxide	1.0	2.73	RM000305

Dissolution profile

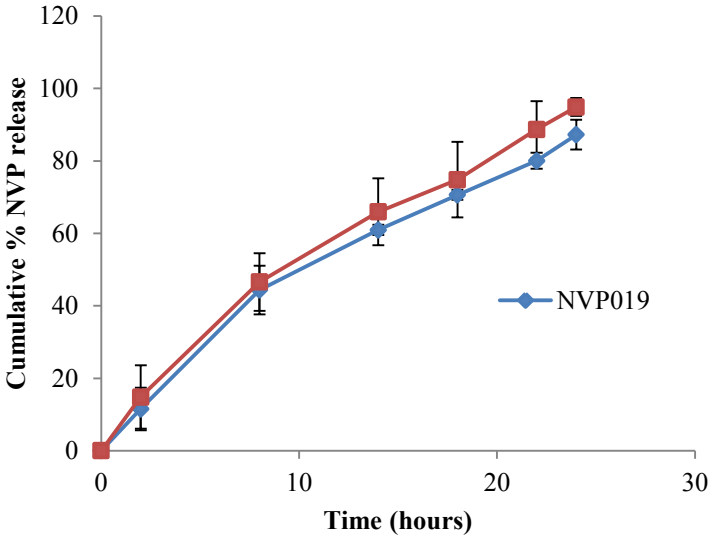

Target weight: 300 mg
Actual weight: 295.7±3.26
Target hardness: 80 – 100 N
Actual hardness:83.7±6.99
Friability: 0.166
%Assay: 96.5±0.29
Temperature: 21.7 °C
Humidity: 36.0 %
Yield: 79.1 %

Comments

-No sticking
-No edge splitting
-No capping
-Smooth surface finish

BATCH SUMMARY – NVP020

Faculty of Pharmacy, Rhodes University

Formulator:	Chiluba Mwila	**Batch size:**	300 g
Product:	Nevirapine tablets	**Blending Time (start):**	15h25 pm
Batch Number:	NVP020	**(end):**	16h00 pm
Blending Date:	18-04-2012	**Tableting Time (start):**	16h30 pm
Tableting Date:	18-04-2012	**(end):**	16h55 pm

Formula

Material	%w/w	Amount added (g)	Rhodes #
NVP	33.3	95.14	RM000260
Methocel® K4M	35.0	100	RM000060
SuperTab® Spray dried lactose	20.0	57.14	RM000161
Avicel® PH102	8.5	38.57	RM000038
Mg stearate	1.1	3.14	RM000304
Talc	1.1	3.14	RM000050
Colloidal silicon dioxide	1.0	2.86	RM000305

Dissolution profile

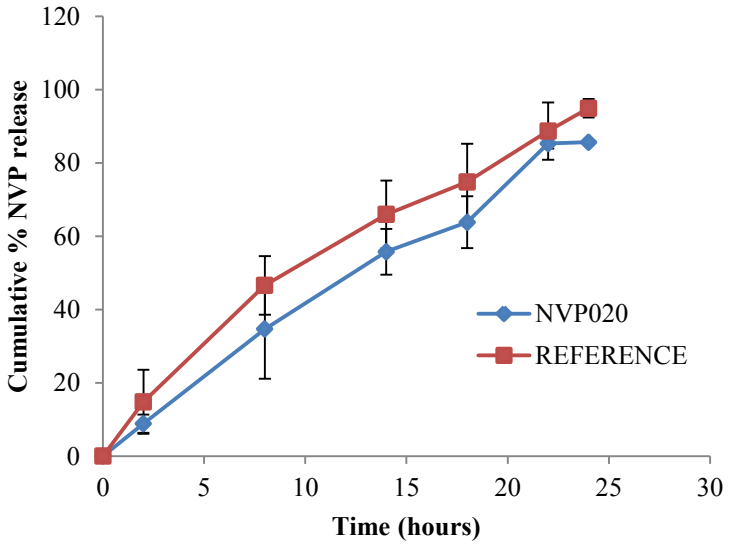

Target weight: 300 mg
Actual weight: 300.4±1.93
Target hardness: 80 – 100 N
Actual hardness:94.9±8.92
Friability: 0.167
%Assay: 100.9±0.37
Temperature: 21.7 °C
Humidity: 36.0 %
Yield: 83.3 %

Comments

-No sticking
-No edge splitting
-No capping
-Smooth surface finish

BATCH SUMMARY – NVP021

Faculty of Pharmacy, Rhodes University

Formulator:	Chiluba Mwila	**Batch size:**	300 g
Product:	Nevirapine tablets	**Blending Time (start):**	16h05 pm
Batch Number:	NVP021	**(end):**	16h40 pm
Blending Date:	18-04-2012	**Tableting Time (start):**	17h01 pm
Tableting Date:	18-04-2012	**(end):**	17h30 pm

Formula

Material	%w/w	Amount added (g)	Rhodes #
NVP	33.3	100	RM000260
Methocel® K4M	30.0	90	RM000060
SuperTab® Spray dried lactose	20.0	60	RM000161
Avicel® PH102	13.5	40.5	RM000038
Mg stearate	1.1	3.3	RM000304
Talc	1.1	3.3	RM000050
Colloidal silicon dioxide	1.0	3.0	RM000305

Dissolution profile

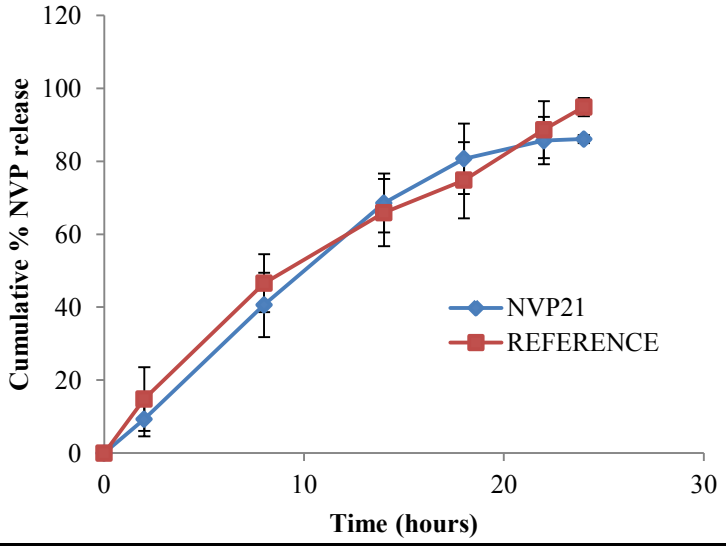

Target weight: 300 mg
Actual weight: 297.8±3.78
Target hardness: 80 – 100 N
Actual hardness:87.3±7.20
Friability: 0.169
%Assay: 94.1±0.21
Temperature: 21.7 °C
Humidity: 36.0 %
Yield: 71.2 %

Comments

-No sticking
-No edge splitting
-No capping
-Smooth surface finish

BATCH SUMMARY – NVP022

Faculty of Pharmacy, Rhodes University

Formulator:	Chiluba Mwila	**Batch size:**	300 g
Product:	Nevirapine tablets	**Blending Time (start):**	11h30 am
Batch Number:	NVP022	**(end):**	12h10 pm
Blending Date:	24-04-2012	**Tableting Time (start):**	12h35 pm
Tableting Date:	24-04-2012	**(end):**	12h50 pm

Formula

Material	%w/w	Amount added (g)	Rhodes #
NVP	33.3	100	RM000260
Methocel® K4M	25.0	75	RM000060
SuperTab® Spray dried lactose	20.0	60	RM000161
Avicel® PH102	18.5	55.5	RM000038
Mg stearate	1.1	3.3	RM000304
Talc	1.1	3.3	RM000050
Colloidal silicon dioxide	1.0	3.0	RM000305

Dissolution profile

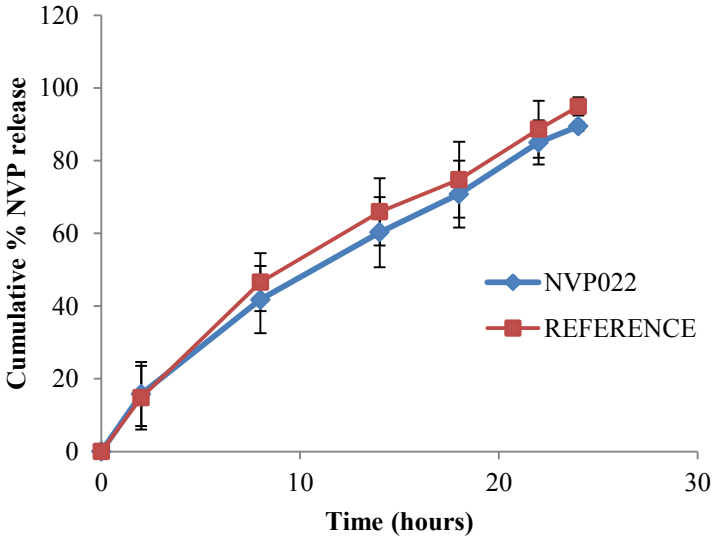

Target weight: 300 mg
Actual weight: 297.7±2.85
Target hardness: 80 – 100 N
Actual hardness:92.1±8.37
Friability: 0.169
%Assay: 96.2±0.31
Temperature: 22.6 °C
Humidity: 39.0 %
Yield: 74.6 %

Comments

-No sticking
-No edge splitting
-No capping
-Smooth surface finish

BATCH SUMMARY – NVP023

Faculty of Pharmacy, Rhodes University

Formulator:	Chiluba Mwila	**Batch size:**	300 g
Product:	Nevirapine tablets	**Blending Time (start):**	12h15 pm
Batch Number:	NVP023	**(end):**	12h50 pm
Blending Date:	24-04-2012	**Tableting Time (start):**	13h06 pm
Tableting Date:	24-04-2012	**(end):**	13h25 pm

Formula

Material	%w/w	Amount added (g)	Rhodes #
NVP	33.3	100	RM000260
Methocel® K4M	35.0	105	RM000060
SuperTab® Spray dried lactose	15.0	45	RM000161
Avicel® PH102	13.5	40.5	RM000038
Mg stearate	1.1	3.3	RM000304
Talc	1.1	3.3	RM000050
Colloidal silicon dioxide	1.0	3.0	RM000305

Dissolution profile

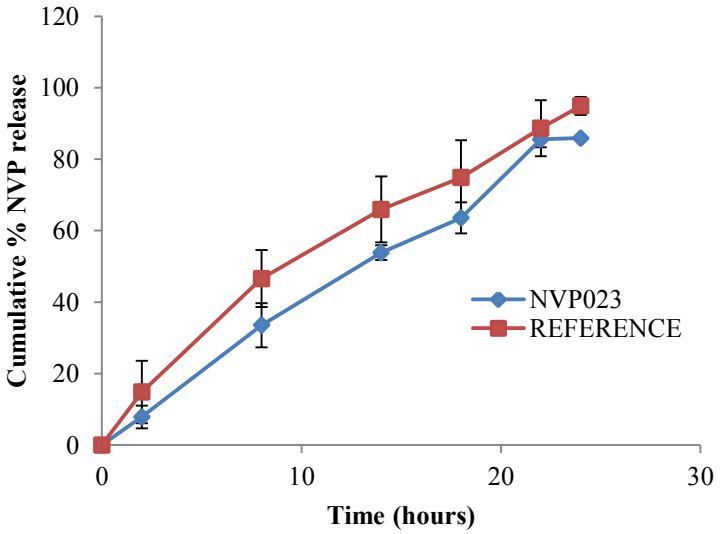

Target weight: 300 mg
Actual weight: 293.5±4.15
Target hardness: 80 – 100 N
Actual hardness:84.7±8.64
Friability: 0.166
%Assay: 96.7±0.31
Temperature: 22.6 °C
Humidity: 39.0 %
Yield: 65.9 %

Comments

-No sticking
-No edge splitting
-No capping
-Smooth surface finish

BATCH SUMMARY – NVP024

Faculty of Pharmacy, Rhodes University

Formulator:	Chiluba Mwila	**Batch size:**	300 g
Product:	Nevirapine tablets	**Blending Time (start):**	12h55 pm
Batch Number:	NVP024	**(end):**	13h30 pm
Blending Date:	24-04-2012	**Tableting Time (start):**	13h32 pm
Tableting Date:	24-04-2012	**(end):**	13h47 pm

Formula

Material	%w/w	Amount added (g)	Rhodes #
NVP	33.3	100	RM000260
Methocel® K4M	30.0	90	RM000060
SuperTab® Spray dried lactose	20.0	60	RM000161
Avicel® PH102	13.5	40.5	RM000038
Mg stearate	1.1	3.3	RM000304
Talc	1.1	3.3	RM000050
Colloidal silicon dioxide	1.0	3.0	RM000305

Dissolution profile

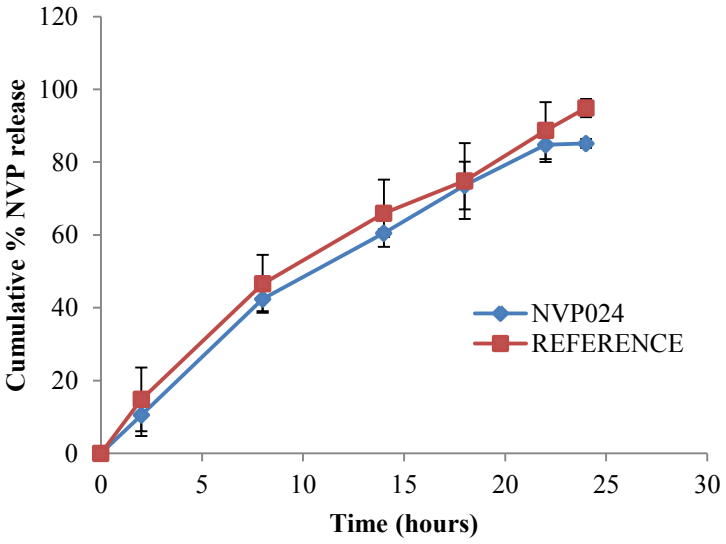

Target weight: 300 mg
Actual weight: 303.9±1.37
Target hardness: 80 – 100 N
Actual hardness:92.0±8.36
Friability: 0.341
%Assay: 96.1±0.20
Temperature: 22.6 °C
Humidity: 39.0 %
Yield: 71.3 %

Comments

-No sticking
-No edge splitting
-No capping
-Smooth surface finish

BATCH SUMMARY – NVP025

Faculty of Pharmacy, Rhodes University

Formulator:	Chiluba Mwila	**Batch size:**	300 g
Product:	Nevirapine tablets	**Blending Time (start):**	10h30 am
Batch Number:	NVP025	**(end):**	11h05 am
Blending Date:	26-04-2012	**Tableting Time (start):**	11h50 am
Tableting Date:	26-04-2012	**(end):**	12h07 pm

Formula

Material	%w/w	Amount added (g)	Rhodes #
NVP	33.3	90.82	RM000260
Methocel® K4M	35.0	95.45	RM000060
SuperTab® Spray dried lactose	20.0	54.55	RM000161
Avicel® PH102	18.5	50.46	RM000038
Mg stearate	1.1	3.0	RM000304
Talc	1.1	3.0	RM000050
Colloidal silicon dioxide	1.0	2.73	RM000305

Dissolution profile

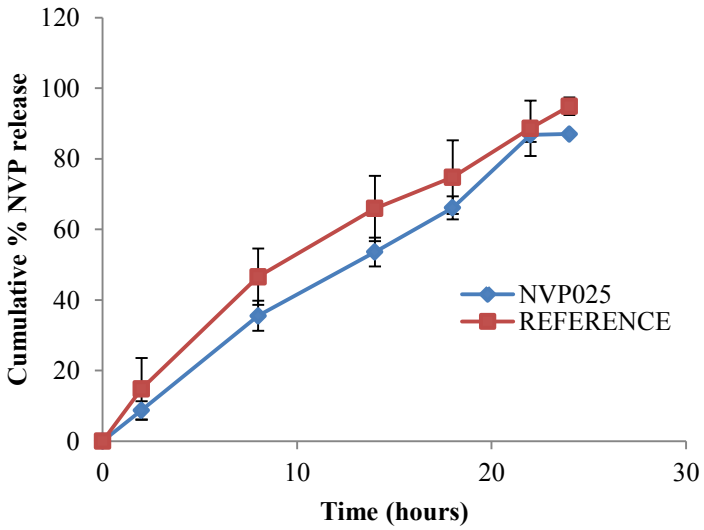

Target weight: 300 mg
Actual weight: 295.7±4.81
Target hardness: 80 – 100 N
Actual hardness:81.8±8.17
Friability: 0.168
%Assay: 97.5±0.18
Temperature: 22.7 °C
Humidity: 52.0 %
Yield: 72.3 %

Comments

-No sticking
-No edge splitting
-No capping
-Smooth surface finish

BATCH SUMMARY – NVP026

Faculty of Pharmacy, Rhodes University

Formulator:	Chiluba Mwila	**Batch size:**	300 g
Product:	Nevirapine tablets	**Blending Time (start):**	11h10 am
Batch Number:	NVP022	**(end):**	11h44 am
Blending Date:	26-04-2012	**Tableting Time (start):**	12h10 pm
Tableting Date:	26-04-2012	**(end):**	12h35 pm

Formula

Material	%w/w	Amount added (g)	Rhodes #
NVP	33.3	111	RM000260
Methocel® K4M	25.0	83.33	RM000060
SuperTab® Spray dried lactose	20.0	66.67	RM000161
Avicel® PH102	8.5	28.33	RM000038
Mg stearate	1.1	3.67	RM000304
Talc	1.1	3.67	RM000050
Colloidal silicon dioxide	1.0	3.33	RM000305

Dissolution profile

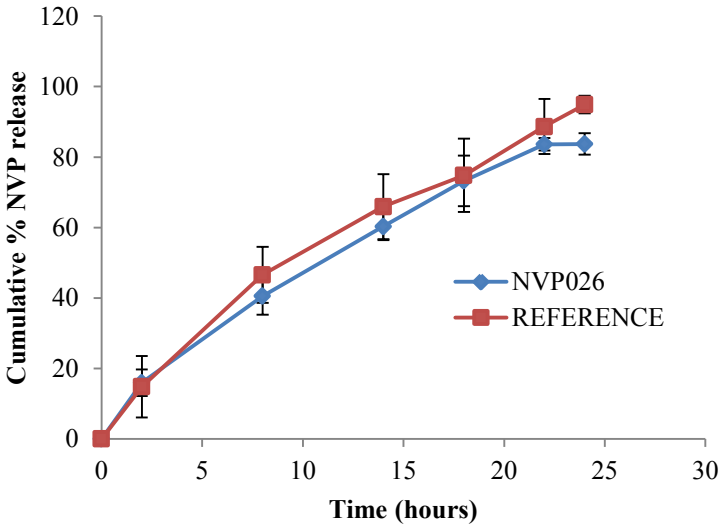

Target weight: 300 mg
Actual weight: 301.2±1.71
Target hardness: 80 – 100 N
Actual hardness:79.6±5.56
Friability: 0.174
%Assay: 99.8±0.28
Temperature: 22.7 °C
Humidity: 52.0 %
Yield: 70.3 %

Comments

-No sticking
-No edge splitting
-No capping
-Smooth surface finish

BATCH SUMMARY – NVP027

Faculty of Pharmacy, Rhodes University

Formulator:	Chiluba Mwila	**Batch size:**	300 g
Product:	Nevirapine tablets	**Blending Time (start):**	12h25 pm
Batch Number:	NVP027	**(end):**	13h09 pm
Blending Date:	27-04-2012	**Tableting Time (start):**	13h46 pm
Tableting Date:	27-04-2012	**(end):**	14h10 pm

Formula

Material	%w/w	Amount added (g)	Rhodes #
NVP	33.3	111	RM000260
Methocel® K4M	30.0	100	RM000060
SuperTab® Spray dried lactose	15.0	50	RM000161
Avicel® PH102	8.5	28.33	RM000038
Mg stearate	1.1	3.67	RM000304
Talc	1.1	3.67	RM000050
Colloidal silicon dioxide	1.0	3.33	RM000305

Dissolution profile

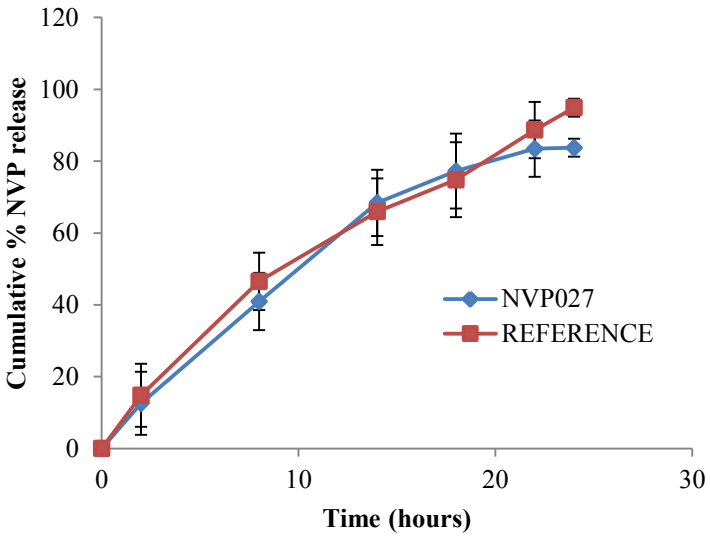

Target weight: 300 mg
Actual weight: 295.2±3.41
Target hardness: 80 – 100 N
Actual hardness:95.4±7.91
Friability: 0.169
%Assay: 96.8±0.07
Temperature: 21.3 °C
Humidity: 48.0 %
Yield: 76.4 %

Comments

-No sticking
-No edge splitting
-No capping
-Smooth surface finish

BATCH SUMMARY – NVP028

Faculty of Pharmacy, Rhodes University

Formulator:	Chiluba Mwila	**Batch size:**	300 g
Product:	Nevirapine tablets	**Blending Time (start):**	13h12 pm
Batch Number:	NVP028	**(end):**	13h48 pm
Blending Date:	27-04-2012	**Tableting Time (start):**	14h17 pm
Tableting Date:	27-04-2012	**(end):**	14h32 pm

Formula

Material	%w/w	Amount added (g)	Rhodes #
NVP	33.3	90.82	RM000260
Methocel® K4M	35.0	95.45	RM000060
SuperTab® Spray dried lactose	25.0	68.18	RM000161
Avicel® PH102	13.5	36.82	RM000038
Mg stearate	1.1	3.0	RM000304
Talc	1.1	3.0	RM000050
Colloidal silicon dioxide	1.0	2.73	RM000305

Dissolution profile

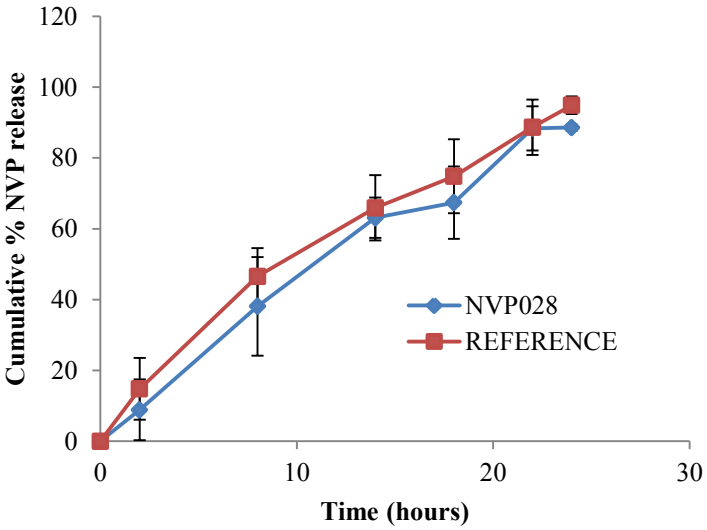

Target weight: 300 mg
Actual weight: 293.8±4.64
Target hardness: 80 – 100 N
Actual hardness:80.9±7.22
Friability: 0.169
%Assay: 94.7±1.34
Temperature: 21.3 °C
Humidity: 48.0 %
Yield: 78.4 %

Comments

-No sticking
-No edge splitting
-No capping
-Smooth surface finish

BATCH SUMMARY – NVP029

Faculty of Pharmacy, Rhodes University

Formulator:	Chiluba Mwila	**Batch size:**	300 g
Product:	Nevirapine tablets	**Blending Time (start):**	13h50 pm
Batch Number:	NVP029	**(end):**	14h25 pm
Blending Date:	27-04-2012	**Tableting Time (start):**	14h37 pm
Tableting Date:	27-04-2012	**(end):**	14h50 pm

Formula

Material	%w/w	Amount added (g)	Rhodes #
NVP	33.3	100	RM000260
Methocel® K4M	30.0	90	RM000060
SuperTab® Spray dried lactose	25.0	75	RM000161
Avicel® PH102	8.5	25.5	RM000038
Mg stearate	1.1	3.3	RM000304
Talc	1.1	3.3	RM000050
Colloidal silicon dioxide	1.0	3.0	RM000305

Dissolution profile

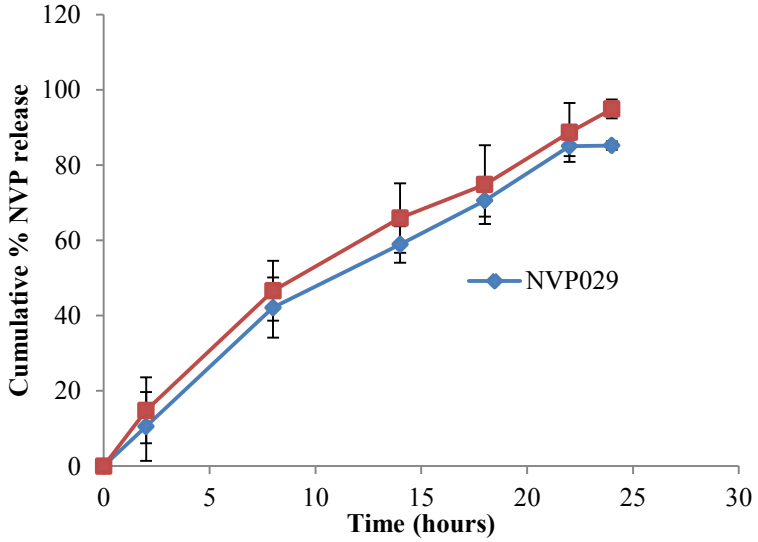

Target weight: 300 mg
Actual weight: 296.2±3.32
Target hardness: 80 – 100 N
Actual hardness:81.5±5.11
Friability: 0.169
%Assay: 98.8±0.94
Temperature: 21.3 °C
Humidity: 48.0 %
Yield: 75.3 %

Comments

-No sticking
-No edge splitting
-No capping
-Smooth surface finish

BATCH SUMMARY – NVP030

Faculty of Pharmacy, Rhodes University

Formulator:	Chiluba Mwila	**Batch size:**	300 g
Product:	Nevirapine tablets	**Blending Time (start):**	10h30 am
Batch Number:	NVP030	**(end):**	11h20 am
Blending Date:	07-06-2012	**Tableting Time (start):**	11h45 am
Tableting Date:	07-06-2012	**(end):**	12h30 pm

Formula

Material	%w/w	Amount added (g)	Rhodes #
NVP	33.3	90.82	RM000260
Methocel® K4M	33.16	90.44	RM000060
SuperTab® Spray dried lactose	25	68.12	RM000161
Avicel® PH102	15.32	41.78	RM000038
Mg stearate	1.1	3.0	RM000304
Talc	1.1	3.0	RM000050
Colloidal silicon dioxide	1.0	2.74	RM000305

Dissolution profile

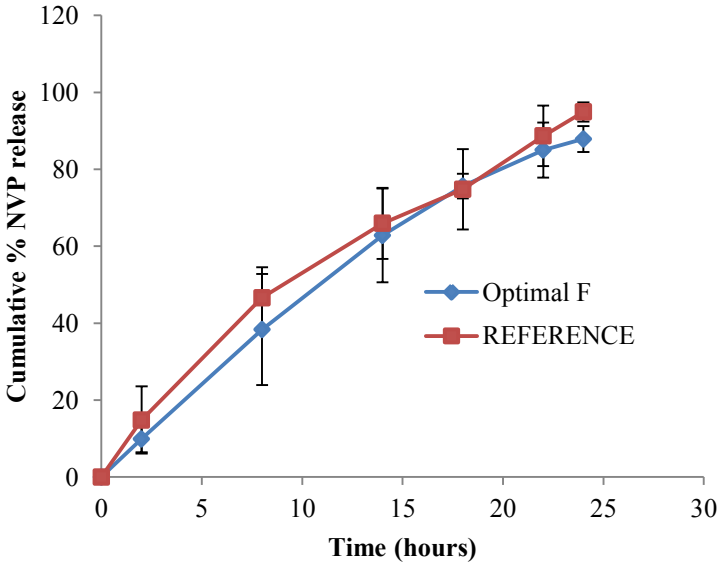

Target weight: 330 mg
Actual weight: 328.5±4.30
Target hardness: 100 – 150 N
Actual hardness:117.0±4.73
Tensile Strength: 1.45±3.70
Friability: 0.171±2.34
%Assay: 99.7±3.80
Temperature: 22.0°C
Humidity: 61.0 %
Yield: 78.5 %

Comments

-No sticking
-No edge splitting
-No capping
-Smooth surface finish

BATCH SUMMARY – NVP031

Faculty of Pharmacy, Rhodes University

Formulator:	Chiluba Mwila	**Batch size:**	300 g
Product:	Nevirapine tablets	**Blending Time (start):**	11h30 am
Batch Number:	NVP031	**(end):**	12h10 pm
Blending Date:	07-06-2012	**Tableting Time (start):**	12h45 pm
Tableting Date:	07-06-2012	**(end):**	13h10 pm

Formula

Material	%w/w	Amount added (g)	Rhodes #
NVP	33.3	90.82	RM000260
Methocel® K4M	33.16	90.44	RM000060
SuperTab® Spray dried lactose	25	68.12	RM000161
Avicel® PH102	15.32	41.78	RM000038
Mg stearate	1.1	3.0	RM000304
Talc	1.1	3.0	RM000050
Colloidal silicon dioxide	1.0	2.74	RM000305

Dissolution profile

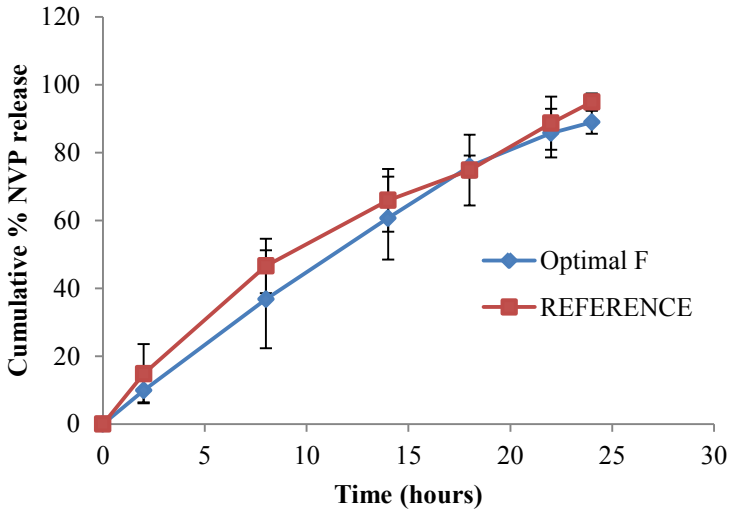

Target weight: 330 mg
Target hardness: 100 – 150 N
Temperature: 22.0°C
Humidity: 61.0 %
Yield: 76.9 %

Comments

-No sticking
-No edge splitting
-No capping
-Smooth surface finish

BATCH SUMMARY – NVP032

Faculty of Pharmacy, Rhodes University

Formulator:	Chiluba Mwila	**Batch size:**	300 g
Product:	Nevirapine tablets	**Blending Time (start):**	12h20 pm
Batch Number:	NVP032	**(end):**	12h55 pm
Blending Date:	07-06-2012	**Tableting Time (start):**	13h20 pm
Tableting Date:	07-06-2012	**(end):**	13h45 pm

Formula

Material	%w/w	Amount added (g)	Rhodes #
NVP	33.3	90.82	RM000260
Methocel® K4M	33.16	90.44	RM000060
SuperTab® Spray dried lactose	25	68.12	RM000161
Avicel® PH102	15.32	41.78	RM000038
Mg stearate	1.1	3.0	RM000304
Talc	1.1	3.0	RM000050
Colloidal silicon dioxide	1.0	2.74	RM000305

Dissolution profile

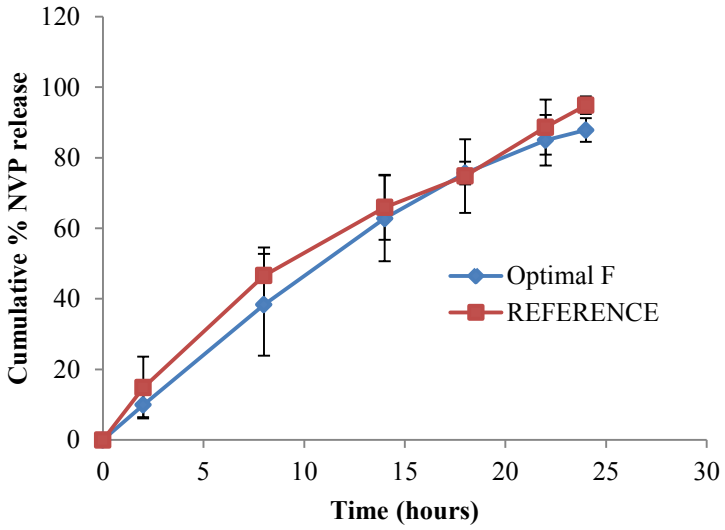

Target weight: 330 mg
Target hardness: 100 – 150 N
Temperature: 22.0°C
Humidity: 61.0 %
Yield: 75.7 %

Comments

-No sticking
-No edge splitting
-No capping
-Smooth surface finish

BATCH SUMMARY – NVP033

Faculty of Pharmacy, Rhodes University

Formulator:	Chiluba Mwila	**Batch size:**	300 g
Product:	Nevirapine tablets	**Blending Time (start):**	22h20 pm
Batch Number:	NVP033	**(end):**	23h03 pm
Blending Date:	20-07-2012	**Tableting Time (start):**	01h30 am
Tableting Date:	20-07-2012	**(end):**	01h50 am

Formula

Material	%w/w	Amount added (g)	Rhodes #
NVP	33.3	90.82	RM000260
Methocel® K15M	33.16	90.44	RM000060
SuperTab® Spray dried lactose	25	68.12	RM000161
Avicel® PH102	15.32	41.78	RM000038
Mg stearate	1.1	3.0	RM000304
Talc	1.1	3.0	RM000050
Colloidal silicon dioxide	1.0	2.74	RM000305

Dissolution profile

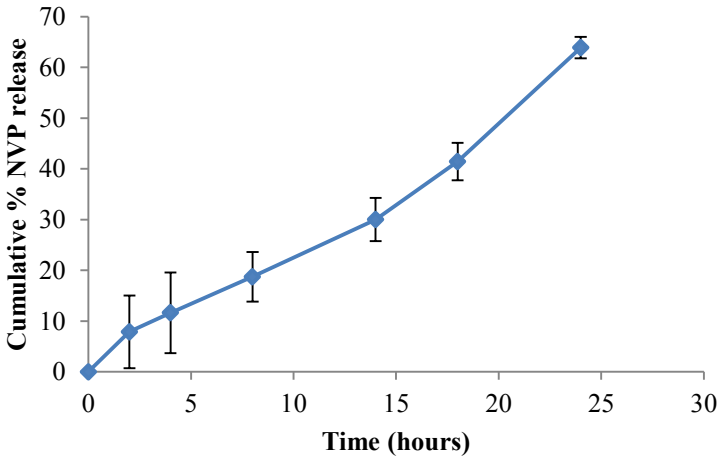

Target weight: 330 mg
Target hardness: 100 – 150 N
Temperature: 22.0°C
Humidity: 61.0 %
Yield: 72.8 %

Comments

-No sticking
-No edge splitting
-No capping
-Smooth surface finish

BATCH SUMMARY – NVP034

Faculty of Pharmacy, Rhodes University

Formulator:	Chiluba Mwila	**Batch size:**	300 g
Product:	Nevirapine tablets	**Blending Time (start):**	23h14 pm
Batch Number:	NVP034	**(end):**	23h50 pm
Blending Date:	20-07-2012	**Tableting Time (start):**	02h00 am
Tableting Date:	20-07-2012	**(end):**	02h15 am

Formula

Material	%w/w	Amount added (g)	Rhodes #
NVP	33.3	90.82	RM000260
Methocel® K100M	33.16	90.44	RM000060
SuperTab® Spray dried lactose	25	68.12	RM000161
Avicel® PH102	15.32	41.78	RM000038
Mg stearate	1.1	3.0	RM000304
Talc	1.1	3.0	RM000050
Colloidal silicon dioxide	1.0	2.74	RM000305

Dissolution profile

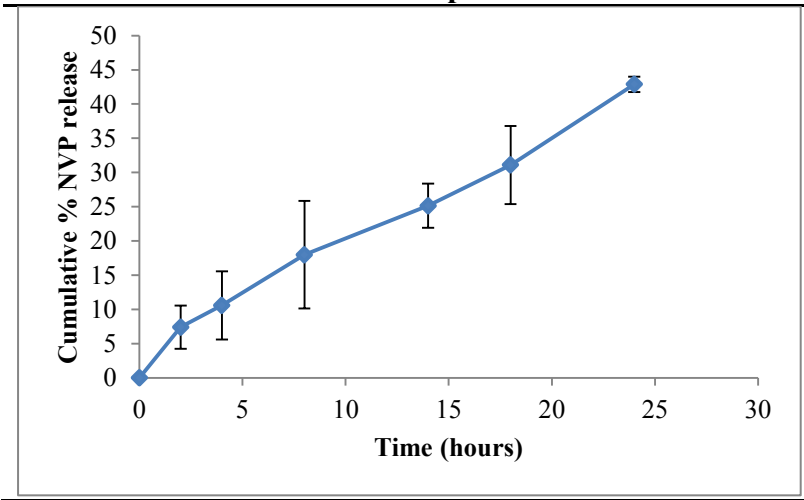

Target weight: 330 mg
Target hardness: 100 – 150 N
Temperature: 22.0°C
Humidity: 61.0 %
Yield: 79.3 %

Comments

-No sticking
-No edge splitting
-No capping
-Smooth surface finish

BATCH SUMMARY – NVP035

Faculty of Pharmacy, Rhodes University

Formulator:	Chiluba Mwila	**Batch size:**	300 g
Product:	Nevirapine tablets	**Blending Time (start):**	24h00 pm
Batch Number:	NVP035	**(end):**	24h37 pm
Blending Date:	20-07-2012	**Tableting Time (start):**	02h30 am
Tableting Date:	20-07-2012	**(end):**	02h42 am

Formula

Material	%w/w	Amount added (g)	Rhodes #
NVP	33.3	90.82	RM000260
Methocel® K4M	33.16	90.44	RM000060
SuperTab® Spray dried lactose	25	68.12	RM000161
Avicel® PH101	15.32	41.78	RM000038
Mg stearate	1.1	3.0	RM000304
Talc	1.1	3.0	RM000050
Colloidal silicon dioxide	1.0	2.74	RM000305

Dissolution profile

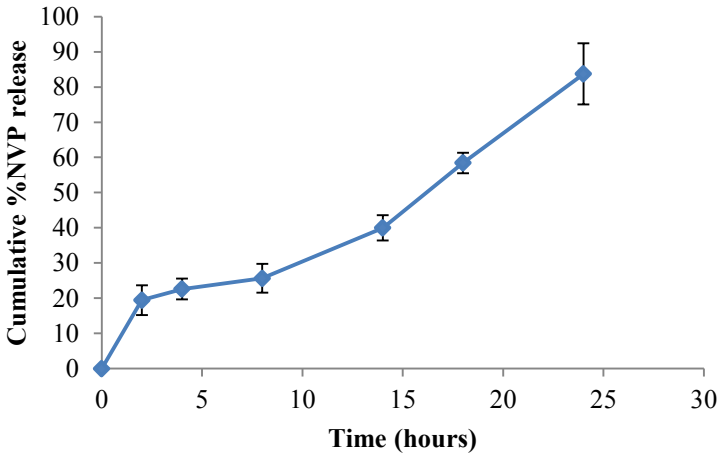

Target weight: 330 mg
Target hardness: 100 – 150 N
Temperature: 22.0°C
Humidity: 61.0 %
Yield: 72.8 %

Comments

-No sticking
-No edge splitting
-No capping
-Smooth surface finish

BATCH SUMMARY – NVP036

Faculty of Pharmacy, Rhodes University

Formulator:	Chiluba Mwila	**Batch size:**	300 g
Product:	Nevirapine tablets	**Blending Time (start):**	24h30 pm
Batch Number:	NVP036	**(end):**	01h10 am
Blending Date:	20-07-2012	**Tableting Time (start):**	02h50 am
Tableting Date:	20-07-2012	**(end):**	03h05 am

Formula

Material	%w/w	Amount added (g)	Rhodes #
NVP	33.3	90.82	RM000260
Methocel® K4M	33.16	90.44	RM000060
SuperTab® Spray dried lactose	25	68.12	RM000161
Avicel® PH200	15.32	41.78	RM000038
Mg stearate	1.1	3.0	RM000304
Talc	1.1	3.0	RM000050
Colloidal silicon dioxide	1.0	2.74	RM000305

Dissolution profile

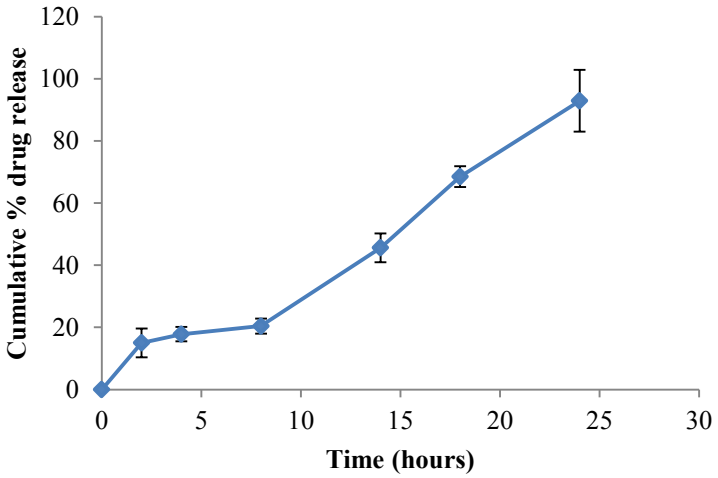

Target weight: 330 mg
Target hardness: 100 – 150 N
Temperature: 22.0°C
Humidity: 61.0 %
Yield: 76.9 %

Comments

-No sticking
-No edge splitting
-No capping
-Smooth surface finish

BATCH SUMMARY – NVP037

Faculty of Pharmacy, Rhodes University

Formulator:	Chiluba Mwila	**Batch size:**	300 g
Product:	Nevirapine tablets	**Blending Time (start):**	01h20 am
Batch Number:	NVP037	**(end):**	01h55 am
Blending Date:	20-07-2012	**Tableting Time (start):**	03h10 am
Tableting Date:	20-07-2012	**(end):**	03h26 am

Formula

Material	%w/w	Amount added (g)	Rhodes #
NVP	33.3	90.82	RM000260
Methocel® K4M	33.16	90.44	RM000060
Tablettose® agglomerated lactose	25	68.12	RM000161
Avicel® PH200	15.32	41.78	RM000038
Mg stearate	1.1	3.0	RM000304
Talc	1.1	3.0	RM000050
Colloidal silicon dioxide	1.0	2.74	RM000305

Dissolution profile

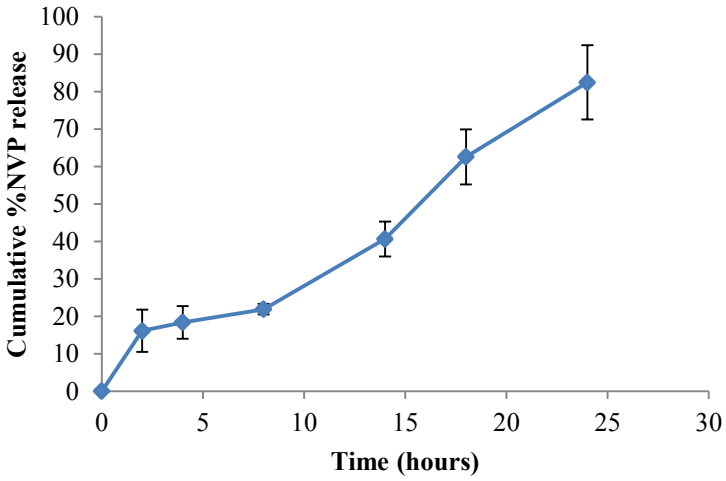

Target weight: 330 mg
Target hardness: 100 – 150 N
Temperature: 22.0°C
Humidity: 61.0 %
Yield: 73.7 %

Comments

-No sticking
-No edge splitting
-No capping
-Smooth surface finish

BATCH SUMMARY – NVP038

Faculty of Pharmacy, Rhodes University

Formulator:	Chiluba Mwila	**Batch size:**	300 g
Product:	Nevirapine tablets	**Blending Time (start):**	02h05 am
Batch Number:	NVP038	**(end):**	02h40 am
Blending Date:	20-07-2012	**Tableting Time (start):**	03h32 am
Tableting Date:	20-07-2012	**(end):**	03h47 am

Formula

Material	%w/w	Amount added (g)	Rhodes #
NVP	33.3	90.82	RM000260
Methocel® K4M	33.16	90.44	RM000060
FlowLac® Spray dried lactose	25	68.12	RM000161
Avicel® PH200	15.32	41.78	RM000038
Mg stearate	1.1	3.0	RM000304
Talc	1.1	3.0	RM000050
Colloidal silicon dioxide	1.0	2.74	RM000305

Dissolution profile

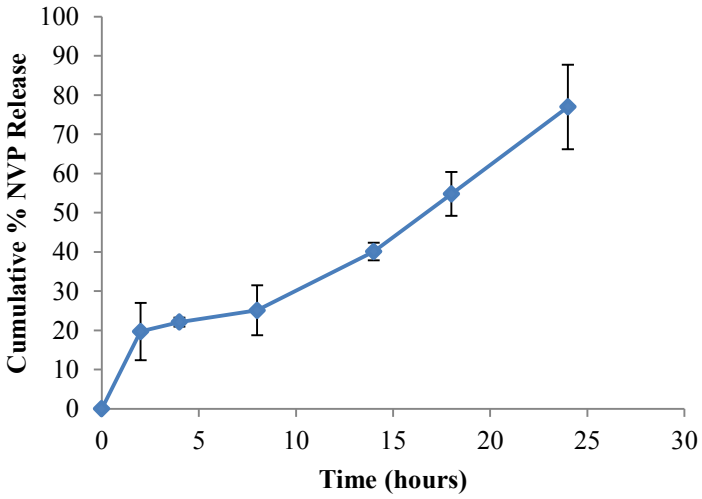

Target weight: 330 mg
Target hardness: 100 – 150 N
Temperature: 22.0°C
Humidity: 61.0 %
Yield: 77.5 %

Comments

-No sticking
-No edge splitting
-No capping
-Smooth surface finish

Diagnostic and response surface plots for responses monitored in Box-Behnken design optimisation process.

1. Diagnostic plots for response Y_1: NVP release at 2 hours – quadratic model.

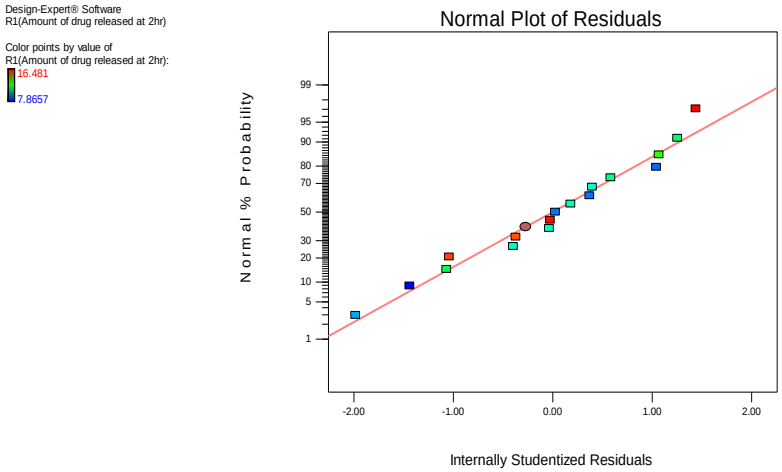

Figure Ap. 3.1. Normal plot of residuals for Y_1.

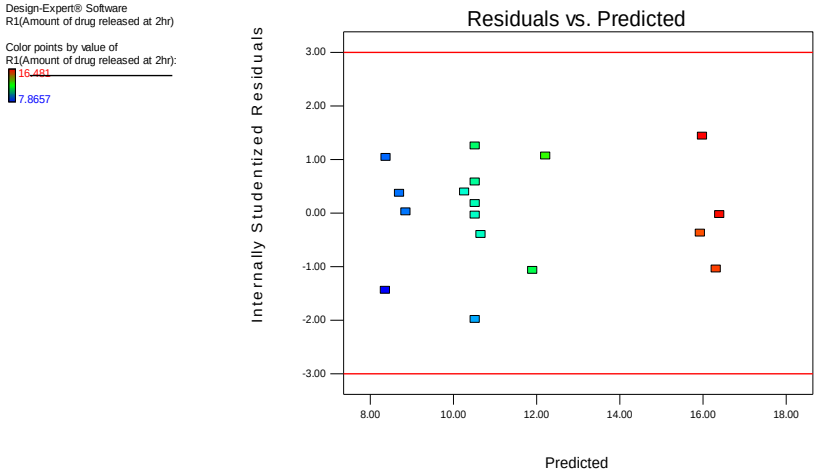

Figure Ap. 3.2. Plot of residuals vs. predicted response for Y_1.

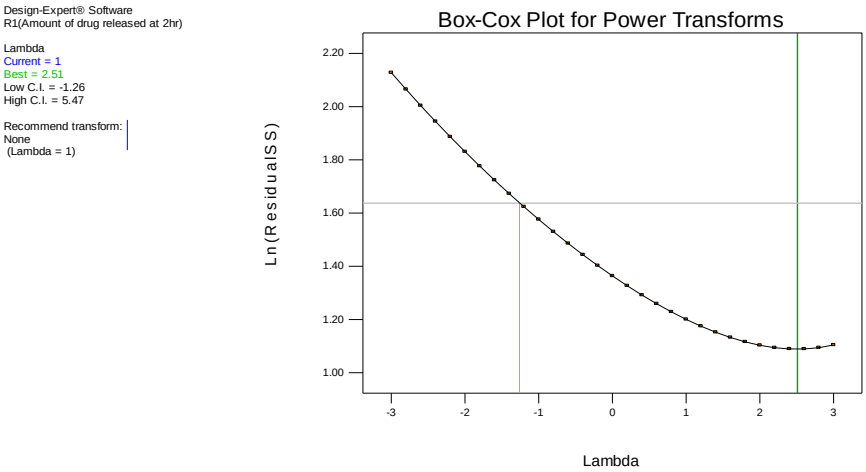

Figure Ap. 3.3. Box-Cox plot for power transforms for response Y_1.

2. Response surface plots for response Y_1

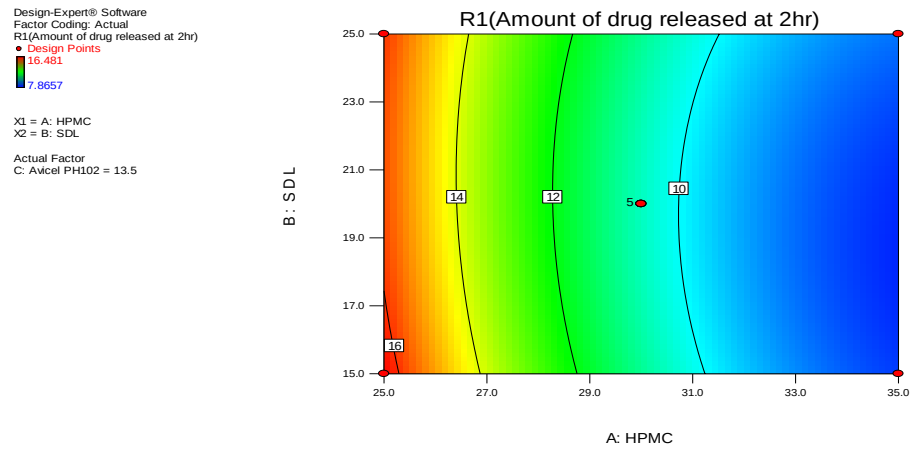

Figure Ap. 3.4. Contour plot of the effect of SDL and HPMC on response Y_1.

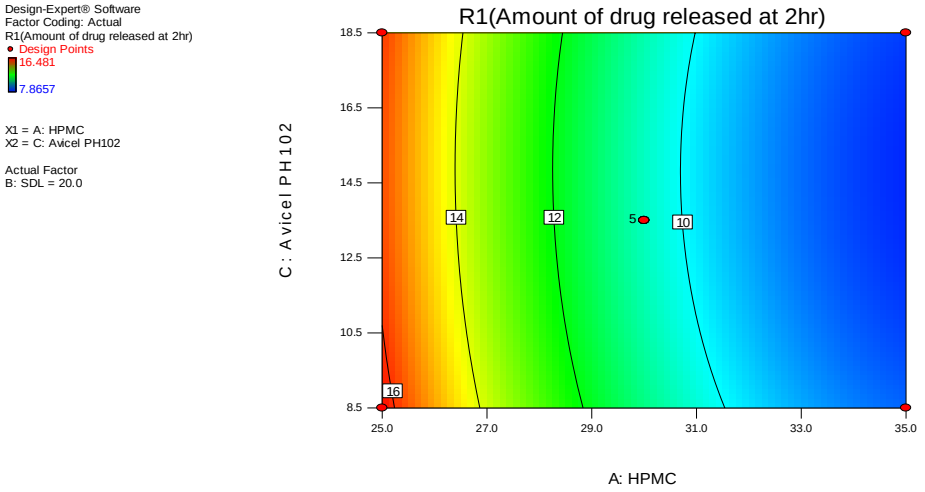

Figure Ap. 3.5. Contour plot of the effect of PH102 and HPMC on response Y_1.

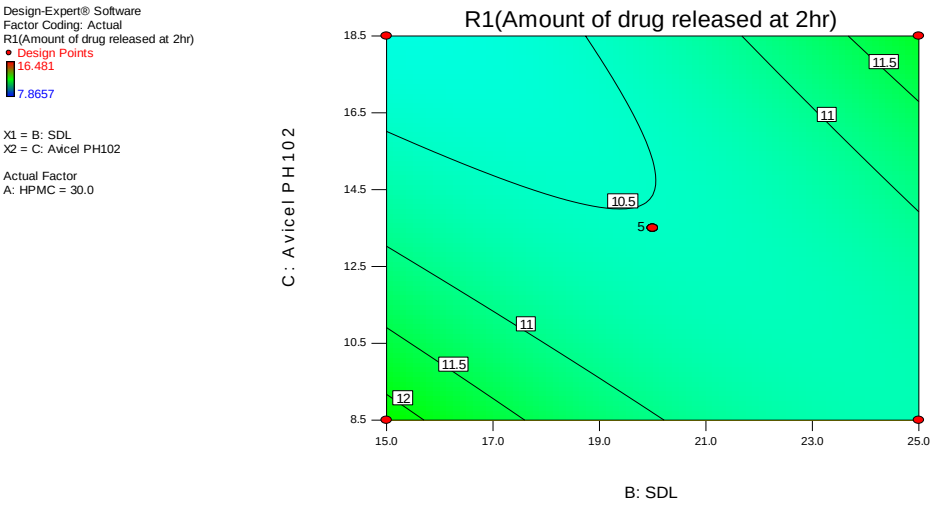

Figure Ap. 3.6. Contour plot of the effect of PH102 and SDL on response Y_1.

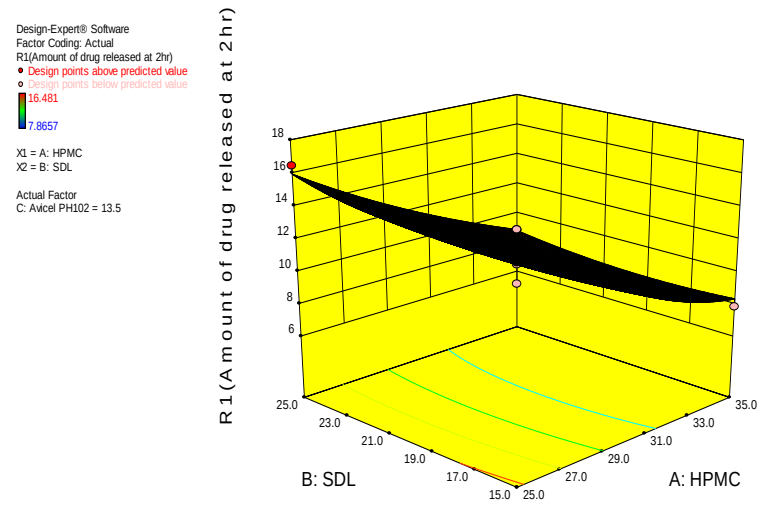

Figure Ap. 3.7. 3-D plot of the effect of SDL and HPMC on response Y_1.

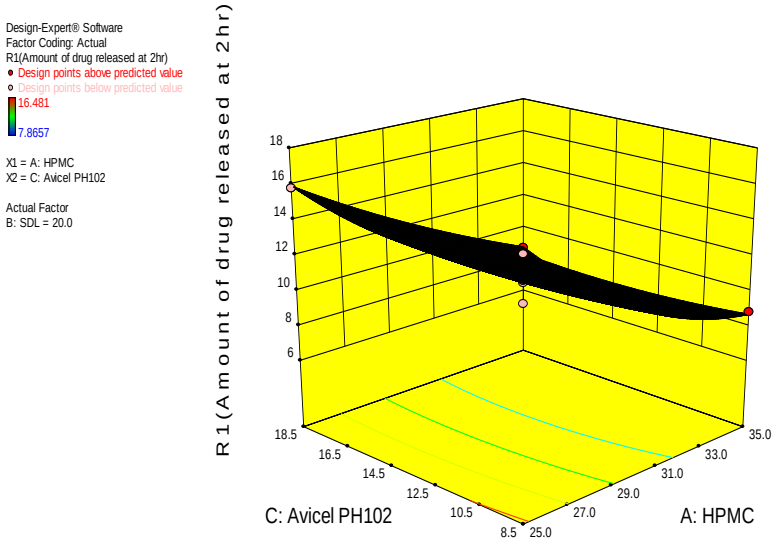

Figure Ap. 3.8. 3-D plot of the effect of PH102 and HPMC on response Y_1.

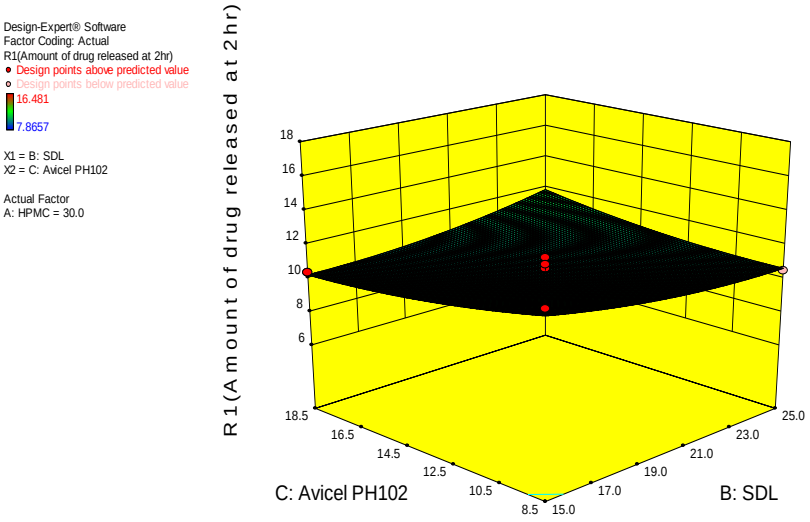

Figure Ap. 3.9. 3-D plot of the effect of PH102 and SDL on response Y_1.

3. Diagnostic plots for response Y_2: NVP release at 8 hours – linear model.

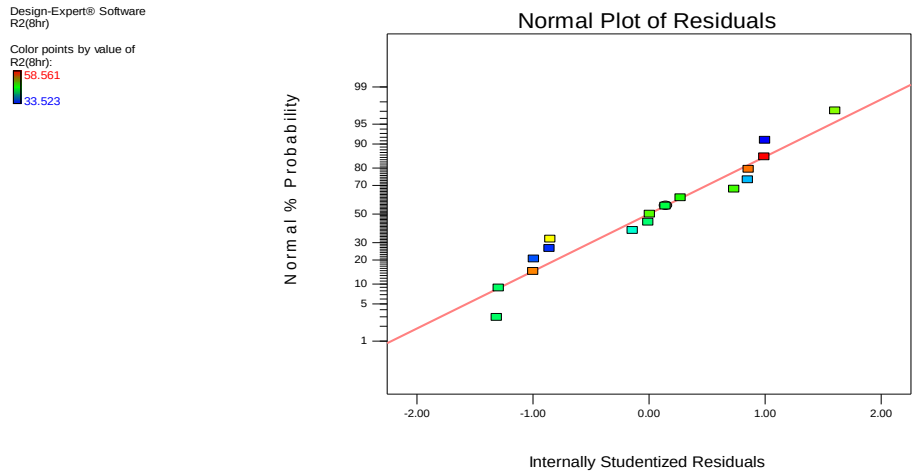

Figure Ap. 3.10. Normal plot of residuals for response Y_2.

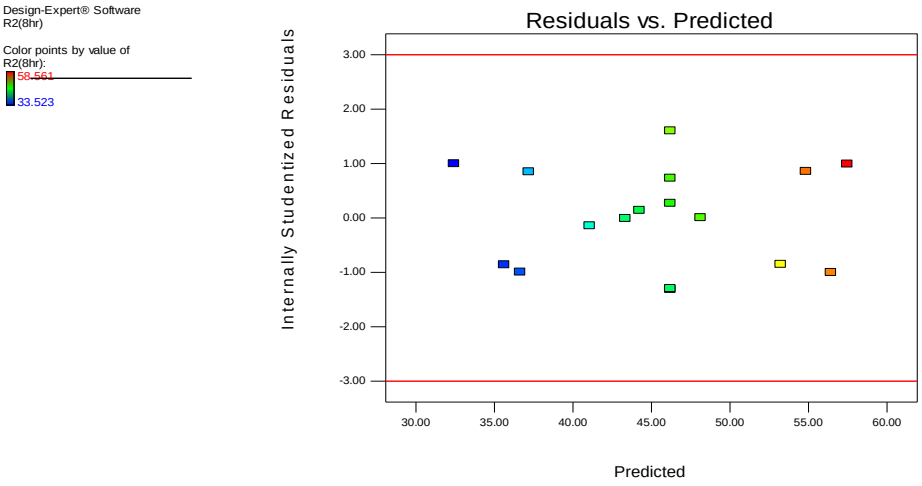

Figure Ap. 3.11. Plot of residuals vs. predicted responses for response Y_2.

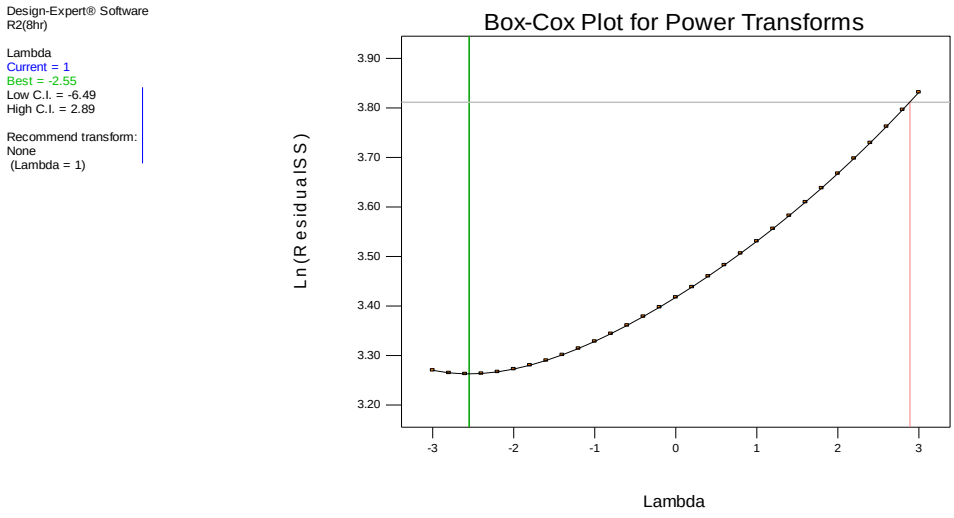

Figure Ap. 3.12. Box-Cox plot for power transforms for response Y_2.

4. Response surface plots for response Y_2

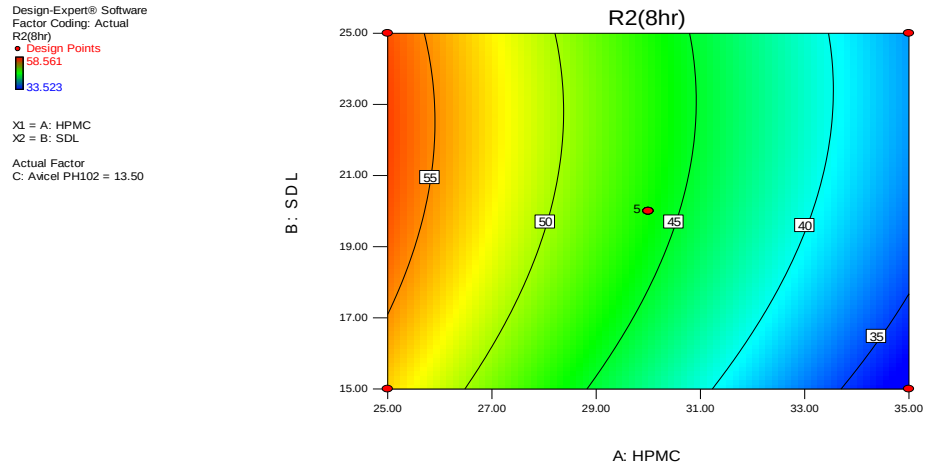

Figure Ap. 3.13. Contour plot of the effect of SDL and HPMC on response Y_2.

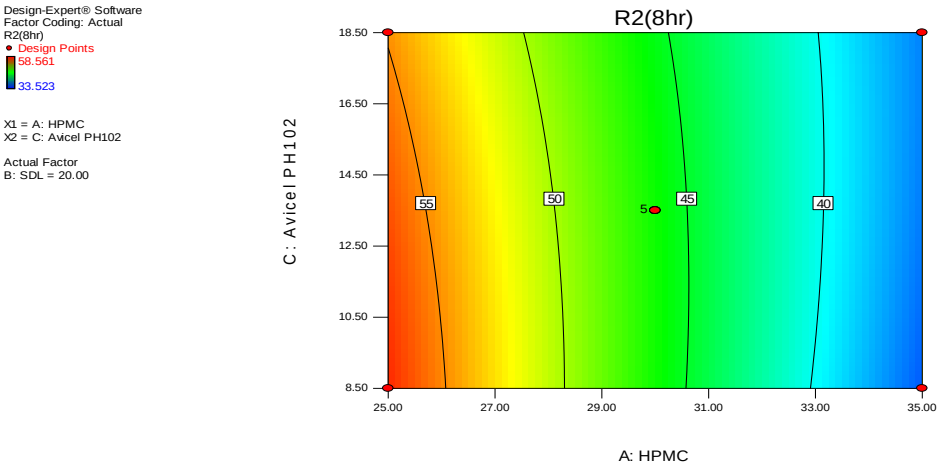

Figure Ap. 3.14. Contour plot of the effect of PH102 and HPMC on response Y_2.

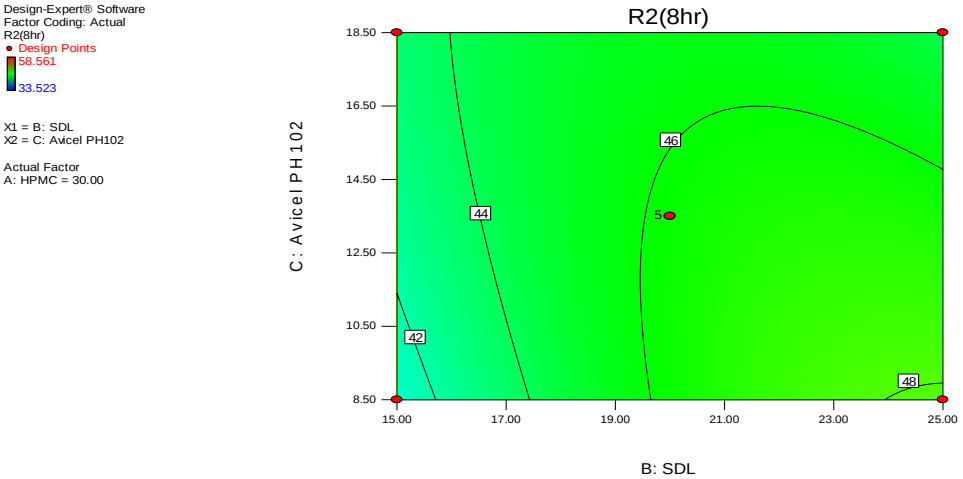

Figure Ap. 3.15. Contour plot of the effect of PH102 and SDL on response Y_2.

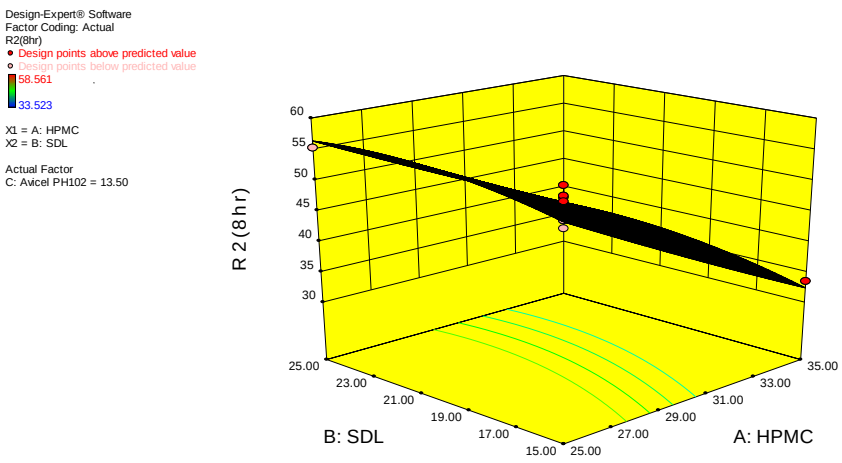

Figure Ap. 3.16. 3-D plot of the effect of SDL and HPMC on response Y_2.

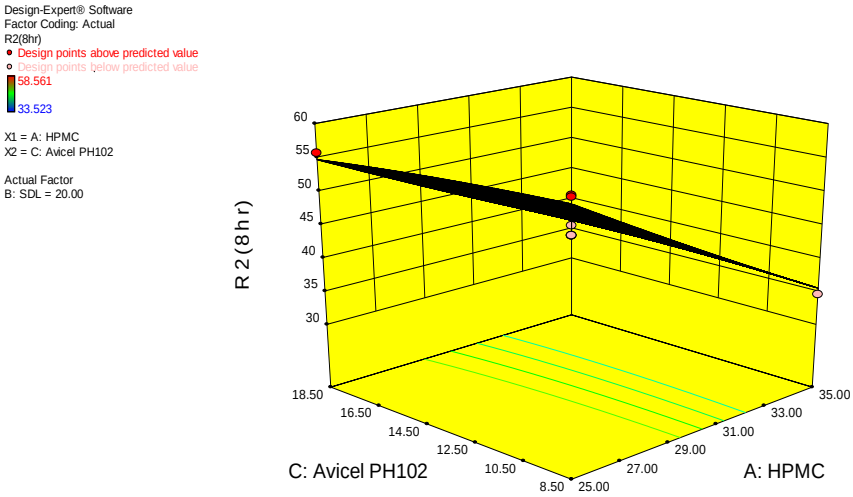

Figure Ap. 3.17. 3-D plot of the effect of PH102 and HPMC on response Y_2.

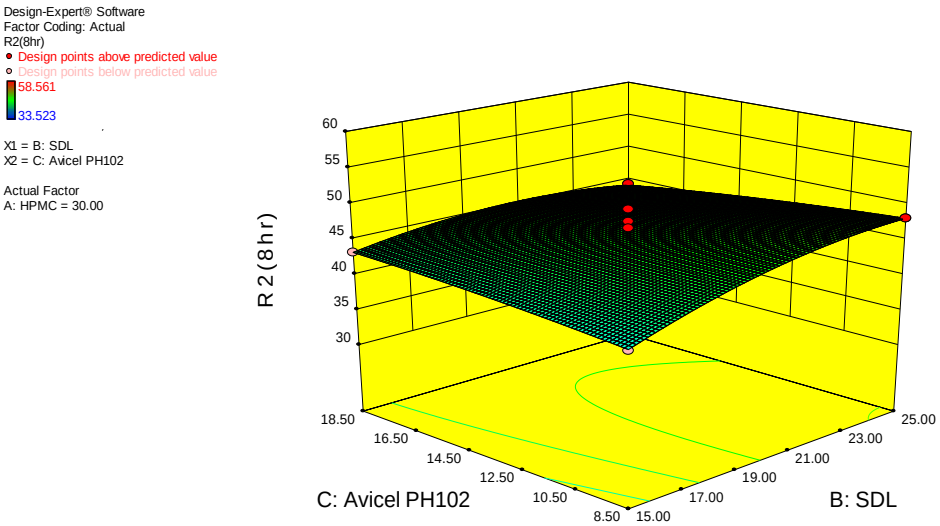

Figure Ap. 3.18. 3-D plot of the effect of PH102 and SDL on response Y_2.

5. Diagnostic plots for response Y_4: NVP release at 24 hours- 2FI model

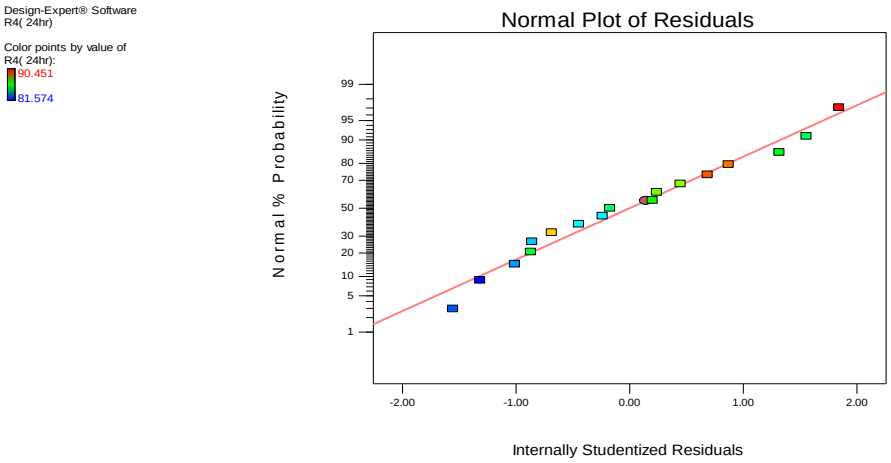

Figure Ap. 3.19. Normal plot of residuals for response Y_4.

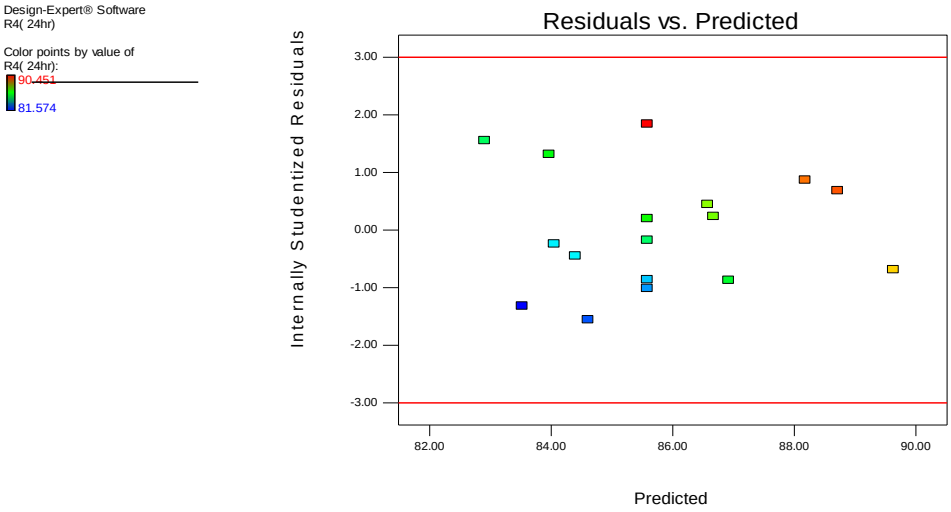

Figure Ap. 3.20. Plot of residuals vs. predicted responses for response Y_4.

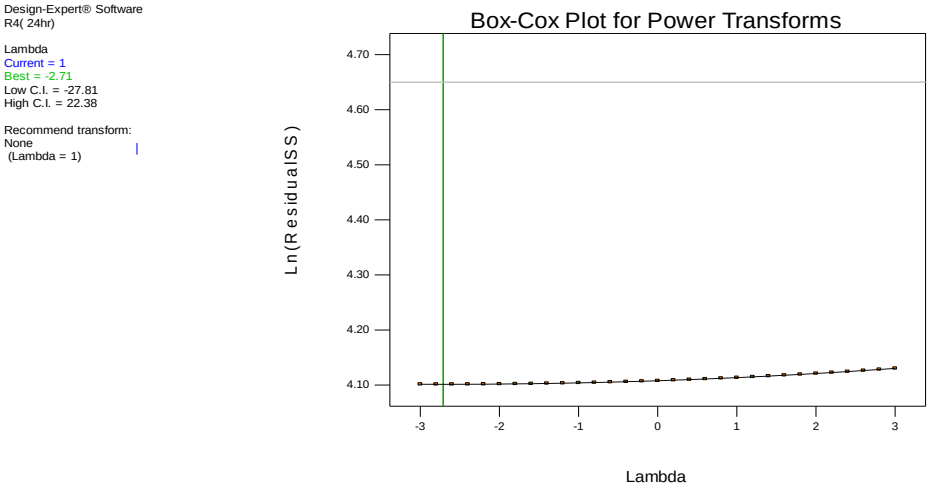

Figure Ap. 3.21. Box-Cox plot for power transforms for response Y_4.

6. Response surface plots for response Y_4

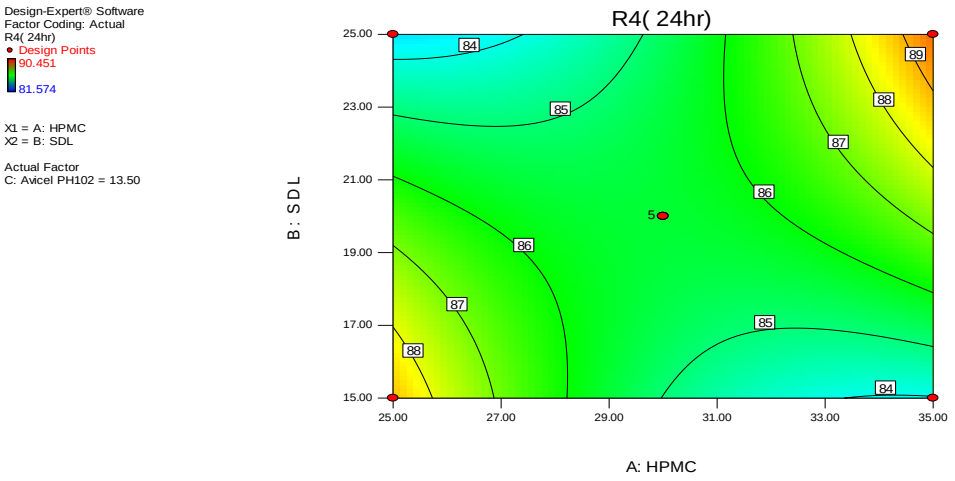

Figure Ap. 3.22. Contour plot of the effect of SDL and HPMC on response Y_4.

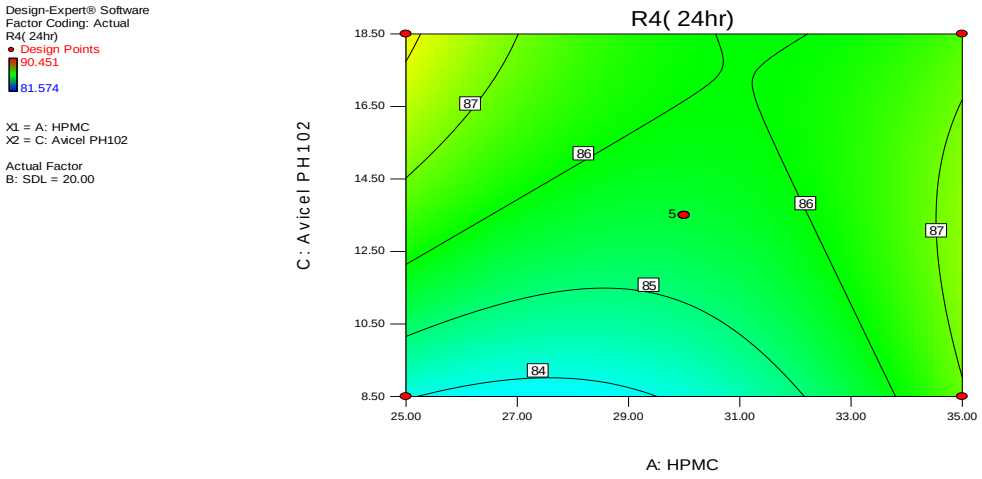

Figure Ap. 3.23. Contour plot of the effect of PH102 and HPMC on response Y_4.

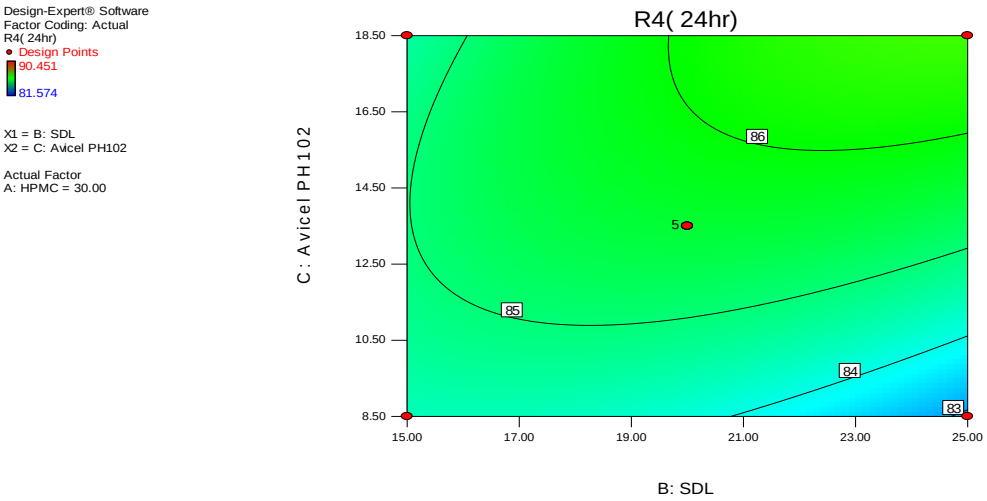

Figure Ap. 3.24. Contour plot of the effect of PH102 and SDL on response Y_4.

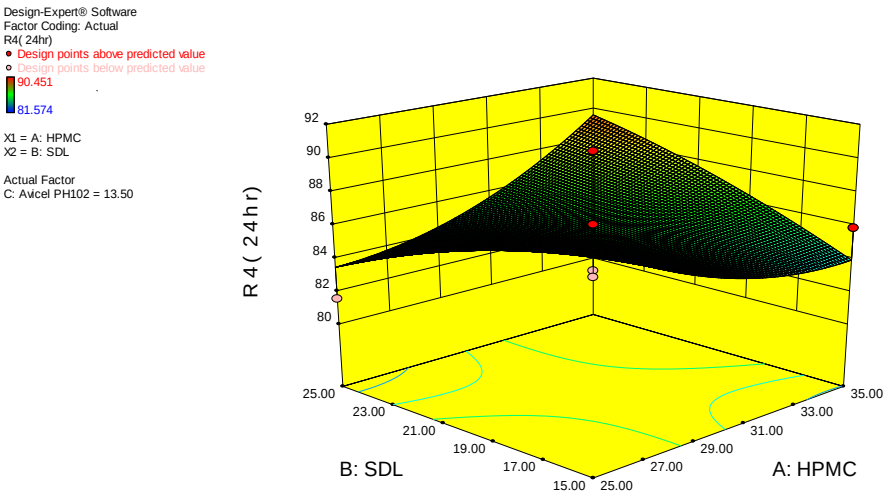

Figure Ap. 3.25. 3-D plot of the effect of SDL and HPMC on response Y_4.

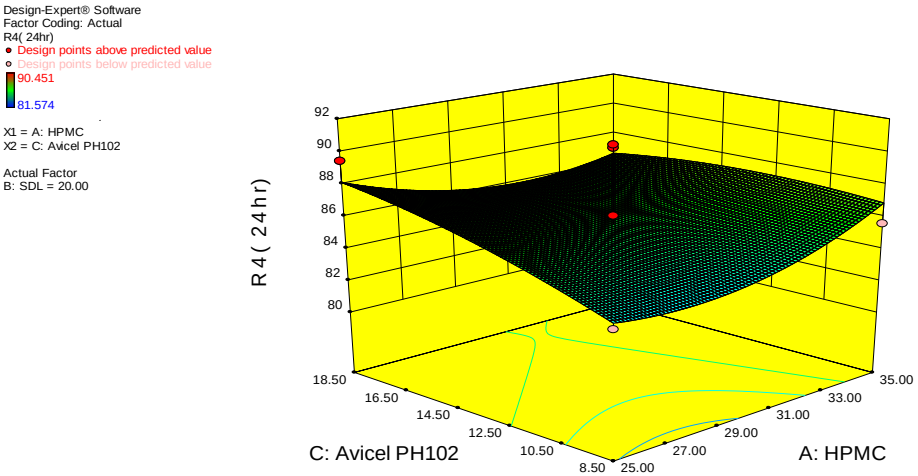

Figure Ap. 3.26. 3-D plot of the effect of PH102 and HPMC on response Y_4.

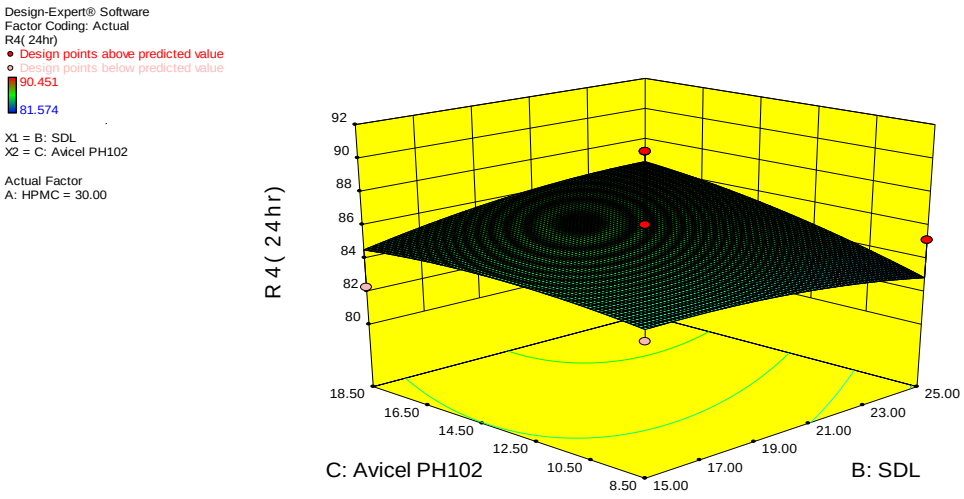

Figure Ap. 3.27. 3-D plot of the effect of PH102 and SDL on response Y_4.

7. Diagnostic plots for response Y_5: f_2 factor – quadratic model

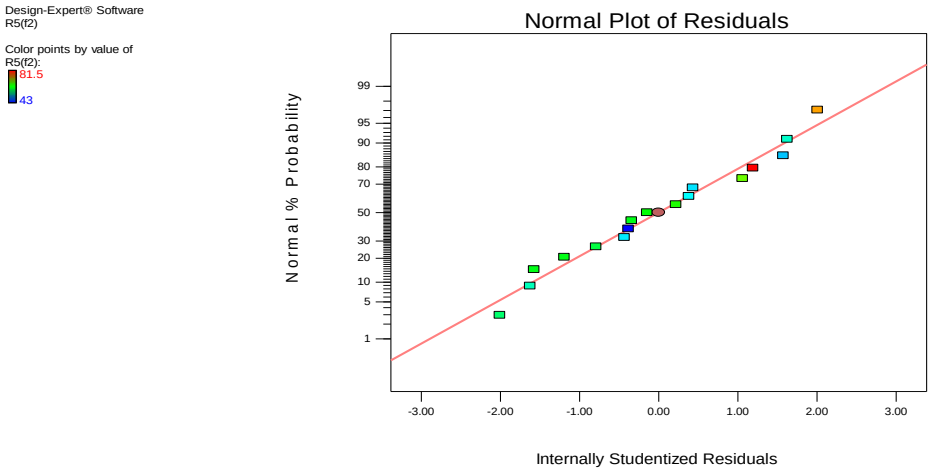

Figure Ap. 3.28. Normal probability plot of residuals for response Y_5.

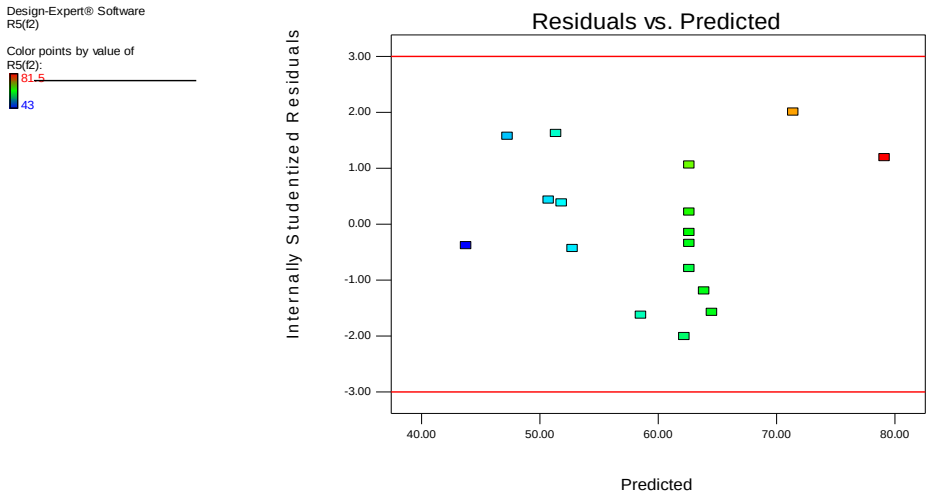

Figure Ap. 3.29. Plot of residuals vs. predicted responses for response Y_5.

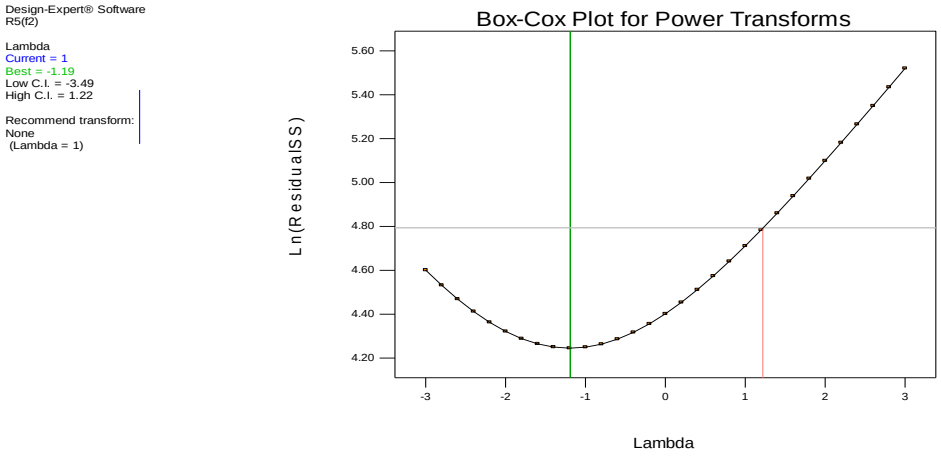

Figure Ap. 3.30. Box-Cox plot for power transforms for response Y_5.

8. Response surface plots for response Y_5

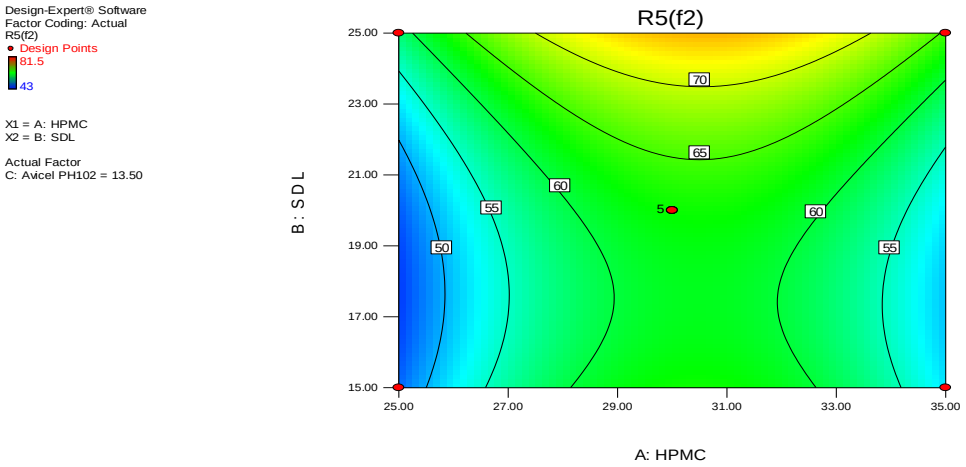

Figure Ap. 3.31. Contour plot of the effect of SDL and HPMC on response Y_5.

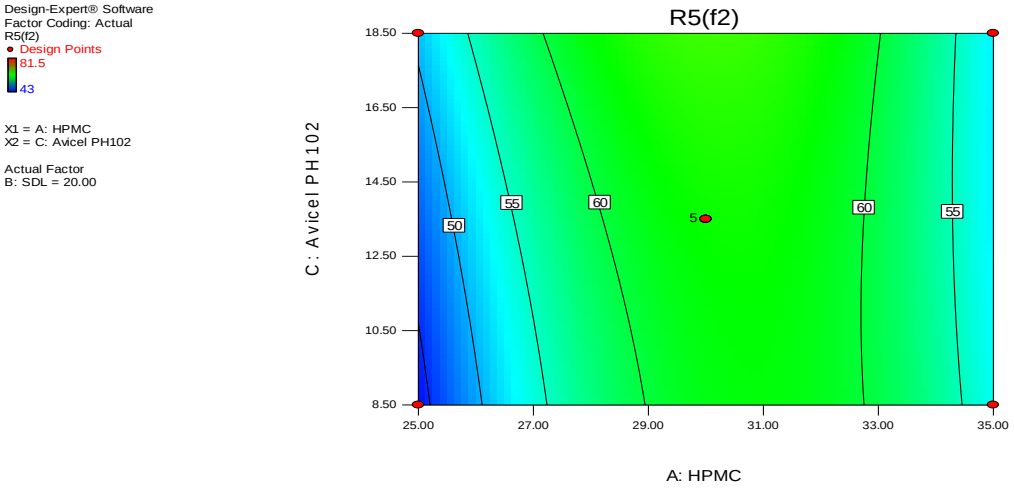

Figure Ap. 3.32. Contour plot of the effect of PH102 and HPMC on response Y_5.

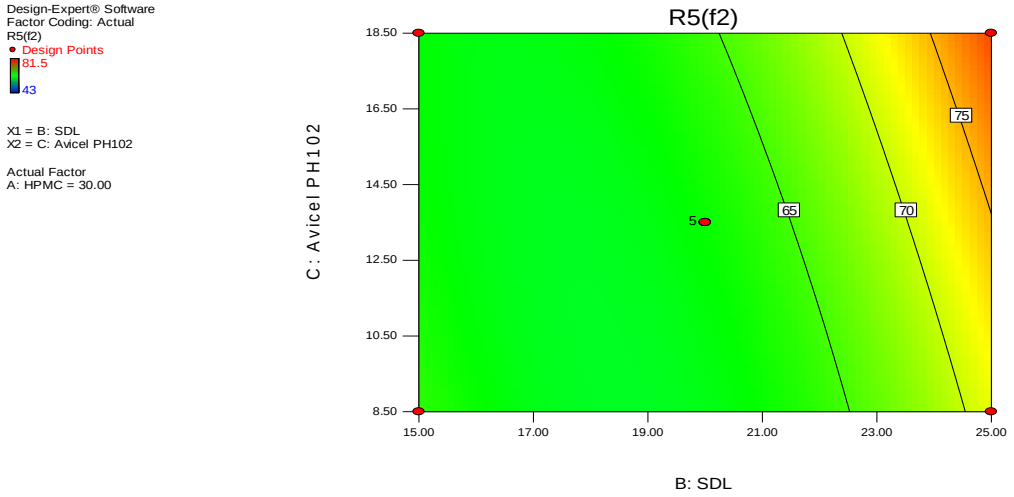

Figure Ap. 3.33. Contour plot of the effect of PH102 and SDL on response Y_5.

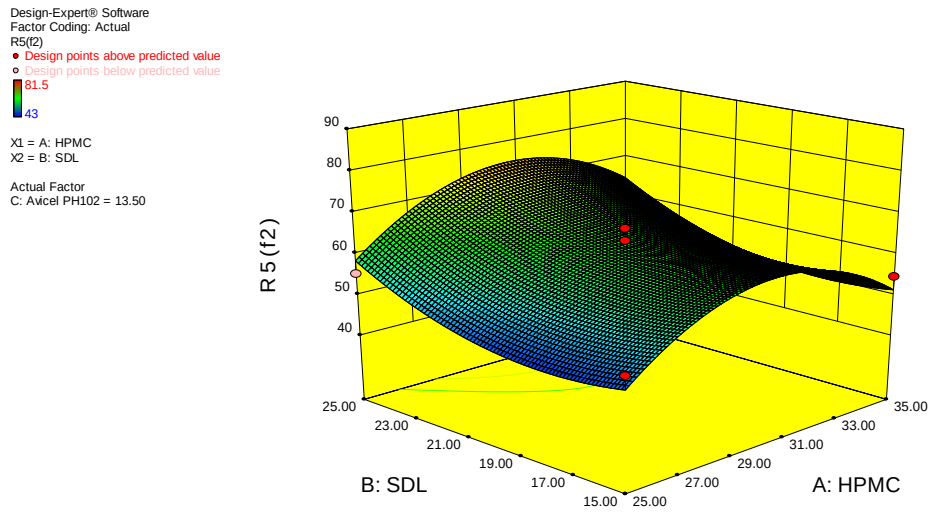

Figure Ap. 3.34. 3-D plot of the effect of SDL and HPMC on response Y_5.

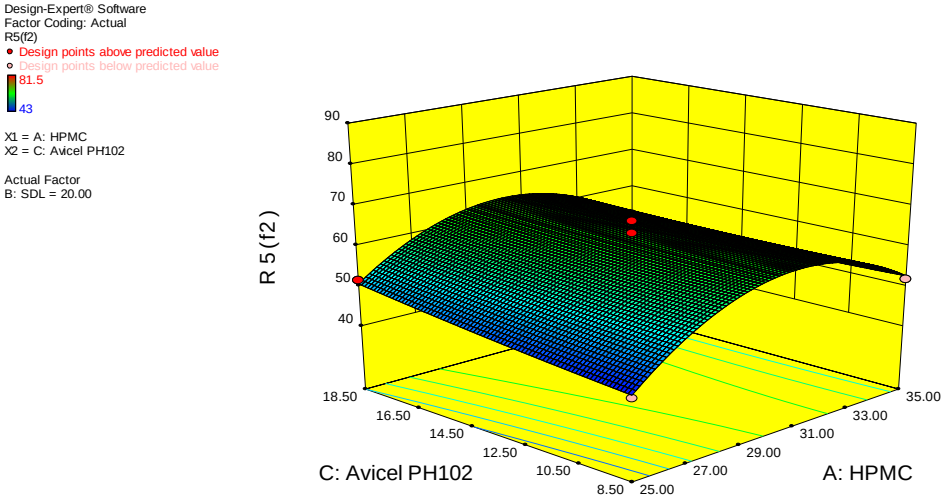

Figure Ap. 3.35. 3-D plot of the effect of PH102 and HPMC on response Y_5.

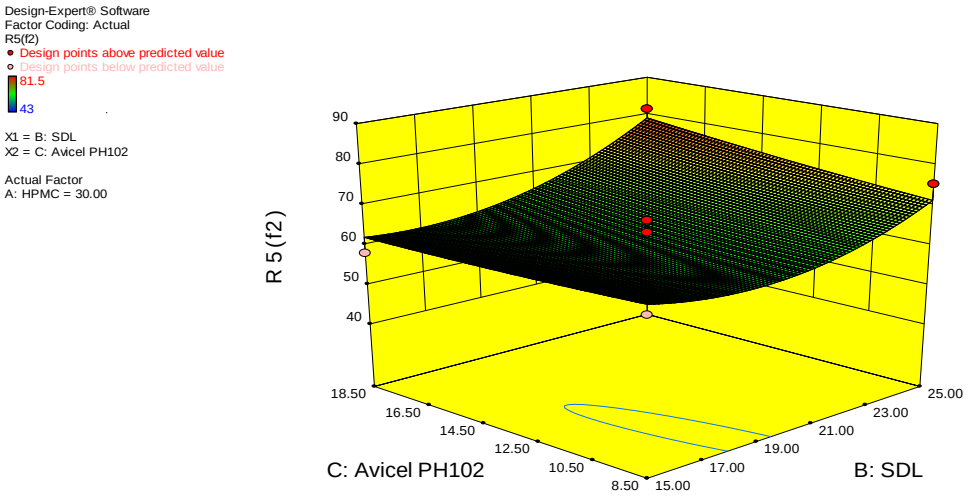

Figure Ap. 3.36. 3-D plot of the effect of PH102 and SDL on response Y_6.

9. Diagnostic plots for response Y_6: n-exponent- linear model

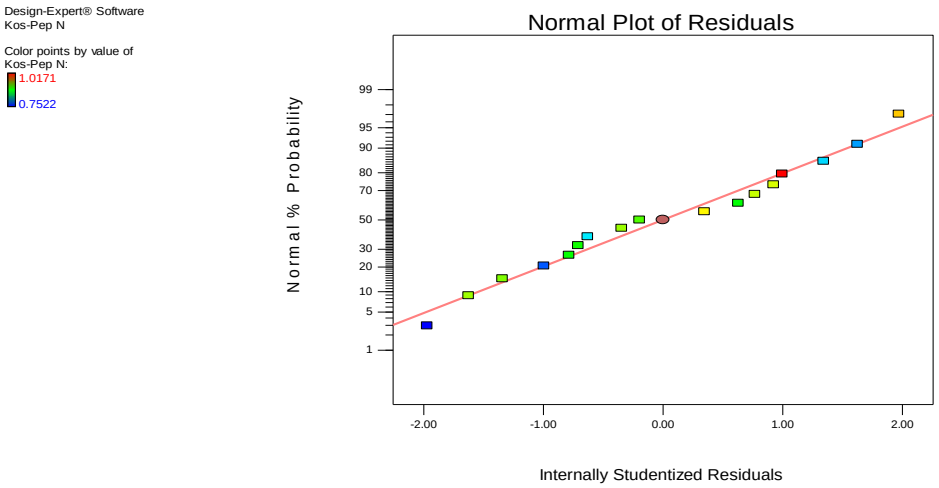

Figure Ap. 3.37. Normal plot of residuals for response Y_6.

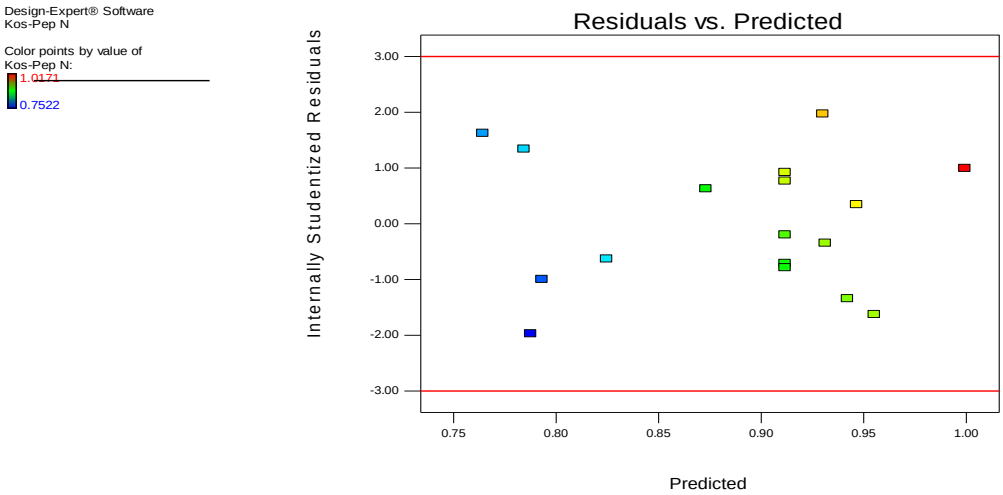

Figure Ap. 3.38. Plot of residuals vs. predicted responses for response Y_6.

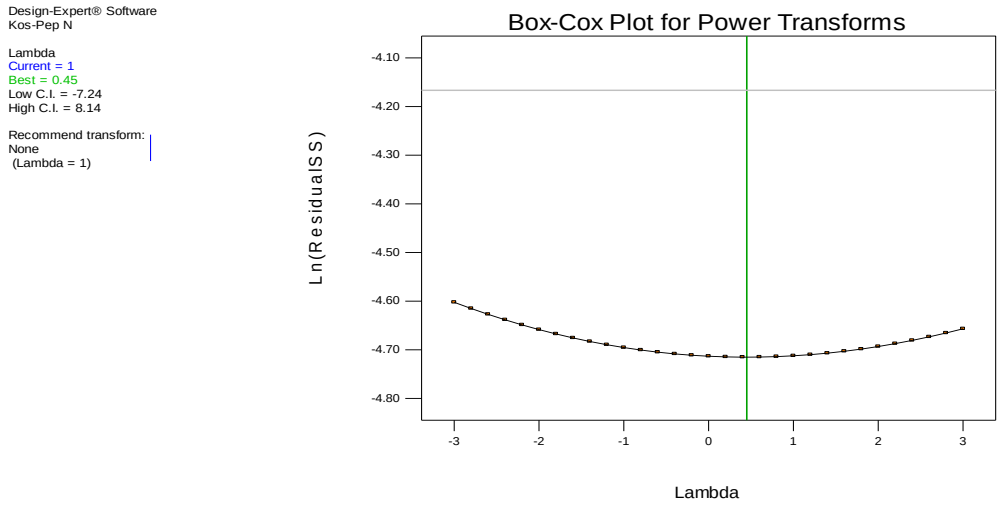

Figure Ap. 3.39. Box-Cox plot for power transforms for response Y_6.

10. Response surface plots for response Y_6

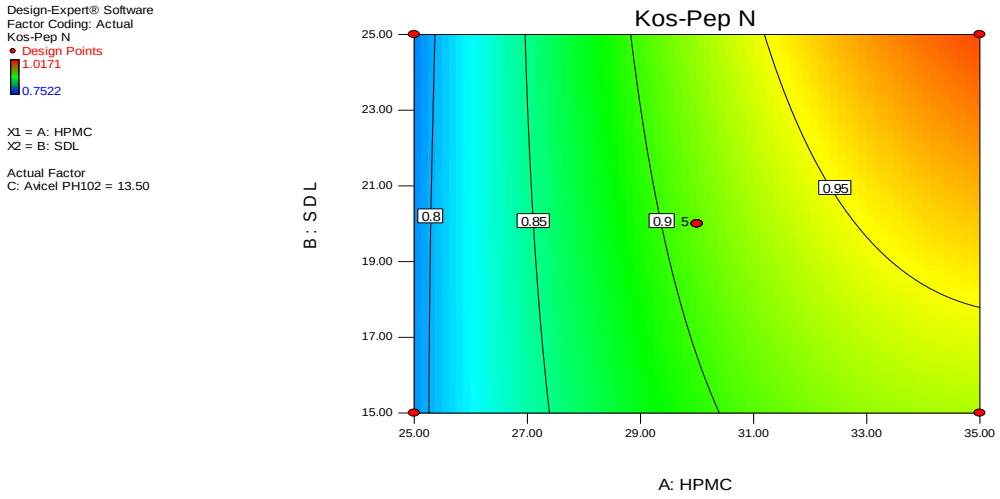

Figure Ap. 3.40. Contour plot of the effect of SDL and HPMC on response Y_6.

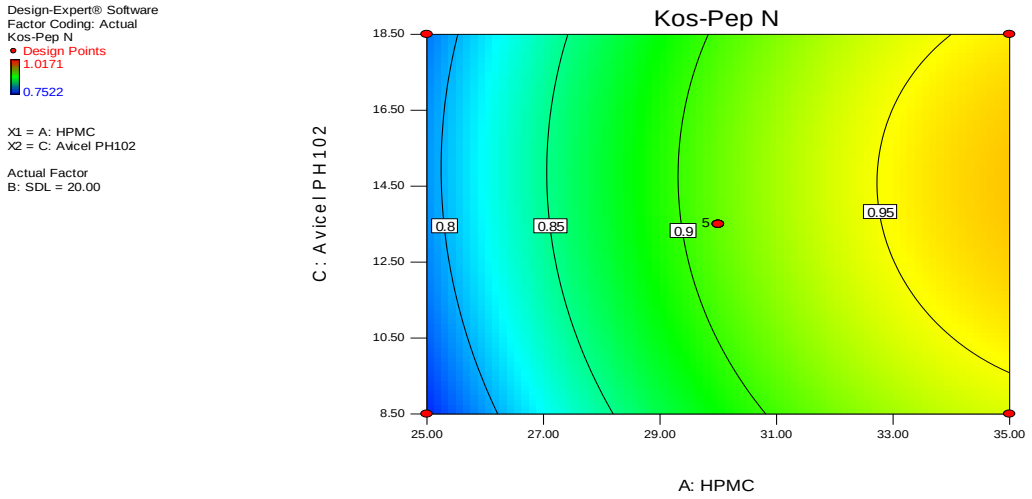

Figure Ap. 3.41. Contour plot of the effect of PH102 and HPMC on response Y_6.

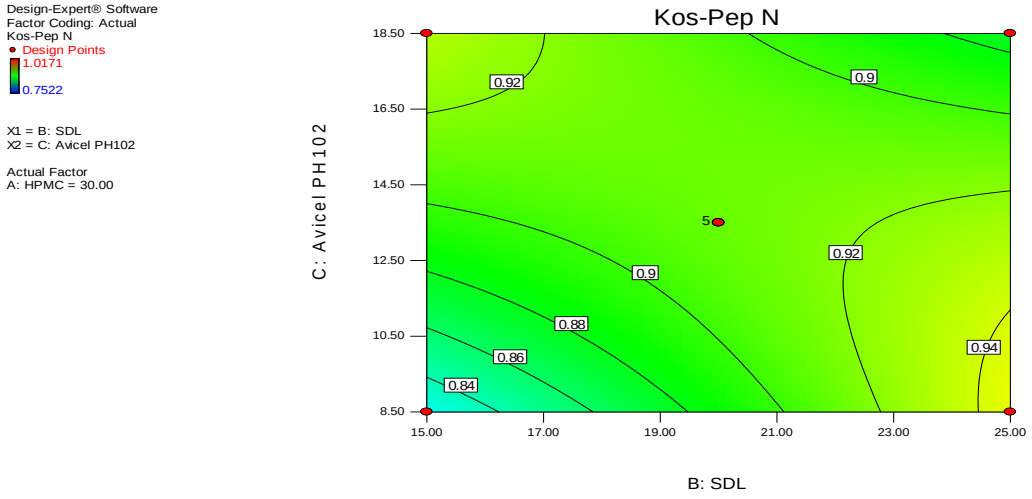

Figure Ap. 3.42. Contour plot of the effect of PH102 and SDL on response Y_6.

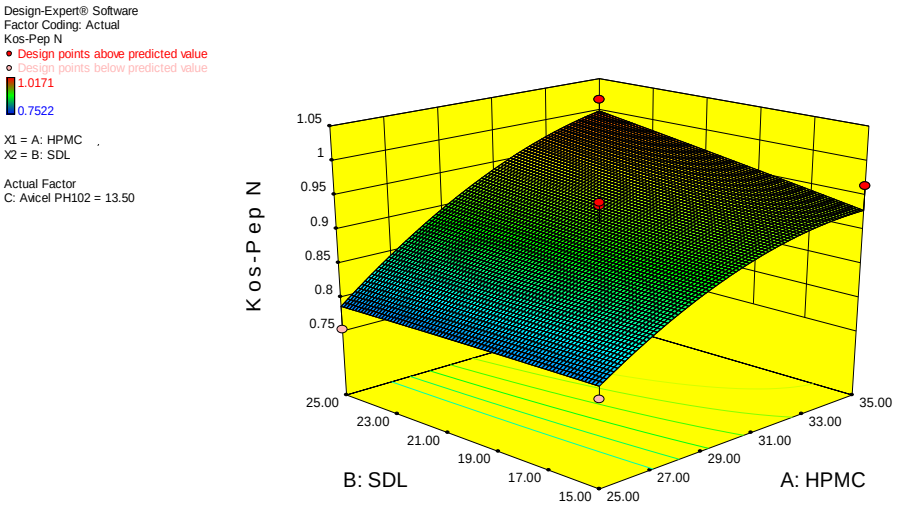

Figure Ap. 3.43. 3-D plot of the effect of SDL and HPMC on response Y_6.

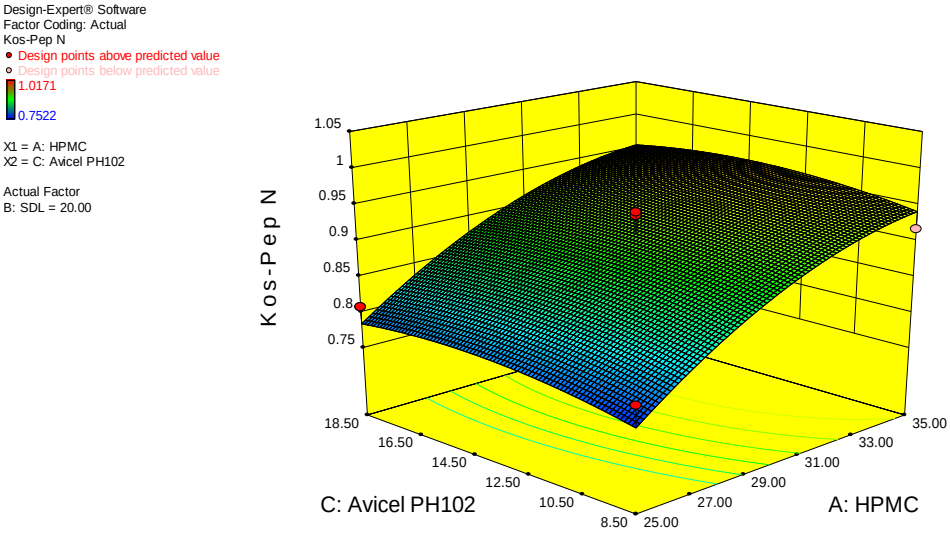

Figure Ap. 3.44. 3-D plot of the effect of PH102 and HPMC on response Y_6.

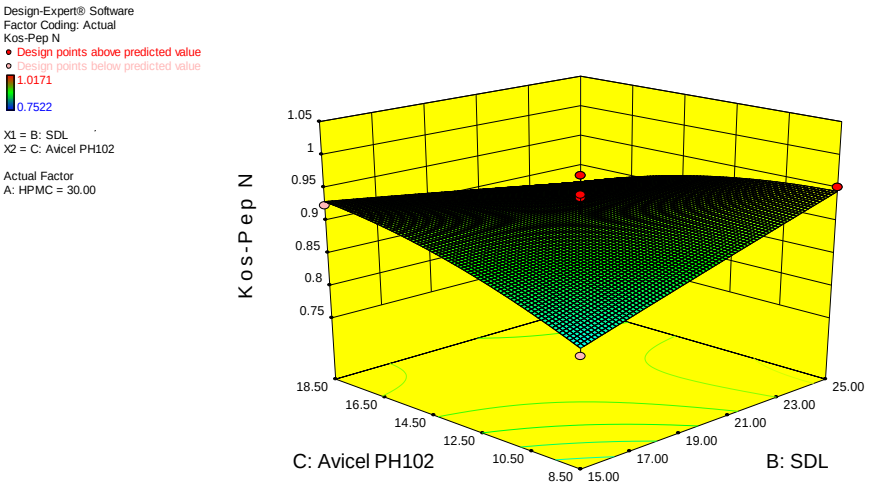

Figure Ap. 3.45. 3-D plot of the effect of PH102 and SDL on response Y_6.